

A Systems Biology Approach to Understand the Influence of SORLA on Amyloidogenic Processing in Alzheimer's Disease

Dissertation

zur

Erlangung des akademischen Grades

Doktor-Ingenieur (Dr.-Ing.)

Promotionsgebiet Systembiologie

Fakultät für Informatik und Elektrotechnik

Universität Rostock

**Universität
Rostock**



Traditio et Innovatio

vorgelegt von

Angelyn Lao

geboren am 30. August 1979 in Manila, Philippinen

Rostock, 13. März 2013

Gutachter:

Prof. Olaf Wolkenhauer (PhD)

Universität Rostock

Prof. Dr. Dr. Thomas E. Willnow

Max-Delbrück-Centrum für Molekulare Medizin Berlin-Buch

Dr. Eduardo Mendoza

Ludwig-Maximilians-Universität München

Tag der Verteidigung: 29. Januar 2013

Where there's a will there's a way.

ABSTRACT

Alzheimer's disease (AD) is a fatal neurodegenerative disorder. It is caused by the formation of neurotoxic beta-amyloid ($A\beta$) peptides, resulting from the proteolytic breakdown of amyloid precursor protein (APP) by secretases. This study aims to model APP processing and evaluate the influence of SORLA, a sortilin-related receptor. Based on a panel of cell lines in which intracellular levels of APP can be controlled, I designed single compartment models encoded in nonlinear ordinary differential equations, describing the kinetics of APP processing and the corresponding influence of SORLA. These models implement either monomeric, dimeric, or both APP forms. The parameter values of each particular model version were estimated with respect to dose-response series for soluble APP α and soluble APP β concentrations, as functions of the total amount of APP for cells in the presence and absence of SORLA. The simulations clearly support the combined model with both monomeric and dimeric APP in a single-compartment; whereby SORLA prevents APP oligomerization that causes secretases to switch from an allosteric to a non-allosteric regulation. However, in order to determine the relative contribution of SORLA to each APP-cleavage step and its effect on β -secretase (the first enzyme in the amyloidogenic pathway), it was crucial to shift from a single compartment to a multi-compartmental model. Comparison of the multi-compartmental model with experimental data shows that SORLA specifically impairs the processing of APP dimer; it is the substrate preferred by the secretases. Furthermore, it implies that SORLA alters the dynamical behavior of β -secretase. Since the multi-compartmental model identifies APP dimers and β -secretase as two distinctive targets of the inhibitory action of SORLA, it represents a major conceptual advancement in our understanding of the complex APP processing, showing SORLA as a promising candidate for AD treatment.

ZUSAMMENFASSUNG

Die Alzheimer-Krankheit (AK) ist eine neurodegenerative Störung, die durch das Auftreten von Amyloid-Plaques im Gehirn gekennzeichnet ist. Diese Plaques entstehen durch den proteolytischen Abbau des Amyloid-Vorläuferprotein (APP) durch Secretasen. Ziel dieser Studie ist die Modellierung der APP-Prozessierung unter Einfluss des sortilin-ähnlichem Rezeptors SORLA. Auf Grundlage von Zelllinien, in denen die intrazellulären Level von APP kontrolliert werden kann, habe ich Differentialgleichungsmodelle in einfachen Kompartimenten zur Beschreibung der Kinetik der APP-Verarbeitung und dem Einfluss von SORLA entwickelt. APP tritt in den Modellen dabei als Monomer und/oder Dimer auf. Zur modellspezifischen Parameterbestimmung habe ich Konzentrationen von löslichem APP α - und APP β verwendet, die in Abhängigkeit zur APP Konzentration in Dosis- Wirkungssexperimenten bei An- und Abwesenheit von SORLA gemessen wurden. Die Ergebnisse verdeutlichen, dass im Fall von Einzelkompartimenten monomeres und dimeres APP gemeinsam vorliegt. SORLA verhindert dabei die APP-Oligomerisation und löst bei den Sekretasen eine Änderung von einer allosterischen zu einer nichtallosterischen Wirkungsweise aus. Um jedoch die Auswirkung von SORLA auf die β -secretase zu bestimmen, der ersten Reaktion der APP-Spaltung in der Amyloidogenese, ist ein Wechsel von einem Einzel- zu einem Multi-Kompartimentmodell nötig. Der Vergleich der Ergebnisse des Multi-Kompartimentmodells mit experimentellen Dosis-Wirkungsdaten zeigt, dass SORLA besonders die Verarbeitung von APP-Dimern, dem bevorzugten Sekretase-Substrat, beeinträchtigt. Weiterhin zeigt das Modell die besondere Bedeutung von SORLA für das dynamische Verhalten der β -s-Sekretase. Der konzeptionelle Fortschritt des Multi-Kompartimentmodells im Bezug zur APP-Prozessierung ist die Trennung der APP-Dimeren und der β -Sekretase als zwei getrennte Wirkungsbereiche von SORLA. Damit rückt SORLA in den Blickpunkt einer medikamentösen Behandlung der AK.

ACKNOWLEDGEMENT

*I am grateful to people who give me chance and opportunity.
I am thankful to people who share with me knowledge and wisdom.
I am indebted to people who stay with me through thick and thin.*

I first offer my gratitude to my advisor, Prof. Dr. Olaf Wolkenhauer, for his guidance and friendship. His passion and commitment to his work and interests have been an incredible source of inspiration for me. I am thankful for all the opportunities he offered me, for a wonderful scientific atmosphere he created, and for his continuous patience and encouragement.

I am deeply grateful to Prof. Dr. Thomas E. Willnow, from Max-Delbrueck Center for Molecular Medicine in Berlin-Buch (MDC), who provided crucial input in the form of scientific advice and research guidance that have led to the completion of this thesis. I thank Dr. Katja Rateitschak for our numerous fruitful discussions that have led to many of the ideas presented in this thesis. I especially thank Dr. Vanessa Schmidt for her scientific input, friendship, and support.

During my PhD years, I have had the good fortune to work with good colleagues and friends whose careful thinking has helped me think better about many matters, both professional and personal. In particular, I am grateful to the whole Department of Systems Biology and Bioinformatics (www.sbi.uni-rostock.de) for the pleasure of doing research and recreational activities together. All these circumstances have made me a better person - more well rounded.

Next, I give thanks to my family, for without their love and support I would not be here. I dedicate all my achievements to my parents, Perla and Simeon Lao, who have taught me to believe in myself, trusted my choices, and always been there for me. I am especially thankful to Dr. Eduardo Mendoza, my mentor way back to my Master days, without whom I would not reach this far. I am also thankful to Dr. Thomas Millat and Dr. Jiří Jablonský for proofreading my dissertation. Finally, I thank all my friends (too many to mention), scattered all over the world, whose presence in my life has made me the person I am now.

My time as a PhD candidate was financially supported through the collaborative project, “Mathematical modeling of neurodegenerative processes in Alzheimer’s disease”, between the University of Rostock and MDC, under the MDC systems biology network that is funded by the Helmholtz alliance of systems biology.

CONTENTS

Abstract	ii
Abbreviations	xi
Model notations	xii
Biochemical network notations	xiv
1. Introduction	1
1.1. A systems biology approach to study Alzheimer's disease	1
1.2. State of the art	7
1.2.1. Amyloid - a hypothesized cause	7
1.2.2. SORLA - a drug candidate	10
1.2.3. Alternatives to the amyloid hypothesis?	14
1.2.4. Previous modeling efforts	16
1.3. Objectives and organization of this thesis	19
2. Materials and methods	21
2.1. Dose-response experimental design	21
2.2. Modeling framework	27
2.2.1. Construction of the model	27
2.2.2. Parameter value estimation	28
3. Mathematical modeling of SORLA's influence on amyloidogenic processing	33
3.1. Pilot simulations based on monomeric APP	34
3.2. Processing of dimeric APP	39
3.3. When one pathway is not enough	46
4. Compartmental-based behavior of the system	59
4.1. Conventional compartmental modeling: pros and cons	60

4.2. Multi-compartmental modeling of APP processing influenced by SORLA . .	61
5. Conclusions	91
Bibliography	93
Appendices	103
A. Description of variables	105
B. Estimated parameter values	111
C. Matlab source code	115
Declaration	
Curriculum Vitae	
Scientific contributions	
Theses	

ABBREVIATIONS

α -secretase	alpha-secretase
β -secretase	beta-secretase
γ -secretase	gamma-secretase
A β	amyloid-beta peptide
A β 40	A β peptide with isoforms of 40 amino acid residues in length
A β 42	A β peptide with isoforms of 42 amino acid residues in length
AICD	APP intracellular domain
APOE	apolipoprotein E
APP	amyloid precursor protein
C83	the 83-amino acid C-terminal fragment
C99	the 99-amino acid C-terminal fragment
CHO	Chinese hamster ovary
CHO-A	Chinese hamster ovary expressing APP 695
CHO-S	Chinese hamster ovary expressing human SORLA
CHO pTet-APP	CHO cells with regulated APP in the absence of SORLA
CHO-A pTet-APP	CHO-A cells with regulated APP in the presence of constant SORLA
CHO-S pTet-SORLA	CHO-S cells with regulated SORLA under constant APP
CMV	cytomegalovirus promoter
CSF	cerebral-spinal fluid
ELISA	enzyme-linked immunosorbent assay
GGA	Golgi-localizing, Gamma-adaptin ear-containing, ARF-interacting protein
LR11	other name for SORLA
ODE	ordinary differential equation
P3	a 3-kDa fragment composed of residues 17-40 or 17-42 of the amyloid beta peptide
PACS	phosphofurin acidic cluster sorting protein
sAPP α	soluble APP-alpha
sAPP β	soluble APP-beta
SORCS	a member of the family of VPS10 domain containing receptors

SORL1	other name for SORLA
SORLA	sortilin-related receptor, L(DLR class) A repeats-containing
TGN	trans-Golgi network
TMS	transmembrane sequence
TRE MOD	modified tetracycline-response
tTA	tetracycline-controlled transcriptional activator
VPS10p	vascular protein sorting 10 protein

MODEL NOTATIONS

IN A SINGLE-COMPARTMENT

APP	monomeric form of APP
α	monomeric form of α -secretase
$sAPP\alpha$	soluble $APP\alpha$, resulting from monomer processing
$C83$	fragment C83, resulting from monomer processing
$C_{APP\alpha}$	complex of APP and α , formed within monomer processing
β	monomeric form of β -secretase
$sAPP\beta$	soluble $APP\beta$, resulting from monomer processing
$C99$	fragment C99 in monomer processing
$C_{APP\beta}$	complex of APP and β , formed within monomer processing
APP_d	dimeric form of APP
α_d	dimeric form of α -secretase
$sAPP\alpha^*$	soluble $APP\alpha$, resulting from dimer processing
$C83_d$	fragment C83-dimer, resulting from dimer processing
$C_{APP_d\alpha_d}$	complex of APP_d and α_d , formed within dimer processing
β_d	dimeric form of β -secretase
$sAPP\beta^*$	soluble $APP\beta$, resulting from dimer processing
$C99_d$	fragment C99-dimer in dimer processing
$C_{APP_d\beta_d}$	complex of APP_d and β_d , formed within dimer processing
$SORLA$	sorting protein-related receptor with A-type repeats
$C_{APPSORLA}$	complex of APP and $SORLA$

IN THE TGN COMPARTMENT

APP_{init}	initial APP
APP_{G1}	monomeric form of APP in the monomer processing
APP_{G2}	monomeric form of APP in the dimer processing
APP_{G2d}	dimeric form of APP in the dimer processing
$SORLA_{G1}$	SORLA in the monomer processing
$SORLA_{G2}$	SORLA in the dimer processing
$C_{APPG1SORLAG1}$	complex of APP_{G1} and $SORLA_{G1}$ in the monomer processing
$C_{APPG2SORLAG2}$	complex of APP_{G2} and $SORLA_{G2}$ in the dimer processing

AT THE CELL SURFACE COMPARTMENT

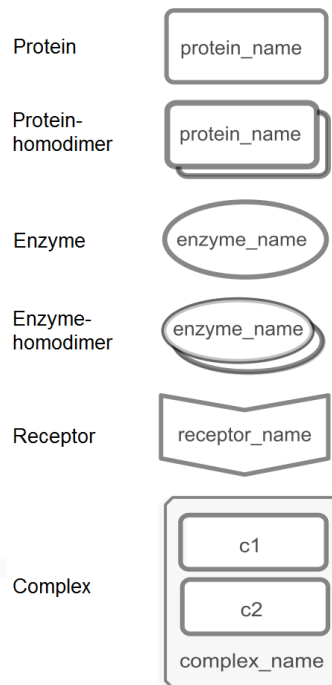
APP_{CS1}	monomeric form of APP in the monomer processing
APP_{CS2d}	dimeric form of APP in the dimer processing
α_{init}	initial α -secretase
α_1	monomeric form of α -secretase in the monomer processing
α_2	monomeric form of α -secretase in the dimer processing
α_{2d}	dimeric form of α -secretase in the dimer processing
$C_{APPCS1\alpha1}$	complex of APP_{CS1} and α_1 , formed within monomer processing
$C_{APPCS2d\alpha2d}$	complex of APP_{CS2d} and α_{2d} , formed within dimer processing
$C83_1$	fragment C83, resulting from monomer processing
$C83_{2d}$	fragment C83-dimer, resulting from dimer processing
$sAPP\alpha_1$	soluble APP α , resulting from monomer processing
$sAPP\alpha_2$	soluble APP α , resulting from dimer processing

IN THE ENDOSOME COMPARTMENT

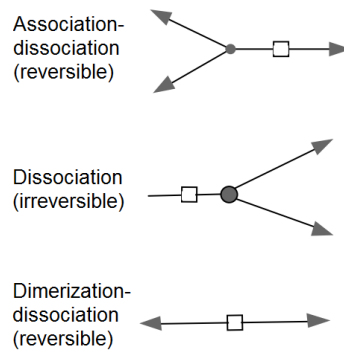
APP_{E1}	monomeric form of APP in the monomer processing
APP_{E2d}	dimeric form of APP in the dimer processing
β_{init}	initial β -secretase
β_1	monomeric form of β -secretase in the monomer processing
β_2	monomeric form of β -secretase in the dimer processing
β_{2d}	dimeric form of β -secretase in the dimer processing
$C_{APPE1\beta1}$	complex of APP_{E1} and β_1 , formed within monomer processing
$C_{APPE2d\beta2d}$	complex of APP_{E2d} and β_{2d} , formed within dimer processing
$C99_1$	fragment C99 in monomer processing
$C99_{2d}$	fragment C99-dimer in dimer processing
$sAPP\beta_1$	soluble APP β , resulting from monomer processing
$sAPP\beta_2$	soluble APP β , resulting from dimer processing

BIOCHEMICAL NETWORK NOTATIONS

State node symbols



Transit nodes and edges



In accordance to the need of our study, the above notations are modified based on those defined in Cell Designer [Kitano et al. 2005].

INTRODUCTION

This introduction will provide the context of Alzheimer's disease (AD) in relation to the work described in this dissertation. Systems biology is an interdisciplinary approach by which biological questions are addressed through integrating experiments in iterative cycles with computational modeling, simulation, and theory [Pastori et al. 2008]. I will describe how systems biology can be used to study AD and highlight the contributions of this thesis to that endeavor.

1.1. A systems biology approach to study Alzheimer's disease

AD is named after the German psychiatrist Dr. Alois Alzheimer. In 1901, Dr. Alzheimer identified the first case of what is now known as AD in a 50-year-old woman called Auguste D. Her symptoms included memory loss, language problems, and unpredictable behavior. After she died, Dr. Alzheimer examined her brain and found tissue changes (Figure 1.1) that included many abnormal clumps (now called amyloid plaques) and tangled bundles of fibers (now called neurofibrillary tangles):

- **Amyloid plaques, also referred to as Beta amyloid($A\beta$) plaques**, accumulate between nerve cells (neurons) in the brain. $A\beta$ is a protein fragment cleaved from amyloid precursor protein (APP). In a healthy brain, these protein fragments are broken down and eliminated. In AD, the fragments accumulate to form hard, insoluble plaques.
- **Neurofibrillary tangles** are insoluble, twisted fibers found inside neurons in the brains of patients with AD. These tangles consist primarily of a protein called tau, which forms part of a structure called a microtubule. Microtubules help to transport nutrients and other substances from one part of the cell to another. In AD, the tau protein is abnormal and the microtubules collapse.

1. Introduction

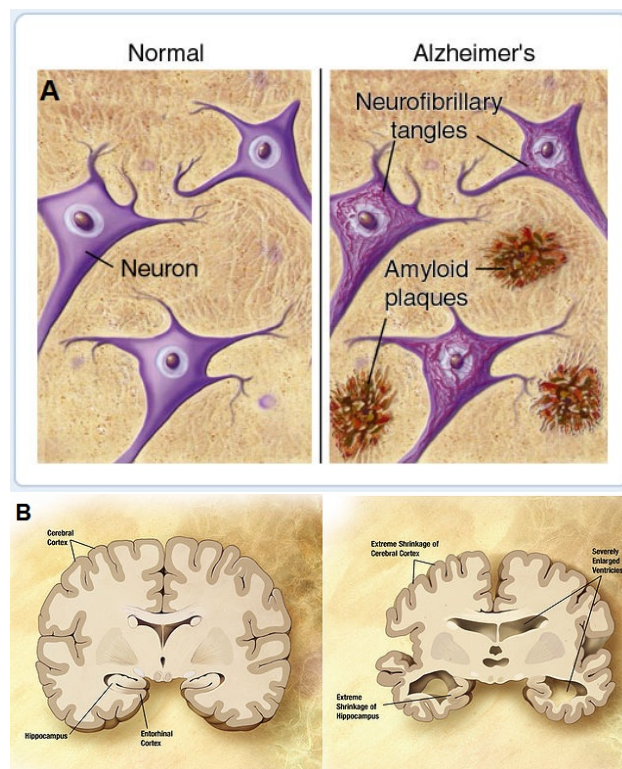


Figure 1.1.: Images of brains with and without AD. On the left side are images of a normally aged brain. On the right side are images of a brain with AD. Image courtesy of the American Health Assistance Foundation (A) and the National Institute on Aging/National Institutes of Health (B).

1.1. A systems biology approach to study Alzheimer's disease

As reported from the Alzheimer's Association, AD is a common form of dementia that accounts for 50 to 80% of all dementia cases. AD is progressive; the symptoms gradually worsen over a number of years. In the early stages, memory loss is mild; but with late-stage AD, individuals lose the abilities to carry on a conversation and respond to their environment. The progression is mild and steady for 8 to 10 years, depending on age and other health conditions. The disease starts in the hippocampus and spreads into different regions of the brain. This progressive spreading is what causes the different stages of AD:

- Stage one: the patient has difficulty finding the right words.
- Stage two: the patient loses the ability to solve problems, grasp concepts, and make plans.
- Stage three: the patient gradually loses control of his/her moods and feelings.
- Stage four: the patient loses senses of things he/she sees, hears, and smells; and experiences hallucinations.
- Stage five: the patient loses his/her oldest and most precious memories.
- Stage six: the patient's balance and coordination are compromised.
- Stage seven: the part of the patients brain that regulates breathing and heart rate is destroyed.

It is, however, a common misconception to regard AD as a normal part of aging. Although the majority of the people who have it are age 65 and older, AD also afflicts younger people. Up to 5% of AD cases are early onset, which often starts when a person is in his/her 40s or 50s [Alzheimer's Association].

As the world's population ages, AD is emerging as a global epidemic. Researchers from Johns Hopkins University concluded in their presentation at an Alzheimer's Association conference in Washington D.C. that 1 in 85 people will have AD by 2050 [Brookmeyer et al. 2007]. Due to the long-term progression of the disease, the responsibilities and burdens of taking care of an AD patient can be emotionally and financially overwhelming. The high costs of providing health insurance to these patients could even cripple the economy of a nation. AD results in personal tragedy for the patients, and family distress and social catastrophe for those around them. Preventing or delaying AD would have a tremendous impact on global public health [Alzheimer's Association].

Today, there is a worldwide effort under way to prevent, delay, and treat AD. However, drug trials are extremely time-consuming and expensive because AD develops very slowly and it takes a long time to determine whether a drug is helping.

Systems biology is an interdisciplinary approach that aims at understanding the dynamic interactions between components of a living system [Pastori et al. 2008]. Starting

1. Introduction

in the 1960s, some researchers began to use systems theory to study and understand general biological principles [Bertalanffy 1950; Mesarovic 1968]. Systems biology has attracted the interest of researchers from different disciplinary backgrounds. Although still in its infancy, systems biology is increasingly considered part of the mainstream in the biological sciences [Hübner et al. 2011].

The interdisciplinary nature of systems biology results in instances where the same process or pathway is modeled in very different frameworks (such as cellular automata, π -calculus, and nonlinear ordinary differential equations) [Wolkenhauer et al. 2004]. Nevertheless, no matter how different one formalism is from another, the aims are generally the same (i.e., the system-level understanding of biological systems) and can be achieved through understanding the following: [Kitano 2002a,b]

- system structure, such as gene regulatory and biochemical networks as well as physical structures;
- system dynamics, through both quantitative and qualitative analysis, as well as construction of a theory/model with powerful predictive capability;
- control methods of the system; and
- design methods of the system.

Different frameworks may be used for different problems, but the workflows in systems biology are generally the same. For this thesis, I used the systems biology workflow shown in Figure 1.2 to understand the influence of sorting receptor-related protein (SORLA), a neuronal sorting receptor, on amyloidogenic processing in AD. **Step one** of the workflow is to survey the literature for related works on: (1) the details of the biological system, (2) existing models of the system and its biological processes, and (3) experimentally measured kinetic parameters of the system. One may dig as deeply as needed and look as far as necessary. The availability of free, online-access databases and journals make collecting this information convenient. The challenge is to identify which information is useful to the study. It is important to carefully consider the purpose of a mathematical model before considering specific mathematical formulations and computational techniques. Next, in **step two** of the workflow, a topological representation of the biological system is constructed. This representation summarizes the hypotheses generated from the literature survey.

When the goals and purposes of the model have been defined, several questions must be answered. Are the data sufficient to construct a model? Can the model be implemented

1.1. A systems biology approach to study Alzheimer's disease

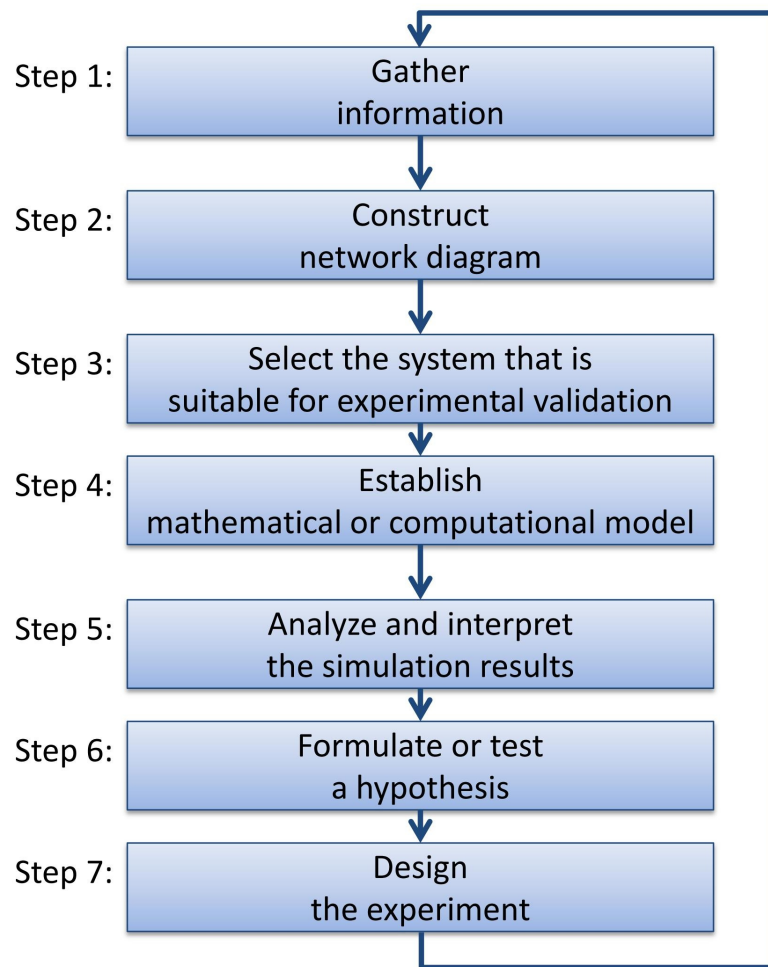


Figure 1.2.: Systems biology workflow. Different analytical frameworks may be applied, but the workflows in systems biology are generally similar.

1. Introduction

and validated? **Step three** of the workflow, is to determine how comprehensive the data are and how they can be applied to the model [Voit et al. 2008]; the type, quality, and quantity of the data, along with the goals and purposes of the study, determine to some extent the type of mathematical representation selected in **step four**. For example, the model can either be static or dynamic, deterministic or stochastic. In particular, a static model is chosen if the system does not change appreciably over a short period of time; otherwise, a dynamic model is chosen. In addition, if the task is to determine how far external random fluctuations could potentially cause the system to deviate from its normal value, the best approach may be to design a stochastic model and evaluate its properties statistically or with simulations. In contrast, if modeling the average behavior or trends of the system is sufficient, a deterministic model might be preferable because it requires considerably less technical effort.

After decisions have been made about the mathematical structure of the model and the variables and processes that will be included, the model is implemented in **step five** of the workflow. Using model parameter estimation, a set of parameters are computed by minimizing the discrepancies between the experimentally measured data and the model output. If the behaviors of the model are inconsistent with the experimental data, changes are made to the model structure or the parameter values. Every model is a compromise among reality, validity, and mathematical tractability, so it is necessary to accept a certain level of inconsistency between the model and reality [Voit et al. 2008]. Moreover, the most typical task in this step of the workflow is the analysis of what-if scenarios. Usually, these types of questions are not addressed experimentally and are best answered with computer simulations that mimic actual experiments. One example is to ask how a particular stimulus leads to an observed response. Another example is to ask how a system could be manipulated for some desired goal or even how it could be optimized [Voit et al. 2008].

In **step six** of the workflow, existing hypotheses are validated or rejected and new hypotheses may be formulated. In **step seven** of the workflow, one determines if new experiments are necessary. If additional experiments are necessary, the mathematical model is often used as a guide to help design them. The workflow is applied repeatedly until the goal of the study is reached.

In each step of the workflow, there are two important components that should be considered [Voit et al. 2008]. One is the “conceptual component” that requires insight into the biological phenomenon under investigation, modeling experience, and common sense. The other is the “technical component” that requires sufficient mastery of mathematical methods to judge what is mathematically feasible, familiarity with computational tech-

niques, and awareness of specialized and/or general-purpose software packages.

In this thesis, a systems biology approach is used to better understand AD. To elucidate the causes and consequences of certain biological processes in AD, mathematical computational models are built. These models do not replicate the physical reality of molecules interacting in space and time, but rather provide an abstract representation of observable principles [Wolkenhauer et al. 2004]; hence, these models are not a substitute for careful empirical observations, but instead are tools to assess hypotheses about the dynamic properties of a system and the mechanisms underlying experimental observations [Wolkenhauer 2007]. The success of this approach relies on close, interdisciplinary interaction between the experimentalist and the theoretician. It is vitally important to address biologically relevant questions and ensure that the models reflect an appreciation for the experimental data [Wolkenhauer et al. 2004]. Ultimately, the goal of systems biology is to discover emergent properties through modeling. In addition, modeling the properties of a system whose theoretical description is difficult can be made more plausible through systems biology approaches [Snoep and Westerhoff 2005].

1.2. State of the art

Most work on the cellular and pathological events underlying the neurodegenerative process in AD is based on the amyloid hypothesis. This hypothesis is also the basis for this thesis, which will focus mainly on a drug candidate called SORLA. In this section, I will discuss the amyloid hypothesis and why it remains popular despite the appearance of several alternatives. I will then introduce SORLA and describe its role in the amyloid hypothesis in detail. I will also briefly review some mathematical models that were built to study amyloidogenic processing.

1.2.1. Amyloid - a hypothesized cause

According to the amyloid hypothesis, $A\beta$ accumulation in the brain is the primary cause of AD; the rest of the disease process, including the formation of neurofibrillary tangles containing the tau protein, is simply a consequence of an imbalance between $A\beta$ production and $A\beta$ clearance [Hardy and Selkoe 2002]. Central to the amyloid hypothesis is the APP, a type-1 membrane protein expressed in many neuronal and non-neuronal cell types [Haass and Selkoe 2007]. The idea is that the onset and progression of the disease are determined by the breakdown of APP to $A\beta$. This idea is supported by the observations that defects in the genes encoding APP are associated with familial forms of the disease,

1. Introduction

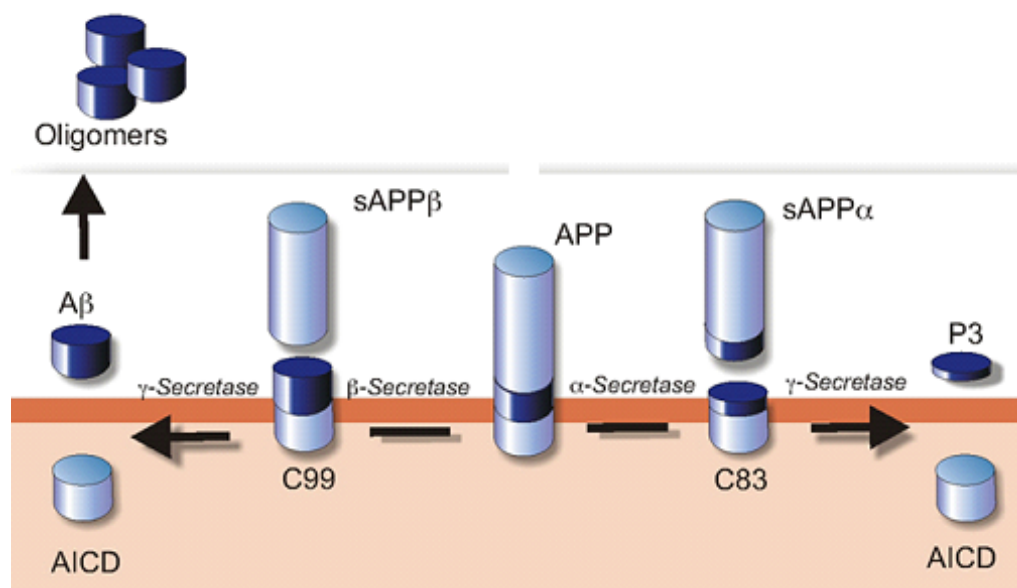


Figure 1.3.: Schematic of APP processing. APP can be cleaved by either α -secretase or β -secretase, but not both at the same time. APP cleaved by α -secretase produces a sAPP α peptide and a C83 peptide. APP cleaved by β -secretase produces a sAPP β peptide and a C99 peptide. Subsequently, γ -secretase either cleaves C83 into peptide P3 and APP intracellular domain (AICD), following α -secretase cleavage, or cleaves C99 into A β plaque and AICD, following β -secretase cleavage. The illustration is adapted from Andersen and Willnow 2006.

and that an extra copy of the APP gene, found in patients with trisomy 21 (Down's syndrome), is invariably associated with the occurrence of early onset AD [Selkoe 1991].

A schematic representation of APP processing is shown in Figure 1.3. In cells, including neurons in the brain, APP is processed via two mutually exclusive pathways, resulting in the formation of different soluble and membrane-associated fragments. Of particular relevance to AD is the amyloidogenic pathway, whereby APP is first cleaved by beta-secretase (β -secretase), producing a soluble APP-beta (sAPP β) peptide and a C99 peptide (the 99-amino acid C-terminal fragment). The C99 peptide is further cleaved by gamma-secretase (γ -secretase), producing AICD and amyloid- β peptide (A β). A β is a 40- to 42-amino acid fragment derived from the extracellular and transmembrane domains of APP. According to the amyloid hypothesis, neurotoxic oligomers and senile plaques formed by A β cause neuronal dysfunction and cell loss in AD [Hardy and Selkoe 2002; Hung et al. 2008]. In the alternative pathway, APP is first cleaved by α -secretase, instead of β -secretase, producing a soluble APP-alpha (sAPP α) peptide and a C83 peptide (the 83-amino acid C-terminal fragment). A subsequent cleavage of APP by α - and γ - secretases produces AICD and P3 (a 3-kDa fragment composed of residues 17-40 or 17-42 of the amyloid beta peptide). This non-amyloidogenic pathway leads to the destruction of the A β peptide [Andersen et al. 2005; Andersen and Willnow 2006].

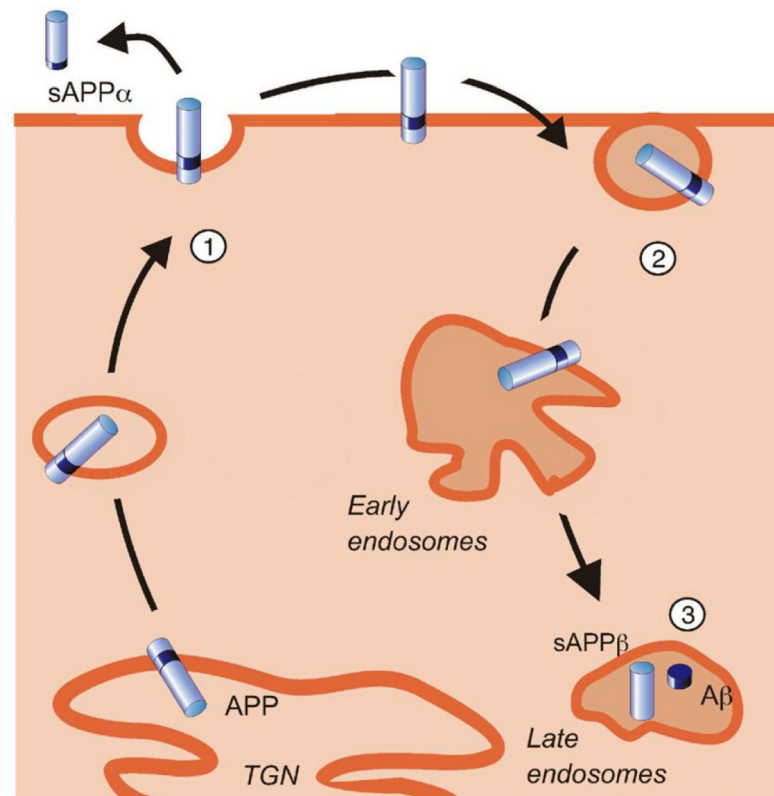


Figure 1.4.: Intraneuronal transport and processing of APP. Newly synthesized APP molecules traverse the trans-Golgi network (TGN) en route to the plasma membrane, where most are cleaved by α -secretase to sAPP α (step 1). Non-processed molecules internalize from the cell surface (step 2) and move from early to late endosomes for processing into sAPP β , initializing the amyloidogenic pathway (step 3). For simplicity, A β formation is indicated in late endosome (step 3). The illustration is adapted from Willnow et al. 2010.

The processing fate of APP is determined by its complex transport through the intracellular compartments of neurons [Willnow et al. 2010]. As shown in Figure 1.4, most APP molecules proceed through the non-amyloidogenic pathway, which occurs at or near the plasma membrane. Some molecules, however, are re-internalized from the cell surface and delivered to late endosomes, where the amyloidogenic pathway takes place. The importance of regulated intracellular APP transport to A β production is underscored by findings that faulty APP transport contributes to AD.

Although APP processing is critical in the development of AD, understanding of the underlying regulatory mechanisms is incomplete. Professor John Hardy [2009], one of the originators of the amyloid hypothesis [Selkoe 1991; Hardy and Allsop 1991; Hardy and Higgins 1992; Hardy and Selkoe 2002], thinks that the main reason for this lack of

1. Introduction

knowledge is incorrect focus. And Willnow et al. [2010] state that the focus should be on identifying neuronal factors that control APP metabolism and determining whether alterations among these factors contribute to the common sporadic forms of the disease that afflict 90% of all patients.

1.2.2. SORLA - a drug candidate

In recent years, much attention was focused on the analysis of factors that influence APP processing and thus may contribute to the elevated $A\beta$ levels seen in patients with AD [Hardy 2009]. One such factor is the SORTilin-related receptor that is L(DLR) class containing A-type repeats (SORLA). It is the neuronal sorting receptor for APP (also known as SORL1 or LR11). It is a 250-kDa type-1 membrane glycoprotein that is widely expressed in neurons in the brain [Jacobsen et al. 1996; Yamazaki et al. 1996].

SORLA is a member of a family of mammalian proteins that are structurally similar to the vacuolar protein sorting 10 protein (VPS10p): a yeast sorting receptor that transports carboxypeptidase Y from the TGN to the vacuole [Marcusson et al. 1994]. Aside from SORLA, the other four VPS10p domain receptors found in humans are sortilin, SORCS-1, SORCS-2, and SORCS-3 (Figure 1.5). These receptors are mainly found in defined populations of cells in the central and peripheral nervous system, and are considered potential neuronal disease factors [Willnow et al. 2008]. In particular, SORLA and SORCS-1 are associated with AD and other age-related dementias. SORCS-2 and sortilin are associated with bipolar disorders and senescence of the nervous system, respectively. The functional relevance of the VPS10p domain receptors was confirmed by Jansen et al. [2007]; they showed that sortilin is a neurotrophin receptor that controls neuronal cell death.

In adult human brain tissue, SORLA expression is strongest in the cerebral and entorhinal cortexes, the hippocampus, the cerebellum, and the brain stem [Offe et al. 2006]. At the subcellular level in primary neurons and established cell lines, SORLA mainly localizes in the intracellular vesicles of the perinuclear region [Andersen et al. 2005], known as the TGN, and in early endosomes [Offe et al. 2006; Spoelgen et al. 2006; Schmidt et al. 2007].

The involvement of SORLA in AD was initially suggested by Scherzer et al. [2004], who used gene expression profiling to demonstrate low levels of SORLA transcript in lymphoblasts from patients with sporadic AD. The reduced SORLA mRNA and protein levels in AD patients suggest that variation in expression levels of SORLA may be under genetic control. Nevertheless, a correlation between distinct SORLA genotypes and protein levels awaits unambiguous documentation [Willnow et al. 2010].

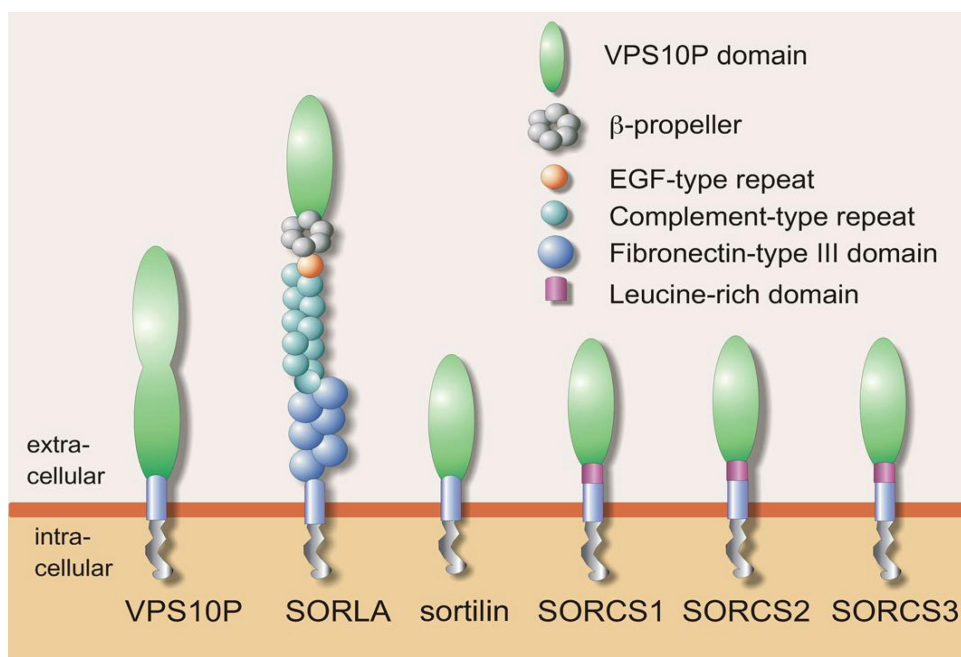


Figure 1.5.: Structure and evolutionary conservation of VPS10P domain receptors.

The structural organizations of VPS10P domain receptors from yeast (VPS10P) and humans (SORLA, sortilin, SORCS-1, -2, -3) are shown. The receptors may carry additional modules involved in protein-protein interaction (leucine-rich domains, complement-type repeats, epidermal growth factor-type repeats, and fibronectin-type III domains) or regulation of ligand binding (β -propeller). The illustration is adapted from Willnow et al. 2008.

1. Introduction

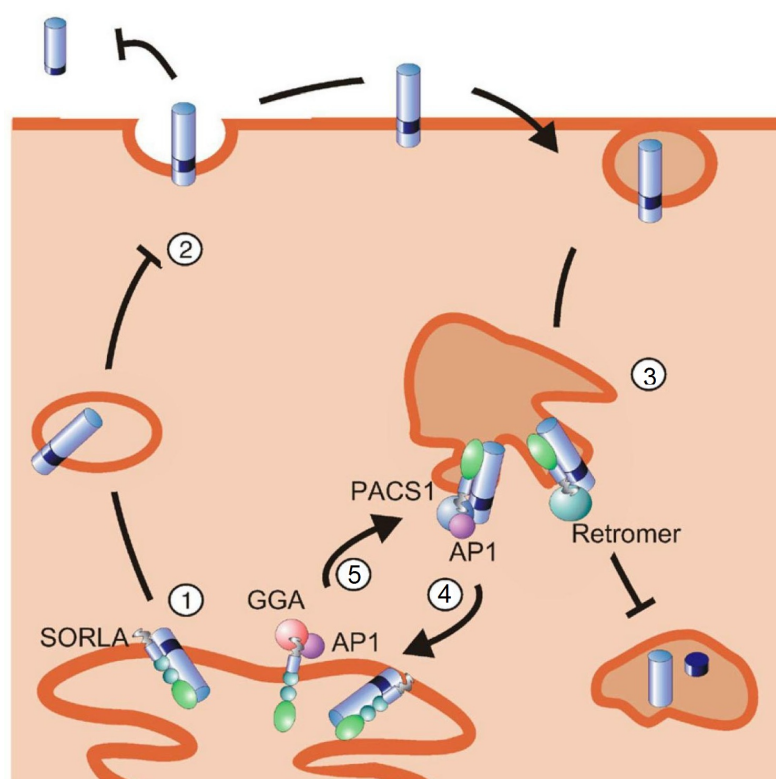


Figure 1.6.: SORLA guides the transport and processing of APP. SORLA acts as a sorting receptor that traps APP in the TGN (step 1), reducing the number of precursor molecules that enter processing pathways at the cell surface (step 2, non-amyloidogenic) or in endocytic compartments (step 3, amyloidogenic). SORLA may also shuttle APP from early endosomes back to the TGN (step 4), further reducing the extent of amyloidogenic processing in late endosomes. Retrograde endosome-to-TGN transport of SORLA-APP complexes may involve association with the retromer complex. Direct sorting of SORLA from the TGN to early endosomes requires golgi-associated, gamma adaptin ear containing, ARF binding proteins (GGAs; step 5). This illustration is adapted from Willnow et al. 2010.

It was Andersen et al. [2005] who first proposed that SORLA acts as a retention factor for APP in AD, preventing the release of precursor molecules into the processing pathways (Figure 1.6). They suggested that SORLA forms a 1:1 stoichiometric complex with the carbohydrate-linked domain of APP [Andersen et al. 2006]. Thus, the over-expression of SORLA in neurons prevents the transport of APP from the TGN to the cell surface and endosomes, effectively reducing the extent of APP cleavage via amyloidogenic and non-amyloidogenic pathways [Andersen et al. 2005; Offe et al. 2006; Schmidt et al. 2007].

The following studies illustrate the roles that SORLA plays in amyloidogenic processing and controlling plaque deposition (reviewed in [Willnow et al. 2010]).

- Andersen et al. [2005] and Rohe et al. [2008] showed in two different mouse models

that the loss of SORLA activity enhances APP and, significantly increases amyloidogenic (sAPP β , A β) and non-amyloidogenic (sAPP α) products in the brain.

- Dodson et al. [2008] and Rohe et al. [2008] showed that introducing the murine SORL1 defect into mice expressing the human APP transgene variants App^{V717F} (Ind) or App^{K595MN596L} (Swe) caused a twofold to threefold increase in A β formation and plaque load.
- Spoelgen et al. [2006] suggested that under high β -secretase levels, SORLA may inhibit APP production. It is possible that SORLA interacts with beta-secretase by coimmunoprecipitation, predominantly in the Golgi, where immature β -secretase resides. APP and β -secretase might compete for SORLA binding within the TGN. SORLA reduces β -secretase activity on APP without affecting the subcellular distribution of either APP or β -secretase.

These initial observations demonstrated a negative correlation between SORLA activity and the conversion of APP to A β , providing a working hypothesis to explain why low levels of SORLA in some individuals may predispose them to enhanced APP turnover and sporadic AD [Andersen and Willnow 2006; Willnow et al. 2010]. This hypothesis is strengthened by the observations of Scherzer et al. [2004], Rogaeva et al. [2007], and Dodson et al. [2008] that patients suffering from AD have low levels of SORLA expression. The importance of SORLA transport in AD is further supported by the studies described below.

Substantial experimental evidence from histopathology and cell biology studies suggest a model in which SORLA acts as a sorting receptor for APP in the TGN (Figure 1.6). SORLA prevents the transport of APP into the intracellular pathways required for processing, and thereby acts as negative regulator of A β production [Haass et al. 1993; Xu et al. 1995; Schmidt et al. 2007]. Schmidt et al. [2007] shed some light on the biology of SORLA through a variety of tests of SORLA's ability to alter APP localization and processing. They found that overexpression of mutated SORLA that is sequestered at the cell surface led to a reduction in A β 40 production and an increase in sAPP α production, thus altering the processing fate of APP from amyloidogenic to non-amyloidogenic. Because SORLA interacts with motifs in both the extracellular [Andersen et al. 2006] and the intracellular domains of APP [Spoelgen et al. 2006], it is tempting to speculate that SORLA may not only sort non-processed APP but also its soluble (sAPP) or membrane-associated (C99 or C83) fragments [Willnow et al. 2010].

Andersen et al. [2005] showed that the uptake of APP is not dependent on SORLA because the loss of SORLA expression has no obvious effect on overall APP levels. There are,

1. Introduction

however, obvious increases in $A\beta$ levels and sAPP α production; but the authors claimed that SORLA mainly affects the transport and processing rather than the synthesis of APP.

Several cytosolic adaptor proteins that control the transport of SORLA between early endosomes and the TGN have been implicated in AD [Andersen et al. 2005]. SORLA can catch APP in the early endosomal compartment and transport it back to the Golgi compartment. This event prevents the transport of APP to the late endosomal compartments that harbor β -secretase activity. The adaptor proteins are named GGA1, GGA2, and GGA3 (**G**olgi-localizing, **G**amma-adaptin ear-containing, **A**RF-interacting proteins) [Jacobsen et al. 2002]. The evidence showing the relation of the GGAs to AD is as follows:

- von Arnim et al. [2006] showed that the overexpression of GGA-1 can decrease $A\beta$ production.
- Wahle et al. [2006] suggested that there is no direct interaction between APP and the GGAs, and that SORLA may be required to tether both components.
- Wahle et al. [2006] and Tesco et al. [2007] observed decreased levels of GGA1 and GGA3 in brain samples from patients who died after suffering from AD.

The GGAs and phosphofurin acidic cluster sorting protein-1 (PACS-1) are adaptor proteins involved in transporting molecular cargo to and from the TGN. To determine the importance of these proteins to SORLA activity, Schmidt et al. [2007] made SORLA mutants with abolished GGA binding, PACS-1 binding, or both. They found that although all the mutant SORLA variants could still bind APP, none of them were capable of retaining its mature form in the Golgi. This confirmed that wild-type SORLA has the unique ability to accumulate mature APP molecules in the Golgi, most likely by extending the transit time.

Despite the fact that SORLA is considered one of the most important risk factors for sporadic AD [Andersen et al. 2005], there is no systematic modeling approach that examines the network cross-talks involving SORLA and the corresponding pathological consequences. This thesis will provide the first evaluation through mathematical modeling of the dynamic network cross-talks among SORLA and the distinct competitive APP-binding processes of the α - and β - secretases.

1.2.3. Alternatives to the amyloid hypothesis?

Regardless of widespread and vocal dissatisfaction with the amyloid hypothesis, there have been very few attempts to formulate alternative hypotheses. One such hypothesis is that

apolipoprotein E plays a role in the development and course of AD [Strittmatter et al. 1993; Corder et al. 1993; Saunders et al. 1993]. Others suggest that environmental or lifestyle factors are the key, and try to associate cognitive decline with vascular and metabolic conditions like heart disease [Ciobica et al. 2011; den Heijer et al. 2012], stroke [Cumming and Brodtmann 2011], high blood pressure [Wysocki et al. 2012], diabetes [Strachan et al. 2008; Cukierman-Yaffe et al. 2009], etc. Below, I discuss the pros and cons of two alternative molecular hypotheses that have rivaled the amyloid hypothesis in popularity: the presenilin inhibition hypothesis [Sambamurti et al. 2006; Shen and Kelleher 3rd 2007] and the dual pathway hypothesis [Small and Duff 2008].

The presenilin inhibition hypothesis, proposed by Sambamurti et al. [2006] and Shen and Kelleher 3rd [2007], suggests that the age-related loss of essential presenilin function leads to progressive neurodegeneration characterized by the loss of synapses, dendrites, and neurons; astrogliosis; and tau hyperphosphorylation. The authors hypothesized that pathogenic mutations in presenilin partially impair γ -secretase-dependent and -independent activities (e.g., the elevation of $A\beta_{42}$ levels). They proposed that γ -secretase inhibitors would aggravate instead of ameliorate neurodegeneration and dementia, and that boosting presenilin-dependent pathways or inhibiting opposing pathways would offer the most promising therapeutic strategies for AD. This hypothesis generated much excitement initially; however, their study did not bear out its most straightforward prediction: that presenilin-mutant mice would show tau-related neurodegeneration. Support for the presenilin inhibition hypothesis is further weakened by the studies conducted by Vidal et al. [1999] and Pickering-Brown et al. [2006]. In particular, Pickering-Brown et al. [2006] shed doubt on the result reported by Shen and Kelleher 3rd [2007]: that some presenilin mutations may lead directly to tangle disease in humans.

The dual pathway hypothesis proposed by Small and Duff [2008] links the elevation of $A\beta$ peptide levels and the hyperphosphorylation of the tau protein in AD. The hypothesis states that elevated levels of $A\beta$ and tau hyperphosphorylation can be linked by separate mechanisms driven by a common upstream molecular defect. The authors emphasized, however, that their hypothesis is offered only as an additional model of causality, and not as a replacement of the amyloid hypothesis. There is currently no evidence that supports the dual pathway hypothesis by showing a relationship between APP or $A\beta$ and tau.

Although these alternative hypotheses are appealing in some ways, there is little evidence to support them, making both unconvincing as replacements for the amyloid hypothesis. For this reason, the amyloid hypothesis is still considered the most plausible hypothesis on which to base research into therapies for AD.

1. Introduction

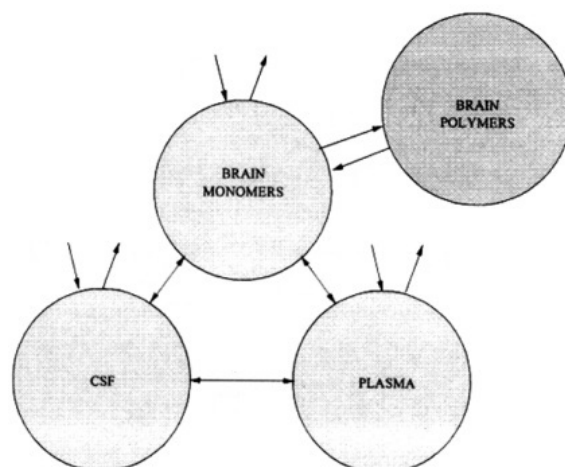


Figure 1.7.: Schematic of the amyloidogenic processing model proposed by Craft et al. [2002]. This is a three-compartment model where $A\beta$ is transported between the brain, CSF, and plasma. The illustration is adapted from Craft et al. 2002.

1.2.4. Previous modeling efforts

In spite of extensive research into the neurodegenerative pathology of AD, it remains poorly understood, mainly due to the complexity of the intercellular cross-talks that take place throughout the pathogenic processes. This situation motivated several studies to use mathematical or computational modeling as a tool to better understand the molecular and cellular processes underlying this complex disease. Such an approach may help identify critical underlying causes of AD and contribute to the development of new treatments. Indeed, there have been several attempts to model amyloidogenic processing [Craft et al. 2002; Das et al. 2011; Puri and Li 2010]. As reported by Craft et al. [2002], there are several mathematical models that focus on either fibrillogenesis [Harper et al. 1999; Inouye and Kirschner 2000; Walsh and Selkoe 2007] or plaque formation [Hyman et al. 1995; Cruz et al. 1997; Urbanc et al. 1999] in the brains of patients with AD. In particular, Naiki et al. [1991, 1996, 1998] and Lomakin et al. [1996, 1997] are the first few to perform kinetic analysis of fibrillogenesis in AD. Below, I briefly review some studies in which mathematical models of the amyloidogenic hypothesis were built. The emphasis of the review is on understanding how the models were established and simplified.

Craft et al. [2002] formulated and analyzed a three-compartment model, where $A\beta$ is transported between the brain, cerebrospinal fluid (CSF), and plasma (see Figure 1.7). They claimed that their paper represented the first attempt to use a mathematical model to assess the effect of AD treatment on $A\beta$ levels in various compartments of the body. They provided simple formulae for the steady-state $A\beta$ levels in the brain, CSF, and

plasma both before and after treatment. They established and simplified the mathematical representation of their model based on some biologically reasonable assumptions. In particular, Craft et al. [2002] made the following assumptions and restrictions:

- Extracellular $A\beta$ is likely to be in a dynamic equilibrium with intracellular $A\beta$.
- The focus is on $A\beta$ polymerization, and the downstream process of plaque formation is ignored. This is because they were primarily interested on the total $A\beta$ burden in the three compartments.
- There is homogeneous mixing within the CSF and plasma compartments. Based on information gathered from the literature, diffusion through the extracellular spaces in the brain is assumed to be much faster than transport across the bloodbrain barrier.
- $A\beta$ appears in the CSF and plasma only as monomers. This assumption is based on the observation that very few oligomers have been found in the CSF or plasma.
- All transport rates are first-order, rather than obeying Michaelis-Menten kinetics; the rate from compartment i to compartment j is denoted by r_{ij} for $i, j = b, c$ or p . The reason for this simplification is that it eases the parameter estimation task.
- Linear (i.e., unsaturated) binding occurs (i.e., free and total A are in direct proportion) and there is a linear relationship between the total $A\beta$ and its clearance rate from the plasma.

Craft et al. [2002] emphasized that although the polymerization and depolymerization processes that they employed are specialized to AD and are less general than many in the literature, the main novelty of their model is the incorporation of multiple compartments with sources (production) and sinks (loss).

Next, Puri and Li [2010] proposed a mechanism for AD involving 16 pathways (Figure 1.8). The mechanism is based on an assumption of constant risk of neuronal death; in other words, a single event randomly initiates cell death independently of the state of any other neuron at any instant. The spatiotemporal influence of diffusion is neglected because local cellular events are assumed to occur on a slower timescale than signal dispersion through chemotaxis. They used an ODE-based model to represent the cell populations and the number of $A\beta$ molecules in an arbitrary local volume. By monitoring neuronal health, they were able to identify intuitive strategies for interventions. They admitted that their mathematical analysis is an initial attempt and may not fully account for the associated intertwined cellular communication pathways. Nevertheless, their model helps

1. Introduction

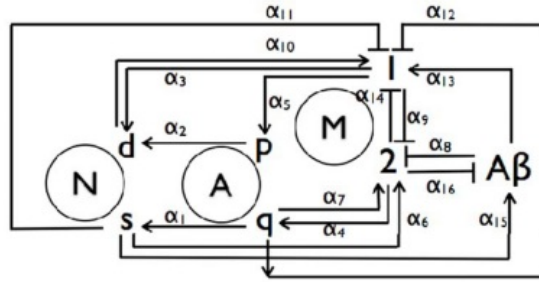


Figure 1.8.: Schematic of amyloidogenic processing proposed by Puri and Li [2010]. This model incorporates feedback from surviving and dead neurons (N_s and N_d), quiescent and proliferating astroglia (A_q and A_p), reactive and normal microglia (M_1 and M_2), and $A\beta$. The illustration is adapted from Puri and Li 2010.

to generate new hypotheses and encourages integrated analyses of pathogenesis.

In the study conducted by Das et al. [2011], the authors examined the temporal dynamics of soluble (un-aggregated) $A\beta$ in the plasma and CSF of rhesus monkeys treated with different oral doses of a γ -secretase inhibitor. They integrated experimental observations with a physiological model of the distribution of γ -secretase inhibitor between the plasma and CSF and the effects of that distribution on $A\beta$ concentrations in the two compartments. The formulation of their model was guided by their observations and their objective to determine the minimal physiological requirements that would explain the observed $A\beta$ relaxation to baseline in the CSF with concurrent elevation and persistence in the plasma. A common approach in systems biology is to start a model with a small subsystem and then expand it. This is precisely what Das et al. [2011] did. Rather than starting from scratch, they based their mathematical model on the model of Craft et al. [2002]. The start-up model, however, was not able to reproduce all of their experimental results. The reason for this is that they were restricted by what could be measured in the laboratory at that time; it was not feasible for them to conduct further experiments that would help to improve the initial model. The only option left for them was to modify the model and assume compartmental details that mimic the dynamics of soluble $A\beta$. The two-compartment model is schematically depicted in Figure 1.9 and its corresponding ODEs are based on biologically reasonable assumptions. For example, they assumed a homeostatic steady state for $A\beta$ which allowed them to assign constant $A\beta$ production rates to the two compartments. Choosing constant production rates is a simplification that ignores certain details and therefore reduces the number of model parameters to be estimated.

Although the studies described above are all based on the amyloidogenic hypothesis, the mathematical or computational designs and approaches differ depending on the questions

1.3. Objectives and organization of this thesis

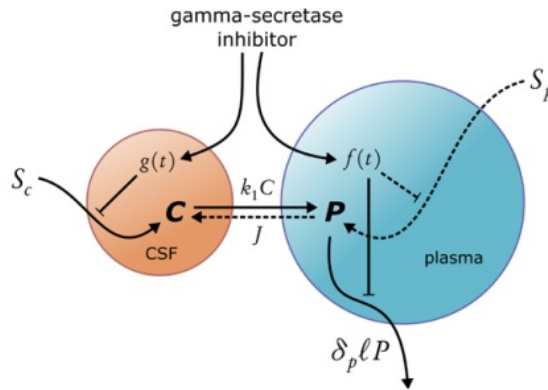


Figure 1.9.: Schematic of the amyloidogenic processing proposed by Das et al. [2011]. A two-compartment model of $A\beta$ dynamics in the presence of a γ -secretase inhibitor. Various production, transport, and clearance terms, and the proposed effects of the γ -secretase inhibitor on $A\beta$ synthesis and clearance are shown schematically. The illustration is adapted from Das et al. 2011.

being addressed, the types of data used, and the materials and methods considered. This thesis focuses more on the transport of APP rather than that of $A\beta$. Nonetheless, the studies reviewed above are starting points for the mathematical models in Chapters 3 and 4.

1.3. Objectives and organization of this thesis

This dissertation is a product of the close collaboration between the group of Prof. Olaf Wolkenhauer from the University of Rostock and Prof. Thomas E. Willnow from Max-Delbrueck-Center (MDC) for molecular medicine in Berlin-Buch. This interdisciplinary project is based on an iterative process from experiments to mathematical modeling, and vice versa. Wolkenhauer's group is composed of Dr. Katja Rateitschak, Yvonne Schmitz, and yours truly. The Rostock group were responsible for the development of mathematical models, based on the experiments conducted by the MDC group. The Berlin group also included Katharina Baum and Dr. Jana Wolf.

The goal of this thesis is to use a systems biology approach to examine APP processing and the network cross-talks among SORLA and the competitive binding of APP by α - and β -secretase to determine their relevance to AD. To achieve this goal, I generated and tested hypotheses about amyloidogenic processing and how it is affected by SORLA using biochemical reaction networks. I used a model, based on ordinary differential equations (ODEs), that describes temporal changes in network components as functions of molecular interactions and cleavage processes. Ultimately, the insights gained from these studies will enhance the understanding of SORLA's role in amyloidogenic processing in AD.

1. Introduction

I reviewed the background for this study earlier in Section 1.2. I elaborated on the importance of understanding APP and its processing fate, which is under the influence of SORLA. I also reviewed some mathematical models of amyloidogenic processing from previous studies. **Chapter 2** contains (1) a description of how the series of experimental dose-response data used in this study was obtained, and (2) a presentation of the mathematical modeling framework I used in this study. Chapter 2 is partially adapted from our publication [Schmidt et al. 2012], where all cell and molecular biology experiments were conducted by V. Schmidt and T.E. Willnow. In **Chapter 3**, I use several models, through a systems biology approach, to study and test different hypotheses about SORLA's influence on the amyloidogenic processing of *monomeric APP*, *dimeric APP*, and *both monomeric and dimeric APP*. Section 3.3 is adapted from our first publication [Schmidt et al. 2012]. Particularly, I carried out the mathematical modelling: designed and established the model, generated the model equations, programmed the MATLAB code that is used to optimize parameter values of the model, performed the simulations, and analyzed the corresponding results. Y. Schmitz supported the analysis of the simulations. K. Rateitschak supervised the work of A. Lao. V. Schmidt and K. Baum performed the analyses of enzyme kinetics under the supervision of J. Wolf. O. Wolkenhauer and T.E. Willnow conceived the research. In **Chapter 4**, I extend the single-compartmental model (presented in Section 3.3) to a multi-compartmental model by including compartment details that determine the distinct transport route of APP through the intracellular compartments where the various secretases reside. Chapter 4 is adapted from our second publication [Lao et al. 2012]. In this publication, I conceived and designed the research. I carried out all the calculations, performed all the simulations, and analyzed the results. V. Schmidt and Y. Schmitz supported my work by checking assumptions, programming codes, and results. T.E. Willnow, and O. Wolkenhauer supervised my work. In the final chapter, **Chapter 5**, I end the thesis with a general discussion of the results and future research directions.

MATERIALS AND METHODS

In this chapter, I describe the series of dose-response data published previously in *The EMBO journal* [Schmidt et al. 2012]. This data series is the basis for all the mathematical models developed in this thesis. Before developing the models, it is important to know exactly the types of experimental data used and understand the experiments in detail. This information is crucial in determining the mathematical framework to use, and vital in making sound assumptions for model reduction. In the second part of this chapter, I present the mathematical modeling framework used in this study and the tools used to establish and analyze the models in chapters 3 and 4.

2.1. Dose-response experimental design

The data generated in wet labs are of crucial importance to the modeling process; in fact, ignoring the nature of data generated in the wet lab and failing to consider the particular technologies involved usually render a model useless to biologists [Wolkenhauer et al. 2004]. In this section, I describe the Tet-off mechanism used to produce the dose-response data, and the technologies (i.e., enzyme-linked immunosorbent assay [ELISA] and Western blot) used to quantify the data.

Mechanism of the Tet-off system

Tetracycline-controlled transcriptional activator (tTA) is a method to induce expression by reversibly turning transcription on or off in the presence of an antibiotic: either tetracycline or one of its derivatives, such as doxycycline. The main advantage of this system over other gene expression systems is that it provides very tight control over gene expression, such that the activation or knock-out of the gene is reversible (Clontech Laboratories,

2. Materials and methods

Mountain View, CA, USA). The tTA system actually comprises two inducible expression systems commonly used in eukaryote cell biology: the Tet-off system and the Tet-on system. Despite what the names suggest, the Tet-on and Tet-off systems do not respectively turn genes on and off; rather they each activate expression in a different manner in response to doxycycline. Tet-on activates expression in the presence of doxycycline, whereas Tet-off activates expression in the absence of doxycycline. The group of Prof. Thomas E. Willnow tried both systems, and their results suggest that the Tet-off system is better suited for this study.

The Tet-off system was developed by Gossen and Bujard [1992] at the University of Heidelberg. Schmidt et al. [2012] applied this system to develop a cellular model with APP and SORLA expression that is tightly controlled over a wide range of molar concentrations. As shown in Figure 2.1, the transcription of the gene or genes of interest, APP and SORLA, is controlled by an upstream regulatory site composed of the modified tetracycline-response element (TRE MOD) and a minimal CMV promoter. The binding of tTA to TRE MOD leads to transcription (Figure 2.1A), whereas the presence of doxycycline releases tTA from the promoter and shuts off transcription in a dose-dependent manner (Figure 2.1B).

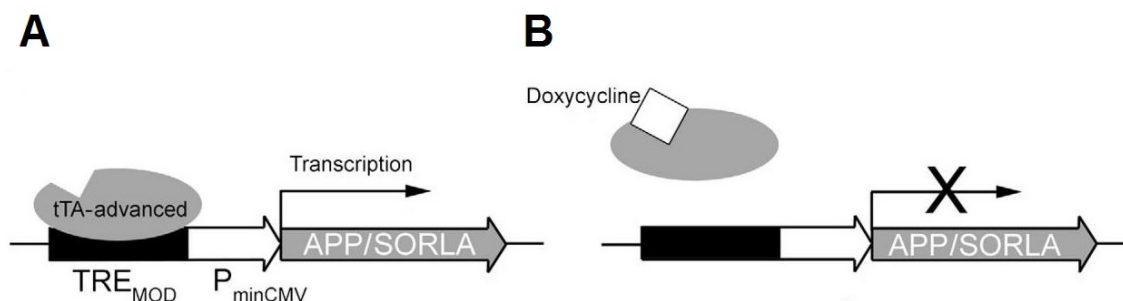


Figure 2.1.: Tet-off system to modulate cellular expression of APP and SORLA.

This is an illustration of the strategy for doxycycline-dependent repression of APP and SORLA expression using the Tet-off system. tTA is the tetracycline-controlled transactivator: without doxycycline (A) and with doxycycline (B). The image is owned by Dr. Vanessa Schmidt from Max-Delbrueck Center Buch-Berlin.

Figure 2.2 shows the general strategy for establishing the Tet-off system. First, target cells are transfected with pTet-off Advanced. Second, a stable Tet-off-Advanced cell line is identified. Third, the cell line is transfected with the customized TRE-based vector containing APP or SORLA. Finally, a stable cell line with doxycycline-induced APP or SORLA is produced.

2.1. Dose-response experimental design

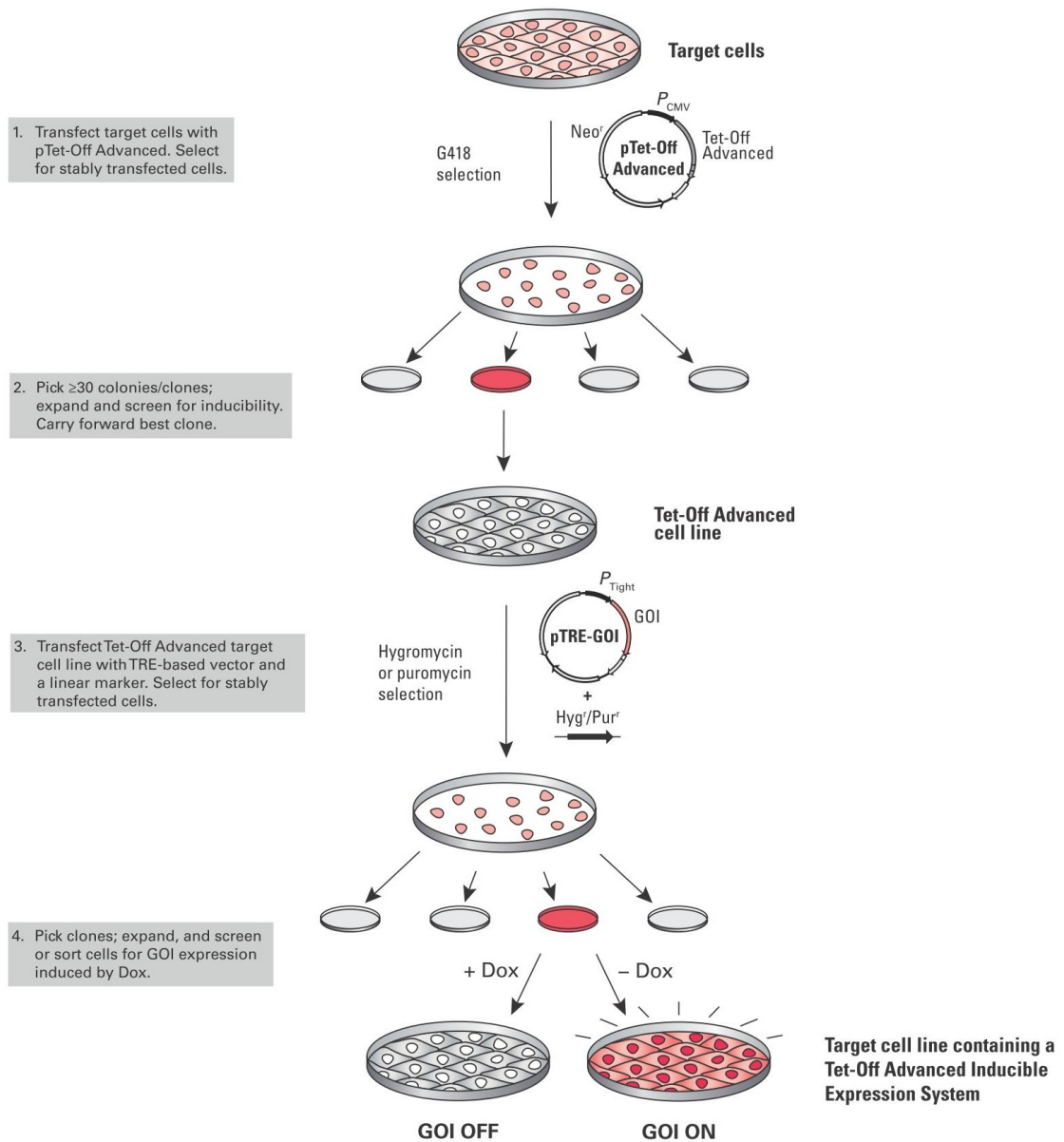


Figure 2.2.: The general strategy for establishing the Tet-off Advanced System. Target cells are first transfected with pTet-off Advanced to create a stable cell line. Once a suitable Tet-off-Advanced cell line is identified, it is transfected with a customized TRE-based vector containing the gene or genes of interest. The illustration is adapted from the user manual provided by Clontech Laboratories, Inc.

2. Materials and methods

The Tet-off system worked faithfully to vary the molar concentrations of APP and SORLA in Chinese hamster ovary (CHO) cells transfected with the expression constructs and constitutively expressing human SORLA (CHO-S) or APP 695 (CHO-A) [Schmidt et al. 2007]. Schmidt et al. [2012] generated three types of cell lines (shown in Figure 2.3), namely:

1. *CHO pTet-APP*, to control APP expression in the absence of SORLA;
2. *CHO-S pTet-APP*, to control APP expression in the presence of constant concentrations of SORLA; and
3. *CHO-A pTet-SORLA*, to control SORLA expression in the presence of constant concentrations of APP.

The application of doxycycline stably reduced the levels of APP and SORLA in cells after 24h. The cells were incubated for 48h with concentrations of doxycycline ranging from 0.025 to 10 ng/ml, thus their APP (from pTet-APP) and SORLA (from pTet-SORLA) levels were modified in a dose-dependent manner. The cells and media were harvested and subjected to ELISA and Western blot analyses. All analyses in this thesis relate to the series of dose-response data produced from the *CHO pTet-APP* and the *CHO-S pTet-APP* cell lines.

Technology for data generation

ELISA

The purpose of an ELISA is to determine if a particular protein is present in a sample, and if so, in what quantity. There are two main variations of this method: one determines how much antibody is in a sample, and one determines how much protein is bound by an antibody. In an ELISA, an unknown amount of antigen in a sample is immobilized on a solid surface and then bound by an enzyme-linked detection antibody. Detection is accomplished by adding the enzymatic substrate to produce a measurable signal. The most crucial element of the assay is a highly specific antigen-antibody interaction.

In this thesis, APP and its processing products were quantified in cell lysates and growth media using commercially available ELISA assays from Invitrogen (Darmstadt, Germany; anti-APP #KHB0051; anti-A β #KHB3482) and IBL (Suite P Minneapolis, MN, USA; anti-sAPP #27734; anti-sAPP β #27732). The ELISAs for sAPP β and A β are specific for their respective processing products, whereas, the ELISAs for APP in cell lysates and sAPP in growth media potentially cross-react. A control experiment confirmed that the immunoreactivity, measured by anti-APP and sAPP ELISAs, of cell extracts exclusively

2.1. Dose-response experimental design

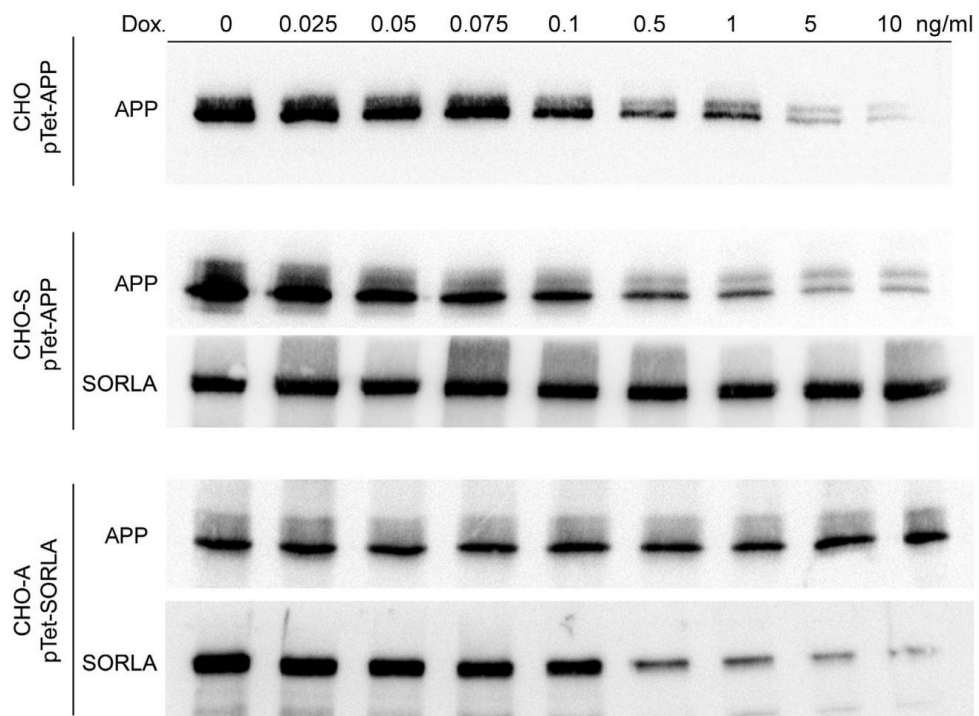


Figure 2.3.: CHO cell models with doxycycline-regulated expression of SORLA and APP. Parental CHO cells or CHO cells constitutively expressing human SORLA (CHO-S) or APP₆₉₅ (CHO-A) were stably transfected with Tet-off constructs for APP (pTet-APP) or SORLA (pTet-SORLA). Protein expression was detected in lysates from cells treated with the indicated concentrations of doxycycline for 48h. This illustration is adapted from Schmidt et al. 2012.

2. Materials and methods

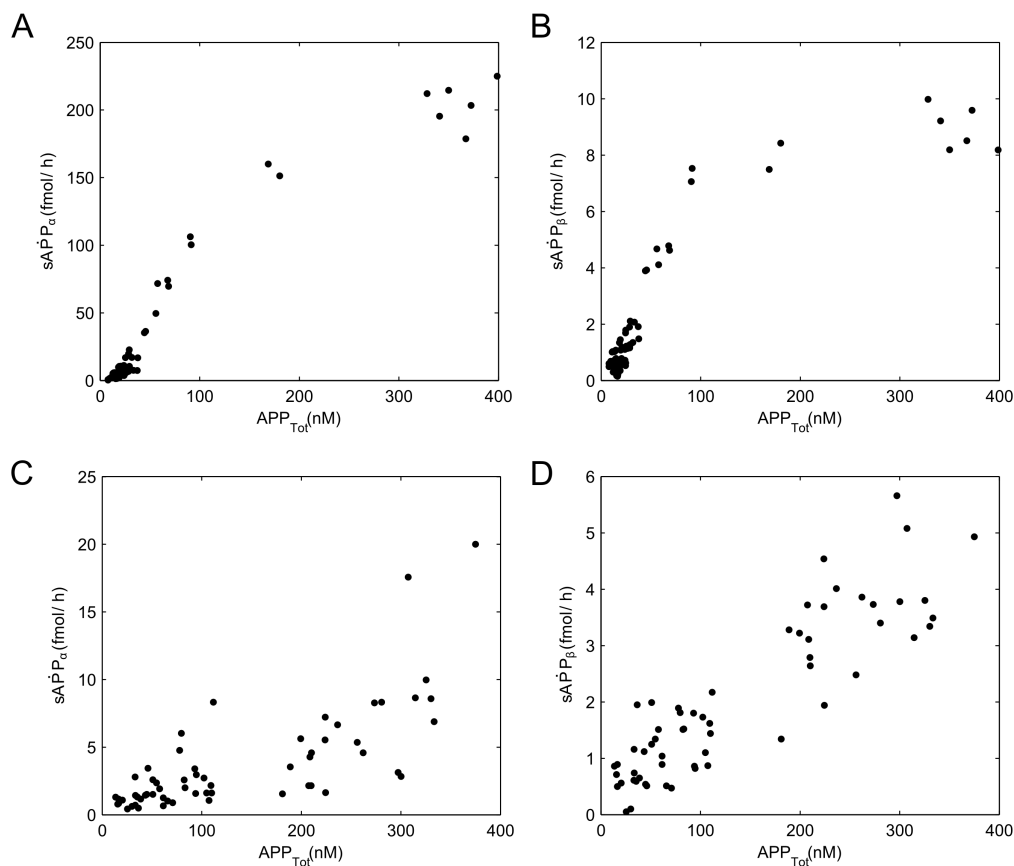


Figure 2.4.: Soluble APP production in the presence or absence of SORLA. CHO pTet-APP (w/o SORLA) (**A, B**) and CHO-S pTet-APP (w/ SORLA) (**C, D**) cells were treated for 48h with concentrations of doxycycline ranging from 0.025 to 10 ng/ml. Concentrations of APP in cell lysates and total amounts of sAPP α (**A, C**) and sAPP β (**B, D**) secreted into the medium within 24h were determined by ELISA. The data are taken from Schmidt et al. 2012.

represented the anticipated peptides. For determination of sAPP α , sAPP β , and A β , media were loaded onto ELISA plates (Meso Scale Discovery; sAPP α /sAPP β Duplex ELISA Cat.#K15120E; A β Single Plex ELISA Cat.#K150FTE) and analyzed according to manufacturers protocols. When the enzyme reaction was complete, the entire plate was placed into a plate reader and the optical density (i.e., the amount of colored product) was determined for each well (Figure 2.4). The amount of color produced is proportional to the amount of primary antibody bound to the proteins on the bottom of the wells.

Western blot

For a clear-cut demonstration of the data used in this thesis, Western blot analysis was performed in addition to ELISA. Western blot is a common way to detect a specific protein or group of proteins in a biological sample. The relative amounts of protein are detected with specific primary antibodies that are separated from one another according

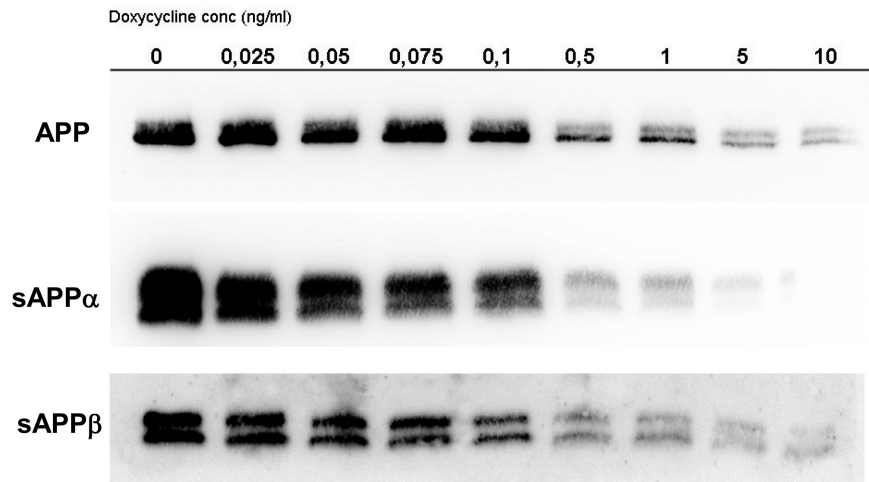


Figure 2.5.: Regulated expression of APP. Western blots showing decreasing concentrations of APP and APP processing products with increasing doxycycline concentrations. Prof. Thomas E. Willnow's group, from Max-Delbrueck Center Buch-Berlin, owns the copyright of the images that are unpublished.

to their size by gel electrophoresis. Smaller proteins migrate through the gel faster than larger proteins. In relation to the dose-response data used in this thesis, anti-serum APP, monoclonal anti-sAPP α , and polyclonal anti-sAPP β are the protein-specific antibodies that were applied to APP, sAPP α , and sAPP β , respectively. Concentrations of APP and SORLA in CHO cell lysates were determined by standard sodium dodecyl sulfate polyacrylamide gel electrophoresis and densitometric scanning of replicate Western blots. Figure 2.5 demonstrates the regulated expression of APP and APP products across a doxycycline concentration range of 0.025 ng/ml to 10 ng/ml.

2.2. Modeling framework

There are many formalisms available for the modeling and/or simulation of biochemical networks, including formal languages, stochastic models, and differential equations. The choice of a suitable framework is guided by more than simply choosing which formalism would provide the most realistic representation of the system. Some assumptions must be made to simplify the large numbers of variables and nonlinear relationships [Wolkenhauer et al. 2005].

2.2.1. Construction of the model

The processing of APP, and the influence of SORLA thereon, have been modeled by ODEs describing the temporal changes in the numbers of molecular network components

2. Materials and methods

as a function of the interaction and cleavage processes. With large numbers of molecules, changes are assumed to be smooth. All of the reversible interactions are split into two irreversible steps. Furthermore, based on the context of the specific experiments carried out, we made the following assumptions to simplify the mathematical equations:

1. APP is in great excess relative to any of the secretases (i.e., $APP \gg \alpha, \beta$) [Schmidt et al. 2007]. The formation of the protein complexes remains approximately constant until APP is nearly exhausted. Hence, a quasi-steady state can be assumed for the $APP - \alpha$ and $APP - \beta$ complexes.
2. The reversible binding between SORLA and APP is rapid. This allows a rapid-equilibrium assumption for $C_{APPSORLA}$.
3. The experimental measurements start when APP reaches steady state at 24 hours time point. Hence, it is reasonable to assume a conservation law for APP.
4. The law of conservation also applies to SORLA, because a constant amount of SORLA was used in the dose-response data series [Schmidt et al. 2012].
5. Without losing generality, the law of conservation is applied to α -secretase and β -secretase.
6. Unlike APP, the productions of $sAPP\alpha$ and $sAPP\beta$ grow over time. The measurements of these proteins were performed 24h after medium exchange; whereas, at the initial time point ($t = 0$), the concentrations of $sAPP\alpha$ and $sAPP\beta$ were zero.

Every model developed in this project uses assumptions similar to those elaborated above. This enables us to simplify the corresponding mathematical equations. The algebraic equations, crucial to this study, include the $APP_{Tot}(APP)$ function and the ODEs that describe the formation of the end products: $sAPP\alpha_{Tot}$ and $sAPP\beta_{Tot}$. This is because these equations correspond to the APP-dose and sAPP-responses measured in the experiments.

2.2.2. Parameter value estimation

We strategically estimated sets of parameter values by nonlinear optimization (Figure 2.6). This method allows the output trajectories of the model to be close to the dose-response series with and without SORLA ($N = 66$ total experimental data points in each series), by finding a set of parameter values that minimizes the weighted least squares function of $sAPP\alpha$ and $sAPP\beta$, where $r = \{1, 2, 3, 4, 5\}$ corresponds to the model number. The

experimental values of $sAPP\alpha$ and $sAPP\beta$ have different orders of magnitude. To avoid bias in the influence of each data set, it is essential to assign weights defined as:

$$w_a = \frac{\sum_{k=1}^N sAPP\alpha_k^E}{N}, w_b = \frac{\sum_{k=1}^N sAPP\beta_k^E}{N}, w_{aS} = \frac{\sum_{k=1}^N sAPP\alpha_{S,k}^E}{N}, w_{bS} = \frac{\sum_{k=1}^N sAPP\beta_{S,k}^E}{N},$$

where the superscript ‘ E ’ indicates an experimentally measured value and the subscript ‘ S ’ if it is measured in the presence of SORLA. The goodness of fit was quantified by calculating the residual value (i.e., the sum of the squared differences between the data and the model outputs divided by the respective weights) [Schittkowski 2002]:

$$residual = \min \sum_{k=1}^N \left[\frac{\left(sAPP\alpha_k^E - sAPP\alpha_{Tot,k} \right)^2}{w_a} + \frac{\left(sAPP\beta_k^E - sAPP\beta_{Tot,k} \right)^2}{w_b} + \frac{\left(sAPP\alpha_{S,k}^E - sAPP\alpha_{Tot,S,k} \right)^2}{w_{aS}} + \frac{\left(sAPP\beta_{S,k}^E - sAPP\beta_{Tot,S,k} \right)^2}{w_{bS}} \right] \quad (2.1)$$

The specific details of how we integrated the method into this study are elaborated below. Whereas the MATLAB source code for the corresponding models, established in Chapter 3 and 4, are given in Appendix C.

Given a series of dose-response data (i.e., $APP_{Tot}-sAPP\alpha_{Tot}$ and $APP-sAPP\beta_{Tot}$), together with a set of simplified equations, we applied the `lsqnonlin` and `fzero` functions in the MATLAB optimization toolbox to estimate the unknown parameter values and solve for free APP. The details of the parameter estimation were as follows:

1. The initial values for the parameters were randomly assigned using the `rand` function.
2. The initial values described in (1) were used for the nonlinear least square fitting function (`lsqnonlin`) to optimize the estimation of the unknown parameter values on the basis of the experimental data.

For curve fitting, `lsqlin`, `lsqcurvefit`, `lsqnonlin`, and `lsqnonneg` are the four candidate functions available in Matlab’s optimization toolbox. `lsqlin` and `lsqnonneg` are excluded from the choices because these functions are designed for linear least squares. With `lsqcurvefit`, the coefficients x are estimated given that the input data $xdata$ and the observed output $ydata$ best fit the following equation:

$$\min_x \frac{1}{2} \|F(x, xdata) - ydata\|_2^2$$

2. Materials and methods

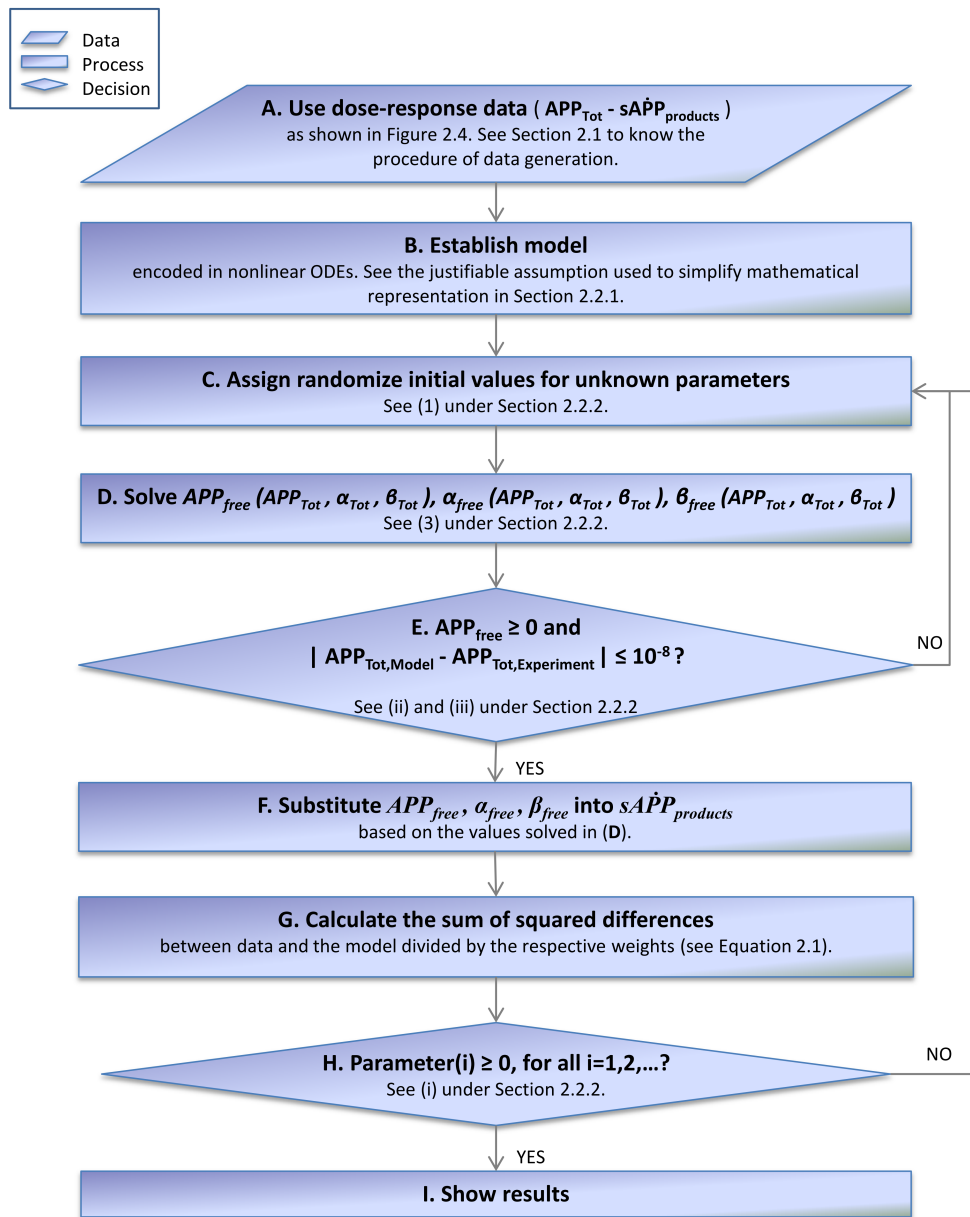


Figure 2.6.: Strategy for parameter value estimation. Based on the dose-response data (A), a model encoded in nonlinear ODEs is established (B). Limited by what can be measured in the experiments, it is crucial in our strategy to simplify the mathematical representation through justifiable assumptions corresponding to the experiments. In step (C), the initial values for the parameters were randomly assigned. (D) We solve for the functions of free APP, α -secretase, and β -secretase with respect to the total amounts of APP, α -secretase, and β -secretase, based on conservation law. This step is essential because what is considered in the ODEs is the free concentration, whereas it is the total concentration that is measured in the experiments. (E) We proceed to the next step if and only if (i) the calculated free APP is non-negative, and (ii) the difference between the total APP concentration measured from experiments and model is not more than 10^{-8} ; otherwise, we go back to step (C). Proceeding to step (F), the calculated free concentrations from (D) are substituted into the mathematical representation of the sAPP products. Lastly, we calculate the sum of squared differences between the data and the model output divided by the respective weights (G). Note that the experimental values of the sAPP products have different orders of magnitude, hence it is substantial to assign weights to avoid bias in the influence of each data set. Furthermore, the estimated values of the unknown parameter must be non-negative in order to make sense biologically (H). We document each set of results (I) and repeat the strategy iteratively.

where $xdata$ and $ydata$ are vectors of length m and $F(x, xdata)$ is a vector-valued function. Whereas for `lsqnonlin`, the equation is represented by

$$\min_x \frac{1}{2} \|F(x, xdata)\|_2^2.$$

Using `lsqnonlin`, the user has more freedom to define the function(s) to be computed, as such that the assigned weights in Equation 2.1 can be considered. For this reason, we applied `lsqnonlin` in fitting the model to the data.

3. Within the `lsqnonlin` function, the `fzero` function was called to solve for free APPs from the corresponding APP_{Tot} function.

For equation solving, there are two candidate functions available in Matlab's optimization toolbox, namely `fsolve` and `fzero`. We chose `fzero` over `fsolve` because the objective is to solve for a zero of a given equation, not a zero of a system of nonlinear equations.

4. (1) - (2) were repeated iteratively.
5. The best match was determined, based on the smallest computed residual value. If the parameter values of the best fit were outside the boundaries of the `rand` function, then the boundaries were increased and the whole process was repeated from (1).

The parameter values were estimated by considering the experimental data (with and without SORLA) and the mathematical equations (with and without SORLA) of each model, as shown in Equation 2.1. In addition, we included the following criteria:

- i The estimated parameter values were non-negative.
- ii The amounts of free APP were non-negative.
- iii The amount of total APP (APP_{Tot}) derived from the mathematical model differs not more than 10^{-8} from the APP_{Tot} measured in the experiments.

MATHEMATICAL MODELING OF SORLA'S INFLUENCE ON
AMYLOIDOGENIC PROCESSING

It is known that SORLA interacts with APP and affects the transportation and processing of APP [Andersen et al. 2005; Schmidt et al. 2007]. However, less is known about the subcellular localization of APP processing and substrate enzyme recognition mechanisms of APP-TACE and APP-BACE. In principle, this interaction decreases TACE and BACE activities at the same ratio; however, our dose-response data indicated different results (Figure 2.4). At half-maximal velocity ($V_{0.5}$), the data show that the amount of sAPP α and sAPP β are reduced by 97% and 75%, respectively, in the presence of SORLA. Unexpected findings such as these underscore the necessity for a thorough understanding of the molecular architecture and function of enzymes (e.g. BACE, TACE) in the process. Studying the binding of substrates in secretase complexes is thus crucial for understanding the molecular mechanism of A β formation. For this reason, we systematically examined the role of SORLA in the processing of APP in AD with the aid of mathematical modeling and a series of dose-response data shown in Figure 2.4. In this chapter, we compare and analyze (a) the model with only monomer processing, (b) the model with only dimer processing, and (c) a combined model with both monomer and dimer processing. All models are developed on the basis of dose-response data. Each of these models includes amyloidogenic and non-amyloidogenic pathways, wherein the proteins in each model are either in monomeric, dimeric, or both monomeric and dimeric forms. Sections 3.1 and 3.2 describe the work conducted as part of the PhD program. The discussion led us to formulate the hypothesis and conduct the work described in Section 3.3, which were subsequently published [Schmidt et al. 2012].

3. Mathematical modeling of SORLA's influence on amyloidogenic processing

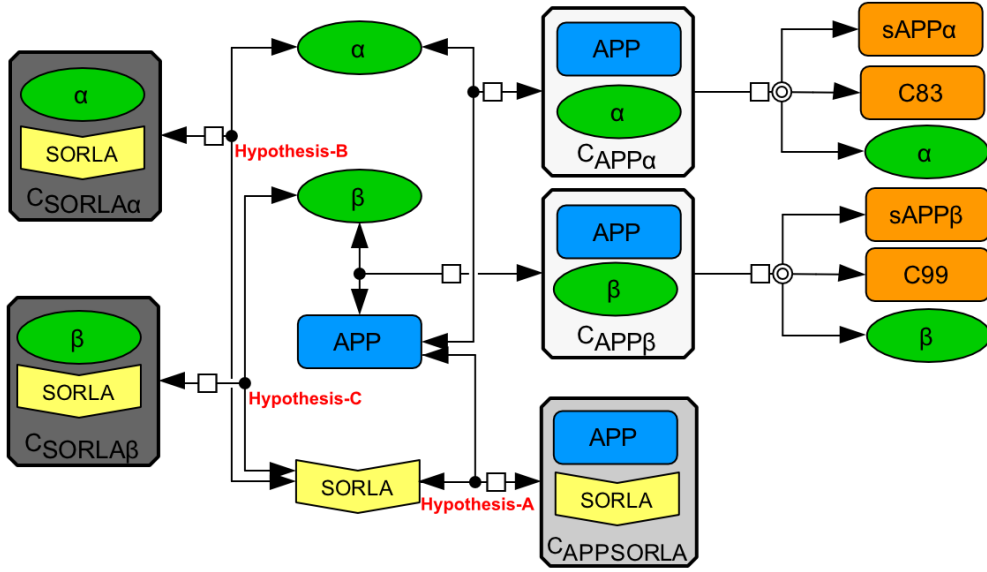


Figure 3.1.: Hypothesized network of the APP processing under the influence of SORLA. Biochemical network of the interaction of reactants APP (blue symbol) with α - and β -secretases (green symbols) and the formation of amyloidogenic and non-amyloidogenic products (orange symbols). Complexes of APP and secretases are indicated as white boxes. The hypothesized complexes of SORLA-APP and SORLA-secretases are indicated as grey boxes. The main consequence of the interaction of SORLA with the APP and the secretases (grey box) is that it lessens the amount of APP and secretases available for processing.

3.1. Pilot simulations based on monomeric APP

Using information from the literature (as discussed in Section 1.2), we established the initial model for APP processing influenced by SORLA in AD. The model includes the amyloidogenic pathway, non-amyloidogenic pathway, and binding relationship of SORLA and APP, wherein all of the proteins are in monomeric forms. The structure of the initial model is established based on the following criteria: (i) simplicity of its form, and (ii) its compatibility to knowledge available from biological database.

Based on our analysis of the dose-response data in Section 2.1, we hypothesized that SORLA interacts with one of the following: (A) APP, (B) α -secretase (i.e. TACE), (C) β -secretase (i.e. BACE), or (D) all of the above. We hypothesized that the additional interaction between SORLA and the enzymes, as shown by Hypotheses B and C in Figure 3.1, may explain the dynamical behavior observed in the experimental data. To validate our hypothesis, experiments were performed. Our findings showed that SORLA does not directly bind with BACE or TACE [Schmidt et al. 2012]. For this reason, it is justifiable to not consider complex formation of SORLA with the secretases, i.e. Hypotheses B and C, in the following models of this thesis.

The biochemical network shown in Figure 3.2 is mainly composed of APP, secretases, SORLA receptor, and the corresponding products, all in monomeric forms. Regardless of SORLA, APP is cleaved by either α -secretase or β -secretase, as such that the non-amyloidogenic pathway produces sAPP α and the amyloidogenic pathway produces sAPP β . When SORLA is present, it binds to APP and reduces the amount of APP available for α -secretase or β -secretase cleavage [Andersen et al. 2005; Andersen and Willnow 2006; Spoelgen et al. 2006; Schmidt et al. 2007].

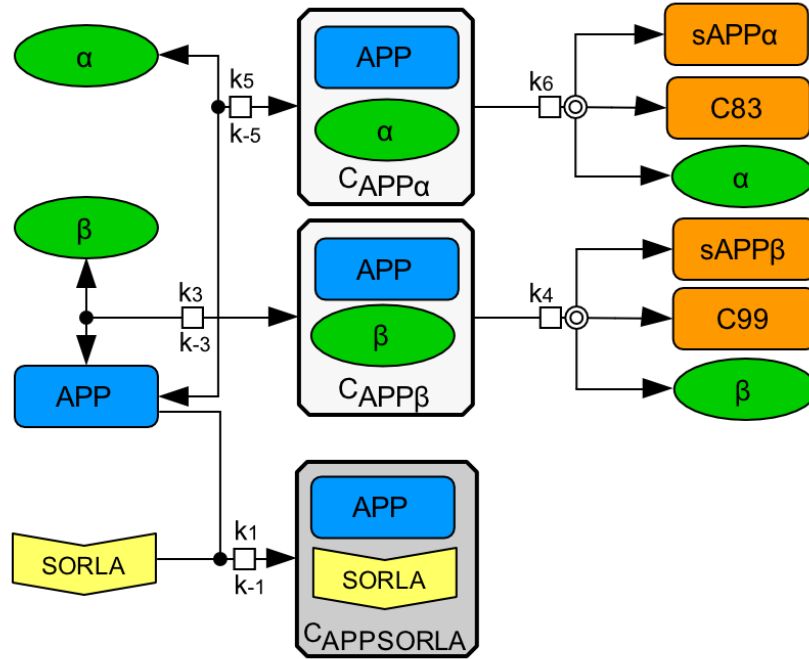


Figure 3.2.: Biochemical network of the processing of APP in monomeric form. Biochemical network of the interaction of reactants APP (blue symbol) with α - and β -secretases (green symbols) and the formation of amyloidogenic and non-amyloidogenic products (orange symbols). Complexes of APP and secretases are indicated as white boxes and complexes of APP and SORLA are indicated in the grey box. Interaction of SORLA with monomeric APP (grey box) lessens the amount of APP monomers available for processing. See the section for “Model notations” for a detailed description of the variables used in the biochemical network.

The biochemical network shown in Figure 3.2 was translated into a system of ODEs. The ODEs in Equations 3.1 describe temporal changes of network components as a function of interactions and cleavage processes.

3. Mathematical modeling of SORLA's influence on amyloidogenic processing

$$\left. \begin{aligned}
 \dot{APP} &= -k_1 \cdot APP \cdot SORLA + k_{-1} \cdot C_{APPSORLA} \\
 &\quad - k_3 \cdot APP \cdot \beta + k_{-3} \cdot C_{APP\beta} \\
 &\quad - k_5 \cdot APP \cdot \alpha + k_{-5} \cdot C_{APP\alpha} \\
 \dot{SORLA} &= -k_1 \cdot APP \cdot SORLA + k_{-1} \cdot C_{APPSORLA} \\
 \dot{\beta} &= -k_3 \cdot APP \cdot \beta + (k_{-3} + k_4) \cdot C_{APP\beta} \\
 \dot{\alpha} &= -k_5 \cdot APP \cdot \alpha + (k_{-5} + k_6) \cdot C_{APP\alpha} \\
 \dot{C}_{APP\beta} &= k_3 \cdot APP \cdot \beta - (k_{-3} + k_4) \cdot C_{APP\beta} \\
 \dot{C}_{APP\alpha} &= k_5 \cdot APP \cdot \alpha - (k_{-5} + k_6) \cdot C_{APP\alpha} \\
 s\dot{APP}\alpha &= k_6 \cdot C_{APP\alpha} \\
 s\dot{APP}\beta &= k_4 \cdot C_{APP\beta} \\
 \dot{C}_{APPSORLA} &= k_1 \cdot APP \cdot SORLA - k_{-1} \cdot C_{APPSORLA}
 \end{aligned} \right\} \quad (3.1)$$

The description of the variables and parameters used in the ODEs are provided in Appendix Table A.1.

Quasi-steady state is assumed for the complexes such that $\dot{C}_{APP\alpha} = 0$ and $\dot{C}_{APP\beta} = 0$. This assumption allows a reduction of the equations, such that

$$\begin{aligned}
 \dot{C}_{APP\alpha} &= k_5 \cdot APP \cdot \alpha - (k_{-5} + k_6) \cdot C_{APP\alpha} \\
 0 &= k_5 \cdot APP \cdot \alpha - (k_{-5} + k_6) \cdot C_{APP\alpha} \\
 C_{APP\alpha} &= \frac{\alpha \cdot APP}{K_{M\alpha}}.
 \end{aligned}$$

A similar simplification approach applies to $\dot{C}_{APP\beta}$. Taken together, we obtain the following equations:

$$\left. \begin{aligned}
 C_{APP\alpha} &= \frac{\alpha \cdot APP}{K_{M\alpha}}, \text{ where } K_{M\alpha} = (k_6 + k_{-5})/k_5 \\
 C_{APP\beta} &= \frac{\beta \cdot APP}{K_{M\beta}}, \text{ where } K_{M\beta} = (k_4 + k_{-3})/k_3.
 \end{aligned} \right\} \quad (3.2)$$

We also take into account the rapid equilibrium assumption for the $C_{APPSORLA}$ complex, such that $\dot{C}_{APPSORLA} = 0$, which implies

$$C_{APPSORLA} = \frac{SORLA \cdot APP}{K_s^{-1}}, \text{ where } K_s = k_1/k_{-1}. \quad (3.3)$$

3.1. Pilot simulations based on monomeric APP

Furthermore, we also assume conservation laws for the enzymes and substrates. This assumption leads to

$$\begin{aligned}
 \alpha_{Tot} &= \alpha + C_{APP\alpha} \\
 \beta_{Tot} &= \beta + C_{APP\beta} \\
 SORLA_{Tot} &= SORLA + C_{APPSORLA} \\
 APP_{Tot} &= APP + C_{APP\alpha} + C_{APP\beta} + C_{APPSORLA}
 \end{aligned}$$

These equations can be expanded and rewritten as follows through substitution of Equations 3.2 and 3.3:

$$\left. \begin{aligned}
 \alpha_{Tot} &= \alpha + \frac{\alpha \cdot APP}{K_{M\alpha}} \\
 \beta_{Tot} &= \beta + \frac{\beta \cdot APP}{K_{M\beta}} \\
 SORLA_{Tot} &= SORLA + \frac{SORLA \cdot APP}{K_s^{-1}} \\
 APP_{Tot}(APP) &= APP \cdot \left(1 + \frac{\alpha}{K_{M\alpha}} + \frac{\beta}{K_{M\beta}} + \frac{SORLA}{K_s^{-1}} \right)
 \end{aligned} \right\} \quad (3.4)$$

The first three equations of (3.4) can be transformed, such that free molecule numbers of α -secretase (α), β -secretase (β), and SORLA ($SORLA$) can be calculated from α_{Tot} , β_{Tot} , and $SORLA_{Tot}$, accordingly:

$$\left. \begin{aligned}
 \alpha &= \frac{\alpha_{Tot} \cdot K_{M\alpha}}{K_{M\alpha} + APP} \\
 \beta &= \frac{\beta_{Tot} \cdot K_{M\beta}}{K_{M\beta} + APP} \\
 SORLA &= \frac{K_s^{-1} \cdot SORLA_{Tot}}{K_s^{-1} + APP}
 \end{aligned} \right\} \quad (3.5)$$

Given (3.5), $APP_{Tot}(APP)$ can be rewritten as

$$APP_{Tot}(APP) = APP \cdot \left(1 + \frac{\alpha_{Tot}}{K_{M\alpha} + APP} + \frac{\beta_{Tot}}{K_{M\beta} + APP} + \frac{SORLA_{Tot}}{K_s^{-1} + APP} \right). \quad (3.6)$$

In addition, the ODEs in Equations 3.1 describing the formation of end products in the processing of the monomeric form of APP under the influence of SORLA can be rewritten in the following form after substituting Equations 3.2:

$$\left. \begin{aligned}
 sA\dot{P}P\alpha &= k_6 \cdot \frac{\alpha \cdot APP}{K_{M\alpha}} \\
 sA\dot{P}P\beta &= k_4 \cdot \frac{\beta \cdot APP}{K_{M\beta}}
 \end{aligned} \right\} \quad (3.7)$$

3. Mathematical modeling of SORLA's influence on amyloidogenic processing

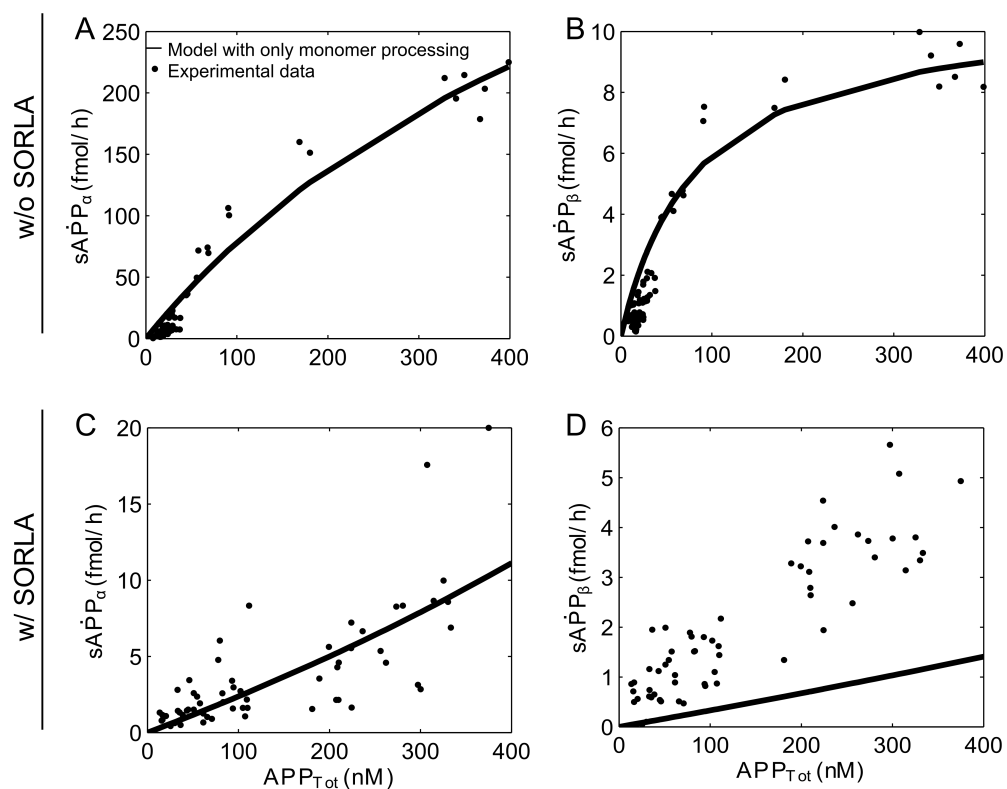


Figure 3.3.: Mathematical modelling of monomeric form of APP processing and its influence by SORLA. Simulation results of the mathematical model (solid lines) for the various APP processing products are shown together with the actual data points obtained from biochemical experiments. Simulation of $sAPP_\alpha$ and $sAPP_\beta$ in the absence (**A-B**) and presence (**C-D**) of SORLA. The list of the estimated parameter values is provided in Table B.1.

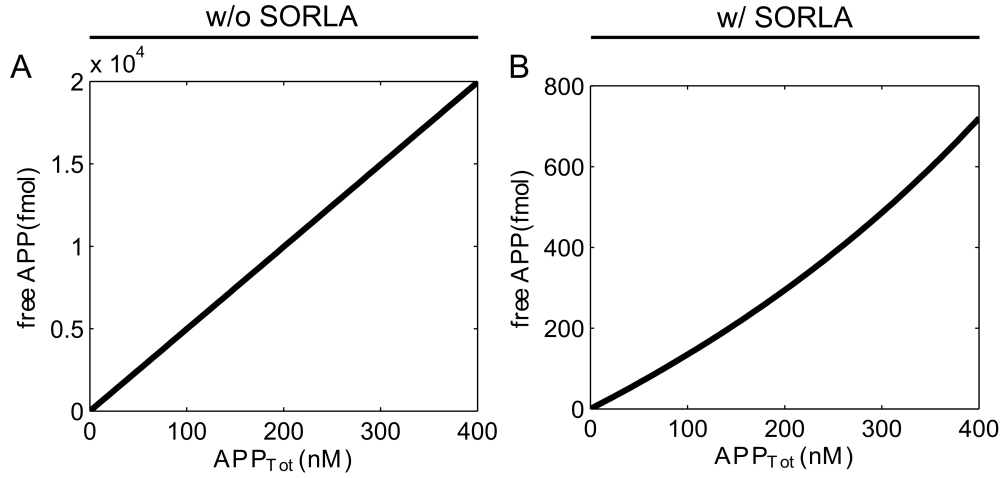


Figure 3.4.: Free APP in the model with monomer processing only. Simulation of the model with only monomer processing (solid lines) for the amount of free APP in the absence (A) and presence (B) of SORLA.

where APP , β , and α can be represented in terms of APP_{Tot} , β_{Tot} , and α_{Tot} , respectively (see Equations 3.5 and 3.6).

Lastly, we followed the procedure for parameter estimation that was discussed in detail in Section 2.2. Following this procedure, we generated the simulations shown in Figure 3.3. The simulations show that, regardless of SORLA, the ODEs derived for $sAPP\alpha$ and $sAPP\beta$ shown in Equations 3.7 are very similar. This is because the levels of APP , α , and β vary in the absence and presence of SORLA. As shown in Figure 3.4, the level of free APP was smaller in the presence of SORLA compared to the absence of SORLA. In contrast, there are higher levels of free α and β in the presence of SORLA compared to the absence of SORLA (Figure 3.5). All 100 global parameter estimations for the simulations of this model with only monomer processing did not achieve a sufficient match to the series of dose-response data. The model either matches the dynamic behavior of $sAPP\beta$ or $sAPP\alpha$ from the experiment, but not both. For example, as shown in Figure 3.3, the simulation of the model does not fit $sAPP\alpha$ without SORLA and $sAPP\beta$ with SORLA from the experiments. As a consequence, further exploration was needed to develop a new hypothesis.

3.2. Processing of dimeric APP

Schmechel et al. [2004], Westmeyer et al. [2004], and Jin et al. [2010] have shown that BACE as a dimer appears to have an effect upon $A\beta$ production. Therefore, dimerization of BACE may help the enzyme acquire specific mechanisms to associate with its sub-

3. Mathematical modeling of SORLA's influence on amyloidogenic processing

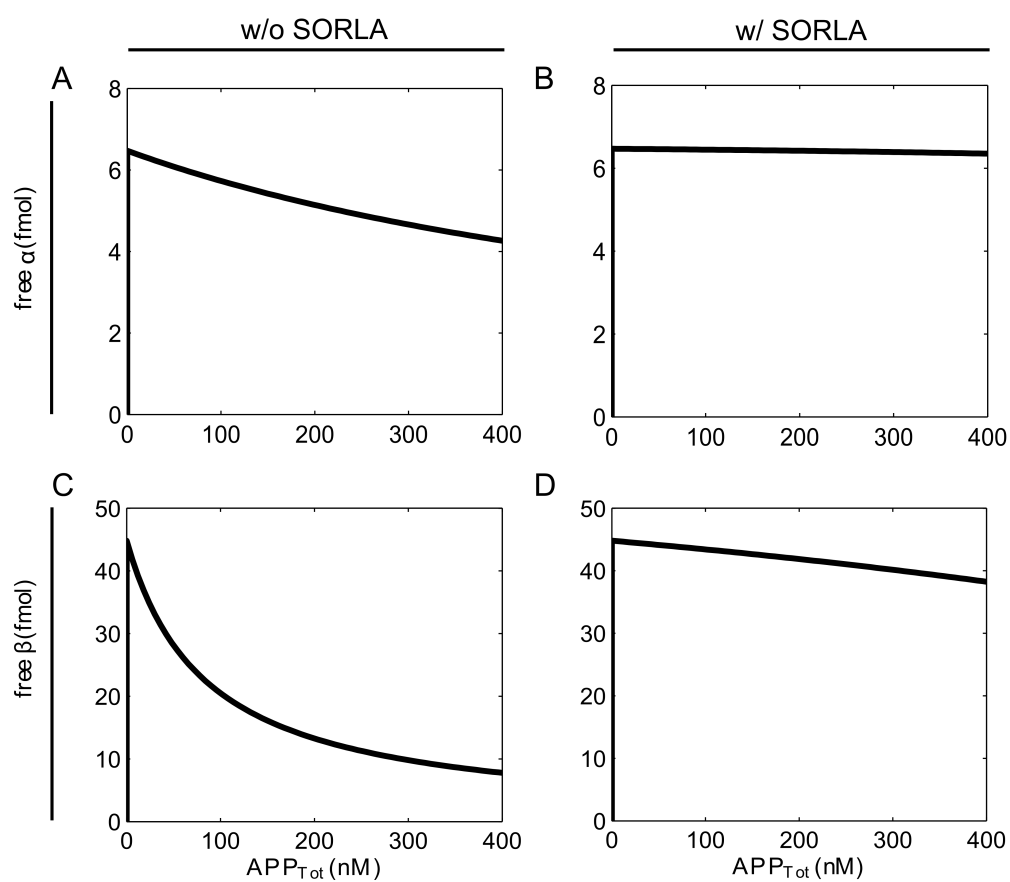


Figure 3.5.: Free secretases in the model with monomer processing only. Simulation of the model with monomer processing only (solid lines) for the amount of free α -secretase (**A-B**) and β -secretase (**C-D**) in the absence and presence of SORLA, respectively.

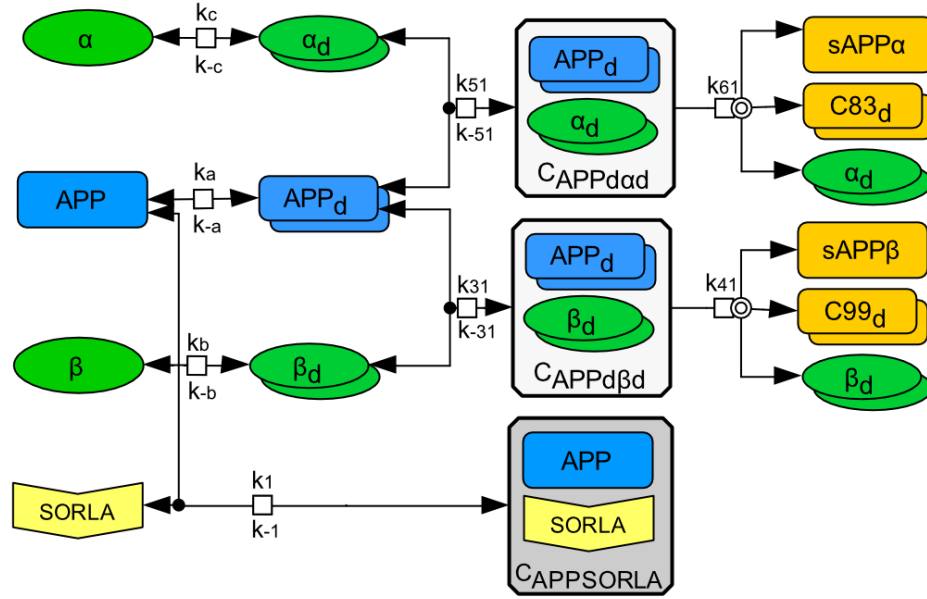


Figure 3.6.: Biochemical network of the processing of dimeric form of APP. Biochemical network of the interaction of reactants APP (blue symbol) with α - and β -secretases (green symbols) and the formation of amyloidogenic and non-amyloidogenic products (orange symbols). Complexes of APP and secretases are indicated as white boxes and complexes of APP and SORLA are indicated in the grey box. The reversible dimerization-dissociation of APP and secretases is included in the model design. Interaction of SORLA with monomeric APP (grey box) has two consequences: it prevents formation of APP dimers, which are the preferred secretase substrates, and it reduces the amount of APP monomers available for processing. Note that dissociation of homodimers of APP (APP_d), α -secretase (α_d), and β -secretase (β_d) results in two identical monomers of the respective proteins. See the section for “Model notations” for a detailed description of the variables used in the biochemical network.

strates and exert catalytic activity. Kinetic analysis has shown that purified native BACE dimer has a higher affinity and turnover rate compared to monomeric soluble BACE (i.e., dimeric and monomeric BACE displayed significant differences in their kinetic profiles). This result implies that inhibitors that interfere with BACE dimerization and lead to an enrichment of monomers could result in a reduction of the activity of this rate-limiting enzyme in amyloid pathology, even if such BACE monomers were stable [Westmeyer et al. 2004; Parsons and Austen 2007].

Multhaup [2006], Munter et al. [2007], Kienlen-Campard et al. [2008], and Kaden et al. [2008, 2009] have also shown an important role of the dimeric form of APP in AD, which is similar to findings by Hung et al. [2008] regarding $A\beta$. Aggregation has long been recognized as a necessary condition for toxicity, and it has been hypothesized that dimers of $A\beta$ are the principal toxic species. Hung et al. [2008] observed that at a given $A\beta$ wild-type (WT) cell viability, the corresponding percentage of monomers present is lower than the percentage of dimers present, which suggests that more $A\beta$ is produced related to $A\beta$ -

3. Mathematical modeling of SORLA's influence on amyloidogenic processing

dimer. Multhaup and colleagues suggested from their results that the γ -secretase cleavage of APP are intimately linked to the dimerization strength of the APP transmembrane sequence (TMS) substrate, and therefore is central to the onset of AD [Multhaup 2006; Munter et al. 2007; Kaden et al. 2008, 2009]. They have also shown that the native APP dimer can be converted entirely into monomers, which implies that strong dimerization of the APP TMS can increase the production of $A\beta$.

Taken together, these results suggest that it is possible to model APP processing in dimeric form. Therefore we established the biochemical network shown in Figure 3.6 and translated the biochemical network into a system of ODEs as shown below:

$$\left. \begin{aligned}
 \dot{APP} &= -k_1 \cdot APP \cdot SORLA + k_{-1} \cdot C_{APPSORLA} \\
 &\quad + 2 \cdot [k_{-a} \cdot APP_d - k_a \cdot APP^2] \\
 \dot{\beta} &= 2 \cdot (k_{-b} \cdot \beta_d - k_b \cdot \beta_2^2) \\
 \dot{\alpha} &= 2 \cdot (k_{-c} \cdot \alpha_d - k_c \cdot \alpha_2^2) \\
 \dot{SORLA} &= -k_1 \cdot APP \cdot SORLA + k_{-1} \cdot C_{APPSORLA} \\
 \dot{C}_{APPSORLA} &= -SORLA \\
 \dot{APP}_d &= -k_{31} \cdot APP_d \cdot \beta_d + k_{-31} \cdot C_{APPd\beta d} \\
 &\quad - k_{51} \cdot APP_d \cdot \alpha_d + k_{-51} \cdot C_{APPd\alpha d} \\
 &\quad - 2 \cdot (k_{-a} \cdot APP_d - k_a \cdot APP^2) \\
 \dot{\beta}_d &= -k_{31} \cdot APP_d \cdot \beta_d + (k_{-31} + k_{41}) \cdot C_{APPd\beta d} \\
 &\quad - 2 \cdot (k_{-b} \cdot \beta_d - k_b \cdot \beta_2^2) \\
 \dot{\alpha}_d &= -k_{51} \cdot APP_d \cdot \alpha_d + (k_{-51} + k_{61}) \cdot C_{APPd\alpha d} \\
 &\quad - 2 \cdot (k_{-c} \cdot \alpha_d - k_c \cdot \alpha_2^2) \\
 \dot{C}_{APPd\beta d} &= k_{31} \cdot APP_d \cdot \beta_d - (k_{-31} + k_{41}) \cdot C_{APPd\beta d} \\
 \dot{C}_{APPd\alpha d} &= k_{51} \cdot APP_d \cdot \alpha_d - (k_{-51} + k_{61}) \cdot C_{APPd\alpha d} \\
 s\dot{APP}\alpha &= 2 \cdot k_{61} \cdot C_{APPd\alpha d} \\
 s\dot{APP}\beta &= 2 \cdot k_{41} \cdot C_{APPd\beta d}
 \end{aligned} \right\} \quad (3.8)$$

A description of the variables and parameters used in the ODEs are provided in Appendix Table A.2.

A quasi-steady state is assumed for the complexes, such that $\dot{C}_{APPd\alpha d} = 0$ and $\dot{C}_{APPd\beta d} =$

0. This assumption allows for a reduction of the equations, such that

$$\begin{aligned} \dot{C}_{APPd\alpha d} &= k_{51} \cdot APP_d \cdot \alpha_d - (k_{-51} + k_{61}) \cdot C_{APPd\alpha d} \\ 0 &= k_{51} \cdot APP_d \cdot \alpha_d - (k_{-51} + k_{61}) \cdot C_{APPd\alpha d} \\ C_{APPd\alpha d} &= \frac{\alpha_d \cdot APP_d}{K_{M\alpha d}}. \end{aligned}$$

A similar approach applies to $\dot{C}_{APP\beta}$. In summary, we arrive at the following equations:

$$\left. \begin{aligned} C_{APPd\alpha d} &= \frac{\alpha_d \cdot APP_d}{K_{M\alpha d}}, \text{ where } K_{M\alpha d} = (k_{61} + k_{-51})/k_{51} \\ C_{APPd\beta d} &= \frac{\beta_d \cdot APP_d}{K_{M\beta d}}, \text{ where } K_{M\beta d} = (k_{41} + k_{-31})/k_{31}. \end{aligned} \right\} \quad (3.9)$$

We also take into account the ratio of the association constants of APP, β -secretase, and α -secretase dimerization as well as the rapid equilibrium assumption for the $C_{APPSORLA}$ complex, such that

$$\left. \begin{aligned} K_A &= \frac{APP_d}{APP^2} \\ K_B &= \frac{\beta_d}{\beta^2} \\ K_C &= \frac{\alpha_d}{\alpha^2} \\ K_s &= \frac{C_{APPSORLA}}{SORLA \cdot APP} \end{aligned} \right\} \quad (3.10)$$

where $K_A = k_a/k_{-a}$, $K_B = k_b/k_{-b}$, $K_C = k_c/k_{-c}$, and $K_s = k_1/k_{-1}$. Note that the dissociation constant is the inverse of the association constant and vice versa (e.g., association constant K_A corresponds to the dissociation constant K_A^{-1}).

Furthermore, we also assume conservation laws for the enzymes and substrates:

$$\begin{aligned} \alpha_{Tot} &= \alpha + 2 \cdot (\alpha_d + C_{APPd\alpha d}) \\ \beta_{Tot} &= \beta + 2 \cdot (\beta_d + C_{APPd\beta d}) \\ SORLA_{Tot} &= SORLA + C_{APPSORLA} \\ APP_{Tot} &= APP + C_{APPSORLA} + 2 \cdot (APP_d + C_{APPd\alpha d} + C_{APPd\beta d}) \end{aligned}$$

3. Mathematical modeling of SORLA's influence on amyloidogenic processing

After substituting Equations 3.9 and 3.10, they are rewritten as:

$$\left. \begin{aligned} \alpha_{Tot} &= \alpha + 2 \cdot \left(K_C \cdot \alpha^2 + \frac{(K_C \cdot \alpha^2) \cdot (K_A \cdot APP^2)}{K_{M\alpha d}} \right) \\ \beta_{Tot} &= \beta + 2 \cdot \left(K_B \cdot \beta^2 + \frac{(K_B \cdot \beta^2) \cdot (K_A \cdot APP^2)}{K_{M\beta d}} \right) \\ SORLA_{Tot} &= SORLA \cdot \left(1 + \frac{APP}{K_s^{-1}} \right) \\ APP_{Tot} &= APP \cdot \left(1 + \frac{SORLA}{K_s^{-1}} \right) + 2 \cdot (K_A \cdot APP^2) \cdot \left(1 + \frac{K_C \cdot \alpha^2}{K_{M\alpha d}} + \frac{K_B \cdot \beta^2}{K_{M\beta d}} \right) \end{aligned} \right\} \quad (3.11)$$

Next, we solve α , β , and $SORLA$ in terms of α_{Tot} , β_{Tot} , and $SORLA_{Tot}$, respectively. Note that only the positive solutions are biologically meaningful. For α ,

$$\alpha = \frac{-B_\alpha + \sqrt{B_\alpha^2 - 4 \cdot A_\alpha \cdot C_\alpha}}{2 \cdot A_\alpha} \quad (3.12)$$

where

$$\begin{aligned} A_\alpha &= 2 \cdot K_C \cdot \left(1 + \frac{K_A \cdot APP^2}{K_{M\alpha d}} \right) \\ B_\alpha &= 1 \\ C_\alpha &= -\alpha_{Tot}. \end{aligned}$$

Similarly for β ,

$$\beta = \frac{-B_\beta + \sqrt{B_\beta^2 - 4 \cdot A_\beta \cdot C_\beta}}{2 \cdot A_\beta} \quad (3.13)$$

where

$$\begin{aligned} A_\beta &= 2 \cdot K_B \cdot \left(1 + \frac{K_A \cdot APP^2}{K_{M\beta d}} \right) \\ B_\beta &= 1 \\ C_\beta &= -\beta_{Tot}. \end{aligned}$$

And for $SORLA$,

$$SORLA = \frac{K_s^{-1} \cdot SORLA_{Tot}}{K_s^{-1} + APP}. \quad (3.14)$$

Substituting Equations 3.12-3.14 into APP_{Tot} in Equations 3.11 will differentiate its value in the presence and absence of SORLA.

The ODEs in Equations 3.8 that describe the formation of end products in the processing of dimeric form of APP under the influence of SORLA can be rewritten in the following

form:

$$\left. \begin{aligned} sAPP\alpha &= 2 \cdot k_{61} \cdot \frac{(K_C \cdot \alpha^2) \cdot (K_A \cdot APP^2)}{K_{M\alpha d}} \\ sAPP\beta &= 2 \cdot k_{41} \cdot \frac{(K_B \cdot \beta^2) \cdot (K_A \cdot APP^2)}{K_{M\beta d}} \end{aligned} \right\} \quad (3.15)$$

where APP , β , and α can be represented in terms of APP_{Tot} , β_{Tot} , and α_{Tot} respectively, as shown in Equations 3.11.

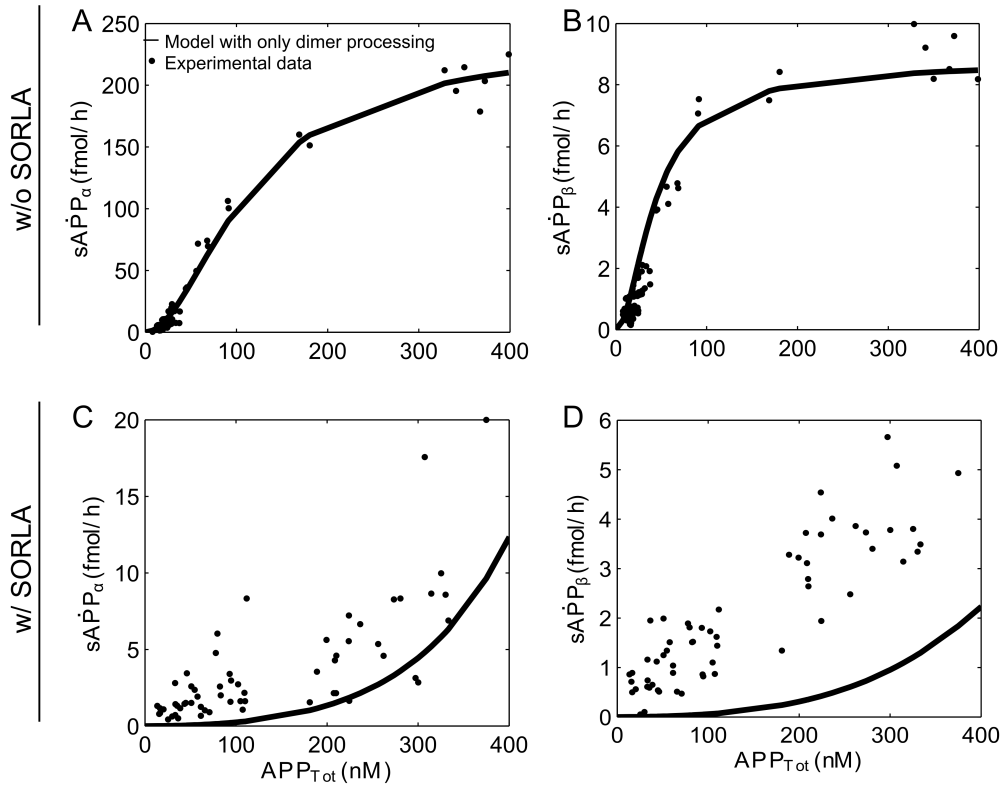


Figure 3.7.: Mathematical modelling of the dimeric form of APP processing and its influence by SORLA. Simulation results of the mathematical model (solid lines) for the various APP processing products are shown together with the actual data points obtained in biochemical experiments. Simulation of $sAPP\alpha$ and $sAPP\beta$ in the absence (A-B) and presence (C-D) of SORLA. The list of the estimated parameter values is provided in Table B.2.

This model, with only dimer processing, has the same limitations as our initial model with only monomer processing. As shown in Figure 3.7, the simulations of the model with only dimer processing also do not fit the series of dose-response data. However, it is interesting to observe that the simulations with only monomer processing (Figure 3.3) have a good fit to the dose-response data with SORLA. Whereas, the simulations with only dimer processing (Figure 3.7) have a good match to the dose-response data without SORLA. These results lead to the formation of the third hypothesis, the “combined model”, which consists of both monomer and dimer processing.

3.3. When one pathway is not enough

The study performed on the previous two models inspired the structure formation of the new model that will be discussed in this section. This model is a straightforward extension of the previous two models and consists of both monomer and dimer processing. This section is adapted from my contribution in Schmidt et al. 2012.

The biochemical network consists of monomer processing (upper panel of Figure 3.8) and dimer processing (lower panel of Figure 3.8). The two modules are connected by the reversible dimerization-dissociation of APP and secretases. Two identical monomeric forms of APP and secretases dimerize to give the corresponding dimeric forms of APP and secretases. In the reverse direction, the dimeric forms of APP and secretases give the respective identical monomeric forms of APP and secretases. In both modules, the interaction of APP with α - and β -secretases leads to the formation of non-amyloidogenic (sAPP α and C83) and amyloidogenic (sAPP β and C99) products. However, APP and secretases are in monomeric form during monomer processing and in dimeric form during dimer processing. The interaction between SORLA and monomeric APP reduces the amount of APP monomers available for processing and prevents the formation of APP dimers. We focused our model in such a way that the dimeric forms of the secretases only act on the dimeric form of APP, and the monomeric forms of the secretases only act on the monomeric form of APP. Descriptions of the variables used in the biochemical network are provided in the section for “Model notations”.

The biochemical network shown in Figure 3.8 is translated into a system of ODEs (Equations 3.16), which describe temporal changes of network components as a function of interactions and cleavage processes. The description of the variables and parameters used in the ODEs are provided in Appendix Table A.3.

In addition to the assumptions stated earlier in Section 2.2, the following additional assumptions are considered in this model:

1. APP as well as α - and β -secretases exist in an equilibrium of monomeric and homodimeric forms;
2. SORLA can reversibly form a complex with monomeric APP to reduce the formation of substrate oligomers (as suggested in Figure 10A-C of [Schmidt et al. 2012]) and impair processing efficiency; and
3. SORLA does not directly impact the enzymatic activity of secretases (as suggested in Figure 8 and 9 of [Schmidt et al. 2012]).

3.3. When one pathway is not enough

4. In agreement with Westmeyer et al. [2004] and Parsons and Austen [2007], monomeric and dimeric forms of proteins display differences in their kinetic profiles. Thus, the parameters and variables for monomer and dimer processing are assigned differently.

$$\left. \begin{aligned}
 \dot{APP} &= -k_1 \cdot APP \cdot SORLA + k_{-1} \cdot C_{APPSORLA} - k_3 \cdot APP \cdot \beta + k_{-3} \cdot C_{APP\beta} \\
 &\quad - k_5 \cdot APP \cdot \alpha + k_{-5} \cdot C_{APP\alpha} + 2 \cdot (k_{-a} \cdot APP_d - k_a \cdot APP^2) \\
 \dot{SORLA} &= -k_1 \cdot APP \cdot SORLA + k_{-1} \cdot C_{APPSORLA} \\
 \dot{\beta} &= -k_3 \cdot APP \cdot \beta + (k_{-3} + k_4) \cdot C_{APP\beta} + 2 \cdot (k_{-b} \cdot \beta_d - k_b \cdot \beta^2) \\
 \dot{\alpha} &= -k_5 \cdot APP \cdot \alpha + (k_{-5} + k_6) \cdot C_{APP\alpha} + 2 \cdot (k_{-c} \cdot \alpha_d - k_c \cdot \alpha^2) \\
 \dot{C}_{APP\beta} &= k_3 \cdot APP \cdot \beta - (k_{-3} + k_4) \cdot C_{APP\beta} \\
 \dot{C}_{APP\alpha} &= k_5 \cdot APP \cdot \alpha - (k_{-5} + k_6) \cdot C_{APP\alpha} \\
 s\dot{APP}\alpha &= k_6 \cdot C_{APP\alpha} \\
 s\dot{APP}\beta &= k_4 \cdot C_{APP\beta} \\
 \dot{C}_{APPSORLA} &= -\dot{SORLA} \\
 \dot{APP}_d &= -k_{31} \cdot APP_d \cdot \beta_d + k_{-31} \cdot C_{APP_d\beta_d} - k_{51} \cdot APP_d \cdot \alpha_d \\
 &\quad + k_{-51} \cdot C_{APP_d\alpha_d} - 2 \cdot (k_{-a} \cdot APP_d - k_a \cdot APP^2) \\
 \dot{\beta}_d &= -k_{31} \cdot APP_d \cdot \beta_d + (k_{-31} + k_{41}) \cdot C_{APP_d\beta_d} + 2 \cdot (k_b \cdot \beta^2 - k_{-b} \cdot \beta_d) \\
 \dot{\alpha}_d &= -k_{51} \cdot APP_d \cdot \alpha_d + (k_{-51} + k_{61}) \cdot C_{APP_d\alpha_d} + 2 \cdot (k_c \cdot \alpha^2 - k_{-c} \cdot \alpha_d) \\
 \dot{C}_{APP_d\beta_d} &= k_{31} \cdot APP_d \cdot \beta_d - (k_{-31} + k_{41}) \cdot C_{APP_d\beta_d} \\
 \dot{C}_{APP_d\alpha_d} &= k_{51} \cdot APP_d \cdot \alpha_d - (k_{-51} + k_{61}) \cdot C_{APP_d\alpha_d} \\
 s\dot{APP}\alpha^* &= 2 \cdot k_{61} \cdot C_{APP_d\alpha_d} \\
 s\dot{APP}\beta^* &= 2 \cdot k_{41} \cdot C_{APP_d\beta_d}
 \end{aligned} \right\} \quad (3.16)$$

Since quasi-steady states can be assumed for the complexes, this allows a reduction of the equations, such that

$$\left. \begin{aligned}
 C_{APP\alpha} &= \frac{\alpha \cdot APP}{K_{M\alpha}}, \\
 C_{APP\beta} &= \frac{\beta \cdot APP}{K_{M\beta}}, \\
 C_{APP_d\alpha_d} &= \frac{\alpha_d \cdot APP_d}{K_{M\alpha_d}}, \\
 C_{APP_d\beta_d} &= \frac{\beta_d \cdot APP_d}{K_{M\beta_d}},
 \end{aligned} \right\} \quad (3.17)$$

3. Mathematical modeling of SORLA's influence on amyloidogenic processing

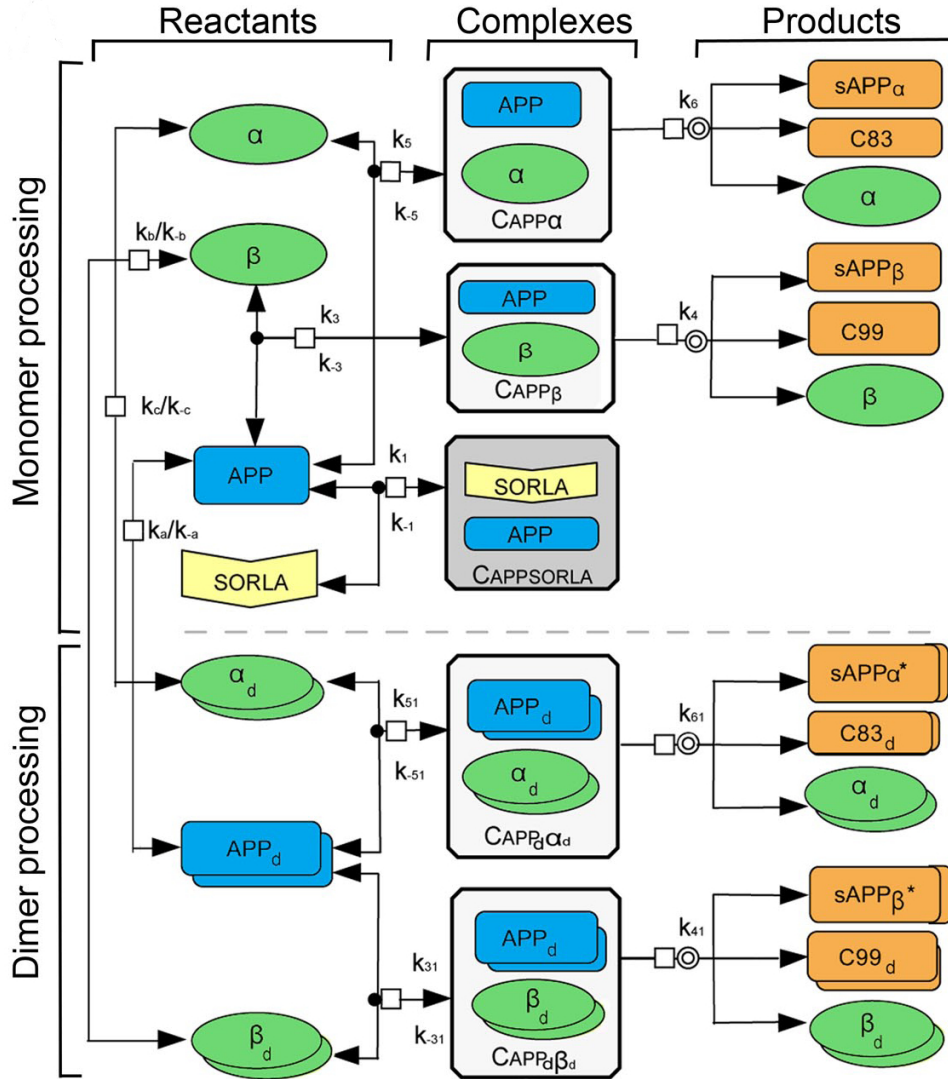


Figure 3.8.: Biochemical network of the processing of both monomeric and dimeric forms of APP. Biochemical network of the interaction of reactants APP (blue symbol) with α - and β -secretases (green symbols) and the formation of amyloidogenic and non-amyloidogenic products (orange symbols). Complexes of APP and secretases are indicated as white boxes and complexes of APP and SORLA are indicated as a grey box. Processing of monomeric (upper panel) and dimeric (lower panel) forms of APP is indicated as separate pathways. The two modules are linked together by the reversible dimerization-dissociation of APP and secretases. Interaction of SORLA with monomeric APP (grey box) has two consequences: it prevents formation of APP dimers, which are the preferred secretase substrates, and it reduces the amount of APP monomers available for processing. Note that dissociation of homodimers of APP (APP_d), α -secretase (α_d), and β -secretase (β_d) results in two identical monomers of the respective proteins. See the section for “Model notations” for a detailed description of the variables used in the biochemical network.

3.3. When one pathway is not enough

where $K_{M\alpha} = (k_6 + k_{-5})/k_5$, $K_{M\beta} = (k_4 + k_{-3})/k_3$, $K_{M\alpha d} = (k_{61} + k_{-51})/k_{51}$, and $K_{M\beta d} = (k_{41} + k_{-31})/k_{31}$.

Next, we take into account the association constants of APP, β -secretase, and α -secretase dimerization as well as the rapid equilibrium assumption for the $C_{APPSORLA}$ complex:

$$\left. \begin{aligned} K_A &= \frac{APP_d}{APP^2}, \\ K_B &= \frac{\beta_d}{\beta^2}, \\ K_C &= \frac{\alpha_d}{\alpha^2}, \\ K_s &= \frac{C_{APPSORLA}}{SORLA \cdot APP}, \end{aligned} \right\} \quad (3.18)$$

where $K_A = k_a/k_{-a}$, $K_B = k_b/k_{-b}$, $K_C = k_c/k_{-c}$, and $K_s = k_1/k_{-1}$.

Furthermore, the ODEs include conservation laws for the enzymes and substrates. This assumption gives

$$\left. \begin{aligned} \alpha_{Tot} &= \alpha + \frac{\alpha \cdot APP}{K_{M\alpha}} + 2 \cdot K_C \cdot \alpha^2 \cdot \left(1 + \frac{K_A \cdot APP^2}{K_{M\alpha d}}\right) \\ \beta_{Tot} &= \beta + \frac{\beta \cdot APP}{K_{M\beta}} + 2 \cdot K_B \cdot \beta^2 \cdot \left(1 + \frac{K_A \cdot APP^2}{K_{M\beta d}}\right) \\ SORLA_{Tot} &= SORLA \cdot \left(1 + \frac{APP}{K_s^{-1}}\right) \end{aligned} \right\} \quad (3.19)$$

In particular, the ODEs include conservation of the APP substrate:

$$\left. \begin{aligned} APP_{Tot}(APP) &= APP \cdot \left(1 + \frac{\alpha}{K_{M\alpha}} + \frac{\beta}{K_{M\beta}} + \frac{SORLA_{Tot}}{K_s^{-1} + APP}\right) + \\ &2 \cdot (K_A \cdot APP^2) \cdot \left(1 + \frac{K_C \cdot \alpha^2}{K_{M\alpha d}} + \frac{K_B \cdot \beta^2}{K_{M\beta d}}\right) \end{aligned} \right\} \quad (3.20)$$

whereas APP_{Tot} is a function of free APP and APP bound to the complexes, with the representation of α and β shown below (Equations 3.21).

The first two equations of Equations 3.19 can be transformed, such that free molecule numbers of α -secretase (α) and β -secretase (β) can be calculated from α_{Tot} and β_{Tot} ,

3. Mathematical modeling of SORLA's influence on amyloidogenic processing

respectively, according to:

$$\left. \begin{aligned} \alpha &= \frac{K_{M\alpha d} \cdot (K_{M\alpha} + APP)}{4 \cdot K_C \cdot K_{M\alpha} \cdot (K_{M\alpha d} + K_A \cdot APP^2)} + \\ &\frac{\sqrt{K_{M\alpha d}^2 \cdot (K_{M\alpha} + APP)^2 + 8 \cdot \alpha_{Tot} \cdot K_{M\alpha d} \cdot K_C \cdot K_{M\alpha}^2 \cdot (K_{M\alpha d} + K_A \cdot APP^2)}}{4 \cdot K_C \cdot K_{M\alpha} \cdot (K_{M\alpha d} + K_A \cdot APP^2)} \\ \beta &= \frac{K_{M\beta d} \cdot (K_{M\beta} + APP)}{4 \cdot K_B \cdot K_{M\beta} \cdot (K_{M\beta d} + K_A \cdot APP^2)} + \\ &\frac{\sqrt{K_{M\beta d}^2 \cdot (K_{M\beta} + APP)^2 + 8 \cdot \beta_{Tot} \cdot K_{M\beta d} \cdot K_B \cdot K_{M\beta}^2 \cdot (K_{M\beta d} + K_A \cdot APP^2)}}{4 \cdot K_B \cdot K_{M\beta} \cdot (K_{M\beta d} + K_A \cdot APP^2)} \end{aligned} \right\} \quad (3.21)$$

where only the positive solutions are biologically meaningful.

The ODEs in Equations 3.16 that describe the formation of end products in the processing of monomeric and dimeric forms of APP under the influence of SORLA can be rewritten in the following form (with the representation of APP , α , and β , in terms of APP_{Tot} , α_{Tot} , and β_{Tot} , respectively; see Equations 3.20 and 3.21):

$$\left. \begin{aligned} s\dot{APP}\alpha &= k_6 \cdot \alpha \cdot \frac{APP}{K_{M\alpha}} \\ s\dot{APP}\beta &= k_4 \cdot \beta \cdot \frac{APP}{K_{M\beta}} \\ s\dot{APP}\alpha^* &= 2 \cdot k_{61} \cdot (K_C \cdot \alpha^2) \cdot \frac{K_A \cdot APP^2}{K_{M\alpha d}} \\ s\dot{APP}\beta^* &= 2 \cdot k_{41} \cdot (K_B \cdot \beta^2) \cdot \frac{K_A \cdot APP^2}{K_{M\beta d}} \end{aligned} \right\} \quad (3.22)$$

Given Equations 3.22, we obtain

$$\left. \begin{aligned} s\dot{APP}\alpha_{Tot} &= s\dot{APP}\alpha + s\dot{APP}\alpha^* \\ s\dot{APP}\beta_{Tot} &= s\dot{APP}\beta + s\dot{APP}\beta^* \end{aligned} \right\} \quad (3.23)$$

Lastly, the parameter values of the model are estimated by optimization from data obtained in the dose-response series for $sAPP\alpha$ and $sAPP\beta$ as a function of APP_{Tot} for cells with or without SORLA, as detailed in Section 2.2. The list of the estimated parameter values is provided in Table B.3.

Global versus global-local parameter estimation

We performed 300 global estimates and 300 global-local estimates to compare the quality of both estimates. In the global-local fit, all parameters are estimated globally, with the exception of $K_{M\beta}$ and $K_{M\beta d}$. Out of the 300 global-local estimation runs ($K_{M\beta}$ and

3.3. When one pathway is not enough

$K_{M\beta d}$ are estimated locally) and 300 global estimation runs, 214 and 216 fits were generated, respectively, satisfying the condition that all parameter values are positive. Note that none of the parameter values were taken from the literature due to the differences in the experimental methods applied. Thus, most kinetic data available in the literature on α - or β - secretase activity were obtained from cell free assays using purified enzyme and artificial peptide substrate. In contrast, our model relies on quantitative data obtained from APP processing in intact cells.

The goodness of a fit is quantified by calculating the residual value. Comparing global-local and purely global parameter estimates, the residual values for the best global fit (i.e. 30.26) are approximately 50% worse than the residual values from the global-local estimations. The simulation for the purely global parameter estimates with the best fits is illustrated in Figure 3.9. The residual values of all 214 global-local estimations are ranked from the lowest residual value of 21.5. A fit with a residual value smaller than 22 was considered a “good fit”. Moreover, the global-local fits, where $K_{M\alpha}$ and $K_{M\alpha d}$ are estimated locally, are slightly weaker (residual value 23.50) than the model where $K_{M\beta}$ and $K_{M\beta d}$ are locally estimated (residual value of 21.50), but better than the model where all parameters were fitted globally. This implies that the model provides the best match to the experimental data where all parameters, except $K_{M\beta}$ and $K_{M\beta d}$, are estimated globally. This observation also suggests a yet unidentified biological process whereby SORLA might indirectly affect the β -secretase, but not other secretases.

In the combined model where all parameters are estimated globally, approximately 75% of the fits show that α cleavage prefers dimer processing (Figures 3.10A and C), while β cleavage prefers monomer processing (Figures 3.10B and D) with and without SORLA. As shown experimentally (Figure 8 of [Schmidt et al. 2012]), SORLA does not interact directly with the α - and β -secretases. Therefore, complex formation with the secretases was not considered in the model.

In this model, where all parameters with the exception of $K_{M\beta}$ and $K_{M\beta d}$ are estimated globally (Figure 3.9), there is support for the hypothesis of a switch from dimer processing in the absence of SORLA to monomer processing in the presence of SORLA in 80% of the global-local fits. This is in agreement with our experimental finding that SORLA disrupts oligomerization of APP (as suggested in Figure 10 of [Schmidt et al. 2012]). The remaining 20% of the fits show beta cleavage prefers monomer processing in both the absence and presence of SORLA.

3. Mathematical modeling of SORLA's influence on amyloidogenic processing

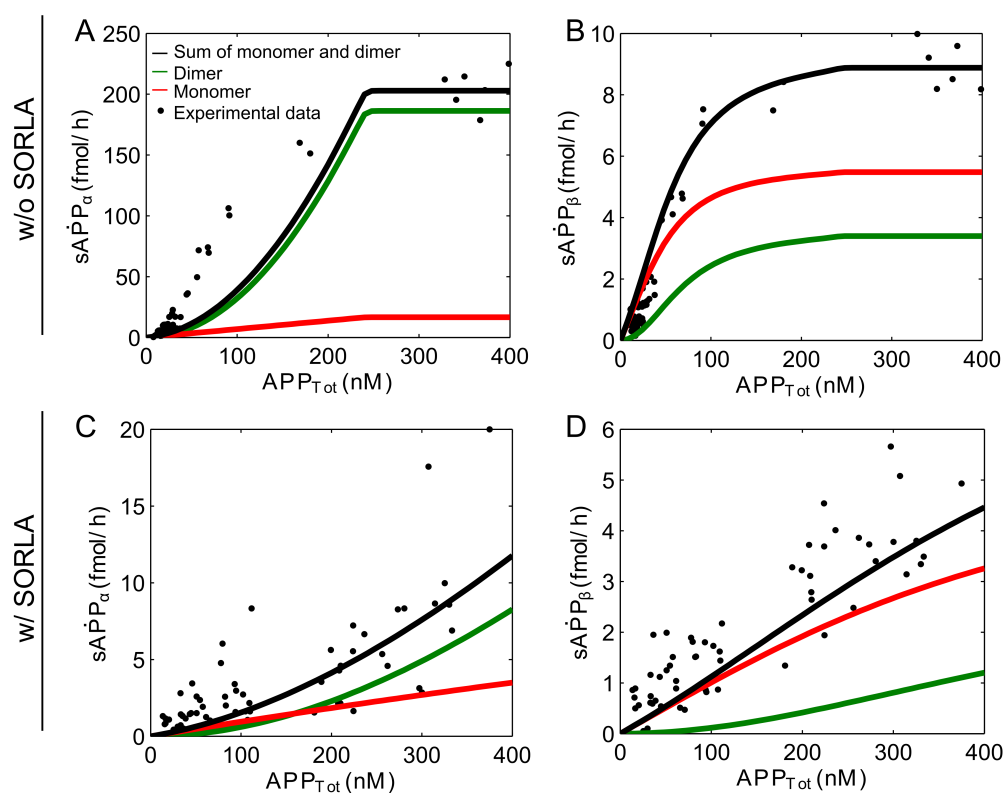


Figure 3.9.: Purely global parameter estimation for the simulation of a model with both monomer and dimer processing. Simulation results of the mathematical model (solid lines) for the various APP processing products are shown together with the actual data points obtained from biochemical experiments. The total amount of products (black line) is the sum of the products produced in the monomer (red line) and dimer processing (green line) pathways. From the simulations of $sAPP\alpha$ and $sAPP\beta$ in the absence (**A-B**) and presence (**A-B**) of SORLA, the simulation of $sAPP\alpha$ (**A**) shows inconsistency with the $sAPP\alpha$ from the experiments.

3.3. When one pathway is not enough

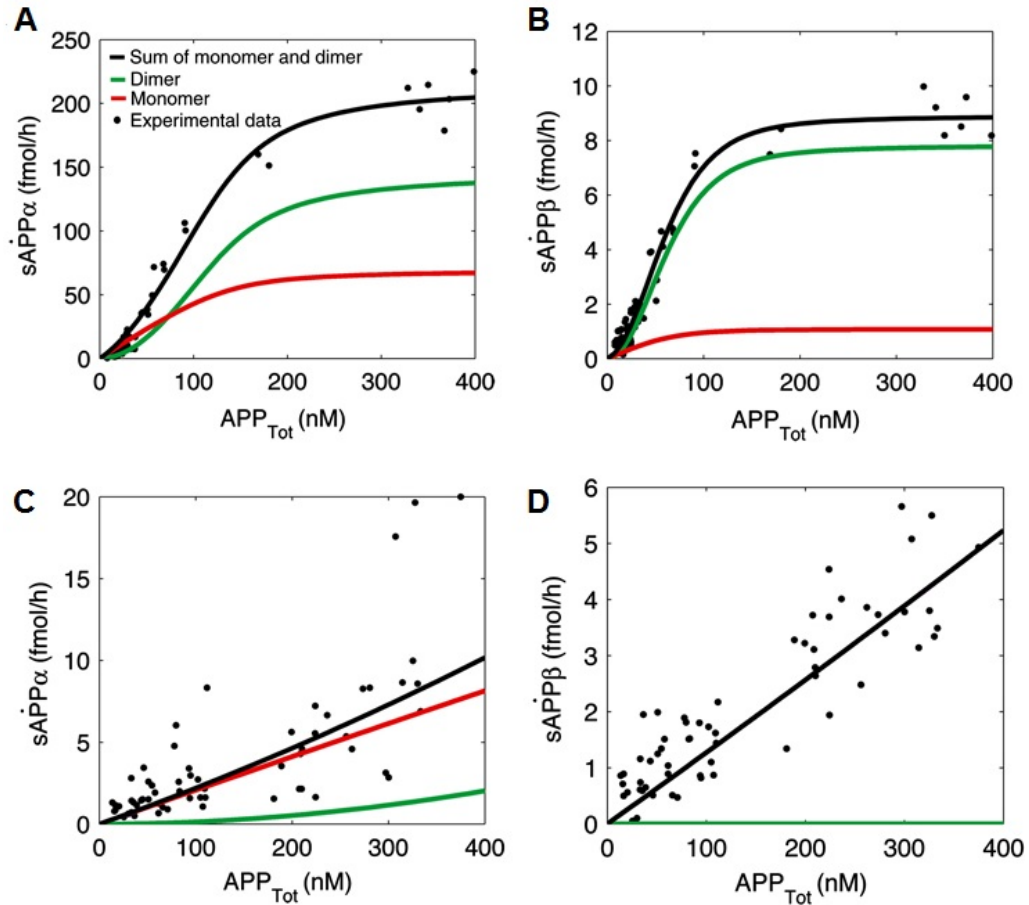


Figure 3.10.: Mathematical modeling of monomeric and dimeric forms of APP processing and its influence by SORLA. Simulation results of the mathematical model (solid lines) for the various APP processing products are shown together with the actual data points obtained from biochemical experiments. The total amount of products (black line) is the sum of the products produced in the monomer (red line) and dimer processing (green line) pathways. In the absence of SORLA, the ‘dimer processing’ more closely resembles the combined model for $sAPP_{\alpha}$ (A) and $sAPP_{\beta}$ (B). In contrast, in the presence of SORLA, it is the ‘monomer processing’ that closely resembles the combined model for both processing products (C, D). In (D), the black and red lines are superimposed.

3. Mathematical modeling of SORLA's influence on amyloidogenic processing

Mathematical modeling confirms SORLA-dependent mode of secretase action

In the absence of SORLA, the sigmoidal curve characteristic for dimer processing (green lines in Figure 3.10A and B) has a strong impact on the combined model (black lines in Figure 3.10A and B) that describes the experimental data sets for sAPP α (black dots in Figure 3.10A) and sAPP β (black dots in Figure 3.10B). In contrast, in the presence of the receptor, the monomer processing (red lines in Figure 3.10C and D) in the combined model (black lines in Figure 3.10C and D) cause the combined model to closely resemble the experimental data for both sAPP α (black dots in Figure 3.10C) and sAPP β (black dots in Figure 3.10D).

Intermediate levels of SORLA

So far, our model has considered the two most extreme scenarios with either no (Figure 3.10A and B) or high levels of SORLA activity (Figure 3.10C and D) as in CHO pTet-APP and CHO-S pTet-APP, respectively. However *in vivo*, subtle alterations in intermediary SORLA levels are likely more relevant for determining the APP processing rates. Accordingly, we next adapt our model to intermediary concentrations of SORLA to define the exact point at which the switch from cooperative to non-cooperative secretase activity may occur. To do so, we have applied several approaches to estimate the relationship between SORLA concentration and quantitative parameter values for secretase activity.

We calculated the intermediate levels of SORLA expression between the cooperative and non-cooperative regimens in an indirect manner. Since the two parameters, $K_{M\beta}$ and $K_{M\beta d}$, are fitted locally, the global-local estimation describes an indirect influence of SORLA. Figure 3.11 shows the empirically derived (almost exponential) dependencies of $K_{M\beta}$ and $K_{M\beta d}$ on the intermediate levels of SORLA, where it is ensured that the simulations of the intermediate curves for $s\dot{A}P\dot{P}\alpha_{Tot}$ and $s\dot{A}P\dot{P}\beta_{Tot}$ (blue dashed curves Figure 3.12A and B) stay smoothly in between the curves with and without SORLA (black curves in Figure 3.12A and B). As we decreased the amount of SORLA, the intermediate curves stay smoothly in between the curves with and without SORLA.

The simulations of the dose response curves of $s\dot{A}P\dot{P}\alpha_{Tot}$, $s\dot{A}P\dot{P}\beta_{Tot}$ (total processing in black curves), $s\dot{A}P\dot{P}\alpha$, $s\dot{A}P\dot{P}\beta$ (monomer processing in red curves) and $s\dot{A}P\dot{P}\alpha^*$, and $s\dot{A}P\dot{P}\beta^*$ (dimer processing in green curves) for intermediate levels of SORLA expression are shown in Figure 3.12C-H. Based on the simulated dose-response kinetics of total sAPP α and sAPP β production that are dependent on three intermediate SORLA expression levels (3%, 12%, and 30% of SORLA $_{Tot}$ of CHO-S pTet-APP; Figure 3.12A and B),

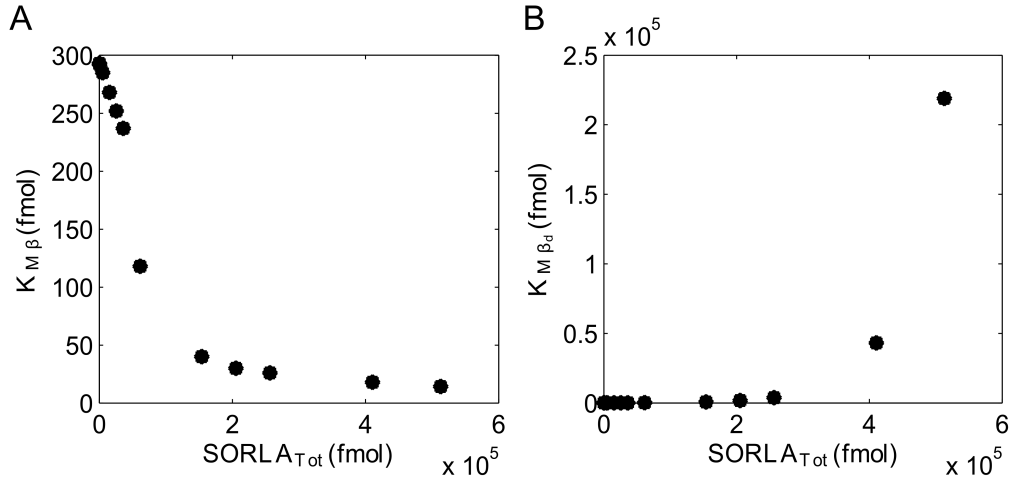


Figure 3.11.: Dependence of $K_{M\beta}$ and $K_{M\beta d}$ on SORLA. The intermediate levels of SORLA expression are calculated in an indirect manner by empirically determining the dependencies of $K_{M\beta}$ (A) and $K_{M\beta d}$ (B) on the intermediate levels of SORLA.

we have predicted that a switch from cooperative (dimer) to less efficient non-cooperative (monomer) processing occurs at a SORLA concentration that is $0.12 \times SORLA_{Tot}$ of CHO-S pTet-APP (where $SORLA_{Tot}$ equals 5.13×10^5 fmol) (Figure 3.12E and F).

Taken together, our quantitative biochemical data and the simulations shown in Figures 3.10 and 3.12 strongly support a model whereby SORLA prevents oligomerization of APP, thereby shifting the mode of secretase action from use of the preferred homodimeric substrate to the less preferred monomer variant.

Summary and conclusions

Mathematical models, in the context of the APP processing influenced by SORLA in AD, were developed to analyze and study the characteristics observed in the series of experimental data that we generated [Schmidt et al. 2012]. We have shown that monomeric APP is insufficient for describing the influence of SORLA during processing, which is similar to the processing of APP in dimeric form. However, by merging the monomer and dimer processing steps, we have shown that the simulation of the combined model, is in line with the experimental observations through global local parameter estimation.

Simulations of the parameterized mathematical model using both monomer and dimer processing are in agreement with the experimental data (Figure 3.10A-D). The combined model has the lowest residual value (2.15×10^1 and 3.10×10^1 for global-local and global parameter estimation, respectively) compared to the model with only monomer processing

3. Mathematical modeling of SORLA's influence on amyloidogenic processing

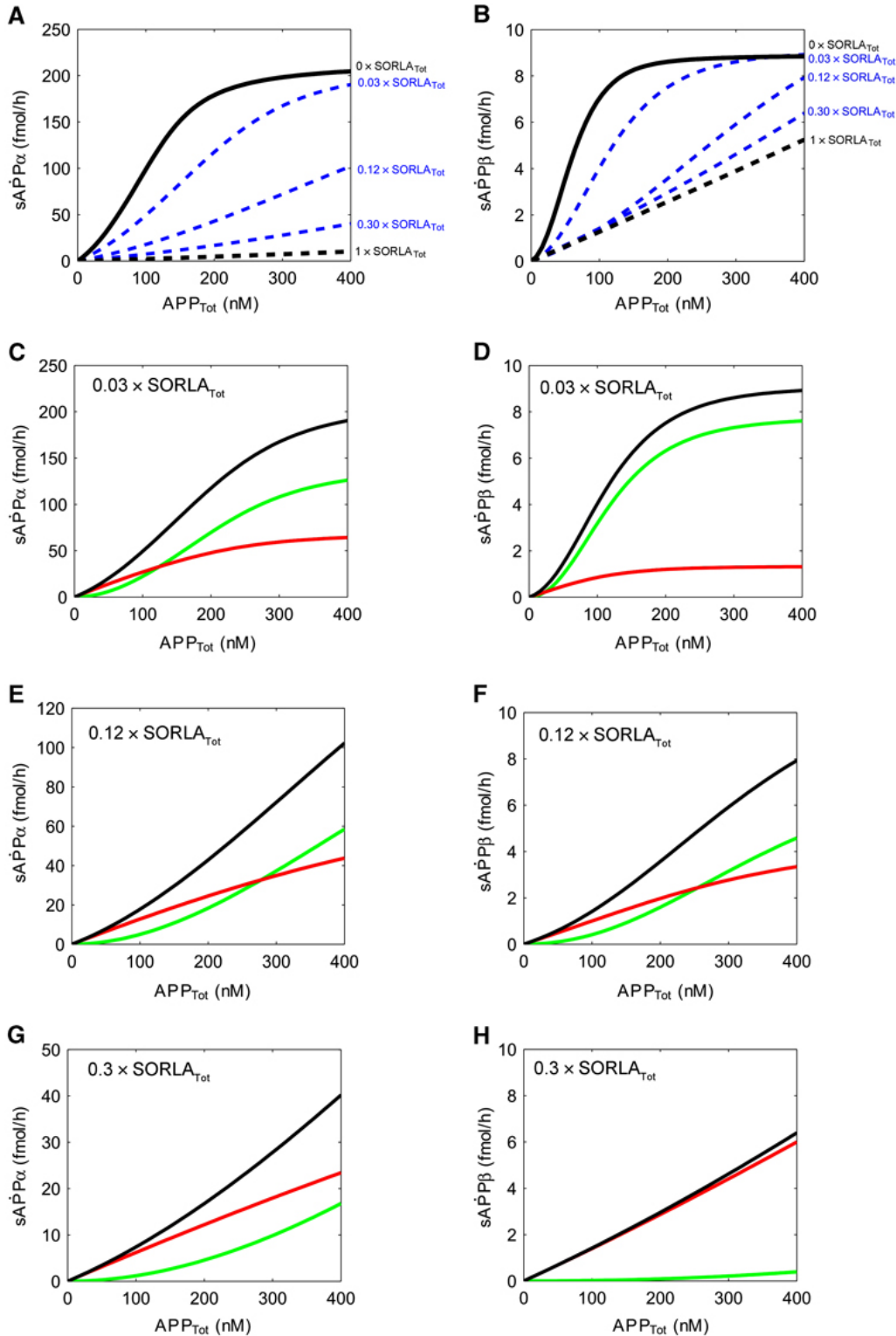


Figure 3.12.: APP processing at intermediate levels of SORLA. (A, B) Simulations of the influence of intermediate levels of SORLA on APP processing into sAPP α (A) and sAPP β (B) are shown. The dashed black lines in (A, B) represent the values for maximum levels of SORLA $_{Tot}$ (5.13×10^5 fmol) as in CHO-S pTet-APP (set at arbitrary value $1 \times SORLA_{Tot}$). The solid black lines represent the situation in the absence of SORLA as in CHO pTet-APP (set at $0 \times SORLA_{Tot}$). Simulations of total processing for three intermediates levels of SORLA (3%, 12%, and 30% of SORLA $_{Tot}$) were calculated as detailed in the Appendix, and are shown as blue stippled lines. (CH) Simulation curves for APP processing into sAPP α and sAPP β for intermediate levels of 3% (C, D), 12% (E, F), and 30% of SORLA $_{Tot}$ (G, H) are given. Total APP processing (black lines) as well as dimer (green lines) and monomer (red lines) processing are indicated for each simulation. A switch from preferred dimer-to-monomer processing is observed at $0.12 \times SORLA_{Tot}$ for both α -secretase (E) and β -secretase (F).

3.3. When one pathway is not enough

(best residual value 1.12×10^2) or the model with only dimer processing (best residual value 1.48×10^2). A comparison of models using statistical criteria, such as the Akaike information criterion, requires standard deviations, which is why we used residuals to compare the models.

For the reasons described above, we used the biochemical evidence gathered in this study to develop the first mathematical model describing the combined action of secretases and SORLA in APP processing. Obviously, this model represents a simplified view of APP processing, as it only considers a single cellular compartment, and regulated trafficking of APP by SORLA through the intracellular compartments critically affects amyloidogenic and non-amyloidogenic processing (reviewed in [Willnow et al. 2008]). In addition, the observation that our model requires a local parameter estimate for β -secretase activity in the presence or absence of SORLA in order to closely resemble the experimental data suggests that additional indirect effects of the receptor on this enzyme contribute to regulation of amyloidogenic processing in the context of an intact cell. Whether these effects entail interference of SORLA with the ability of BACE to bind APP [Spoelgen et al. 2006] or other yet unknown mechanisms remains to be elucidated. Nevertheless, the fact that secretases switch their mode of action in the presence of the receptor demonstrates that its function is more complex than simply preventing transport of APP into compartments where the enzymes reside. The strong agreement of the mathematical model with the experimental data strongly argues that depletion of APP dimer processing represents a major molecular mechanism whereby SORLA affects the fate of APP processing. Conceptually, this model represents a unique tool for mapping the quantitative contribution of additional cis-acting factors to APP processing and perhaps even to stratify the amyloidogenic burden in individuals with a given ratio of APP and SORLA.

COMPARTMENTAL-BASED BEHAVIOR OF THE SYSTEM

In our initial attempts to simulate amyloidogenic processing in AD, we developed a single-compartment model to describe APP processing in Section 3.3 [Schmidt et al. 2012]. While this model has been valuable for establishing the kinetics of amyloidogenic processing and the quantitative contribution of SORLA to this pathway, a single-compartment model is expected to fall short of accurately describing the complexity of APP processing in cells that have a heterogeneous spatial environment. It remained unclear to what extent SORLA may affect APP monomer versus dimer processing and in what compartment of the cell its activity may be most relevant. Moreover, the possible influence of SORLA on the dynamics of β -secretase remains unclear. Such an effect have been previously postulated based on studies in cultured cells [Spoelgen et al. 2006]. Therefore, to answer these questions, in this chapter, we establish a multi-compartment model that represents APP processing in both its monomeric and dimeric forms [Lao et al. 2012]. The formalism of this model was developed to integrate experimental evidence from previous biochemical and cell biological studies by Andersen et al. [2005, 2006], Offe et al. [2006], Spoelgen et al. [2006], Rogaeva et al. [2007], Schmidt et al. [2007], and Dodson et al. [2008]. We combine our multi-compartment model with the dose-response data of APP and soluble APP products. The data shown in Figure 2.4 were then used to estimate the parameter values of our model. Using our multi-compartment model, we (i) establish the activity distribution of APP in various compartments, and (ii) trace the activity distribution of APP, α -secretase, β -secretase, and SORLA in the monomeric and dimeric processing of APP.

4. Compartmental-based behavior of the system

4.1. Conventional compartmental modeling: pros and cons

Compartmental models play a key role in understanding many processes in biological and medical sciences. Such models are composed of homogeneous interconnected subsystems (or compartments) that exchange variable nonnegative quantities of material with conservation laws that describe transfer, accumulation, and outflows between compartments and the environment. The range of applications of compartmental systems is not limited to biological and medical systems. They are also applied to chemical reaction systems, queuing systems, ecological systems, economic systems, telecommunication systems, transportation systems, and power systems, to name but a few examples. In conventional compartmental systems that are used to model chemical reaction systems, the compartments represent quantities of different chemical substances contained within the compartment, and the compartmental flows characterize transformation rates of reactant to products [Haddad et al. 2010].

Take for example the three compartment system that is illustrated below (in Figure 4.1):

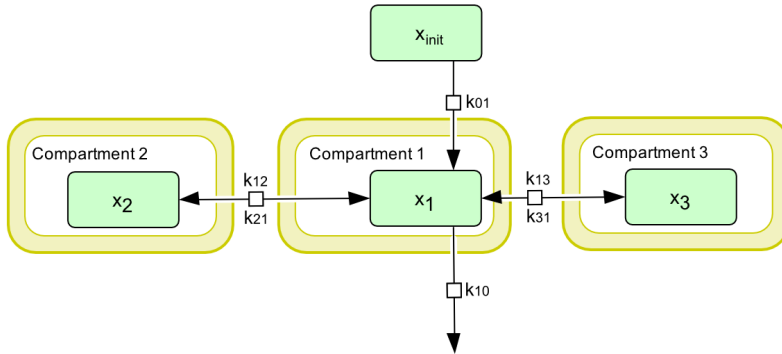


Figure 4.1.: Three-compartment toy model for disposition of protein X . Initial amount of protein X , x_{init} , transfers to Compartment 1, and further transfers to either Compartment 2 or Compartment 3. At an elimination rate of k_{10} , a certain amount of protein X from Compartment 1 flows out to another environment.

The toy model in Figure 4.1 describes the distribution of protein X into three compartments. Assuming mass balance for the entire compartmental system, it yields the following ODEs:

$$\left. \begin{aligned} \dot{x}_{init} &= -k_{01} \cdot x_{init} \\ \dot{x}_1 &= -(k_{12} + k_{13} + k_{10}) \cdot x_1 + k_{21} \cdot x_2 + k_{31} \cdot x_3 + k_{01} \cdot x_{init} \\ \dot{x}_2 &= -k_{21} \cdot x_2 + k_{12} \cdot x_1 \\ \dot{x}_3 &= -k_{31} \cdot x_3 + k_{13} \cdot x_1 \end{aligned} \right\} \quad (4.1)$$

where (1) $x_1, x_2, x_3 \geq 0$ are the quantities of protein X in compartment 1, 2, and 3, respectively; (2) x_{init} is the initial amount of protein X in quantity; (3) k_{01} and $k_{ij} \geq 0, i \neq j$

4.2. Multi-compartmental modeling of APP processing influenced by SORLA

$j, i, j = \{1, 2, 3\}$, are the rate constant in time^{-1} for the transfer between compartments; and (4) k_{10} in time^{-1} is the rate constant for elimination from compartment 1. Assuming 100 units of quantity for x_{init} , the simulations of the model in Equations 4.1 are shown below (Figure 4.2). The model shows the quantities of protein X in all three compartments versus time.

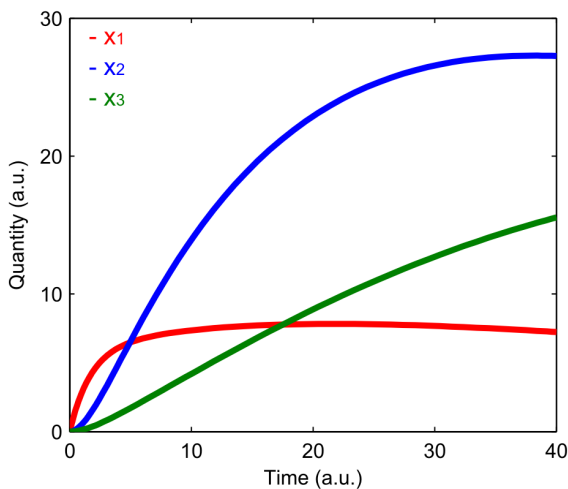


Figure 4.2.: Simulations of a three-compartmental toy model. The compartmental quantities of x_1 , x_2 , and x_3 versus time.

The conventional compartmental modeling inspired the structure of our multi-compartmental model. However, as we have emphasized earlier in Section 2.1, the type of experimental data we have (i.e. dose-response data) is different than the time series data that is conventionally used in compartmental modeling. Therefore, additional assumptions and constraints are necessary when building our model.

4.2. Multi-compartmental modeling of APP processing influenced by SORLA

This section is adapted from Lao et al. 2012. The multi-compartmental model [Lao et al. 2012] is an extension of the single-compartment model [Schmidt et al. 2012] presented in Section 3.3. The choice of the compartments considered in Figure 4.3 was based on the different locations where APP is shown to interact with SORLA as well as with α - and β -secretases. The corresponding three compartments are the TGN, the cell surface, and the endosomes [Andersen et al. 2005; Spoelgen et al. 2006; Willnow et al. 2008]. Note that the transport of APP among these compartments indirectly interconnects these three compartments to one another. As SORLA affects the initial cleavage of APP by α - and β -secretases [Schmidt et al. 2007], which are the rate limiting steps that determine the extent of amyloidogenic processing. Further processing steps involving γ -secretase, are

4. Compartmental-based behavior of the system

not included in this model.

In order to accommodate the monomeric and dimeric forms of APP, each compartment shown in Figure 4.3 is further divided into two subcompartments: a “red” subcompartment for APP monomer processing and a “green” subcompartment for APP dimer processing. Notice that the monomeric forms of APP, SORLA, α -secretase, and β -secretase, within the two subcompartments, are annotated differently: APP_{G1} , $SORLA_{G1}$, α_1 , and β_1 for monomer processing, and APP_{G2} , $SORLA_{G2}$, α_2 , and β_2 for dimer processing. Even so, the components from the two subcompartments are linked to each other through APP_{init} , α_{init} , and β_{init} . Moreover, APP_{G2} , α_2 , and β_2 undergo dimerization before the start of APP dimer processing. That is, two APP_{G2} , α_2 , and β_2 monomers dimerize in order to form the corresponding dimeric forms. Conversely, these dimers can dissociate to generate their respective monomers. Note that subscript ‘1’ is assigned to the reactants and products in monomer processing, while subscript ‘2’ is assigned to those in dimer processing. In addition, we use subscripts ‘G’, ‘CS’, and ‘E’ for APP in the TGN, at the cell surface, and in the endosomes, respectively.

Up to this point, we have described the different forms of APP, α -secretase, and β -secretase in the diverse compartments prior to the beginning of APP processing. Because SORLA interacts with APP in a 1:1 stoichiometric complex [Andersen et al. 2005, 2006], the model describes how SORLA strictly interacts with APP-monomers (but not dimers) to form an APP-SORLA complex. Consequently, this interaction is responsible for the diminished level of APP-monomers (APP_{G1}) and APP-dimers (APP_{G2d}) transported from the TGN to the cell surface. This interaction decreases the amount of APP-monomers (APP_{CS1}) and APP-dimers (APP_{CS2d}) that end up in the endosomes as APP_{E1} and APP_{E2d} , respectively. Moreover, in order to determine whether SORLA will have a similar influence on the monomer and dimer processing, the binding affinity assigned to APP_{G1} - $SORLA_{G1}$ during monomer processing is different to that of APP_{G2} - $SORLA_{G2}$ during dimer processing [Lao et al. 2012].

After the interaction of SORLA and APP in the TGN, the remaining APP_{G1} and APP_{G2d} are transported to the cell surface where APP processing begins within the non-amyloidogenic pathway. Then, a small portion of APP_{CS1} and APP_{CS2d} , which is not cleaved by α -secretase, is further transported from the cell surface to the endosomes where the amyloidogenic pathway takes over. Notably, the interaction of APP and α -secretase at the cell surface leads to the formation of non-amyloidogenic products, such as $sAPP\alpha$ and C83, whereas the interaction of APP and β -secretase in the endosome yields amyloidogenic products, such as $sAPP\beta$ and C99. The model is established in such a way that

4.2. Multi-compartmental modeling of APP processing influenced by SORLA

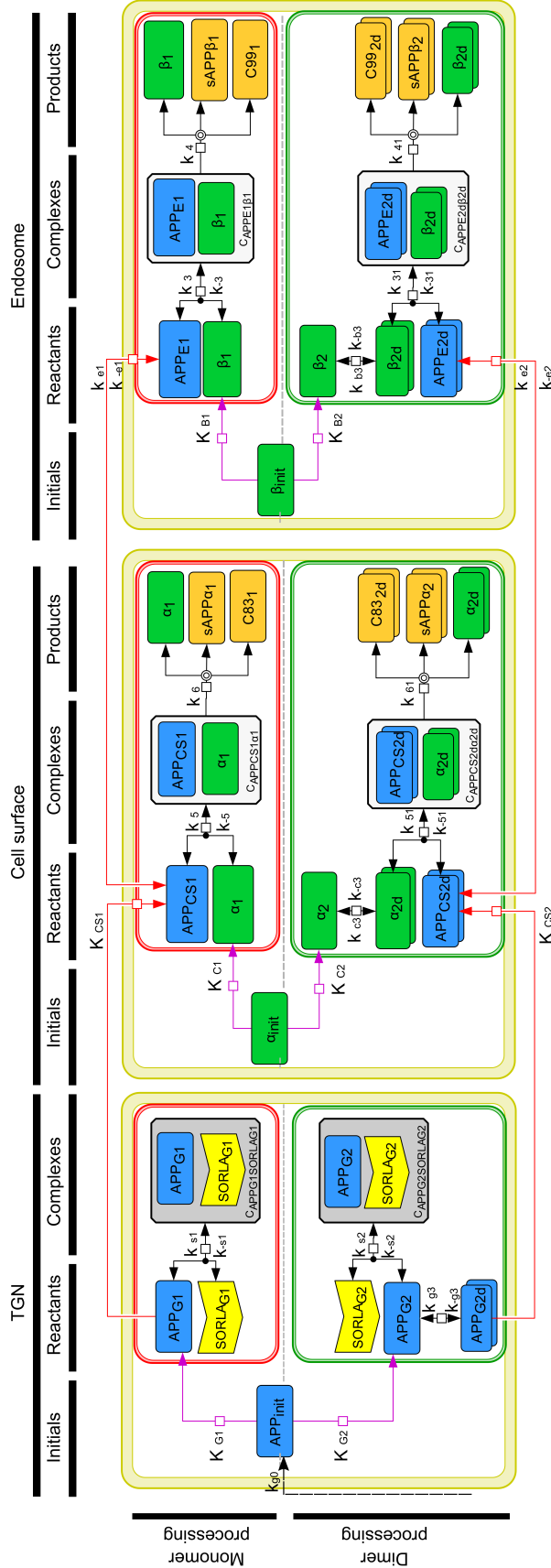


Figure 4.3.: Biochemical network of a multi-compartmental model describing the influence of SORLA in APP processing. The three main yellow compartments in the network are the trans-Golgi network (TGN), the cell surface, and the endosomes. Each compartment is subdivided into two subcompartments: a red subcompartment for APP monomer processing and a green subcompartment for dimer processing. The monomeric forms of APP, SORLA, α -secretase, and β -secretase, within the two subcompartments, are annotated differently: APP_{G1}, SORLA_{G1}, α_1 , and β_1 for monomer processing, and APP_{G2}, SORLA_{G2}, α_2 , and β_2 for dimer processing. Moreover, APP_{G1} binds to APP_{G1} while SORLA_{G2} binds to APP_{G2} in the green subcompartment. At the cell surface, APP_{C51} and APP_{C52d} are cleaved by α_1 and α_2 , respectively, producing soluble fragments encompassing the extracellular domain of APP. These fragments are called soluble (s) APP α_1 and sAPP α_2 , respectively. In addition, α -secretase cleavage produces a membrane-associated fragment containing the membrane anchor and the cytoplasmic tail, denoted as C83. In the endosomes, APP molecules that escaped cleavage by α -secretase (APP_{E1} and APP_{E2d}) are cleaved by β_1 and β_2 . Cleavage results in production of the soluble fragments of the extracellular APP domain (sAPP β_1 and sAPP β_2) and in the membrane-tethered fragments C99₁ and C99_{2d}. C99 includes the A β peptide sequence and represents the substrate for γ -secretase cleavage.

4. Compartmental-based behavior of the system

the dimeric form of secretases act only on the dimeric form of APP and the monomeric form of secretases act only on the monomeric form of APP [Lao et al. 2012].

Model equations

Based on the biochemical network shown in Figure 4.3, we established ODEs [Lao et al. 2012] that describe temporal changes of molecule numbers for the network components as a function of interaction and cleavage processes, such that the changes with large numbers of molecules can be assumed to be smooth. The components in our multi-compartment model [Lao et al. 2012], separated by the three different compartments and two different subcompartments, are annotated differently. Distinctly labeling the components allows for differentiation of the results generated from these multi-compartments. The notations that are used in the equations are described in Tables A.4 and A.5 of the Appendix section.

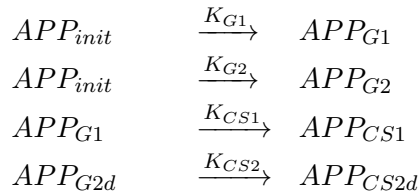
$$\begin{aligned}
\dot{APP}_{init} &= k_{g0} - (k_{g1} + k_{g2}) \cdot APP_{init} + k_{-g1} \cdot APP_{G1} + k_{-g2} \cdot APP_{G2} \\
\dot{APP}_{G1} &= k_{g1} \cdot APP_{init} - (k_{-g1} + k_{cs1}) \cdot APP_{G1} + k_{-cs1} \cdot APP_{CS1} - \\
&\quad k_{s1} \cdot APP_{G1} \cdot SORLAG1 + k_{-s1} \cdot C_{APPG1SORLAG1} \\
\dot{APP}_{G2} &= k_{g2} \cdot APP_{init} - k_{-g2} \cdot APP_{G2} + 2 \cdot (k_{-g3} \cdot APP_{G2d} - k_{g3} \cdot APP_{G2}^2) - \\
&\quad k_{s2} \cdot APP_{G2} \cdot SORLAG2 + k_{-s2} \cdot C_{APPG2SORLAG2} \\
\dot{APP}_{G2d} &= 2 \cdot (k_{g3} \cdot APP_{G2}^2 - k_{-g3} \cdot APP_{G2d}) - k_{cs2} \cdot APP_{G2d} + k_{-cs2} \cdot APP_{CS2d} \\
\dot{APP}_{CS1} &= k_{cs1} \cdot APP_{G1} - (k_{-cs1} + k_{e1}) \cdot APP_{CS1} + k_{-e1} \cdot APP_{E1} - \\
&\quad k_5 \cdot APP_{CS1} \cdot \alpha_1 + k_{-5} \cdot C_{APPCS1\alpha1} \\
\dot{APP}_{CS2d} &= k_{cs2} \cdot APP_{G2d} - (k_{-cs2} + k_{e2}) \cdot APP_{CS2d} + k_{-e2} \cdot APP_{E2d} - \\
&\quad k_{51} \cdot APP_{CS2d} \cdot \alpha_{2d} + k_{-51} \cdot C_{APPCS2d\alpha2d} \\
\dot{APP}_{E1} &= k_{e1} \cdot APP_{CS1} - k_{-e1} \cdot APP_{E1} - k_3 \cdot APP_{E1} \cdot \beta_1 + k_{-3} \cdot C_{APPE1\beta1} \\
\dot{APP}_{E2d} &= k_{e2} \cdot APP_{CS2d} - k_{-e2} \cdot APP_{E2d} - k_{31} \cdot APP_{E2d} \cdot \beta_{2d} + k_{-31} \cdot C_{APPE2d\beta2d} \\
\dot{\alpha}_{init} &= k_{-c1} \cdot \alpha_1 + k_{-c2} \cdot \alpha_2 - (k_{c1} + k_{c2}) \cdot \alpha_{init} \\
\dot{\alpha}_1 &= k_{c1} \cdot \alpha_{init} - k_{-c1} \cdot \alpha_1 - \dot{C}_{APPCS1\alpha1} \\
\dot{\alpha}_2 &= k_{c2} \cdot \alpha_{init} - k_{-c2} \cdot \alpha_2 - 2 \cdot (k_{c3} \cdot \alpha_2^2 - k_{-c3} \cdot \alpha_{2d}) \\
\dot{\alpha}_{2d} &= 2 \cdot (k_{c3} \cdot \alpha_2^2 - k_{-c3} \cdot \alpha_{2d}) - \dot{C}_{APPCS2d\alpha2d} \\
\dot{\beta}_{init} &= k_{-b1} \cdot \beta_1 + k_{-b2} \cdot \beta_2 - (k_{b1} + k_{b2}) \cdot \beta_{init} \\
\dot{\beta}_1 &= k_{b1} \cdot \beta_{init} - k_{-b1} \cdot \beta_1 - \dot{C}_{APPE1\beta1} \\
\dot{\beta}_2 &= k_{b2} \cdot \beta_{init} - k_{-b2} \cdot \beta_2 - 2 \cdot (k_{b3} \cdot \beta_2^2 - k_{-b3} \cdot \beta_{2d}) \\
\dot{\beta}_{2d} &= 2 \cdot (k_{b3} \cdot \beta_2^2 - k_{-b3} \cdot \beta_{2d}) - \dot{C}_{APPE2d\beta2d}
\end{aligned}$$

4.2. Multi-compartmental modeling of APP processing influenced by SORLA

$$\begin{aligned}
\dot{S}ORLA_{G1} &= -\dot{C}_{APPG1SORLAG1} \\
\dot{S}ORLA_{G2} &= -\dot{C}_{APPG2SORLAG2} \\
\dot{C}_{APPG1SORLAG1} &= k_{s1} \cdot APP_{G1} \cdot SORLA_{G1} - k_{-s1} \cdot C_{APPG1SORLAG1} \\
\dot{C}_{APPG2SORLAG2} &= k_{s2} \cdot APP_{G2} \cdot SORLA_{G2} - k_{-s2} \cdot C_{APPG2SORLAG2} \\
\dot{C}_{APPCS1\alpha1} &= k_5 \cdot APP_{CS1} \cdot \alpha_1 - (k_{-5} + k_6) \cdot C_{APPCS1\alpha1} \\
\dot{C}_{APPCS2d\alpha2d} &= k_{51} \cdot APP_{CS2d} \cdot \alpha_{2d} - (k_{-51} + k_{61}) \cdot C_{APPCS2d\alpha2d} \\
\dot{C}_{APPE1\beta1} &= k_3 \cdot APP_{E1} \cdot \beta_1 - (k_{-3} + k_4) \cdot C_{APPE1\beta1} \\
\dot{C}_{APPE2d\beta2d} &= k_{31} \cdot APP_{E2d} \cdot \beta_{2d} - (k_{-31} + k_{41}) \cdot C_{APPE2d\beta2d} \\
s\dot{A}PP\alpha_1 &= k_6 \cdot C_{APPCS1\alpha1} \\
\dot{C}83_1 &= k_6 \cdot C_{APPCS1\alpha1} \\
s\dot{A}PP\alpha_2 &= 2 \cdot k_{61} \cdot C_{APPCS2d\alpha2d} \\
\dot{C}83_{2d} &= k_{61} \cdot C_{APPCS2d\alpha2d} \\
s\dot{A}PP\beta_1 &= k_4 \cdot C_{APPE1\beta1} \\
\dot{C}99_1 &= k_4 \cdot C_{APPE1\beta1} \\
s\dot{A}PP\beta_2 &= 2 \cdot k_{41} \cdot C_{APPE2d\beta2d} \\
\dot{C}99_{2d} &= k_{41} \cdot C_{APPE2d\beta2d}
\end{aligned}$$

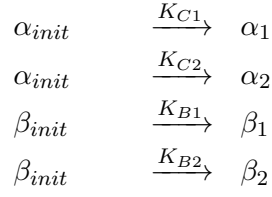
Herein, we show a series of assumptions that allow for the reduction of the equations [Lao et al. 2012]. Firstly, we start with the transportation of APP, α -secretase, and β -secretase among the three compartments and between the two subcompartments. Recall that the (i) APP-monomers and APP-dimers are transported from the TGN to the cell surface, and are then further transported to the endosomes, (ii) monomeric forms of APP, SORLA, α -secretase, and β -secretase within the two subcompartments are annotated differently, and (iii) components within the two subcompartments are linked to each other through APP_{init} , α_{init} , and β_{init} . These properties are reflected by introducing the following biochemical reactions:

For APP,



and for the secretases,

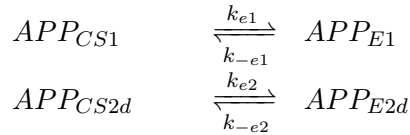
4. Compartmental-based behavior of the system



where the second reactant is assumed to be in quasi-equilibrium with the first reactant. Without loss of generality, the concentration of the second reactant is related to the first reactant by an ordinary equilibrium expression, such as

$$\left. \begin{array}{l}
 APP_{G1} = K_{G1} \cdot APP_{init} , \text{ where } K_{G1} = \frac{k_{g1}}{k_{-g1}}, \\
 APP_{G2} = K_{G2} \cdot APP_{init} , \text{ where } K_{G2} = \frac{k_{g2}}{k_{-g2}}, \\
 APP_{CS1} = K_{CS1} \cdot APP_{G1} , \text{ where } K_{CS1} = \frac{k_{cs1}}{k_{-cs1}}, \\
 APP_{CS2d} = K_{CS2} \cdot APP_{G2d} , \text{ where } K_{CS2} = \frac{k_{cs2}}{k_{-cs2}}, \\
 \alpha_1 = K_{C1} \cdot \alpha_{init} , \text{ where } K_{C1} = \frac{k_{c1}}{k_{-c1}}, \\
 \alpha_2 = K_{C2} \cdot \alpha_{init} , \text{ where } K_{C2} = \frac{k_{c2}}{k_{-c2}}, \\
 \beta_1 = K_{B1} \cdot \beta_{init} , \text{ where } K_{B1} = \frac{k_{b1}}{k_{-b1}}, \\
 \beta_2 = K_{B2} \cdot \beta_{init} , \text{ where } K_{B2} = \frac{k_{b2}}{k_{-b2}}.
 \end{array} \right\} \quad (4.2)$$

As for

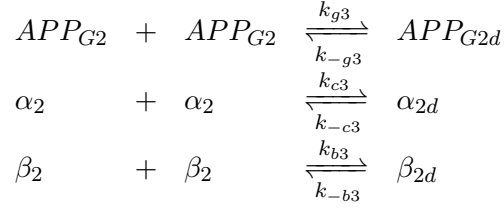


the ratio of the association constant is taken into consideration. This assumption permits the two reactants to be related to each other by an association constant, such that

$$\left. \begin{array}{l}
 APP_{E1} = K_{E1} \cdot APP_{CS1} , \text{ where } K_{E1} = \frac{k_{e1}}{k_{-e1}}, \\
 APP_{E2d} = K_{E2} \cdot APP_{CS2d} , \text{ where } K_{E2} = \frac{k_{e2}}{k_{-e2}}.
 \end{array} \right\} \quad (4.3)$$

Secondly, the monomeric forms of APP, α -secretase, and β -secretase in dimer processing undergo dimerization. In other words, two monomeric forms of APP, α -secretase, or β -secretase are dimerized, and a dimeric form of APP, α -, or β -secretase is dissociated, as shown by the reactions below:

4.2. Multi-compartmental modeling of APP processing influenced by SORLA

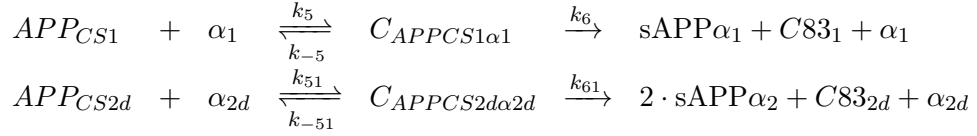


As we take into account the association constant of each reaction above, it allows us to generate the following representation of the equation:

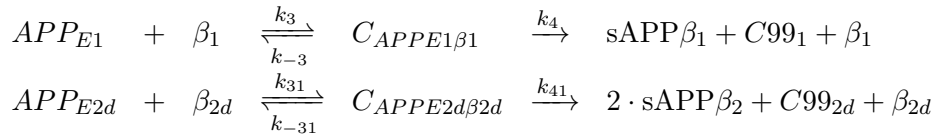
$$\left. \begin{array}{l}
 APP_{G2d} = K_{G3} \cdot APP_{G2}^2, \text{ where } K_{G3} = \frac{k_{g3}}{k_{-g3}}, \\
 \alpha_{2d} = K_{C3} \cdot \alpha_2^2, \text{ where } K_{C3} = \frac{k_{c3}}{k_{-c3}}, \\
 \beta_{2d} = K_{B3} \cdot \beta_2^2, \text{ where } K_{B3} = \frac{k_{b3}}{k_{-b3}}.
 \end{array} \right\} \quad (4.4)$$

So far, we have established equations that describe the relationship of APP, α -secretase, or β -secretase, which are defined in the three different compartments.

Thirdly, at the cell surface, APP interacts with α -secretase through the following reactions



Whereas in the endosomes, the following reactions take place:



For the ODEs of the complexes above, a quasi-steady state can be assumed. This allows the complexes to be represented as:

$$\left. \begin{array}{l}
 C_{APPCS1\alpha1} = \frac{\alpha_1 \cdot APP_{CS1}}{K_{M\alpha1}}, \text{ where } K_{M\alpha1} = \frac{k_{-5} + k_6}{k_5} \\
 C_{APPE1\beta1} = \frac{\beta_1 \cdot APP_{E1}}{K_{M\beta1}}, \text{ where } K_{M\beta1} = \frac{k_{-3} + k_4}{k_3} \\
 C_{APPCS2d\alpha2d} = \frac{\alpha_{2d} \cdot APP_{CS2d}}{K_{M\alpha2d}}, \text{ where } K_{M\alpha2d} = \frac{k_{-51} + k_{61}}{k_{51}} \\
 C_{APPE2d\beta2d} = \frac{\beta_{2d} \cdot APP_{E2d}}{K_{M\beta2d}}, \text{ where } K_{M\beta2d} = \frac{k_{-31} + k_{41}}{k_{31}}
 \end{array} \right\} \quad (4.5)$$

These equations for the complexes are substituted into the ODEs that describe the formation of the sAPP products: the ODEs of the sAPP products in the monomeric form of

4. Compartmental-based behavior of the system

APP processing can be rewritten as

$$\left. \begin{aligned} sA\dot{P}P\alpha_1 &= k_6 \cdot \frac{\alpha_1 \cdot APP_{CS1}}{K_{M\alpha 1}} \\ sA\dot{P}P\beta_1 &= k_4 \cdot \frac{\beta_1 \cdot APP_{E1}}{K_{M\beta 1}} \end{aligned} \right\} \quad (4.6)$$

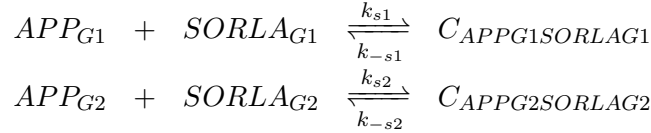
whereas those in the dimeric form of APP processing can be written in the following form

$$\left. \begin{aligned} sA\dot{P}P\alpha_2 &= 2 \cdot k_{61} \cdot \frac{\alpha_{2d} \cdot APP_{CS2d}}{K_{M\alpha 2d}} \\ sA\dot{P}P\beta_2 &= 2 \cdot k_{41} \cdot \frac{\beta_{2d} \cdot APP_{E2d}}{K_{M\beta 2d}} \end{aligned} \right\} \quad (4.7)$$

From Equations 4.6 and 4.7, we obtain

$$\left. \begin{aligned} sA\dot{P}P\alpha_{Tot} &= sA\dot{P}P\alpha_1 + sA\dot{P}P\alpha_2 \\ sA\dot{P}P\beta_{Tot} &= sA\dot{P}P\beta_1 + sA\dot{P}P\beta_2 \end{aligned} \right\} \quad (4.8)$$

Fourthly, recall that APP_{G1} binds to $SORLA_{G1}$ with a binding affinity of K_{S1} in monomer processing, whereas APP_{G2} binds to $SORLA_{G2}$ with a different affinity K_{S2} in dimer processing, where $K_{S1} = k_{s1}/k_{-s1}$ and $K_{S2} = k_{s2}/k_{-s2}$, respectively. These properties are reflected in the biochemical reactions below:



We then take into consideration the rapid-equilibrium assumption for the $C_{APPG1SORLAG1}$ and $C_{APPG2SORLAG2}$ complexes, which gives

$$\left. \begin{aligned} C_{APPG1SORLAG1} &= K_{S1} \cdot SORLA_{G1} \cdot APP_{G1}, \text{ where } K_{S1} = \frac{k_{s1}}{k_{-s1}}, \\ C_{APPG2SORLAG2} &= K_{S2} \cdot SORLA_{G2} \cdot APP_{G2}, \text{ where } K_{S2} = \frac{k_{s2}}{k_{-s2}}. \end{aligned} \right\} \quad (4.9)$$

Lastly, the ODEs include conservation laws for the enzymes and substrates. Herein, we take into account Equations 4.2 to 4.5 and 4.9 that are shown above. Regardless of SORLA, the total amount of APP, α -secretase, β -secretase, and SORLA that are conserved in the system are represented by the following equations:

$$\alpha_{Tot} = \alpha_{init} + \alpha_{monomer} + \alpha_{dimer} \quad (4.10)$$

$$\beta_{Tot} = \beta_{init} + \beta_{monomer} + \beta_{dimer} \quad (4.11)$$

$$APP_{Tot} = APP_{init} + APP_{monomer} + APP_{dimer} \quad (4.12)$$

$$SORLA_{Tot} = SORLA_{monomer} + SORLA_{dimer} \quad (4.13)$$

4.2. Multi-compartmental modeling of APP processing influenced by SORLA

In order to differentiate the functions in the presence and absence of SORLA, the reactants and complexes are denoted as functions with respect to the reactants that they depend on in the process of computation. For example, $f(x_1, y_1)$ is the function f that is dependent on the representation of x_1 and y_1 .

In the absence of SORLA,

$$\left. \begin{aligned}
 \alpha_{monomer} &= \alpha_1(\alpha_{init}) + C_{APPCS1\alpha1}(APP_{init}, \alpha_{init}) \\
 \alpha_{dimer} &= \alpha_2(\alpha_{init}) + 2 \cdot [\alpha_{2d}(\alpha_{init}) + C_{APPCS2d\alpha2d}(APP_{init}, \alpha_{init})] \\
 \beta_{monomer} &= \beta_1(\beta_{init}) + C_{APPE1\beta1}(APP_{init}, \beta_{init}) \\
 \beta_{dimer} &= \beta_2(\beta_{init}) + 2 \cdot [\beta_{2d}(\beta_{init}) + C_{APPE2d\beta2d}(APP_{init}, \beta_{init})] \\
 APP_{monomer} &= APP_{G1}(APP_{init}) + APP_{CS1}(APP_{init}) + APP_{E1}(APP_{init}) + \\
 &\quad C_{APPCS1\alpha1}(APP_{init}, \alpha_{init}) + C_{APPE1\beta1}(APP_{init}, \beta_{init}) \\
 APP_{dimer} &= APP_{G2}(APP_{init}) + 2 \cdot [APP_{G2d}(APP_{init}) + \\
 &\quad APP_{CS2d}(APP_{init}) + APP_{E2d}(APP_{init}) + \\
 &\quad C_{APPCS2d\alpha2d}(APP_{init}, \alpha_{init}) + C_{APPE2d\beta2d}(APP_{init}, \beta_{init})]
 \end{aligned} \right\} \quad (4.14)$$

The equations above are substituted into Equations 4.10 to 4.12, and APP_{init} , α_{init} and β_{init} are solved with respect to APP_{Tot} , α_{Tot} and β_{Tot} .

For APP_{Tot} without SORLA,

$$\left. \begin{aligned}
 APP_{Tot} &= APP_{init} + K_{G2} \cdot APP_{init} + K_{G1} \cdot APP_{init} \cdot \left\{ 1 + \right. \\
 &\quad \left. K_{CS1} \cdot \left[1 + \frac{K_{C1} \cdot \alpha_{init}}{K_{M\alpha1}} \right] + K_{E1} \cdot K_{CS1} \cdot \left[1 + \frac{K_{B1} \cdot \beta_{init}}{K_{M\beta1}} \right] \right\} + \\
 &\quad 2 \cdot K_{G3} \cdot (K_{G2} \cdot APP_{init})^2 \cdot \left\{ 1 + K_{CS2} \cdot \left[1 + \frac{K_{C3} \cdot (K_{C2} \cdot \alpha_{init})^2}{K_{M\alpha2d}} \right] + \right. \\
 &\quad \left. K_{E2} \cdot K_{CS2} \cdot \left[1 + \frac{K_{B3} \cdot (K_{B2} \cdot \beta_{init})^2}{K_{M\beta2d}} \right] \right\}
 \end{aligned} \right\} \quad (4.15)$$

Due to the complexity of Equation 4.15, the computation of APP_{init} with respect to APP_{Tot} will not be shown algebraically, but rather will be solved using the `fzero` function that is available in MATLAB. Nevertheless, the algebraic computation for α_{init} and β_{init} are shown below. We will show the computation for α_{init} and the solution for β_{init} will follow similarly. Take α_{Tot} for example: $\alpha_{monomer}$ and α_{dimer} from Equation 4.14 are substituted into Equation 4.10, which leads to

$$\begin{aligned}
 \alpha_{Tot} &= \alpha_{init} + [\alpha_1(\alpha_{init}) + C_{APPCS1\alpha1}(APP_{init}, \alpha_{init})] + \\
 &\quad \{\alpha_2(\alpha_{init}) + 2 \cdot [\alpha_{2d}(\alpha_{init}) + C_{APPCS2d\alpha2d}(APP_{init}, \alpha_{init})]\}
 \end{aligned}$$

4. Compartmental-based behavior of the system

Further substitutions of the equations shown above give

$$\alpha_{Tot} = \alpha_{init} + K_{C1} \cdot \alpha_{init} \cdot \left(1 + \frac{APP_{CS1}}{K_{M\alpha 1}}\right) + K_{C2} \cdot \alpha_{init} + 2 \cdot K_{C3} \cdot (K_{C2} \cdot \alpha_{init})^2 \cdot \left(1 + \frac{APP_{CS2d}}{K_{M\alpha 2d}}\right)$$

that can be rewritten as

$$\alpha_{Tot} = \alpha_{init} + K_{C1} \cdot \alpha_{init} \cdot \left(1 + \frac{K_{CS1} \cdot K_{G1} \cdot APP_{init}}{K_{M\alpha 1}}\right) + K_{C2} \cdot \alpha_{init} + \left. \begin{aligned} & 2 \cdot K_{C3} \cdot (K_{C2} \cdot \alpha_{init})^2 \cdot \left(1 + \frac{K_{CS2} \cdot K_{G3} \cdot (K_{G2} \cdot APP_{init})^2}{K_{M\alpha 2d}}\right) \end{aligned} \right\} \quad (4.16)$$

such that

$$\alpha_{init} = \frac{-B_{\alpha} \pm \sqrt{B_{\alpha}^2 - 4 \cdot A_{\alpha} \cdot C_{\alpha}}}{2 \cdot A_{\alpha}} \quad (4.17)$$

where

$$\begin{aligned} A_{\alpha} &= 2 \cdot K_{C3} \cdot K_{C2}^2 \cdot \left(1 + \frac{K_{CS2} \cdot K_{G3} \cdot (K_{G2} \cdot APP_{init})^2}{K_{M\alpha 2d}}\right) \\ B_{\alpha} &= 1 + K_{C1} \cdot \left(1 + \frac{K_{CS1} \cdot K_{G1} \cdot APP_{init}}{K_{M\alpha 1}}\right) + K_{C2} \\ C_{\alpha} &= -\alpha_{Tot}. \end{aligned}$$

Similarly, for β_{Tot} shown in Equation 4.11:

$$\beta_{init} = \frac{-B_{\beta} \pm \sqrt{B_{\beta}^2 - 4 \cdot A_{\beta} \cdot C_{\beta}}}{2 \cdot A_{\beta}} \quad (4.18)$$

where

$$\begin{aligned} A_{\beta} &= 2 \cdot K_{B3} \cdot K_{B2}^2 \cdot \left(1 + \frac{K_{E2} \cdot K_{CS2} \cdot K_{G3} \cdot (K_{G2} \cdot APP_{init})^2}{K_{M\beta 2d}}\right) \\ B_{\beta} &= 1 + K_{B1} \cdot \left(1 + \frac{K_{E1} \cdot K_{CS1} \cdot K_{G1} \cdot APP_{init}}{K_{M\beta 1}}\right) + K_{B2} \\ C_{\beta} &= -\beta_{Tot}. \end{aligned}$$

Note that only the positive solutions are biologically meaningful.

One of the main objectives of our study is to differentiate the influence of SORLA in monomer and in dimer processing. Therefore, it is necessary to further assume the law of conservation in each processing step. Otherwise, the SORLA assigned in each processing will indirectly affect the other processing, which can easily be shown by simple algebraic equations. In this relationship, we consider SORLA to directly influence the amounts of free *APP* available in monomer and dimer processing without affecting APP_{init} . In the presence of SORLA, the effect of SORLA on free *APP* starts with APP_{G1} for monomer

4.2. Multi-compartmental modeling of APP processing influenced by SORLA

processing and APP_{G2} for dimer processing. As such, the equations shown in Equation 4.14 can be rewritten in the following ways:

In the presence of SORLA,

$$\left. \begin{aligned}
 \alpha_{monomer} &= \alpha_1 + C_{APPCS1\alpha1}(APP_{G1}, \alpha_1) \\
 \alpha_{dimer} &= \alpha_2 + 2 \cdot (\alpha_{2d}(\alpha_2) + C_{APPCS2d\alpha2d}(APP_{G2}, \alpha_2)) \\
 \beta_{monomer} &= \beta_1 + C_{APPE1\beta1}(APP_{G1}, \beta_1) \\
 \beta_{dimer} &= \beta_2 + 2 \cdot [\beta_{2d}(\beta_2) + C_{APPE2d\beta2d}(APP_{G2}, \beta_2)] \\
 APP_{monomer} &= APP_{G1} + APP_{CS1}(APP_{G1}) + APP_{E1}(APP_{G1}) + \\
 &\quad C_{APPCS1\alpha1}(APP_{G1}, \alpha_1) + C_{APPE1\beta1}(APP_{G1}, \beta_1) + \\
 &\quad C_{APPG1SORLAG1}(APP_{G1}, SORLAG1) \\
 APP_{dimer} &= APP_{G2} + C_{APPG2SORLAG2}(APP_{G2}, SORLAG2) + \\
 &\quad 2 \cdot [APP_{G2d}(APP_{G2}) + APP_{CS2d}(APP_{G2}) + \\
 &\quad APP_{E2d}(APP_{G2}) + C_{APPCS2d\alpha2d}(APP_{G2}, \alpha_2) + \\
 &\quad C_{APPE2d\beta2d}(APP_{G2}, \beta_2)] \\
 SORLA_{monomer} &= SORLAG1 + C_{APPG1SORLAG1}(APP_{G1}, SORLAG1) \\
 SORLA_{dimer} &= SORLAG2 + C_{APPG2SORLAG2}(APP_{G2}, SORLAG2)
 \end{aligned} \right\} \quad (4.19)$$

Similarly, the equations above are substituted into Equations 4.10 to 4.13. APP_{G1} , α_1 , and β_1 are solved with respect to the total amount of $APP_{monomer}$, $\alpha_{monomer}$, and $\beta_{monomer}$ concentrations calculated from the case without SORLA, respectively. Likewise, APP_{G2} , α_2 , and β_2 are solved with respect to the total amount of APP_{dimer} , α_{dimer} , and β_{dimer} concentrations derived from the case without SORLA.

Moreover,

$$\begin{aligned}
 SORLA_{monomer} &= SORLAG1 + C_{APPG1SORLAG1}(APP_{G1}, SORLAG1) \\
 &= SORLAG1 \cdot (1 + K_{S1} \cdot APP_{G1})
 \end{aligned}$$

implies that

$$SORLAG1 = SORLA_{monomer} \cdot (1 + K_{S1} \cdot APP_{G1})^{-1}$$

and thus

$$C_{APPG1SORLAG1} = K_{S1} \cdot APP_{G1} \cdot [SORLA_{monomer} \cdot (1 + K_{S1} \cdot APP_{G1})^{-1}]$$

Similarly,

$$C_{APPG2SORLAG2} = K_{S2} \cdot APP_{G2} \cdot [SORLA_{dimer} \cdot (1 + K_{S2} \cdot APP_{G2})^{-1}]$$

4. Compartmental-based behavior of the system

Given the equations above, APP_{Tot} with SORLA can be rewritten as

$$APP_{Tot} = APP_{init} + APP_{G2} + K_{S1} \cdot APP_{G1} \cdot \left[\frac{SORLA_{monomer}}{1 + K_{S1} \cdot APP_{G1}} \right] + \left. \begin{aligned} & APP_{G1} \cdot \left\{ 1 + K_{CS1} \cdot \left[1 + \frac{\alpha_1}{K_{M\alpha 1}} \right] + K_{E1} \cdot K_{CS1} \cdot \left[1 + \frac{\beta_1}{K_{M\beta 1}} \right] \right\} + \\ & K_{S2} \cdot APP_{G2} \cdot \left[\frac{SORLA_{dimer}}{1 + K_{S2} \cdot APP_{G2}} \right] + 2 \cdot K_{G3} \cdot APP_{G2}^2 \cdot \{ 1 + \\ & K_{CS2} \cdot \left[1 + \frac{K_{C3} \cdot \alpha_2^2}{K_{M\alpha 2d}} \right] + K_{E2} \cdot K_{CS2} \cdot \left[1 + \frac{K_{B3} \cdot \beta_2^2}{K_{M\beta 2d}} \right] \} \end{aligned} \right\} \quad (4.20)$$

Due to the complexity of Equation 4.20, the computations of APP_{G1} and APP_{G2} will not be shown algebraically, but rather will be calculated using the `fzero` function in MATLAB. Nevertheless, the algebraic computation for α_1 , α_2 , β_1 , and β_2 are shown below. We will show the computation for α_1 and α_2 , and the solutions for β_1 and β_2 will follow a similar approach.

First, we compute the amounts of $\alpha_{monomer}$ and α_{dimer} without SORLA (see Equation 4.14) given APP_{init} (in Equation 4.15), α_{init} (in Equation 4.17), and β_{init} (in Equation 4.18) that were solved previously, i.e.

$$\left. \begin{aligned} \alpha_{monomer} &= K_{C1} \cdot \alpha_{init} \cdot \left(1 + \frac{K_{CS1} \cdot K_{G1} \cdot APP_{init}}{K_{M\alpha 1}} \right) \\ \alpha_{dimer} &= K_{C2} \cdot \alpha_{init} + 2 \cdot K_{C3} \cdot (K_{C2} \cdot \alpha_{init})^2 \cdot \left[1 + \frac{K_{CS2} \cdot K_{G3} \cdot (K_{G2} \cdot APP_{init})^2}{K_{M\alpha 2d}} \right] \end{aligned} \right\} \quad (4.21)$$

Next, we use the calculated values of $\alpha_{monomer}$ and α_{dimer} in Equations 4.21, and substitute them into Equation 4.19:

$$\begin{aligned} \alpha_{monomer} &= \alpha_1 + C_{APPCS1\alpha 1}(APP_{G1}, \alpha_1) \\ \alpha_{dimer} &= \alpha_2 + 2 \cdot [\alpha_{2d}(\alpha_2) + C_{APPCS2d\alpha 2d}(APP_{G2}, \alpha_2)] \end{aligned}$$

which can be rewritten as

$$\begin{aligned} \alpha_{monomer} &= \alpha_1 \cdot \left(1 + \frac{K_{CS1} \cdot APP_{G1}}{K_{M\alpha 1}} \right) \\ \alpha_{dimer} &= \alpha_2 + 2 \cdot K_{C3} \cdot \alpha_2^2 \cdot \left(1 + \frac{K_{CS2} \cdot K_{G3} \cdot APP_{G2}^2}{K_{M\alpha 2d}} \right) \end{aligned}$$

Lastly, we solved for α_1 and α_2 with respect to the conserved amount of $\alpha_{monomer}$ and

4.2. Multi-compartmental modeling of APP processing influenced by SORLA

α_{dimer} that were previously calculated in Equations 4.21:

$$\left. \begin{aligned} \alpha_1 &= \alpha_{\text{monomer}} \cdot \left(1 + \frac{K_{CS1} \cdot APP_{G1}}{K_{M\alpha1}} \right)^{-1} \\ \alpha_2 &= \frac{-1 \pm \sqrt{1 + 8 \cdot \alpha_{\text{dimer}} \cdot \left[K_{C3} \cdot \left(1 + \frac{K_{CS2} \cdot K_{G3} \cdot APP_{G2}^2}{K_{M\alpha2d}} \right) \right]}}{4 \cdot K_{C3} \cdot \left(1 + \frac{K_{CS2} \cdot K_{G3} \cdot APP_{G2}^2}{K_{M\alpha2d}} \right)} \end{aligned} \right\} \quad (4.22)$$

Similarly, take

$$\begin{aligned} \beta_{\text{monomer}} &= \beta_1 + C_{APPE1\beta1}(APP_{G1}, \beta_1) \\ \beta_{\text{dimer}} &= \beta_2 + 2 \cdot (\beta_{2d}(\beta_2) + C_{APPE2d\beta2d}(APP_{G2}, \beta_2)) \end{aligned}$$

such that

$$\left. \begin{aligned} \beta_1 &= \beta_{\text{monomer}} \cdot \left(1 + \frac{K_{E1} \cdot K_{CS1} \cdot APP_{G1}}{K_{M\beta1}} \right)^{-1} \\ \beta_2 &= \frac{-1 \pm \sqrt{1 + 8 \cdot \beta_{\text{dimer}} \cdot \left[K_{B3} \cdot \left(1 + \frac{K_{E2} \cdot K_{CS2} \cdot K_{G3} \cdot APP_{G2}^2}{K_{M\beta2d}} \right) \right]}}{4 \cdot K_{B3} \cdot \left(1 + \frac{K_{E2} \cdot K_{CS2} \cdot K_{G3} \cdot APP_{G2}^2}{K_{M\beta2d}} \right)} \end{aligned} \right\} \quad (4.23)$$

Note that only the positive solutions are biologically meaningful.

Below, we discuss in more detail the properties behind the equations above: (I) each conserved equation is a function of free reactant and of reactant bound in the complexes, and therefore the reactant can be the APP, SORLA, α -, or β -secretase. (II) Each Reactant_{Tot} function is represented differently in the presence and absence of SORLA. In particular, each Reactant_{Tot} function without SORLA is transcribed as a function of APP_{init} , α_{init} , and β_{init} , whereas those with SORLA are transcribed as a function of APP_{G1} , APP_{G2} , α_1 , α_2 , β_1 , and β_2 . (III) The amount of the Reactant_{init} in each Reactant_{Tot} with SORLA is set to be the same as that calculated from the corresponding Reactant_{Tot} without SORLA. (IV) Similarly, the total amount of $\text{Reactant}_{monomer}$ and Reactant_{dimer} in each Reactant_{Tot} with SORLA is equivalent to that calculated from the corresponding Reactant_{Tot} without SORLA. (V) The amount of SORLA_{Tot} , α_{Tot} , and β_{Tot} are assumed to be constant for different APP_{Tot} concentrations. This assumption is based on the experimental design applied to the series of dose-response data [Schmidt et al. 2012] that are used in this thesis. (VI) Without loss of generality, $\text{SORLA}_{monomer}$ and SORLA_{dimer} are also assumed to be constant for different APP_{Tot} concentrations.

The properties defined above are, in particular, necessary and important. Without these properties, the presence of SORLA in monomer processing will not only affect the

4. Compartmental-based behavior of the system

monomeric form of APP processing, but will also indirectly influence the dimeric form of APP processing, and vice versa [Lao et al. 2012]. As such, it defeats the main purpose of this study, which is to differentiate the level of influence of SORLA in monomer and in dimer processing.

Model parameter estimation

The development of the model [Lao et al. 2012] that is described above reduced the number of free parameters from 77 to 27. The reduced number of parameter values of the model are estimated by nonlinear optimization, such that the model simulations fit four biological independent dose-response series without SORLA (a total of $N = 64$ experimental data points) and five biological independent dose-response series with SORLA (also a total of $N = 64$ experimental data points). We looked for a set of parameter values that minimizes the weighted least squares function of APP_{Tot} with SORLA (Equations 4.15), and $sAPP\alpha_{Tot}$ and $sAPP\beta_{Tot}$ regardless of the presence of SORLA (Equation 4.8). On account of the different orders of magnitude of the experimental values of APP, $sAPP\alpha$, and $sAPP\beta$, weights are assigned such that the influence of each data set in the process of optimization will be equal. The weights are defined as

$$w_a = \frac{\sum_{k=1}^N sAPP\alpha_k^E}{N}, w_b = \frac{\sum_{k=1}^N sAPP\beta_k^E}{N},$$

$$w_{aS} = \frac{\sum_{k=1}^N sAPP\alpha_{S,k}^E}{N}, w_{bS} = \frac{\sum_{k=1}^N sAPP\beta_{S,k}^E}{N}, \text{ and } w_{appS} = \frac{\sum_{k=1}^N APP_{S,k}^E}{N},$$

where the superscript ‘E’ and the subscript ‘S’ denotes experimental data points and the influence of SORLA, respectively. The goodness of fit is quantified by calculating the residual value given the respective weights above:

$$residual = \min \sum_{k=1}^N \left[\frac{\left(APP_{S,k}^E - APP_{Tot,S,k} \right)^2}{w_{appS}} + \frac{\left(sAPP\alpha_k^E - sAPP\alpha_{Tot,k} \right)^2}{w_a} + \frac{\left(sAPP\beta_k^E - sAPP\beta_{Tot,k} \right)^2}{w_b} + \frac{\left(sAPP\alpha_{S,k}^E - sAPP\alpha_{Tot,S,k} \right)^2}{w_{aS}} + \frac{\left(sAPP\beta_{S,k}^E - sAPP\beta_{Tot,S,k} \right)^2}{w_{bS}} \right]$$

4.2. Multi-compartmental modeling of APP processing influenced by SORLA

The estimation of parameter values is performed using the steps shown in Table 4.1 (see Appendix C for the corresponding Matlab source code) [Lao et al. 2012]. We performed 500 global estimates, satisfying the condition that all parameter values are positive. Due to the differences in the experimental methods applied, none of the parameter values were taken from the literature. Most kinetic data available in the literature on α/β -secretase activity were obtained in cell free assays using purified enzyme and artificial peptide substrate. This is in contrast to our model, which relies on quantitative data obtained from APP processing in intact cells. Furthermore, the parameter values that are estimated for our multi-compartment model are expected to differ from those of the single-compartment model by Schmidt et al. [2012]. Out of the 500 simulation runs, we took the set of estimated parameter values that had the smallest residual value (as shown in Appendix Table B.4).

Decrease in total amounts of sAPP products is mainly due to the influence of SORLA in dimer processing

Using the multi-compartmental model, we show in Figure 4.4 the corresponding model simulations for various APP products, namely, the products that are produced in monomer, dimer, and in both processing pathways. The simulations of the parameterized mathematical model are in agreement with our experimental data shown in Figure 2.4.

In the absence of SORLA, the sigmoidal curve that is characteristic for products produced in dimer processing (green lines in Figure 4.4A and B) has a strong impact on the sum of the products produced in monomer and dimer processing pathways (black lines in Figure 4.4A and B). As such, it describes the experimental data sets for sAPP α and sAPP β very well (black dots in Figure 4.4A and B, respectively).

Surprisingly, in the presence of SORLA, a significant decrease in the products produced during dimer processing is observed (green lines in Figure 4.4C and D) compared to those in monomer processing (red lines in Figure 4.4C and D). In particular, the analysis shows that at a high level of SORLA activity (i.e. 100% of SORLA $_{Tot}$ where SORLA $_{Tot}$ equals 2.43×10^5 fmol), there is obviously more APP bound to SORLA during dimer processing (Figure 4.5B) than during monomer processing (Figure 4.5A).

Taken together, the simulations shown in Figure 4.4 and Figure 4.5 strongly support the hypothesis whereby SORLA prevents oligomerization of APP and has a larger impact on the products produced in dimer processing compared to monomer processing [Lao et al. 2012].

4. Compartmental-based behavior of the system

Table 4.1.: Steps in the estimation of parameter values in a multi-compartmental model.

-
1. Sort experimental data according to the total amount of APP values.
 2. For simulation purpose, the unit of measurements is unified into fmol (i.e. the values of APP_{Tot} is converted from Molar to fmol, wherein the unit of measurement for sAPP α and sAPP β remains as fmol).
 3. The initial values of the parameters are randomly assigned using the `rand` function.
 4. The initial values described in Step 3 are used by the `lsqnonlin` function to estimate the parameter values of the mathematical model, whereby the following tasks are performed:
 - a) Given the total amount of APP values from the experimental data without SORLA, the `fzero` function is used to solve for APP_{init} .
 - b) Use the APP_{init} that is solved in (4a) to solve for α_{init} and β_{init} while simultaneously estimating the values for α_{Tot} and β_{Tot} .
 - c) The total amount of APP values measured between the experimental data without SORLA and the experimental data with SORLA are different. Thus, it is necessary to compute the corresponding free APP levels in both cases (i.e. with and without SORLA).
 - d) Use the values of APP_{init} , α_{init} , and β_{init} that are calculated in (4a) and (4b) to solve for the conserved amount of APP, α -secretase, and β -secretase in monomer and dimer processing without SORLA (i.e. $APP_{monomer}$, APP_{dimer} , $\alpha_{monomer}$, α_{dimer} , $\beta_{monomer}$, and β_{dimer}).
 - e) Use $APP_{monomer}$, APP_{dimer} , $\alpha_{monomer}$, α_{dimer} , $\beta_{monomer}$, and β_{dimer} that are solved in (4d) to recalculate for the values of APP_{G1} , APP_{G2} , α_1 , α_2 , β_1 , and β_2 , respectively, which are influenced by SORLA.
 - f) Then, apply APP, α -secretase, and β -secretase that are calculated in (4a) and (4b) into the production rate equations of sAPP α and sAPP β without SORLA, and those in (4e) into that with SORLA.
 - g) Lastly, the sum of weighted squares of differences between the experimental data and results in (4f) are minimized, i.e. the predicted and observed total amount of
 - i. sAPP α without SORLA
 - ii. sAPP β without SORLA
 - iii. sAPP α with SORLA
 - iv. sAPP β with SORLA
 - v. APP with SORLA. (This step is necessary because the free APP in the case with SORLA are computed indirectly)
-

4.2. Multi-compartmental modeling of APP processing influenced by SORLA

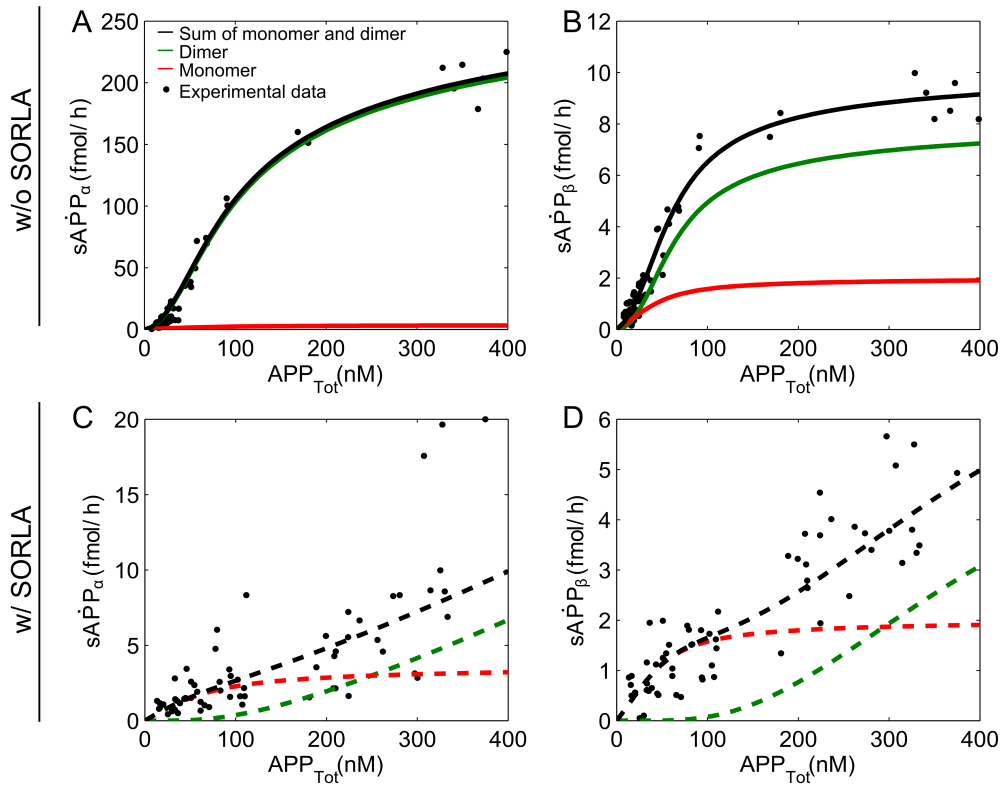


Figure 4.4.: Simulation results of the $sAPP\alpha$ and $sAPP\beta$ end products. Simulation results of the multi-compartmental model (lines) for the various APP products are shown together with the actual data points obtained from biochemical experiments by Schmidt et al. [2012]. The total amount of products (black line) is the sum of the products produced in monomer (red line) and in dimer processing (green line) pathways. In the absence of SORLA, the products produced in the dimer processing pathways more closely resemble the total amount of $sAPP\alpha$ (A) and $sAPP\beta$ (B). With SORLA, the amounts of $sAPP\alpha$ and $sAPP\beta$ that are produced in dimer processing are significantly reduced compared to those in monomer processing (C, D).

4. Compartmental-based behavior of the system

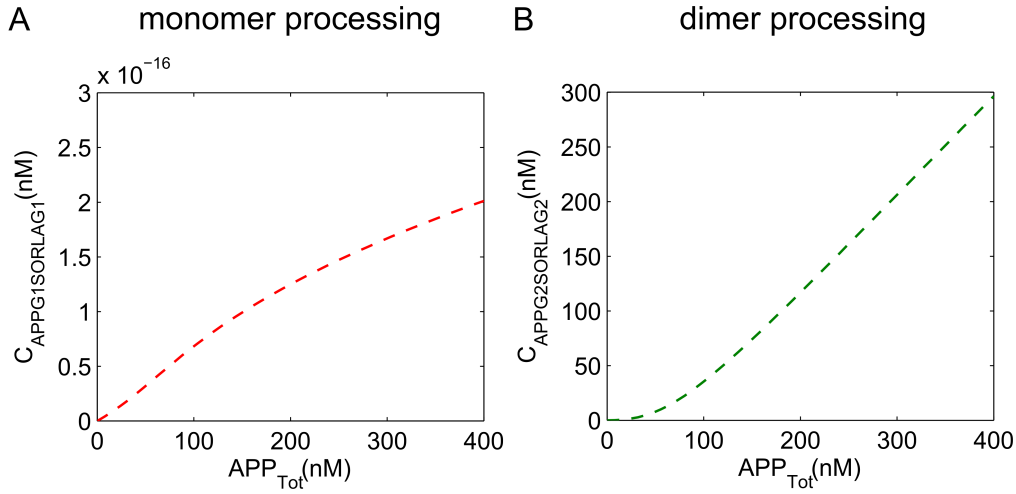


Figure 4.5.: Complex formation of APP-SORLA in monomer and dimer processing. Simulations of the influence of SORLA on APP processing on the complex formation of APP-SORLA in monomer (A) and dimer (B) processing are shown. There is more APP bound to SORLA in dimer processing (B) than in monomer processing (A).

Intermediate levels of SORLA

So far, we have only shown simulations of our model in the two most extreme scenarios: with no (Figure 4.4A and B) or high levels (Figure 4.4C and D) of SORLA activity. However, subtle alterations of SORLA concentration are likely to be more relevant for the determination of its influence on APP processing pathways. Accordingly, we adapted our multi-compartment model to intermediate concentrations of SORLA. As shown in Figures 4.6 to 4.10, the simulations are all dependent on three intermediate SORLA expression levels, namely, 3%, 12%, and 30% of $SORLA_{Tot}$.

Remarkably, we observed in Figure 4.6 that the simulations that are dependent on the three intermediate SORLA expression levels are either “spread” (as in Figure 4.6A and Figure 4.6D) or “clustered” (as in Figure 4.6B and Figure 4.6C) into the two most extreme scenarios of SORLA concentration [Lao et al. 2012]. This came as a surprise, because the dose-response kinetics of total sAPP α production that is dependent on the intermediate SORLA expression levels (Figure 4.6A) is expected to be “clustered” similar to that of sAPP β (Figure 4.6B). This is similar to the amount of APP bound to SORLA in monomer (Figure 4.6C) and in dimer processing (Figure 4.6D). We say that the simulations are “clustered” when

$$X_Y \approx (X_{100\%} - X_{0\%}) \cdot Y + X_{0\%}$$

where $Y = \{3\%, 12\%, 30\%\}$, and X denotes the concentration at a given percentage value

4.2. Multi-compartmental modeling of APP processing influenced by SORLA

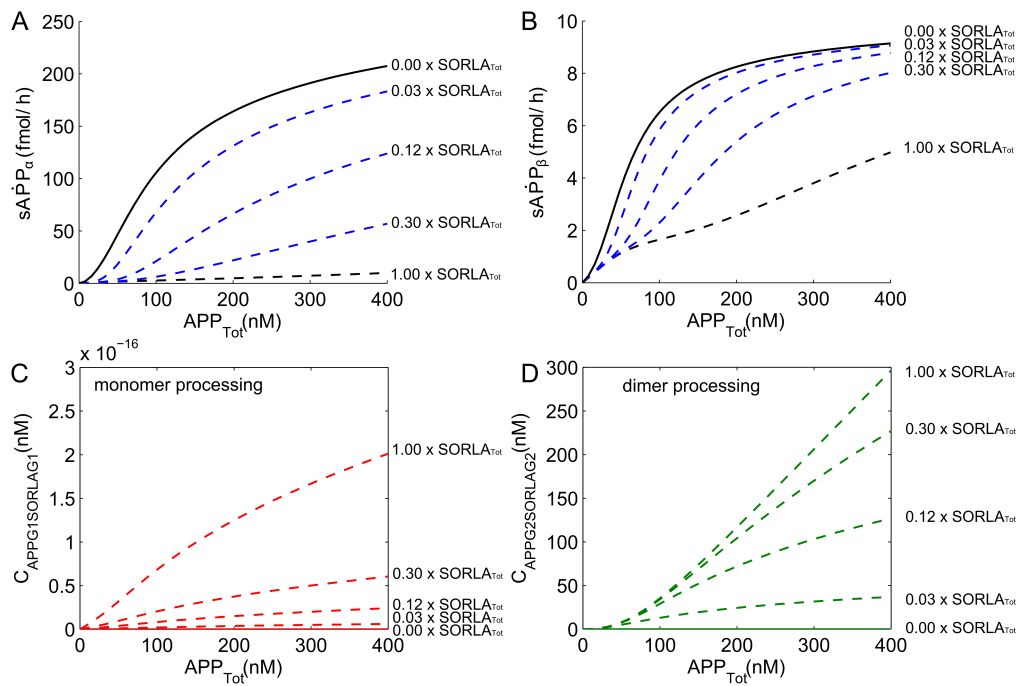


Figure 4.6.: APP processing at intermediate levels of SORLA. Simulations of the influence of intermediate levels of SORLA on APP processing into the total amount of $sAPP_{\alpha}$ (A) and total amount of $sAPP_{\beta}$ (B), and on the complex formation of APP-SORLA in monomer (C) and dimer (D) processing are shown. They are simulated in different intermediate levels of SORLA: from without SORLA, to 3%, 12%, 30%, and 100% of $SORLA_{Tot}$ (where $SORLA_{Tot} = 2.43 \times 10^5$ fmol).

4. Compartmental-based behavior of the system

of $SORLA_{Tot}$ that is specified by its subscript. Otherwise, we say that the simulations are “spread”. Next, we investigate what leads to the observation shown in Figure 4.6, which is dependent on the intermediate SORLA expression levels.

SORLA indirectly affects the dynamical behavior of the β -secretase but not that of α -secretase

First, we analyzed the simulations of the influence of intermediate levels of SORLA on APP processing on α -secretase (Figure 4.7A-F) and β -secretase (Figure 4.7G-L) concentrations [Lao et al. 2012]. In Figure 4.7, the term “used” refers to the complex formation of the secretases and APP, while the term “free” refers to the secretases that are not bound in a complex.

The total amounts of α -secretase and β -secretase are assumed to be constant (depicted by the black lines in Figure 4.7E-F and Figure 4.7K-L, respectively). Due to the conservation law assumption, the total amount of each secretase in each subcompartment is conserved (i.e. $\alpha_{monomer}$ and $\beta_{monomer}$ depicted by red lines in Figure 4.7F and Figure 4.7L, respectively; α_{dimer} and β_{dimer} depicted by green lines in Figure 4.7F and Figure 4.7L), respectively. Consequently, the total amount of each secretase in the entire system is thus also conserved (α_{Tot} and β_{Tot} shown by the black lines in Figure 4.7E-F and Figure 4.7K-L, respectively).

The simulations of the influence of intermediate levels of SORLA on APP processing on the α -secretase (Figure 4.7A-F) concentration show that (i) more α -secretases are used (Figure 4.7C) than are left free (Figure 4.7A) in monomer processing, (ii) more α -secretases remain free (Figure 4.7B) than are used (Figure 4.7D) in the dimer processing, (iii) the total amount of α -secretase that is free and used (blue and orange lines in Figure 4.7E, respectively) is dominated by the corresponding amount of α -secretase concentration in dimer (Figure 4.7B) and in monomer processing (Figure 4.7C), (iv) SORLA has a relatively larger influence on the amount of α -secretase concentration that is used in dimer processing (Figure 4.7D) compared to other simulations on the α -secretase concentration (Figure 4.7A-C), and (v) its simulations that are dependent on the three intermediate SORLA expression levels (Figure 4.7D) is consistent with the dose-response kinetics of total sAPP α production ((Figure 4.6A).

The significant difference in the concentration of free (Figure 4.7B) and used (Figure 4.7D) α -secretase in dimer processing is a consequence of the large concentration of α -secretase used in monomer processing (shown in Figure 4.7C). As the total APP con-

4.2. Multi-compartmental modeling of APP processing influenced by SORLA

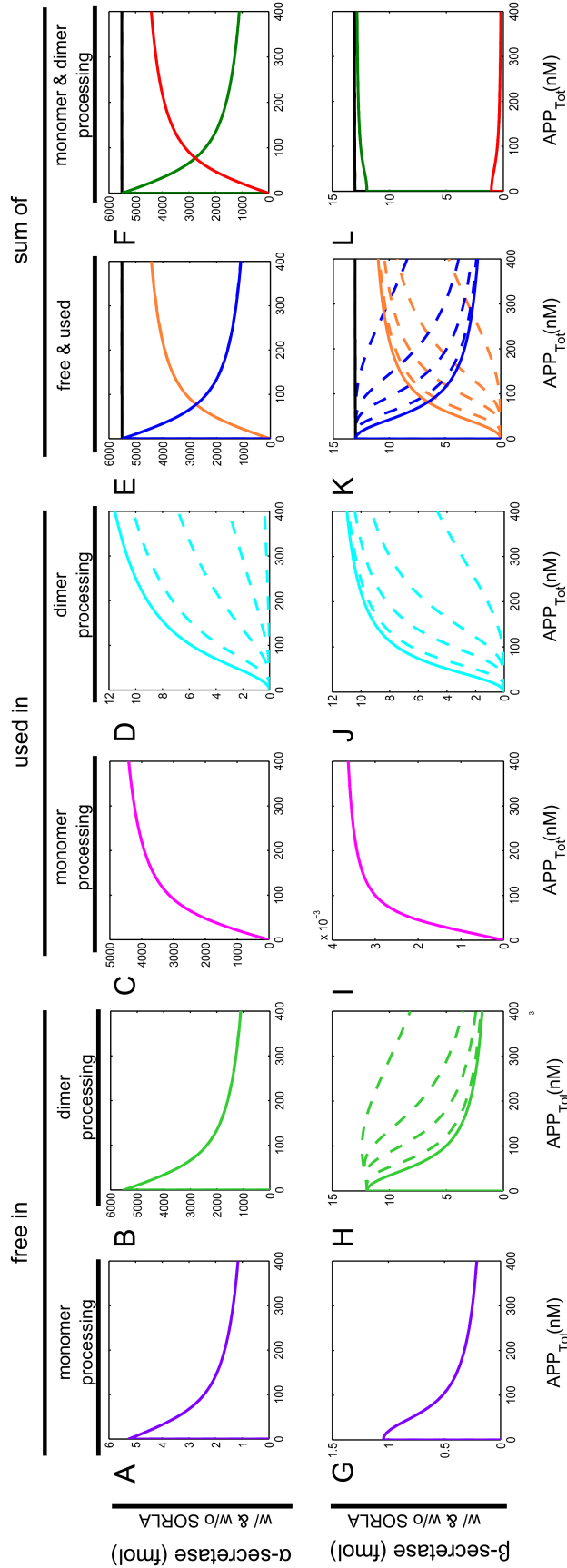


Figure 4.7.: Concentration values of the secretases at intermediate levels of SORLA. Simulations of the influence of intermediate levels of SORLA on APP processing on the α -secretase (**A-F**) and β -secretase (**G-L**) concentrations. The term “used” refers to the complex formation of the secretases and APP, while the term “free” refers to the secretases that are not bound in a complex. The first four columns show the simulations of secretase concentration that is free (1st and 2nd columns), in monomer processing (3rd and 4th columns), used (3rd and 4th columns), and in dimer processing (2nd and 4th columns). In the last two columns, the corresponding total concentration of secretase molecules that is free (blue line in **E** and **K**), used (orange line in **E** and **K**), in monomer processing (red line in **F** and **L**) and in dimer processing (green line in **F** and **L**) are also shown. Moreover, the black line in (**E**, **K**) represents the sum of the secretase concentration depicted by the blue and orange lines, while the black line (**F**, **L**) indicates the sum of the secretase concentration depicted by the red and green lines. There are five intermediate levels of SORLA, namely, 0% (solid line), 3%, 12%, 30%, and 100% (dashed line) of SORLA_{Total} (where SORLA_{Total} = 2.43×10^5 fmol). When there is only a solid line in a plot, it is because solid and dashed lines are superimposed. Notice that the solid and dashed lines for both blue and orange colors deviates in (**K**). This, however, is not the case in (**E**).

4. Compartmental-based behavior of the system

centration increases (from 0 nM to 400 nM), the concentration of α -secretase that is free in dimer processing decreases (Figure 4.7B), while the concentration of α -secretase used in monomer processing increases (Figure 4.7C). As the amount of SORLA concentration increases, the curves representing the secretases transition from solid to dashed lines. SORLA affects α -secretase in dimer processing (Figure 4.7B and 4.7D): the molecules used in dimer processing decrease (Figure 4.7D), while the concentration of those that are free in dimer processing increases (Figure 4.7B). In the latter figure, the increase is not obvious because the change is very small compared to the concentration values of α -secretase.

Regarding the influence of intermediate levels of SORLA on APP processing on the amount of β -secretase (Figure 4.7G-L) concentration, the simulations show that (i) there are more free β -secretases (Figure 4.7G) than used (Figure 4.7I) in monomer processing, (ii) SORLA has no influence on β -secretase in monomer processing (Figure 4.7G and Figure 4.7I), (iii) SORLA alters the dynamical behaviors of β -secretase in dimer processing (Figure 4.7H and Figure 4.7J), (iv) the total amount of β -secretase that is free and used (blue and orange lines in Figure 4.7K, respectively) is dominated by the β -secretase concentration in dimer processing (Figure 4.7H and Figure 4.7J, correspondingly), and (v) its simulations that are dependent on the three intermediate SORLA expression levels (Figure 4.7H and Figure 4.7J) are consistent with those of the dose-response kinetics of total sAPP β production ((Figure 4.6B). The curves for β -secretase with SORLA (dashed lines in Figure 4.7H) are greater in values compared to those without SORLA (solid line in Figure 4.7H), which is a consequence of SORLA's influence on β -secretase used in dimer processing (Figure 4.7J).

When a comparison is made between the total concentration of α - and β -secretase that are free (blue lines in Figure 4.7E and Figure 4.7K, respectively) and used (orange lines in Figure 4.7E and Figure 4.7K, respectively) that are dependent on the three intermediate SORLA expression levels, it can be observed that the total β -secretase concentration for both free and used deviated (Figure 4.7K), which was not the case for α -secretase (Figure 4.7E). This observation suggests that SORLA indirectly affects the dynamics of β -secretase, but not that of α -secretase [Lao et al. 2012]. This result supports our hypothesis presented in Section 3.3 that “the global-local estimation of the parameter values in the model suggests a yet unidentified biological process whereby SORLA might indirectly affect β -secretase, but not α -secretase”. The present result therefore clarifies what was unidentified in Section 3.3.

With a SORLA concentration greater than the estimated total SORLA concentration (i.e. $SORLA_{Tot} = 2.43 \times 10^5 \text{ fmol}$), we arrive at Figure 4.8. Figures 4.8D and J show that

4.2. Multi-compartmental modeling of APP processing influenced by SORLA

for a very large concentration of $SORLA_{Tot}$ (greater than $1 \times SORLA_{Tot}$ for α -secretase and greater than $10 \times SORLA_{Tot}$ for β -secretase), α - and β -secretase are barely “used”. Consequently, the concentration of α -secretase (Figure 4.8B) and β -secretase (Figure 4.8H) are all “free” in dimer processing, and there will be no sAPP products produced in dimer processing [Lao et al. 2012].

SORLA is more influential in dimer processing than in monomer processing

We also investigated the concentration of APP molecules that was either free or used in monomer or in dimer processing, and which are in the TGN, at the cell surface, or in the endosomes [Lao et al. 2012], as shown in Figure 4.9. The term “used” refers to the complex formation of (i) APP and SORLA in the TGN, (ii) APP and α -secretase at the cell surface, and (iii) APP and β -secretase in the endosomes. Wherein, the term “free” refers to the APP that is not bound in the respective compartments.

First, we show the simulations of the concentration of APP molecules that are free or used in monomer and in dimer processing. The simulations under dimer processing show that the concentration of APP molecules that are free or used in each compartment are significantly affected by the presence of SORLA (last two columns of Figure 4.9: Figure 4.9D-E, Figure 4.9H-I, Figure 4.9L-M, and Figure 4.9P-Q) compared to those under monomer processing (first three columns of Figure 4.9: Figure 4.9A-C, Figure 4.9F-G, Figure 4.9J-K, and Figure 4.9N-O). In particular, one observes from the simulations that the concentration of APP molecules that are used to bind with SORLA in dimer processing of the TGN tremendously increases from 0 M up to 300 nM (Figure 4.9E), wherein those in monomer processing are so small that they can be neglected (Figure 4.9C). Consequently, SORLA decreases the concentration of APP molecules that are free or used at the cell surface and in the endosomes (Figure 4.9H-I and Figure 4.9L-M, respectively). In addition, the total APP concentrations in dimer processing is dominated by the total amount of free APP in the absence of SORLA and by the total amount of used APP in the presence of SORLA (depicted by the two outermost lines in Figure 4.9P and Figure 4.9Q, respectively).

Next, in each compartment, the simulations for the total APP concentrations that are free, used, in monomer processing, or in dimer processing, are shown in Figure 4.10. Consistent with previous observations (Figure 4.9), the simulations for total APP concentrations in monomer processing for the three different compartments (3rd column of Figure 4.10) are not influenced by SORLA, while those in dimer processing are affected by the presence of SORLA (4th column of Figure 4.10). Moreover, the simulations shown in the first two columns of Figure 4.10 also indicate that the presence of SORLA in the TGN

4. Compartmental-based behavior of the system

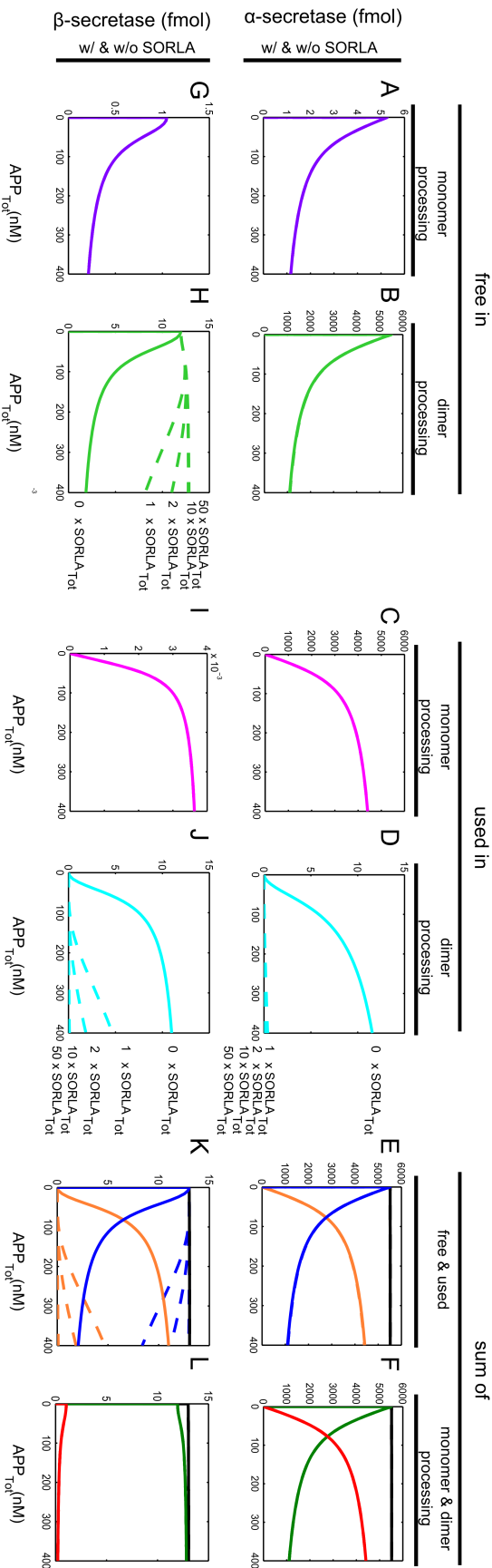


Figure 4.8.: Concentration values of the secretases with higher SORLA_{Tot} values. Simulations of the influence of intermediate levels of SORLA on APP processing on the amount of α-secretase (A-F) and β-secretase (G-I) concentration. The term “used” refers to the complex formation of the secretases and APP, while the term “free” refers to the secretases that are not bound in a complex. There are five intermediate levels of SORLA, namely, 0% (solid line), 100%, 200%, 1000%, and 5000% (dashed line) of SORLA_{Tot} (where SORLA_{Tot} = 2.43 × 10⁵ fmol). When there is only a solid line in a plot, it is because the solid and dashed lines are superimposed. Starting from the first column, the figure shows the amount of α-secretase (A) and β-secretase (G) that is free in monomer processing. In the second column, it shows the amount of α-secretase (B) and β-secretase (H) that is free in dimer processing. The amount of α-secretase (C) and β-secretase (I) used in monomer processing are shown in the third column, whereas those used in dimer processing (D, J) are shown in the fourth column. In the fifth column, it shows the total amount of α-secretase (E) and β-secretase (K) that is free (blue line) and used (orange line) in the system. Lastly, there is the total amount of α-secretase (F) and β-secretase (L) in monomer (blue line) and in dimer (orange line) processing of the system. The black lines in (E, F) and in (K, L) are the estimated total amounts of α- and β-secretase, respectively. In particular, the black line in (E, K) represents the sum of the secretase concentration depicted by the blue and orange lines. Notice that the solid and dashed lines for both blue and orange colors deviates in (K). This, however, is not the case in (E).

4.2. Multi-compartmental modeling of APP processing influenced by SORLA

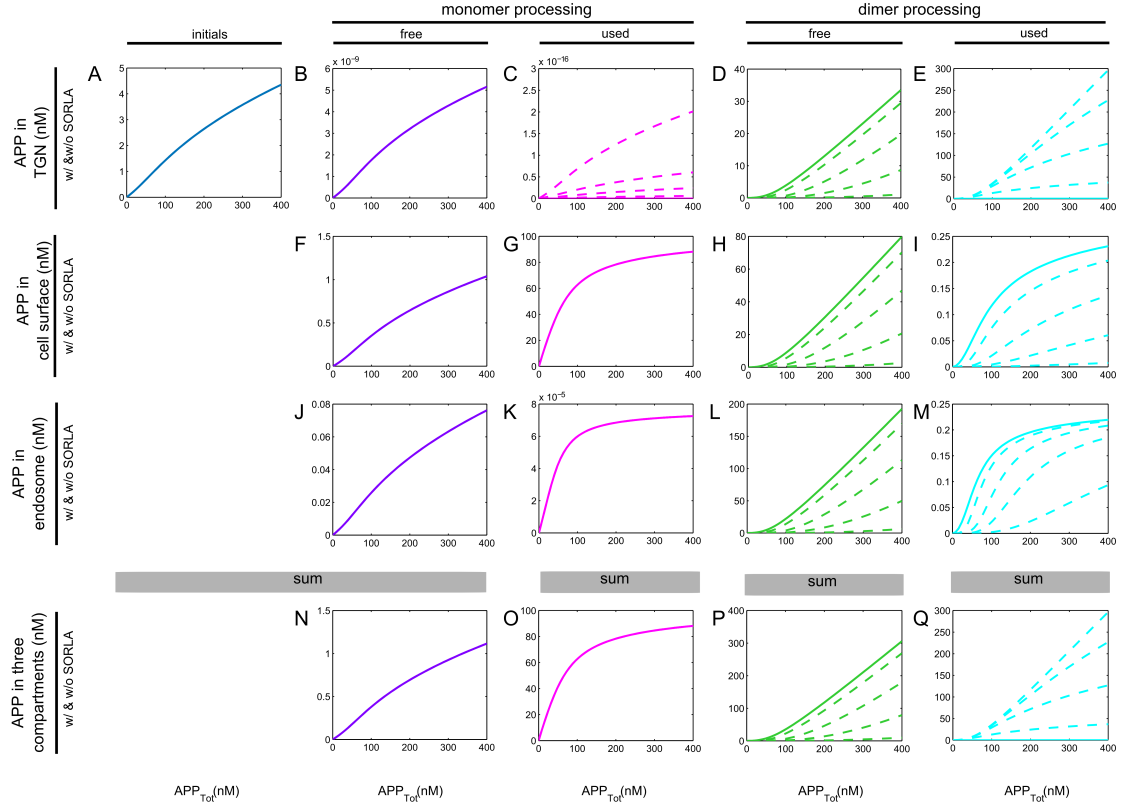


Figure 4.9.: Distribution of free and used APP within monomer and dimer processing in each compartment. Simulations of the influence of intermediate levels of SORLA on APP processing into the amounts of APP concentrations in the TGN (A-E), at the cell surface (F-I), in the endosomes (J-M), and in all three compartments (N-Q). There are five intermediate levels of SORLA, namely, 0% (solid line), 3%, 12%, 30%, and 100% (dashed line) of $SORLA_{Tot}$ (where $SORLA_{Tot} = 2.43 \times 10^5$ fmol). If the dashed line is not seen in a plot, it is because the solid and dashed lines are superimposed. In the first column, the initial APP concentrations that are left free is shown (A). Next, in the second and third columns, the APP concentrations that are free and used in monomer processing are also shown, respectively. In the last two columns, the APP concentrations that are free and used in dimer processing are also given. Notice that the APP concentrations in monomer processing are not influenced by SORLA (2nd and 3rd columns). Conversely, SORLA shows a strong influence on the concentration of APP in dimer processing (last two columns). The term “used” refers to the complex formation of (i) APP and SORLA in the TGN, (ii) APP and α -secretase at the cell surface, and (iii) APP and β -secretase in the endosomes. Wherein, the term “free” refers to the APP that is not bound in the respective compartments.

4. Compartmental-based behavior of the system

decreases the total amount of free APP (Figure 4.10P) and increases the total amount of used APP (Figure 4.10Q). In particular, total amount of used APP under the influence of SORLA, it is (i) enormously increased in the TGN (Figure 4.10B), (ii) not affected at the cell surface (Figure 4.10G), and (iii) reduced by up to half in the endosomes (Figure 4.10L). Taken together, the presence of SORLA increases the total APP concentration in the TGN (Figure 4.10E), and subsequently decreases the total APP concentration at the cell surface (Figure 4.10J) and in the endosomes (Figure 4.10O).

The simulations for the total APP concentration in monomer processing (Figure 4.10R), dimer processing (Figure 4.10S), and both monomer and dimer processing (Figure 4.10T) show that the conservation law is assumed for APP in monomer and in dimer processing. Above all, one observes that there is a higher APP concentration in dimer processing (Figure 4.10S) than in monomer processing (Figure 4.10R).

The spread and clustering of SORLA expression levels

As mentioned in subsection “Intermediate levels of SORLA”, the simulations of SORLA expression levels are either “spread” (Figure 4.6A) or “clustered” (Figure 4.6B). This is due to the effect of SORLA on the processing of APP dimer [Lao et al. 2012]. With respect to the total concentration of APP, the APP concentration (Figure 4.9I) and α -secretase concentration (Figure 4.7D) that is “used” at the cell surface in dimer processing “spread”. Considering the relevance of APP and α -secretase at the cell surface for the production of sAPP α , this observation suggests that a “spread” is observed in Figure 4.6A for sAPP α . Similarly, for the “clustering” observed in Figure 4.6B for sAPP β , it is a consequence of the “clustering” that is observed for APP (Figure 4.9M) and β -secretase (Figure 4.7J) that are “used” in the endosome during dimer processing, which are relevant in producing sAPP β . Moreover, the change from “spread” at the cell surface (Figure 4.6A) to “clustered” in the endosome (Figure 4.6B) is due to the indirect influence of SORLA on the dynamic behavior of β -secretase observed in Figure 4.7 [Lao et al. 2012].

The effect of different SORLA concentrations in switching sAPP α and sAPP β from preferred dimer-to-monomer processing

Lastly, Figure 4.11 shows simulations of the influence of SORLA on APP processing into sAPP α (Figure 4.11A and Figure 4.11C) and sAPP β (Figure 4.11B and Figure 4.11D). The simulations show that the switch from preferred dimer-to-monomer processing is observed at 25% of SORLA $_{Tot}$ for α -secretase (Figure 4.11A) and at 3% of SORLA $_{Tot}$ for β -secretase (Figure 4.11B), where SORLA $_{Tot} = 2.43 \times 10^5$ fmol. In agreement with

4.2. Multi-compartmental modeling of APP processing influenced by SORLA

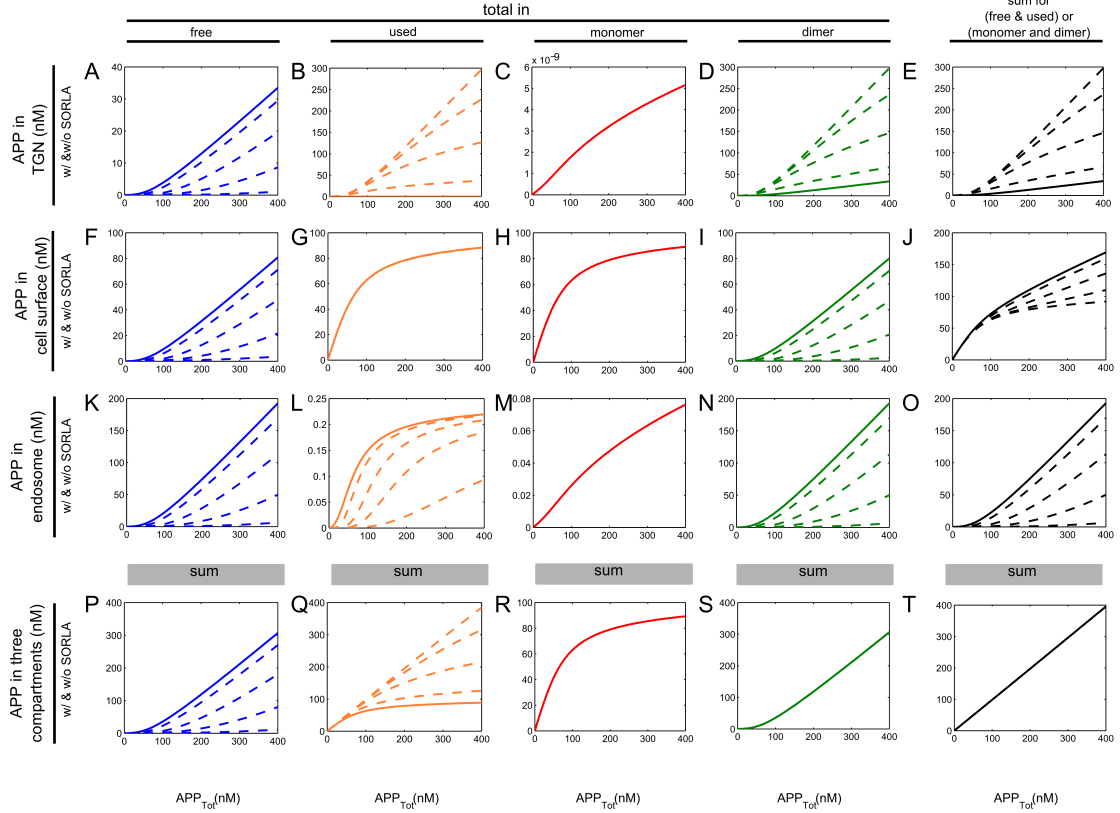


Figure 4.10.: Total amount of APP that is free, used, in monomer processing, and in dimer processing in each compartment. Simulations of the influence of intermediate levels of SORLA on APP processing for APP concentration in the TGN (A-E), at the cell surface (F-J), in the endosomes (K-O), and in all three compartments (P-T). There are five intermediate levels of SORLA, namely, 0% (solid line), 3%, 12%, 30%, and 100% (dashed line) of $SORLA_{Tot}$ (where $SORLA_{Tot} = 2.43 \times 10^5$ fmol). When only a solid line exists in a plot, it is because the solid and dashed lines are superimposed. Note that the term “used” refers to the complex formation of (i) APP and SORLA in the TGN, (ii) APP and α -secretase at the cell surface, and (iii) APP and β -secretase in the endosomes. Wherein, the term “free” refers to the APP that is not bound in the respective compartments. The first two columns show the total concentration of APP that is free and used. In the third and fourth columns, the total APP concentration in monomer and in dimer processing is shown, respectively. Each line in the last column has two meanings: (i) the sum of the corresponding APP concentrations shown in the first two columns, or (ii) the sum of the respective APP concentrations shown in the third and fourth columns. The plots aligned along the first column show that SORLA significantly decreases the total concentration of free APP in each compartment. The plots in the second column show that the total APP concentration in the TGN increases significantly (B), while not affecting and minimally decreasing those at the cell surface (G) and in the endosomes (L), respectively. The plots in the third column show that SORLA has no influence on the total APP concentration in monomer processing. Moreover the plots in the fourth column show that as the level of SORLA concentration in dimer processing increases, the total APP concentration in the TGN also increases (D), while the concentration at the cell surface (I) and in the endosomes (N) decreases.

4. Compartmental-based behavior of the system

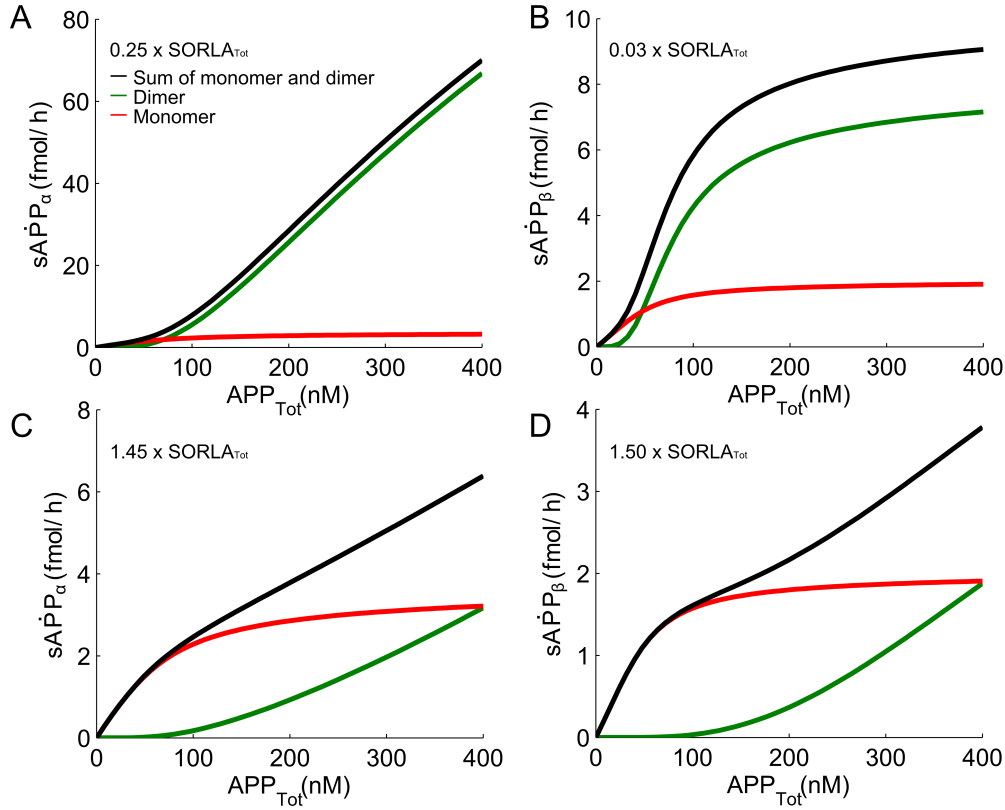


Figure 4.11.: Switch from preferred dimer-to-monomer processing. Simulations of the influence of SORLA on APP processing into sAPP α (A, C) and sAPP β (B, D) are shown (where $SORLA_{Tot} = 2.43 \times 10^5$ fmol). The total amount of products produced from both processing (black line) as well as the products produced from dimer (green line) and monomer (red line) processing are indicated for each simulation. A switch from preferred dimer-to-monomer processing is seen at 25% of $SORLA_{Tot}$ for α -secretase (A) and at 3% of $SORLA_{Tot}$ for β -secretase (B). The amount of product obtained from “red” monomer is greater than that of “green” dimer at 145% of $SORLA_{Tot}$ for α -secretase (C) and 150% of $SORLA_{Tot}$ for β -secretase (D).

the study performed in Section 3.3, the switch from cooperative (dimer) to less efficient non-cooperative (monomer) processing occurs at a low SORLA concentration [Lao et al. 2012]. Moreover, the end product obtained from monomer processing dominates the total amount of end product at 145% of $SORLA_{Tot}$ for α -secretase (Figure 4.11C) and 150% of $SORLA_{Tot}$ for β -secretase (Figure 4.11D). Similar to the results obtained in Figure 4.6 for the simulations of the influence of intermediate levels of SORLA on APP processing into sAPP α (Figure 4.6A) and sAPP β (Figure 4.6B), these two sets of results (Figure 4.6 and Figure 4.11) suggest that SORLA reduces the products produced in non-amyloidogenic and amyloidogenic pathways of APP processing, respectively, at different rates [Lao et al. 2012].

Summary and conclusions

The multi-compartment model is an extension of the single-compartment model that was established earlier in Chapter 3. To the best of our knowledge, this is the first multi-compartmental model developed to analyze APP processing in the context of AD [Lao et al. 2012]. In addition, the model represents the regulated trafficking of APP by SORLA through the intracellular compartments, which critically affects amyloidogenic and non-amyloidogenic processing pathways [Willnow et al. 2008]. This model was established to answer questions that arose from a study based on a single-compartment model (presented in Section 3.3).

The first question that emerged concerns the relative contributions of SORLA to monomer and dimer processing. Based on the study conducted in Section 3.3 [Schmidt et al. 2012], it was shown that SORLA influences the combined products obtained by monomer and dimer processing. However, due to the structural limitations of the single-compartment model, it was not possible to investigate the relative contribution of SORLA in monomer and dimer processing. Therefore, using the multi-compartment model, we have shown that the decrease in the total sAPP α and sAPP β is mainly due to the influence of SORLA in dimer processing [Lao et al. 2012]. This observation confirms the previous hypothesis that SORLA prevents oligomerization of APP, thereby eliminating the preferred substrates for secretases.

The second question was how does SORLA affect the dynamics of β -secretase? In Section 3.3, it is suggested that there is an indirect effect of the SORLA receptor on β -secretase, which contributes to the regulation of amyloidogenic processing in the context of an intact cell [Schmidt et al. 2012]. However, in order for the single-compartment model to closely resemble the experimental data, the model required a local parameter estimate for β -secretase activity in the presence or absence of SORLA. Through the multi-compartment model, where all parameters are estimated globally, we now confirm that SORLA affects the interaction between APP and β -secretase, but not that of APP with α -secretase [Lao et al. 2012]. A previous study suggests that SORLA directly interacts with β -secretase, preventing access of the enzyme to its substrate APP [Spoelgen et al. 2006]. While the simulations confirm an important influence of SORLA on β -secretase, this influence may also be indirect, such as by having an effect on the trafficking of cofactors essential for enzyme activity [Lao et al. 2012]. An indirect effect of SORLA is in agreement with our findings that the receptor does not impair β -secretase activity in cell-free assays [Schmidt et al. 2012].

In addition, we investigated the regulated trafficking of APP by SORLA in monomer and

4. Compartmental-based behavior of the system

dimer processing, considering several cellular compartments, including the TGN, cell surface, and endosomes [Lao et al. 2012]. Simulations of the multi-compartment model show that SORLA increases the total amount of APP concentrations in the TGN (Figure 4.10E) and subsequently decreases the total amount of APP at the cell surface (Figure 4.10J) and endosomes (Figure 4.10O). In agreement with Andersen and Willnow [2006], this result suggests that overexpression of SORLA prevents the localization of APP from the TGN to the cell surface and endosomes, whereby overexpression of SORLA decreases the products produced in the amyloidogenic and non-amyloidogenic pathways of APP processing. Furthermore, our study confirms that SORLA is more influential in dimer than in monomer processing. This observation is in agreement with the previous model that APP dimers represent the preferred substrate for α -secretase and β -secretase, as they enable cooperativity in substrate binding [Schmidt et al. 2012]. Taken together, data obtained both in single and in multi-compartment models strongly suggest that depletion of APP dimer processing represents a major molecular mechanism in the pathology of AD [Lao et al. 2012].

Our multi-compartment model was used to simulate pathological situations involving APP under different SORLA concentrations [Lao et al. 2012]. However, the model can also be used as a kinetic-dynamic model to study the effects of SORLA on α -secretase and β -secretase. Whereas, as the SORLA concentration increases, there is a relatively large decrease in the production rate of sAPP α compared to that of sAPP β (Figure 4.6 and Figure 4.11) [Lao et al. 2012].

CONCLUSIONS

Over the last 20 years much progress has been made in understanding the molecular biology of the pathogenesis of AD. There has been a growing focus on the cellular pathways that control APP processing and their potential contribution to neurodegenerative processes in patients. Results from various studies shed light on a previously poorly understood process concerning the targeted transport of APP to distinct intraneuronal compartments harbouring the various secretase activities. In particular, some of these research studies suggested that the functional characterization of SORLA, a unique sorting receptor for APP, plays an important role in sporadic AD. Although much still remains to be learned about SORLA and its role in this exciting AD pathway, SORLA certainly holds great promise as a novel biomarker and perhaps even as a new drug target in the treatment of this devastating disease [Willnow et al. 2010]. Given the ageing population and the concomitant increase in the number of Alzheimer sufferers, fully understanding the effect of SORLA in the context of AD is of extreme importance for a sustainable society.

To push the development of drug like SORLA, the systems biology approach is crucial to understand the influence of SORLA in the processing of APP. In our first attempt, we employed the quantitative modeling to approach risk factors in AD [Schmidt et al. 2012]. Furthermore, we have simulated the quantitative contribution of SORLA to proteolytic processing of APP through a single-compartment model. In particular, we have confirmed the strict linear relationship between SORLA concentrations and efficiency of APP processing, and we have uncovered the ability of SORLA to prevent dimerization of APP, thereby preventing the formation of high affinity substrates for secretases.

While our initial study [Schmidt et al. 2012] has been met with great enthusiasm in the field, it falls short of addressing major aspects of SORLA activity in the cell biology of AD. Our earlier study assumed, for sake of simplification, a single-compartment model

5. Conclusions

describing the effects of SORLA on APP processing. It also neglects the fact that APP follows a complex intracellular transportation whereby the protein moves between the TGN, cell surface, and endosomes, which is where the various interacting proteins reside. Finally, the model does not possess the ability to show how SORLA affects APP transport between various cell compartments in neurons, which is what initially sparked interest in this protein.

Since the single-compartment model [Schmidt et al. 2012] does not explain the APP transport mechanism, we have designed a new multi-compartmental model [Lao et al. 2012]. The new model addresses the important aspect of the cell biology of SORLA by assuming three compartments. Using the new model together with the estimated parameter values, our results suggest the following biological implications of SORLA: (1) a decrease in the total amount of sAPP products is mainly due to the high SORLA concentration in dimer processing, and not due to the low SORLA concentration in monomer processing; (2) SORLA indirectly affects the dynamic behavior of the β -secretase, but not that of α -secretase. The receptor targets β -secretase which is responsible for the initial amyloidogenic cleavage. This supports the initial biochemical data showing that SORLA can bind to β -secretase [Spoelgen et al. 2006]; and (3) SORLA is more influential in dimer processing than in monomer processing, which confirms our initial hypothesis that blockade of APP dimerization is an important aspect of SORLA action in AD. These findings represents a major conceptual advancement in our understanding of the complex APP processing.

In order to establish a model that will test the potential effects of SORLA on APP processing in the context of AD therapy, the multi-compartmental model presented in Section 4.2 [Lao et al. 2012] can be extended by including additional cleavage activity of γ -secretase in monomer and dimer processing for research interests that focus on the influence of SORLA on γ -secretase and $A\beta$ peptide. Whereas, for researchers interested in other risk factors, it will be an endeavor to extend the model by adding more risk factors.

BIBLIOGRAPHY

- Alzheimer's Association. What is Alzheimer's disease? <http://www.alz.org>.
- O. M. Andersen and T. E. Willnow. Lipoprotein receptors in Alzheimer's disease. *Trends Neurosci.*, 29(12):687–694, Dec. 2006.
- O. M. Andersen, J. Reiche, V. Schmidt, M. Gotthardt, R. Spoelgen, J. Behlke, C. A. F. von Arnim, T. Breiderhoff, P. Jansen, X. Wu, K. R. Bales, R. Cappai, C. L. Masters, J. Gliemann, E. J. Mufson, B. T. Hyman, S. M. Paul, A. Nykjaer, and T. E. Willnow. Neuronal sorting protein-related receptor sorLA/LR11 regulates processing of the amyloid precursor protein. *Proc. Natl. Acad. Sci. USA*, 102(38):13461–13466, 2005.
- O. M. Andersen, V. Schmidt, R. Spoelgen, J. Gliemann, J. Behlke, D. Galatis, W. J. McKinstry, M. W. Parker, C. L. Masters, B. T. Hyman, R. Cappai, and T. E. Willnow. Molecular dissection of the interaction between amyloid precursor protein and its neuronal trafficking receptor SorLA/LR11. *Biochemistry*, 45(8):2618–2628, Feb. 2006.
- L. V. Bertalanffy. An outline of general system theory. *Br. J. Philos. Sci.*, 1(2):134–165, 1950.
- R. Brookmeyer, E. Johnson, K. Ziegler-Graham, and H. M. Arrighi. Forecasting the global burden of Alzheimer's disease. *Alzheimers Dement.*, 3(3):186–191, July 2007.
- A. Ciobica, M. Padurariu, W. Bild, and C. Stefanescu. Cardiovascular risk factors as potential markers for mild cognitive impairment and Alzheimer's disease. *Psychiatria Danubina*, 23(4):340–346, Dec. 2011.
- E. H. Corder, A. M. Saunders, W. J. Strittmatter, D. E. Schmechel, P. C. Gaskell, G. W. Small, A. D. Roses, J. L. Haines, and M. A. Pericak-Vance. Gene dose of apolipoprotein E type 4 allele and the risk of Alzheimer's disease in late onset families. *Science*, 261(5123):921–923, Aug. 1993.

Bibliography

- D. L. Craft, L. M. Wein, and D. J. Selkoe. A mathematical model of the impact of novel treatments on the A-beta burden in the Alzheimer's brain, CSF and plasma. *B. Math. Biol.*, 64(5):1011–1031, Sept. 2002.
- L. Cruz, B. Urbanc, S. V. Buldyrev, R. Christie, T. Gómez-Isla, S. Havlin, M. McNamara, H. E. Stanley, and B. T. Hyman. Aggregation and disaggregation of senile plaques in Alzheimer's disease. *Proc. Natl. Acad. Sci. USA*, 94(14):7612–7616, July 1997.
- T. Cukierman-Yaffe, H. C. Gerstein, J. D. Williamson, R. M. Lazar, L. Lovato, M. E. Miller, L. H. Coker, A. Murray, M. D. Sullivan, S. M. Marcovina, and L. J. Launer. Relationship between baseline glycemic control and cognitive function in individuals with type 2 diabetes and other cardiovascular risk factors: the action to control cardiovascular risk in diabetes-memory in diabetes (ACCORD-MIND) trial. *Diabetes Care*, 32(2):221–226, Feb. 2009.
- T. B. Cumming and A. Brodtmann. Can stroke cause neurodegenerative dementia? *Int. J. Stroke.*, 6(5):416–424, Oct. 2011.
- R. Das, R. B. Nachbar, L. Edelstein-Keshet, J. S. Saltzman, M. C. Wiener, A. Bagchi, J. Bailey, D. Coombs, A. J. Simon, R. J. Hargreaves, and J. J. Cook. Modeling effect of a gamma-secretase inhibitor on amyloid-beta dynamics reveals significant role of an amyloid clearance mechanism. *B. Math. Biol.*, 73(1):230–247, Jan. 2011.
- T. den Heijer, F. van der Lijn, A. Ikram, P. J. Koudstaal, A. van der Lugt, G. P. Krestin, H. A. Vrooman, A. Hofman, W. J. Niessen, and M. M. B. Breteler. Vascular risk factors, apolipoprotein E, and hippocampal decline on magnetic resonance imaging over a 10-year follow-up. *Alzheimers Dement.*, Jan. 2012.
- S. E. Dodson, O. M. Andersen, V. Karmali, J. J. Fritz, D. Cheng, J. Peng, A. I. Levey, T. E. Willnow, and J. J. Lah. Loss of LR11/SORLA enhances early pathology in a mouse model of amyloidosis: evidence for a proximal role in Alzheimer's disease. *J. Neurosci.*, 28(48):12877–12886, Nov. 2008.
- M. Gossen and H. Bujard. Tight control of gene expression in mammalian cells by tetracycline-responsive promoters. *Proc. Natl. Acad. Sci. USA*, 89(12):5547–5551, June 1992.
- C. Haass and D. J. Selkoe. Soluble protein oligomers in neurodegeneration: lessons from the Alzheimer's amyloid beta-peptide. *Nat. Rev. Mol. Cell Biol.*, 8(2):101–112, Feb. 2007.
- C. Haass, A. Y. Hung, M. G. Schlossmacher, D. B. Teplow, and D. J. Selkoe. beta-Amyloid peptide and a 3-kDa fragment are derived by distinct cellular mechanisms. *J. Biol. Chem.*, 268(5):3021–3024, Feb. 1993.

- W. M. Haddad, V. Chellaboina, and Q. Hui. *Nonnegative and Compartmental Dynamical Systems*. Princeton University Press, Jan. 2010.
- J. Hardy. The amyloid hypothesis for Alzheimer's disease: a critical reappraisal. *J. Neurochem.*, 110(4):1129–1134, Aug. 2009.
- J. Hardy and D. Allsop. Amyloid deposition as the central event in the aetiology of Alzheimer's disease. *Trends Pharmacol. Sci.*, 12(10):383–388, Oct. 1991.
- J. Hardy and D. J. Selkoe. The amyloid hypothesis of Alzheimer's disease: progress and problems on the road to therapeutics. *Science*, 297(5580):353–356, July 2002.
- J. A. Hardy and G. A. Higgins. Alzheimer's disease: the amyloid cascade hypothesis. *Science*, 256(5054):184–185, Apr. 1992.
- J. D. Harper, S. S. Wong, C. M. Lieber, and J. Lansbury, P T. Assembly of a beta amyloid protofibrils: an in vitro model for a possible early event in alzheimer's disease. *Biochemistry*, 38(28):8972–8980, July 1999.
- K. Hübner, S. Sahle, and U. Kummer. Applications and trends in systems biology in biochemistry. *FEBS J.*, 278(16):2767–2857, Aug. 2011.
- L. W. Hung, G. D. Ciccotosto, E. Giannakis, D. J. Tew, K. Perez, C. L. Masters, R. Cappai, J. D. Wade, and K. J. Barnham. Amyloid-beta peptide (A β) neurotoxicity is modulated by the rate of peptide aggregation: A β dimers and trimers correlate with neurotoxicity. *J. Neurosci.*, 28(46):11950–11958, Nov. 2008.
- B. T. Hyman, H. L. West, G. W. Rebeck, S. V. Buldyrev, R. N. Mantegna, M. Ukleja, S. Havlin, and H. E. Stanley. Quantitative analysis of senile plaques in Alzheimer's disease: observation of log-normal size distribution and molecular epidemiology of differences associated with apolipoprotein E genotype and trisomy 21 (Down syndrome). *Proc. Natl. Acad. Sci. USA*, 92(8):3586–3590, Apr. 1995.
- H. Inouye and D. A. Kirschner. A beta fibrillogenesis: kinetic parameters for fibril formation from congo red binding. *J. Struct. Biol.*, 130(2-3):123–129, June 2000.
- L. Jacobsen, P. Madsen, S. K. Moestrup, A. H. Lund, N. Tommerup, A. Nykjaer, L. Sottrup-Jensen, J. Gliemann, and C. M. Petersen. Molecular characterization of a novel human hybrid-type receptor that binds the alpha2-Macroglobulin receptor-associated protein. *J. Biol. Chem.*, 271(49):31379–31383, Dec. 1996.
- L. Jacobsen, P. Madsen, M. S. Nielsen, W. P. M. Geraerts, J. Gliemann, A. B. Smit, and C. M. Petersen. The sorLA cytoplasmic domain interacts with GGA1 and -2 and defines minimum requirements for GGA binding. *FEBS Letters*, 511(1-3):155–158, Jan. 2002.

Bibliography

- P. Jansen, K. Giehl, J. R. Nyengaard, K. Teng, O. Lioubinski, S. S. Sjoegaard, T. Breiderhoff, M. Gotthardt, F. Lin, A. Eilers, C. M. Petersen, G. R. Lewin, B. L. Hempstead, T. E. Willnow, and A. Nykjaer. Roles for the pro-neurotrophin receptor sortilin in neuronal development, aging and brain injury. *Nat. Neurosci.*, 10(11):1449–1457, Nov. 2007.
- S. Jin, K. Agerman, K. Kolmodin, E. Gustafsson, C. Dahlqvist, A. Jureus, G. Liu, J. Fältling, S. Berg, J. Lundkvist, and U. Lendahl. Evidence for dimeric BACE-mediated APP processing. *Biochem. Biophys. Res. Commun.*, 393(1):21–27, Feb. 2010.
- D. Kaden, L. Munter, M. Joshi, C. Treiber, C. Weise, T. Bethge, P. Voigt, M. Schaefer, M. Beyermann, B. Reif, and G. Multhaup. Homophilic interactions of the amyloid precursor protein (APP) ectodomain are regulated by the loop region and affect beta-Secretase cleavage of APP. *J. Biol. Chem.*, 283(11):7271–7279, Mar. 2008.
- D. Kaden, P. Voigt, L. M. Munter, K. D. Bobowski, M. Schaefer, and G. Multhaup. Subcellular localization and dimerization of APLP1 are strikingly different from APP and APLP2. *J. Cell Sci.*, 122(Pt 3):368, 2009.
- P. Kienlen-Campard, B. Tasiaux, J. Van Hees, M. Li, S. Huysseune, T. Sato, J. Z. Fei, S. Aimoto, P. J. Courttoy, S. O. Smith, S. N. Constantinescu, and J. Octave. Amyloidogenic processing but not amyloid precursor protein (APP) intracellular C-terminal domain production requires a precisely oriented APP dimer assembled by transmembrane GXXXG motifs. *J. Biol. Chem.*, 283(12):7733–7744, Mar. 2008.
- H. Kitano. Computational systems biology. *Nature*, 420(6912):206–210, Nov. 2002a.
- H. Kitano. Systems biology: a brief overview. *Science*, 295(5560):1662–1664, Mar. 2002b.
- H. Kitano, A. Funahashi, Y. Matsuoka, and K. Oda. Using process diagrams for the graphical representation of biological networks. *Nat. Biotechnol.*, 23(8):961–966, 2005.
- A. Lao, V. Schmidt, Y. Schmitz, T. E. Willnow, and O. Wolkenhauer. Multi-compartmental modeling of SORLA’s influence on amyloidogenic processing in Alzheimer’s disease. *BMC Syst. Biol.*, 6(1):74, June 2012.
- A. Lomakin, D. S. Chung, G. B. Benedek, D. A. Kirschner, and D. B. Teplow. On the nucleation and growth of amyloid beta-protein fibrils: detection of nuclei and quantitation of rate constants. *Proc. Natl. Acad. Sci. USA*, 93(3):1125–1129, Feb. 1996.
- A. Lomakin, D. B. Teplow, D. A. Kirschner, and G. B. Benedek. Kinetic theory of fibrillogenesis of amyloid beta-protein. *Proc. Natl. Acad. Sci. USA*, 94(15):7942–7947, July 1997.

- E. G. Marcusson, B. F. Horazdovsky, J. L. Cereghino, E. Gharakhanian, and S. D. Emr. The sorting receptor for yeast vacuolar carboxypeptidase Y is encoded by the VPS10 gene. *Cell*, 77(4):579–586, May 1994.
- M. D. Mesarovic. *Systems Theory and Biology*. Springer-Verlag, Berlin, 1968.
- G. Multhaup. Amyloid precursor protein and BACE function as oligomers. *Neurodegener Dis.*, 3(4-5):270–274, 2006.
- L. Munter, P. Voigt, A. Harmeier, D. Kaden, K. E. Gottschalk, C. Weise, R. Pipkorn, M. Schaefer, D. Langosch, and G. Multhaup. GxxxG motifs within the amyloid precursor protein transmembrane sequence are critical for the etiology of Abeta42. *EMBO J.*, 26(6):1702–1712, Mar. 2007.
- H. Naiki and K. Nakakuki. First-order kinetic model of Alzheimer’s beta-amyloid fibril extension in vitro. *Lab Invest.*, 74(2):374–383, Feb. 1996.
- H. Naiki, K. Higuchi, K. Nakakuki, and T. Takeda. Kinetic analysis of amyloid fibril polymerization in vitro. *Lab Invest.*, 65(1):104–110, July 1991.
- H. Naiki, K. Hasegawa, I. Yamaguchi, H. Nakamura, F. Gejyo, and K. Nakakuki. Apolipoprotein E and antioxidants have different mechanisms of inhibiting Alzheimer’s beta-amyloid fibril formation in vitro. *Biochemistry*, 37(51):17882–17889, Dec. 1998.
- K. Offe, S. E. Dodson, J. T. Shoemaker, J. J. Fritz, M. Gearing, A. I. Levey, and J. J. Lah. The lipoprotein receptor LR11 regulates amyloid beta production and amyloid precursor protein traffic in endosomal compartments. *J. Neurosci.*, 26(5):1596–1603, Feb. 2006.
- R. Parsons and B. Austen. Protein-protein interactions in the assembly and subcellular trafficking of the BACE (beta-site amyloid precursor protein-cleaving enzyme) complex of Alzheimer’s disease. *Biochem. Soc. Trans.*, 35(5):974, Oct. 2007.
- G. Pastori, V. Simons, and M. van Bogaert. Systems biology in the European research area. <http://www.erasysbio.net>, Mar. 2008.
- S. M. Pickering-Brown, M. Baker, J. Gass, B. F. Boeve, C. T. Loy, W. S. Brooks, I. R. A. Mackenzie, R. N. Martins, J. B. J. Kwok, G. M. Halliday, J. Kril, P. R. Schofield, D. M. A. Mann, and M. Hutton. Mutations in progranulin explain atypical phenotypes with variants in MAPT. *Brain*, 129(Pt 11):3124–3126, Nov. 2006.
- I. K. Puri and L. Li. Mathematical modeling for the pathogenesis of Alzheimer’s disease. *PLoS One*, 5(12):e15176, Dec. 2010.

Bibliography

- E. Rogaeva, Y. Meng, J. H. Lee, Y. Gu, T. Kawarai, F. Zou, T. Katayama, C. T. Baldwin, R. Cheng, H. Hasegawa, F. Chen, N. Shibata, K. L. Lunetta, R. Pardossi-Piquard, C. Bohm, Y. Wakutani, L. A. Cupples, K. T. Cuenco, R. C. Green, L. Pinessi, I. Rainero, S. Sorbi, A. Bruni, R. Duara, R. P. Friedland, R. Inzelberg, W. Hampe, H. Bujo, Y. Song, O. M. Andersen, T. E. Willnow, N. Graff-Radford, R. C. Petersen, D. Dickson, S. D. Der, P. E. Fraser, G. Schmitt-Ulms, S. Younkin, R. Mayeux, L. A. Farrer, and P. St George-Hyslop. The neuronal sortilin-related receptor SORL1 is genetically associated with Alzheimer disease. *Nat. Genet.*, 39(2):168–177, Feb. 2007.
- M. Rohe, A.-S. Carlo, H. Breyhan, A. Sporbert, D. Militz, V. Schmidt, C. Wozny, A. Harmeier, B. Erdmann, K. R. Bales, S. Wolf, G. Kempermann, S. M. Paul, D. Schmitz, T. A. Bayer, T. E. Willnow, and O. M. Andersen. Sortilin-related receptor with A-type repeats (SORLA) affects the amyloid precursor protein-dependent stimulation of ERK signaling and adult neurogenesis. *J. Biol. Chem.*, 283(21):14826–14834, May 2008.
- K. Sambamurti, A. Suram, C. Venugopal, A. Prakasam, Y. Zhou, D. K. Lahiri, and N. H. Greig. A partial failure of membrane protein turnover may cause Alzheimer’s disease: a new hypothesis. *Curr. Alzheimer Res.*, 3(1):81–90, Feb. 2006.
- A. M. Saunders, W. J. Strittmatter, D. Schmechel, P. H. George-Hyslop, M. A. Pericak-Vance, S. H. Joo, B. L. Rosi, J. F. Gusella, D. R. Crapper-MacLachlan, and M. J. Alberts. Association of apolipoprotein E allele epsilon 4 with late-onset familial and sporadic Alzheimer’s disease. *Neurology*, 43(8):1467–1472, Aug. 1993.
- C. R. Scherzer, K. Offe, M. Gearing, H. D. Rees, G. Fang, C. J. Heilman, C. Schaller, H. Bujo, A. I. Levey, and J. J. Lah. Loss of apolipoprotein E receptor LR11 in Alzheimer disease. *Arch. Neurol.*, 61(8):1200–1205, Aug. 2004.
- K. Schittkowski. *Numerical Data Fitting in Dynamical Systems: A Practical Introduction with Applications and Software*. Springer, 1 edition, Dec. 2002.
- A. Schmechel, M. Strauss, A. Schlicksupp, R. Pipkorn, C. Haass, T. A. Bayer, and G. Multhaup. Human BACE forms dimers and colocalizes with APP. *J. Biol. Chem.*, 279(38):39710–39717, 2004.
- V. Schmidt, A. Sporbert, M. Rohe, T. Reimer, A. Rehm, O. M. Andersen, and T. E. Willnow. SorLA/LR11 regulates processing of amyloid precursor protein via interaction with adaptors GGA and PACS-1. *J. Biol. Chem.*, 282(45):32956–32964, Nov. 2007.
- V. Schmidt, K. Baum, A. Lao, K. Rateitschak, Y. Schmitz, A. Teichmann, B. Wiesner, C. M. Petersen, A. Nykjaer, J. Wolf, O. Wolkenhauer, and T. E. Willnow. Quantita-

- tive modelling of amyloidogenic processing and its influence by SORLA in Alzheimer's disease. *EMBO J.*, 31(1):187–200, Jan. 2012.
- D. J. Selkoe. The molecular pathology of Alzheimer's disease. *Neuron*, 6(4):487–498, Apr. 1991.
- J. Shen and R. J. Kelleher 3rd. The presenilin hypothesis of Alzheimer's disease: evidence for a loss-of-function pathogenic mechanism. *Proc. Natl. Acad. Sci. USA*, 104(2):403–409, Jan. 2007.
- S. A. Small and K. Duff. Linking Abeta and tau in late-onset Alzheimer's disease: a dual pathway hypothesis. *Neuron*, 60(4):534–542, Nov. 2008.
- J. L. Snoep and H. V. Westerhoff. Systems biology: Definitions and perspectives. In *From isolation to integration, a systems biology approach for building the Silicon Cell*, volume 13 of *Topics in Current Genetics*, page pp. 1330. Springer-Verlag, Berlin, 2005.
- R. Spoelgen, C. A. F. von Arnim, A. V. Thomas, I. D. Peltan, M. Koker, A. Deng, M. C. Irizarry, O. M. Andersen, T. E. Willnow, and B. T. Hyman. Interaction of the cytosolic domains of sorLA/LR11 with the amyloid precursor protein (APP) and beta-Secretase beta-Site APP-Cleaving enzyme. *J. Neurosci.*, 26(2):418–428, Jan. 2006.
- M. W. J. Strachan, R. M. Reynolds, B. M. Frier, R. J. Mitchell, and J. F. Price. The relationship between type 2 diabetes and dementia. *Br. Med. Bull.*, 88(1):131–146, 2008.
- W. J. Strittmatter, A. M. Saunders, D. Schmechel, M. Pericak-Vance, J. Enghild, G. S. Salvesen, and A. D. Roses. Apolipoprotein E: high-avidity binding to beta-amyloid and increased frequency of type 4 allele in late-onset familial Alzheimer disease. *Proc. Natl. Acad. Sci. USA*, 90(5):1977–1981, Mar. 1993.
- G. Tesco, Y. H. Koh, E. L. Kang, A. N. Cameron, S. Das, M. Sena-Esteves, M. Hiltunen, S. Yang, Z. Zhong, Y. Shen, J. W. Simpkins, and R. E. Tanzi. Depletion of GGA3 stabilizes BACE and enhances beta-secretase activity. *Neuron*, 54(5):721–737, June 2007.
- B. Urbanc, L. Cruz, S. V. Buldyrev, S. Havlin, M. C. Irizarry, H. E. Stanley, and B. T. Hyman. Dynamics of plaque formation in Alzheimer's disease. *Biophys. J.*, 76(3):1330–1334, Mar. 1999.
- R. Vidal, B. Frangione, A. Rostagno, S. Mead, T. Révész, G. Plant, and J. Ghiso. A stop-codon mutation in the BRI gene associated with familial British dementia. *Nature*, 399(6738):776–781, June 1999.

Bibliography

- E. O. Voit, Z. Qi, and G. W. Miller. Steps of modeling complex biological systems. *Pharmacopsychiatry*, 41 Suppl 1:S78–84, Sept. 2008.
- C. A. F. von Arnim, R. Spoelgen, I. D. Peltan, M. Deng, S. Courchesne, M. Koker, T. Matsui, H. Kowa, S. F. Lichtenthaler, M. C. Irizarry, and B. T. Hyman. GGA1 acts as a spatial switch altering amyloid precursor protein trafficking and processing. *J. Neurosci.*, 26(39):9913–9922, Sept. 2006.
- T. Wahle, D. R. Thal, M. Sastre, A. Rentmeister, N. Bogdanovic, M. Famulok, M. T. Heneka, and J. Walter. GGA1 is expressed in the human brain and affects the generation of amyloid beta-peptide. *J. Neurosci.*, 26(49):12838–12846, Dec. 2006.
- D. M. Walsh and D. J. Selkoe. Abeta oligomers - a decade of discovery. *J. Neurochem.*, 101(5):1172–1184, June 2007.
- G. G. Westmeyer, M. Willem, S. F. Lichtenthaler, G. Lurman, G. Multhaup, I. Assfalg-Machleidt, K. Reiss, P. Saftig, and C. Haass. Dimerization of beta-site beta-Amyloid precursor protein-cleaving enzyme. *J. Biol. Chem.*, 279(51):53205–53212, Dec. 2004.
- T. E. Willnow, C. M. Petersen, and A. Nykjaer. VPS10P-domain receptors - regulators of neuronal viability and function. *Nat. Rev. Neurosci.*, 9(12):899–909, Dec. 2008.
- T. E. Willnow, A. Carlo, M. Rohe, and V. Schmidt. SORLA/SORL1, a neuronal sorting receptor implicated in Alzheimer’s disease. *Rev. Neurosci.*, 21(4):315–329, 2010.
- O. Wolkenhauer. Defining systems biology: an engineering perspective. *IET Syst. Biol.*, 1(4):204–206, July 2007.
- O. Wolkenhauer, B. Ghosh, and K. Cho. Control and coordination in biochemical networks. *IEEE Contr. Syst.*, 24(4):30–34, Aug. 2004.
- O. Wolkenhauer, M. Ullah, P. Wellstead, and K. Cho. The dynamic systems approach to control and regulation of intracellular networks. *FEBS letters*, 579(8):1846–1853, Mar. 2005.
- M. Wysocki, X. Luo, J. Schmeidler, K. Dahlman, G. T. Lesser, H. Grossman, V. Haroutunian, and M. S. Beeri. Hypertension is associated with cognitive decline in elderly people at high risk for dementia. *Am. J. Geriatr. Psychiatry.*, 20(2):179–187, Feb. 2012.
- H. Xu, P. Greengard, and S. Gandy. Regulated formation of golgi secretory vesicles containing Alzheimer beta-amyloid precursor protein. *J. Biol. Chem.*, 270(40):23243–23245, Oct. 1995.

Bibliography

H. Yamazaki, H. Bujo, J. Kusunoki, K. Seimiya, T. Kanaki, N. Morisaki, W. J. Schneider, and Y. Saito. Elements of neural adhesion molecules and a yeast vacuolar protein sorting receptor are present in a novel mammalian low density lipoprotein receptor family member. *J. Biol. Chem.*, 271(40):24761 –24768, Oct. 1996.

APPENDICES

APPENDIX

A

DESCRIPTION OF VARIABLES

A. Description of variables

Table A.1.: Description of the variables and parameters used in the equations found in Section 3.1.

Notation	Unit	Description
APP	fmol	free APP-monomer
α	fmol	free α -secretase-monomer
β	fmol	free β -secretase-monomer
$C_{APP\alpha}$	fmol	complex of APP and α , formed within monomer processing
$C_{APP\beta}$	fmol	complex of APP and β , formed within monomer processing
$sAPP\alpha$	fmol	soluble $APP\alpha$ resulting from monomer processing
$sAPP\beta$	fmol	soluble $APP\beta$ resulting from monomer processing
$SORLA$	fmol	free sorting protein-related receptor
$C_{APPSORLA}$	fmol	complex of APP and $SORLA$
APP_{Tot}	fmol	total APP conserved in the whole system
$SORLA_{Tot}$	fmol	total SORLA conserved in the whole system
α_{Tot}	fmol	total α -secretase conserved in the whole system
β_{Tot}	fmol	total β -secretase conserved in the whole system
$sAPP\alpha_{Tot}$	fmol	total soluble $APP\alpha$
$sAPP\beta_{Tot}$	fmol	total soluble $APP\beta$
K_s	fmol^{-1}	association constant of APP and $SORLA$
k_i	$\text{fmol}^{-1} \cdot \text{h}^{-1}$	binding rate constant (where $i = 1, 3, 5$)
k_j	h^{-1}	dissociation rate constant (where $j = -1, -3, -5, 4, 6$)
$K_{M\alpha}$	fmol	defined by $(k_6 + k_{-5})/k_5$
$K_{M\beta}$	fmol	defined by $(k_4 + k_{-3})/k_3$

Table A.2.: Description of the variables and parameters used in the equations found in Section 3.2.

Notation	Unit	Description
APP	fmol	free APP-monomer
α	fmol	free α -secretase-monomer
β	fmol	free β -secretase-monomer
APP_d	fmol	free APP-dimer
α_d	fmol	free α -secretase-dimer
β_d	fmol	free β -secretase-dimer
$C_{APPd\alpha d}$	fmol	complex of APP_d and α_d , formed within dimer processing
$C_{APPd\beta d}$	fmol	complex of APP_d and β_d , formed within dimer processing
$sAPP\alpha^*$	fmol	soluble $APP\alpha$ resulting from dimer processing
$sAPP\beta^*$	fmol	soluble $APP\beta$ resulting from dimer processing
$SORLA$	fmol	free sorting protein-related receptor
$C_{APPSORLA}$	fmol	complex of APP and $SORLA$
APP_{Tot}	fmol	total APP conserved in the whole system
$SORLA_{Tot}$	fmol	total SORLA conserved in the whole system
α_{Tot}	fmol	total α -secretase conserved in the whole system
β_{Tot}	fmol	total β -secretase conserved in the whole system
$sAPP\alpha_{Tot}$	fmol	total soluble $APP\alpha$
$sAPP\beta_{Tot}$	fmol	total soluble $APP\beta$
K_A	fmol^{-1}	association constant of APP dimerization
K_B	fmol^{-1}	association constant of β -secretase dimerization
K_C	fmol^{-1}	association constant of α -secretase dimerization
K_s	fmol^{-1}	association constant of APP and $SORLA$
k_i	$\text{fmol}^{-1} \cdot \text{h}^{-1}$	binding rate constant (where $i = 1, 31, 51$)
k_j	h^{-1}	dissociation rate constant (where $j = -1, -31, -51, -a, -b, -c, 41, 61$)
k_h	$\text{fmol}^{-1} \cdot \text{h}^{-1}$	dimerization rate constant (where $h = a, b, c$)
$K_{M\alpha d}$	fmol	defined by $(k_{61} + k_{-51})/k_{51}$
$K_{M\beta d}$	fmol	defined by $(k_{41} + k_{-31})/k_{31}$

A. Description of variables

Table A.3.: Description of the variables and parameters used in the equations found in Section 3.3.

Notation	Unit	Description
APP	fmol	free APP-monomer
α	fmol	free α -secretase-monomer
β	fmol	free β -secretase-monomer
$C_{APP\alpha}$	fmol	complex of APP and α , formed within monomer processing
$C_{APP\beta}$	fmol	complex of APP and β , formed within monomer processing
$sAPP\alpha$	fmol	soluble $APP\alpha$ resulting from monomer processing
$sAPP\beta$	fmol	soluble $APP\beta$ resulting from monomer processing
APP_d	fmol	free APP-dimer
α_d	fmol	free α -secretase-dimer
β_d	fmol	free β -secretase-dimer
$C_{APP_d\alpha_d}$	fmol	complex of APP_d and α_d , formed within dimer processing
$C_{APP_d\beta_d}$	fmol	complex of APP_d and β_d , formed within dimer processing
$sAPP\alpha^*$	fmol	soluble $APP\alpha$ resulting from dimer processing
$sAPP\beta^*$	fmol	soluble $APP\beta$ resulting from dimer processing
$SORLA$	fmol	free sorting protein-related receptor
$C_{APPSORLA}$	fmol	complex of APP and $SORLA$
APP_{Tot}	fmol	total APP conserved in the whole system
$SORLA_{Tot}$	fmol	total $SORLA$ conserved in the whole system
α_{Tot}	fmol	total α -secretase conserved in the whole system
β_{Tot}	fmol	total β -secretase conserved in the whole system
$sAPP\alpha_{Tot}$	fmol	total soluble $APP\alpha$
$sAPP\beta_{Tot}$	fmol	total soluble $APP\beta$
K_A	fmol^{-1}	association constant of APP dimerization
K_B	fmol^{-1}	association constant of β -secretase dimerization
K_C	fmol^{-1}	association constant of α -secretase dimerization
K_s	fmol^{-1}	association constant of APP and $SORLA$
k_i	$\text{fmol}^{-1} \cdot \text{h}^{-1}$	binding rate constant (where $i = 1, 3, 5, 31, 51$)
k_j	h^{-1}	dissociation rate constant (where $j = -1, -3, -5, -31, -51, -a, -b, -c, 4, 6, 41, 61$)
k_h	$\text{fmol}^{-1} \cdot \text{h}^{-1}$	dimerization rate constant (where $h = a, b, c$)
$K_{M\alpha}$	fmol	defined by $(k_6 + k_{-5})/k_5$
$K_{M\beta}$	fmol	defined by $(k_4 + k_{-3})/k_3$
$K_{M\alpha_d}$	fmol	defined by $(k_{61} + k_{-51})/k_{51}$
$K_{M\beta_d}$	fmol	defined by $(k_{41} + k_{-31})/k_{31}$

Table A.4.: Description of the variables used in the equations found in Section 4.2.

Notation	Unit	Description
APP_{init}	fmol	free initial APP-monomer in TGN
APP_{G1}	fmol	free APP-monomer in monomer processing of TGN
APP_{G2}	fmol	free APP-monomer in dimer processing of TGN
APP_{G2d}	fmol	free APP-dimer in dimer processing of TGN
APP_{CS1}	fmol	free APP-monomer in monomer processing of cell surface
APP_{CS2d}	fmol	free APP-dimer in dimer processing of cell surface
APP_{E1}	fmol	free APP-monomer in monomer processing of endosome
APP_{E2d}	fmol	free APP-dimer in dimer processing of endosome
α_{init}	fmol	free initial α -secretase within cell surface
α_1	fmol	free α -secretase-monomer in monomer processing within cell surface
α_2	fmol	free α -secretase-monomer in dimer processing within cell surface
α_{2d}	fmol	free α -secretase-dimer in dimer processing within cell surface
β_{init}	fmol	free initial β -secretase within endosome
β_1	fmol	free β -secretase-monomer in monomer processing within endosome
β_2	fmol	free β -secretase-monomer in dimer processing within endosome
β_{2d}	fmol	free β -secretase-dimer in dimer processing within endosome
$C_{APPCS1\alpha1}$	fmol	complex of APP_{CS1} and α_1 , formed within monomer processing of cell surface
$C_{APPE1\beta1}$	fmol	complex of APP_{E1} and β_1 , formed within monomer processing of endosome
$C_{APPCS2d\alpha2d}$	fmol	complex of APP_{CS2d} and α_{2d} , formed within dimer processing of cell surface
$C_{APPE2d\beta2d}$	fmol	complex of APP_{E2d} and β_{2d} , formed within dimer processing of endosome
$sAPP\alpha_1$	fmol	soluble $APP\alpha$ resulting from monomer processing of cell surface
$sAPP\beta_1$	fmol	soluble $APP\beta$ resulting from monomer processing of endosome
$sAPP\alpha_2$	fmol	soluble $APP\alpha$ resulting from dimer processing of cell surface
$sAPP\beta_2$	fmol	soluble $APP\beta$ resulting from dimer processing of endosome
$SORLAG_1$	fmol	free SORLA in the monomer processing of TGN
$SORLAG_2$	fmol	free SORLA in the dimer processing of TGN
$C_{APPG1SORLAG1}$	fmol	complex of APP_{G1} and $SORLAG_1$ in the monomer processing of TGN
$C_{APPG2SORLAG2}$	fmol	complex of APP_{G2} and $SORLAG_2$ in the dimer processing of TGN
$APP_{monomer}$	fmol	total APP conserved in the monomer processing
APP_{dimer}	fmol	total APP conserved in the dimer processing
APP_{Tot}	fmol	total APP conserved in the whole system
$SORLA_{monomer}$	fmol	total SORLA conserved in the monomer processing
$SORLA_{dimer}$	fmol	total SORLA conserved in the dimer processing
$SORLA_{Tot}$	fmol	total SORLA conserved in the whole system
$\alpha_{monomer}$	fmol	total α -secretase conserved in the monomer processing
α_{dimer}	fmol	total α -secretase conserved in the dimer processing
α_{Tot}	fmol	total α -secretase conserved in the whole system
$\beta_{monomer}$	fmol	total β -secretase conserved in the monomer processing
β_{dimer}	fmol	total β -secretase conserved in the dimer processing
β_{Tot}	fmol	total β -secretase conserved in the whole system
$sAPP\alpha_{Tot}$	fmol	total soluble $APP\alpha$
$sAPP\beta_{Tot}$	fmol	total soluble $APP\beta$

A. Description of variables

Table A.5.: Description of the parameters used in the equations found in Section 4.2.

Notation	Unit	Description
K_{G1}		equilibrium constant of APP_{init} and APP_{G1}
K_{G2}		equilibrium constant of APP_{init} and APP_{G2}
K_{CS1}		equilibrium constant of APP_{G1} and APP_{CS1}
K_{CS2}		equilibrium constant of APP_{G2d} and APP_{CS2d}
K_{E1}		equilibrium constant of APP_{CS1} and APP_{E1}
K_{E2}		equilibrium constant of APP_{CS2d} and APP_{E2d}
K_{C1}		equilibrium constant of α_{init} and α_1
K_{C2}		equilibrium constant of α_{init} and α_2
K_{B1}		equilibrium constant of β_{init} and β_1
K_{B2}		equilibrium constant of β_{init} and β_2
K_{G3}	fmol^{-1}	association constant of APP dimerization
K_{B3}	fmol^{-1}	association constant of β -secretase dimerization
K_{C3}	fmol^{-1}	association constant of α -secretase dimerization
K_{S1}	fmol^{-1}	association constant of APP_{G1} and $SORLAG1$
K_{S2}	fmol^{-1}	association constant of APP_{G2} and $SORLAG2$
k_i	$\text{fmol}^{-1} \cdot \text{h}^{-1}$	binding rate constant (where $i = 1, 3, 5, 31, 51$)
k_j	h^{-1}	dissociation rate constant (where $j = -1, -3, -5, -31, -51, -g3, -b3, -c3, 4, 6, 41, 61$)
k_h	$\text{fmol}^{-1} \cdot \text{h}^{-1}$	dimerization rate constant (where $h = g3, b3, c3$)
k_q	h^{-1}	inflow rate constant (where $q = g1, g2, cs1, cs2, e1, e2, c1, c2, b1, b2$)
k_t	h^{-1}	outflow rate constant (where $q = -g1, -g2, -cs1, -cs2, -e1, -e2, -c1, -c2, -b1, -b2$)
k_r	$\text{fmol} \cdot \text{h}^{-1}$	initial rate (where $r = g0$)
$K_{M\alpha 1}$	fmol	defined by $(k_6 + k_{-5})/k_5$
$K_{M\beta 1}$	fmol	defined by $(k_4 + k_{-3})/k_3$
$K_{M\alpha 2d}$	fmol	defined by $(k_{61} + k_{-51})/k_{51}$
$K_{M\beta 2d}$	fmol	defined by $(k_{41} + k_{-31})/k_{31}$

APPENDIX

B

ESTIMATED PARAMETER VALUES

B. Estimated parameter values

Table B.1.: Estimated parameter values corresponding to the simulations shown in Figure 3.3.

parameter	(units)	values	parameter	(units)	values
α_{Tot}	(fmol)	6.47×10^0	β_{Tot}	(fmol)	4.48×10^1
$SORLA_{Tot}$	(fmol)	6.05×10^4	K_s	(fmol ⁻¹)	1.54×10^3
k_6	(h ⁻¹)	1.01×10^2	k_4	(h ⁻¹)	2.42×10^{-1}
$K_{M\alpha}$	(fmol)	3.85×10^4	$K_{M\beta}$	(fmol)	4.19×10^3

Table B.2.: Estimated parameter values corresponding to the simulations shown in Figure 3.7.

parameter	(units)	values	parameter	(units)	values
α_{Tot}	(fmol)	1.74×10^0	β_{Tot}	(fmol)	3.73×10^{-1}
$SORLA_{Tot}$	(fmol)	3.59×10^4	K_s	(fmol ⁻¹)	1.14×10^3
K_B	(fmol ⁻¹)	3.38×10^2	K_C	(fmol ⁻¹)	2.53×10^2
K_A	(fmol ⁻¹)	1.17×10^{-5}			
k_{61}	(h ⁻¹)	1.37×10^2	k_{41}	(h ⁻¹)	2.37×10^1
$K_{M\alpha d}$	(fmol)	3.13×10^2	$K_{M\beta d}$	(fmol)	5.02×10^1

Table B.3.: Estimated parameter values corresponding to the simulations shown in Figure 3.10.

parameter	(units)	values	parameter	(units)	values
α_{Tot}	(fmol)	7.34×10^3	β_{Tot}	(fmol)	6.05×10^1
$SORLA_{Tot}$	(fmol)	5.13×10^5	K_s	(fmol ⁻¹)	7.19×10^{-3}
K_B	(fmol ⁻¹)	2.10×10^3	K_C	(fmol ⁻¹)	7.41×10^1
K_A	(fmol ⁻¹)	1.25×10^{-1}			
Monomer processing			Dimer processing		
without SORLA					
k_6	(h ⁻¹)	9.87×10^{-3}	k_{61}	(h ⁻¹)	4.75×10^{-1}
$K_{M\alpha}$	(fmol)	4.32×10^{-2}	$K_{M\alpha d}$	(fmol)	5.51×10^3
k_4	(h ⁻¹)	1.16×10^2	k_{41}	(h ⁻¹)	1.30×10^{-1}
$K_{M\beta}$	(fmol)	2.93×10^2	$K_{M\beta d}$	(fmol)	6.53×10^1
with SORLA					
k_6	(h ⁻¹)	9.87×10^{-3}	k_{61}	(h ⁻¹)	4.75×10^{-1}
$K_{M\alpha}$	(fmol)	4.32×10^{-2}	$K_{M\alpha d}$	(fmol)	5.51×10^3
k_4	(h ⁻¹)	1.16×10^2	k_{41}	(h ⁻¹)	1.30×10^{-1}
$K_{M\beta}$	(fmol)	1.42×10^1	$K_{M\beta d}$	(fmol)	2.19×10^5

B. Estimated parameter values

Table B.4.: Estimated parameter values corresponding to the simulations shown in Figure 4.4.

parameter	(units)	values	parameter	(units)	values
α_{Tot}	(fmol)	5.52×10^3	β_{Tot}	(fmol)	1.31×10^1
K_{B3}	(fmol ⁻¹)	2.55×10^{-2}	K_{C3}	(fmol ⁻¹)	1.52×10^{-5}
K_{G3}	(fmol ⁻¹)	4.45×10^{11}			
Monomer processing			Dimer processing		
K_{G1}		1.19×10^{-9}	K_{G2}		2.00×10^{-7}
K_{CS1}		2.01×10^8	K_{CS2}		2.38×10^0
K_{E1}		7.33×10^{-2}	K_{E2}		2.41×10^0
K_{C1}		1.80×10^1	K_{C2}		1.64×10^3
K_{B1}		2.37×10^1	K_{B2}		1.90×10^2
$SORLA_{monomer}$	(fmol)	1.23×10^1	$SORLA_{dimer}$	(fmol)	2.43×10^5
K_{S1}	(fmol ⁻¹)	3.16×10^{-9}	K_{S2}	(fmol ⁻¹)	8.35×10^3
k_6	(h ⁻¹)	7.29×10^{-4}	k_{61}	(h ⁻¹)	1.77×10^1
$K_{M\alpha 1}$	(fmol)	1.37×10^{-2}	$K_{M\alpha 2d}$	(fmol)	5.91×10^3
k_4	(h ⁻¹)	5.25×10^2	k_{41}	(h ⁻¹)	6.59×10^{-1}
$K_{M\beta 1}$	(fmol)	2.23×10^2	$K_{M\beta 2d}$	(fmol)	6.50×10^1

APPENDIX

C

MATLAB SOURCE CODE

Single-compartmental model I

(For Sections 3.1 and 3.2 - with either monomeric or dimeric form of APP)

```
function SingleCompartmentModell

%% clear screen
clc

%% global variables
global data;
global datas;
global parameter;

%% APPROACH:
% Global estimation of parameter values for Single compartment model with only
% (7) monomeric APP
% (99) dimeric APP
approach=7;

%% load experimental data
PREdata= load('CHO.txt'); %without SORLA
PREdatas= load('CHO_S.txt'); %with SORLA

%% open file to record parameter values that will be estimated
if (approach==7)
    fid = fopen('SingleCompartmentMonomer_global.txt', 'at');
elseif (approach==99)
    fid = fopen('SingleCompartmentDimer_global.txt', 'at');
end

%% sort experimental data according to the total amount of APP measured in the experiments
data = sortrows(PREdata, 1); %without SORLA
datas = sortrows(PREdatas, 1); %with SORLA

%% data sets
% without SORLA
xdata = data(:, 1).* 50;%convert total APP from nM into fmol
ydataA = data(:, 2);%sAPPA
ydataB = data(:, 3);%sAPPB
% with SORLA
xdatas = datas(:, 1).* 50;%convert total APP from nM into fmol
ydataAs = datas(:, 2);%sAPPA
ydataBs = datas(:, 3);%sAPPB
% back up vectors of the experimental data
xdata8=xdata;
ydataA8=ydataA;
ydataB8=ydataB;
xdatas8=xdatas;
ydataAs8=ydataAs;
ydataBs8=ydataBs;
% a copy of vector APP in nM for plotting purpose
xdata8P= data(:, 1);
xdatas8P= datas(:, 1);

%%%%%%%%%%%%%%%%%%%%%%%%%%%%%%%%%%%%%%%%%%%%%%%%%%%%%%%%%%%%%%%%%%%%%%%%
%% initial loop
loop=1;
%% row denotes the number of repetitions
for row=1:500

%% initial parameter values
% for monomer processing model
if (approach==7)
    k6=100* rand(1);
    Atot=100* rand(1);%total amount of alpha-secretase
    Kma=100* rand(1);
    k4=100* rand(1);
    Btot=100* rand(1);%total amount of beta-secretase
    Kmb=100* rand(1);
    s=100* rand(1);%SORLA
    Ks=100* rand(1);%dissociation constant of SORLA and APP
    Ka=0;%constant ratio for APP dimerization
    Kb=0;%constant ratio for beta dimerization
```

```

Kc=0;%constant ratio for alpha dimerization
% for dimer processing model
% Note that the dimerization effect is not shown in the model because the appF.^2 is denoted as appF.
elseif (approach==99)
    k6=100* rand(1); %corresponds to k61 of the model
    Atot=100* rand(1);%total amount of alpha-secretase
    Kma=100* rand(1); %corresponds to Kmad of the model
    k4=100* rand(1); %corresponds to k41 of the model
    Btot=100* rand(1);%total amount of beta-secretase
    Kmb=100* rand(1); %corresponds to Kmbd of the model
    s=100* rand(1);%SORLA
    Ks=100* rand(1);%dissociation constant of SORLA and APP
    Ka=1* rand(1);%constant ratio for APP dimerization
    Kb=1* rand(1);%constant ratio for beta dimerization
    Kc=1* rand(1);%constant ratio for alpha dimerization
end

%%%%%%%%%%%%%%%%%%%%%%%%%%%%%%%%%%%%%%%%%%%%%%%%%%%%%%%%%%%%%%%%%%%%%%%%
%% call the nonlinear least square function lsqnonlin()
options = optimset('PrecondBandwidth', 0);
if (approach==7)
    [parameter, resi] = lsqnonlin(@mycurve, [k6, Atot, Kma, k4, Btot, Kmb, s, Ks], [0 0 0 0
0 0 0 0], [], options);
    s=parameter(7);
    Ks=parameter(8);
    parameter(21)=parameter(2);%Atot
    parameter(31)=parameter(3);%Kma
    parameter(51)=parameter(5);%Btot
    parameter(61)=parameter(6); %Kmb
elseif (approach==99)
    [parameter, resi] = lsqnonlin(@mycurve, [k6, Atot, Kma, k4, Btot, Kmb, s, Ks, Ka, Kb,
Kc], [0 0 0 0 0 0 0], [], options);
    s=parameter(7);
    Ks=parameter(8);
    Ka=parameter(9);
    Kb=parameter(10);
    Kc=parameter(11);
    parameter(21)=parameter(2);%2* Atot
    parameter(31)=parameter(3);%Kma
    parameter(51)=parameter(5);%2* Btot
    parameter(61)=parameter(6); %Kmb
end

%%%%%%%%%%%%%%%%%%%%%%%%%%%%%%%%%%%%%%%%%%%%%%%%%%%%%%%%%%%%%%%%%%%%%%%%
%% to check if there is negative parameter estimated
if (parameter(1)>0 && parameter(2)>0 && parameter(3)>0 && parameter(4)>0 && parameter(5)>0 &&
parameter(6)>0 && parameter(7)>0 && parameter(8)>0 && (Ka==0 || Ka>0) && (Kb==0 || Kb>0) && (Kc==0 ||
Kc>0))

%%%%%%%%%%%%%%%%%%%%%%%%%%%%%%%%%%%%%%%%%%%%%%%%%%%%%%%%%%%%%%%%%%%%%%%%
%% Mathematical representation
% See Equations 3.4 and 3.11 for monomer and dimer processing, respectively

% without SORLA
appF= appFSOLVE';
datum= xdata8(:, 1);
if (approach==7)
    appTOT=appF.* (1+ (parameter(2)./ (parameter(3)+ appF))+ (parameter(5)./ (parameter(6)+ appF)));
elseif (approach==99)
    appTOT=appF+ (2.* Ka.* (appF.^2)).* (1 + ((- 1+ sqrt(1.^2+ (8.* Kc.* (1+ Ka.* appF.^2./
parameter(3)).* parameter(2))))./ (4.* Kc.* (1+ Ka.* appF.^2./ parameter(3))))./ parameter(3)+ ((- 1+
sqrt(1.^2+ (8.* Kb.* (1+ Ka.* appF.^2./ parameter(6)).* parameter(5))))./ (4.* Kb.* (1+ Ka.* appF.^2./
parameter(6))))./ parameter(6));
end

% with SORLA
appFs= appFSOLVES';
datums= xdatas8(:, 1);
if (approach==7)
    appTOTs=appFs.* (1+ (parameter(21)./ (parameter(31)+ appFs))+ (parameter(51)./ (parameter(61)+
appFs)))+ s./ (Ks+ appFs));
elseif (approach==99)
    appTOTs=appFs.* (1+ s./ (Ks+ appFs))+ (2.* Ka.* (appFs.^2)).* (1 + ((- 1+ sqrt(1.^2+ (8.* Kc.*
(1+ Ka.* appFs.^2./ parameter(31)).* parameter(21))))./ (4.* Kc.* (1+ Ka.* appFs.^2./
parameter(31))))./ parameter(31)+ ((- 1+ sqrt(1.^2+ (8.* Kb.* (1+ Ka.* appFs.^2./ parameter(61)).*
parameter(51))))./ (4.* Kb.* (1+ Ka.* appFs.^2./ parameter(61))))./ parameter(61));
end

% solve for secretases
% See Equations 3.12 and 3.13

```

```

if (approach==99)
alpha=(- 1+ sqrt(1.^2+ (8.* Kc.* (1+ Ka.* appF.^2./ parameter(3)).* parameter(2))))./ (4.* Kc.* (1+
Ka.* appF.^2./ parameter(3)));
beta =(- 1+ sqrt(1.^2+ (8.* Kb.* (1+ Ka.* appF.^2./ parameter(6)).* parameter(5))))./ (4.* Kb.* (1+
Ka.* appF.^2./ parameter(6)));
alphas=(- 1+ sqrt(1.^2+ (8.* Kc.* (1+ Ka.* appFs.^2./ parameter(31)).* parameter(21))))./ (4.* Kc.*
(1+ Ka.* appFs.^2./ parameter(31)));
betas =(- 1+ sqrt(1.^2+ (8.* Kb.* (1+ Ka.* appFs.^2./ parameter(61)).* parameter(51))))./ (4.* Kb.*
(1+ Ka.* appFs.^2./ parameter(61)));
end

%%%%%%%%%%%%%%%%%%%%%%%%%%%%%%%%%%%%%%%%%%%%%%%%%%%%%%%%%%%%%%%%%%%%%%%%
%% check if the difference between the given appTOT and estimated appTOT
% increment count if
% (1) the Difference is larger than the threshold value
% (2) free APPs is negative
Diff=abs(appTOT- datum);
Diffs=abs(appTOTs- datums);

u=length(appF);
uu=length(appFs);
threshold = 0.00000001;
count=0;
count2=0;
for t=1:u
    if ( Diff(t) > threshold)
        count = count + 1;
    end

    if (appF(t) < 0)
        count2 = count2 + 1;
    end
end

for t=1:uu
    if ( Diffs(t) > threshold)
        count = count + 1;
    end

    if (appFs(t) < 0)
        count2 = count2 + 1;
    end
end

% checkpoint: restart if count or count2 <0
if ((count >0) || (count2 >0))
    continue;
else

%%%%%%%%%%%%%%%%%%%%%%%%%%%%%%%%%%%%%%%%%%%%%%%%%%%%%%%%%%%%%%%%%%%%%%%%
%% Plotting: plot the original data together with simulation results of the model
% See Equations 3.7 and 3.15 for monomer and dimer processing model, respectively

appTOT=appTOT./ 50;%convert to Molar from fmol for plots
appTOTs=appTOTs./ 50;%convert to Molar from fmol for plots
appTOT=vertcat(0, appTOT);
appTOTs=vertcat(0, appTOTs);
if (approach==7)
    appF=vertcat(0, appF);
    appFs=vertcat(0, appFs);
elseif (approach==99)
    appF=Ka.* (appF).^2;
    appF=vertcat(0, appF);
    appFs=Ka.* (appFs).^2;
    appFs=vertcat(0, appFs);
    alpha=vertcat(0, alpha);
    alphas=vertcat(0, alphas);
    beta=vertcat(0, beta);
    betas=vertcat(0, betas);
end

% without SORLA
figure(3000+ loop)
plot(xdata8P, ydataA8, 'k.', 'MarkerSize', 10)
hold on
if (approach==7)
    fitted = appF .* parameter(1).* parameter(2)./ (parameter(3) + appF);
elseif (approach==99)
    fitted = 2.* appF .* parameter(1).* Kc.* alpha.^2./ parameter(3);
end
end

```

```

plot(appTOT, fitted, 'k- ', 'LineWidth', 2)
xlabel('APP_{Tot}(nM)', 'interpreter', 'latex');
ylabel('sAPP_{alpha} (fmol/ h)', 'interpreter', 'latex')
xlim([0 400])
ylim([0 250])

figure(4000+ loop)
plot(xdata8P, ydataB8, 'k.', 'MarkerSize', 10)
hold on
if (approach==7)
    fitted1 = appF .* parameter(4).* parameter(5)./ (parameter(6)+ appF);
elseif (approach==99)
    fitted1 = 2.* appF .* parameter(4).* Kb.* beta.^2./ parameter(6);
end
plot(appTOT, fitted1, 'k- ', 'LineWidth', 2)
xlabel('APP_{Tot}(nM)', 'interpreter', 'latex');
ylabel('sAPP_{beta} (fmol/ h)', 'interpreter', 'latex')
xlim([0 400])
ylim([0 12])

%with SORLA
figure(6000+ loop)
plot(xdatas8P, ydataAs8, 'k.', 'MarkerSize', 10)
hold on
if (approach==7)
    fitteds = appFs .* parameter(1).* parameter(21)./ (parameter(31) + appFs);
elseif (approach==99)
    fitteds = 2.* appFs .* parameter(1).* Kc.* alphas.^2./ parameter(31);
end
plot(appTOTs, fitteds, 'k- ', 'LineWidth', 2)
xlabel('APP_{Tot}(nM)', 'interpreter', 'latex');
ylabel('sAPP_{alpha} (fmol/ h)', 'interpreter', 'latex')
xlim([0 400])
ylim([0 250])

figure(7000+ loop)
plot(xdatas8P, ydataBs8, 'k.', 'MarkerSize', 10)
hold on
if (approach==7)
    fittedls = appFs .* parameter(4).* parameter(51)./ (parameter(61)+ appFs);
elseif (approach==99)
    fittedls = 2.* appFs .* parameter(4).* Kb.* betas.^2./ parameter(61);
end
plot(appTOTs, fittedls, 'k- ', 'LineWidth', 2)
xlabel('APP_{Tot}(nM)', 'interpreter', 'latex');
ylabel('sAPP_{beta} (fmol/ h)', 'interpreter', 'latex')
xlim([0 400])
ylim([0 12])

%%%%%%%%%%%%%%%%%%%%%%%%%%%%%%%%%%%%%%%%%%%%%%%%%%%%%%%%%%%%%%%%%%%%%%%%
%% Record the estimated parameters into the text file
%% (1 residue + 11 parameters = 12 variables)
fprintf(fid,
'%12.12f %12.12f %12.12f %12.12f %12.12f %12.12f %12.12f %12.12f %12.12f %12.12f %12.12f\n',
resi, parameter(1), parameter(2), parameter(3), parameter(4), parameter(5), parameter(6), s, Ks,
Ka, Kb, Kc);

%% increment to the next loop
loop=loop+ 1;
end
end
end
fclose(fid);

%%%%%%%%%%%%%%%%%%%%%%%%%%%%%%%%%%%%%%%%%%%%%%%%%%%%%%%%%%%%%%%%%%%%%%%%
%% Subroutine to calculate the sum of squared of error by Least Square Method
%%%%%%%%%%%%%%%%%%%%%%%%%%%%%%%%%%%%%%%%%%%%%%%%%%%%%%%%%%%%%%%%%%%%%%%%
function err = mycurve(p)

%% initial assumptions:
% Initialization of vectors for the computed amount of free APP in the presence and absence of SORLA
% without SORLA
P = xdata8(:, 1);
w=length(P);
appFSOLVE=zeros(1, w);
% with SORLA
Ps = xdatas8(:, 1);
ws=length(Ps);
appFSOLVES=zeros(1, ws);

```

```

% Unless specified otherwise, p(i)=parameter(i) where i={1,2,...,15}
if (approach==7)
    s=p(7); Ks=p(8); Atot=p(2); Kma=p(3); Btot=p(5); Kmb=p(6);
elseif (approach==99)
    s=p(7); Ks=p(8); Ka=p(9); Kb=p(10); Kc=p(11); Kma=p(3); Kmb=p(6);
    Atot=p(2);%2* Atot
    Btot=p(5);%2* Btot
end

%% solve for free APP (See Equations 3.4 and 3.11)
% without SORLA
for j=1:w
    if (approach==7)
        func=@(appF)(appF.* (1+ (p(2)./(p(3)+ appF)))+(p(5)./(p(6)+ appF)))- P(j, 1));
    elseif (approach==99)
        func=@(appF)(appF+ (2.* Ka.* (appF.^2)).*(1+ ((-1+ sqrt(1.^2+(8.* Kc.* (1+ Ka.* appF.^2./ p(3)).* p(2)))))/(4.* Kc.* (1+ Ka.* appF.^2./ p(3)))))/p(3)+ ((-1+ sqrt(1.^2+(8.* Kb.* (1+ Ka.* appF.^2./ p(6)).* p(5)))))/(4.* Kb.* (1+ Ka.* appF.^2./ p(6)))))/p(6)- xdata8(j, 1));
    end
    appFSOLVE(1, j)=fzero(func, [0 P(j)], optimset('fzero'));
end

% with SORLA
for js=1:ws
    if (approach==7)
        funcs=@(appFs)(appFs.* (1+ (Atot./ (Kma+ appFs)))+(Btot./ (Kmb+ appFs))+ s./ (Ks+ appFs))- Ps(js, 1));
    elseif (approach==99)
        funcs=@(appFs)(appFs.* (1+ s./ (Ks+ appFs))+ (2.* Ka.* (appFs.^2)).*(1+ ((-1+ sqrt(1.^2+(8.* Kc.* (1+ Ka.* appFs.^2./ p(3)).* p(2)))))/(4.* Kc.* (1+ Ka.* appFs.^2./ p(3)))))/p(3)+ ((-1+ sqrt(1.^2+(8.* Kb.* (1+ Ka.* appFs.^2./ p(6)).* p(5)))))/(4.* Kb.* (1+ Ka.* appFs.^2./ p(6)))))/p(6)- xdatas8(js, 1));
    end
    appFSOLVES(1, js)=fzero(funcs, [0 Ps(js)], optimset('fzero'));
end

% amount of free APP
appF=appFSOLVE';
appFs=appFSOLVES';

%% solve for secretases (See Equations 3.12 and 3.13)
if (approach==99)
    alpha=(-1+ sqrt(1.^2+(8.* Kc.* (1+ Ka.* appF.^2./ p(3)).* p(2))))/(4.* Kc.* (1+ Ka.* appF.^2./ p(3)));
    beta=(-1+ sqrt(1.^2+(8.* Kb.* (1+ Ka.* appF.^2./ p(6)).* p(5))))/(4.* Kb.* (1+ Ka.* appF.^2./ p(6)));
    alphas=(-1+ sqrt(1.^2+(8.* Kc.* (1+ Ka.* appFs.^2./ Kma).* Atot))/(4.* Kc.* (1+ Ka.* appFs.^2./ Kma));
    betas=(-1+ sqrt(1.^2+(8.* Kb.* (1+ Ka.* appFs.^2./ Kmb).* Btot))/(4.* Kb.* (1+ Ka.* appFs.^2./ Kmb));
end

%%%%%%%%%%%%%%%%%%%%%%%%%%%%%%%%%%%%%%%%%%%%%%%%%%%%%%%%%%%%%%%%%%%%%%%%%%%%%%
%% fitting to the experimental data (See Equations 3.7 and 3.15)
%without SORLA
if (approach==7)
    fit1 = appF .* p(1).* p(2)./(p(3)+ appF);
    fit2 = appF .* p(4).* p(5)./(p(6)+ appF);
elseif (approach==99)
    fit1 = 2.* appF .* p(1).* Kc.* alpha.^2./ p(3);
    fit2 = 2.* appF .* p(4).* Kb.* beta.^2./ p(6);
end
%with SORLA
if (approach==7)
    fit1s = appFs .* p(1).* Atot./ (Kma + appFs);
    fit2s = appFs .* p(4).* Btot./ (Kmb+ appFs);
elseif (approach==99)
    fit1s = 2.* appFs .* p(1).* Kc.* alphas.^2./ Kma;
    fit2s = 2.* appFs .* p(4).* Kb.* betas.^2./ Kmb;
end
% RECALL: w and ws denote the number of experimental data without and with SORLA, respectively
err11 = (fit1 - data(:, 2))./ sqrt((sum(data(:, 2))./ w));
err22 = (fit2 - data(:, 3))./ sqrt((sum(data(:, 3))./ w));
err11s = (fit1s - datas(:, 2))./ sqrt((sum(datas(:, 2))./ ws));
err22s = (fit2s - datas(:, 3))./ sqrt((sum(datas(:, 3))./ ws));
errWO = [err11, err22];
errW = [err11s, err22s];
% error vector
err=vertcat(errWO, errW);
end end

```

Single-compartmental model II

(For Sections 3.3 - with both monomeric and dimeric forms of APP)

```
function SingleCompartmentModel2

%% clear screen
clc

%% global variables
global data;
global datas;
global Parameter;

%% load experimental data
PREdata= load('CHO.txt'); %without SORLA
PREdatas= load('CHO_S.txt'); %with SORLA

%% Choices
% 12: local estimation of parameter values - affect Kma of both monomer and dimer
% 13: local estimation of parameter values - affect Kmb of both monomer and dimer
% 14: global estimation of parameter values
choice=13;

%% open file to record parameter values that will be estimated
if (choice==12)
    fid = fopen('SingleCompartmentBoth_localKma.txt', 'at');
elseif (choice==13)
    fid = fopen('SingleCompartmentBoth_localKmb.txt', 'at');
elseif (choice==14)
    fid = fopen('SingleCompartmentBoth_global.txt', 'at');
end

%% sort experimental data according to the total amount of APP measured in the experiments
data = sortrows(PREdata, 1); %without SORLA
datas = sortrows(PREdatas, 1); %with SORLA

%% data sets
%without SORLA
xdata = data(:, 1).* 50; %convert total APP from nM into fmol
ydataA = data(:, 2); %sAPPa
ydataB = data(:, 3); %sAPPb
% with SORLA
xdatas = datas(:, 1) .* 50; %convert total APP from nM into fmol
ydataAs = datas(:, 2); %sAPPa
ydataBs = datas(:, 3); %sAPPb
% back up vectors of the experimental data
xdata8=xdata;
ydataA8=ydataA;
ydataB8=ydataB;
xdata8s=xdatas;
ydataA8s=ydataAs;
ydataB8s=ydataBs;
% a copy of vector APP in nM for plotting purpose
xdata8P= data(:, 1);
xdata8sP= datas(:, 1);

%%%%%%%%%%%%%%%%%%%%%%%%%%%%%%%%%%%%%%%%%%%%%%%%%%%%%%%%%%%%%%%%%%%%%%%%
%% initial loop
loop=1;
%% row denotes the number of repetitions
for row=1:500

%% initial parameter values
% for dimer processing
k6d=100* rand(1);
Kmad=100* rand(1);
k4d=100* rand(1);
Kmbd=100* rand(1);
% for monomer processing
k6=100* rand(1);
Kma=100* rand(1);
k4=100* rand(1);
Kmb=100* rand(1);
% shared by both processing
```

```

Atot=100* rand(1); %total amount of alpha-secretase
Btot=100.* rand(1); %total amount of beta-secretase
Ka=100* rand(1); %constant ratio for APP dimerization
Kb=100* rand(1); %constant ratio for beta dimerization
Kc=100* rand(1); %constant ratio for alpha dimerization
sor=100* rand(1); %SORLA
Ksor=100* rand(1);%dissociation constant of SORLA and APP
tune=100* rand(1);%variable that may varies for local estimation of Km values
tune2=100* rand(1);%variable that may varies for local estimation of Km values

%%%%%%%%%%%%%%%%%%%%%%%%%%%%%%%%%%%%%%%%%%%%%%%%%%%%%%%%%%%%%%%%%%%%%%%%
%% call the nonlinear least square function lsqnonlin()
options = optimset('PrecondBandWidth', 0);
if (choice==12 || choice==13)
[Parameter, resi] = lsqnonlin(@mycurve, [Atot, Btot, k6d, Kmad, k4d, Kmbd, k6, Kma, k4, Kmb, Ka,
Kb, Kc, sor, Ksor, tune, tune2], [0 0 0 0 0 0 0 0 0 0 0 0 0 0 0], [], options);
elseif (choice==14)
[Parameter, resi] = lsqnonlin(@mycurve, [Atot, Btot, k6d, Kmad, k4d, Kmbd, k6, Kma, k4, Kmb, Ka,
Kb, Kc, sor, Ksor], [0 0 0 0 0 0 0 0 0 0 0 0 0 0], [], options);
end
%with SORLA (temporarily assignment)
Parameter(101)=Parameter(1);%Atot
Parameter(102)=Parameter(2);%Btot
Parameter(103)=Parameter(3);%k6d
Parameter(105)=Parameter(5);%k4d
Parameter(107)=Parameter(7);%k6
Parameter(109)=Parameter(9);%k4
Parameter(111)=Parameter(11);%Ka
Parameter(112)=Parameter(12);%Kb
Parameter(113)=Parameter(13);%Kc
if (choice==12)
Parameter(104)=Parameter(16);%Kma dimer
Parameter(106)=Parameter(6);%Kmb dimer
Parameter(108)=Parameter(17);%Kma monomer
Parameter(110)=Parameter(10);%Kmb monomer
elseif (choice==13)
Parameter(104)=Parameter(4);%Kma dimer
Parameter(106)=Parameter(16);%Kmb dimer
Parameter(108)=Parameter(8);%Kma monomer
Parameter(110)=Parameter(17);%Kmb monomer
elseif (choice==14)
Parameter(104)=Parameter(4);%Kma dimer
Parameter(106)=Parameter(6);%Kmb dimer
Parameter(108)=Parameter(8);%Kma monomer
Parameter(110)=Parameter(10);%Kmb monomer
end
Ka=Parameter(11);
Kb=Parameter(12);
Kc=Parameter(13);
s=Parameter(14);
Ks=Parameter(15);

%%%%%%%%%%%%%%%%%%%%%%%%%%%%%%%%%%%%%%%%%%%%%%%%%%%%%%%%%%%%%%%%%%%%%%%%
%% to check if there is negative parameter estimated
if (s>0 && Ks>0 && Parameter(101)>0 && Parameter(102)>0 && Parameter(103)>0 && Parameter(104)>0 &&
Parameter(105)>0 && Parameter(106)>0 && Parameter(107)>0 && Parameter(108)>0 && Parameter(109)>0 &&
Parameter(110)>0 && Parameter(111)>0 && Parameter(112)>0 && Parameter(113)>0)

%%%%%%%%%%%%%%%%%%%%%%%%%%%%%%%%%%%%%%%%%%%%%%%%%%%%%%%%%%%%%%%%%%%%%%%%
%% Mathematical representation
%% See Equations 3.20 and 3.21 for monomer and dimer processing, respectively

appF= appFSOLVE';
appFs= appFSOLVEs';
datum= xdata8(:, 1);
datums= xdata8s(:, 1);

%without SORLA
alpha=(- appF.* Parameter(4) - Parameter(8).* Parameter(4) + sqrt((- appF.* Parameter(4) -
Parameter(8).* Parameter(4)).^2 - 4.* Parameter(1).* Parameter(8).* Parameter(4).* (- 2.*
appF.^2.* Ka.* Kc.* Parameter(8) - 2.* Kc.* Parameter(8).* Parameter(4))))./ (4.* (appF.^2 .*
Ka.* Kc.* Parameter(8) + Kc.* Parameter(8).* Parameter(4)));
beta =(- appF.* Parameter(6) - Parameter(10).* Parameter(6) + sqrt((- appF.* Parameter(6) -
Parameter(10).* Parameter(6)).^2 - 4.* Parameter(2).* Parameter(10).* Parameter(6).* (- 2.*
appF.^2 .* Ka.* Kb.* Parameter(10) - 2.* Kb.* Parameter(10).* Parameter(6))))./ (4.*
(appF.^2 .* Ka.* Kb.* Parameter(10) + Kb.* Parameter(10).* Parameter(6)));
appTOT=appF.* (1+ alpha./ Parameter(8)+ beta./ Parameter(10)) + (2.* Ka.* appF.^2).* (1 + Kc.*
(alpha.^2)./ Parameter(4) + Kb.*(beta.^2)./ Parameter(6));

%with SORLA

```

```

alphas=(- appFs.* Parameter(104) - Parameter(108).* Parameter(104) + sqrt((- appFs.* Parameter(104)
- Parameter(108).* Parameter(104)).^2 - 4.* Parameter(101).* Parameter(108).* Parameter(104).*
(- 2.* appFs.^2.* Ka.* Kc.* Parameter(108) - 2.* Kc.* Parameter(108).* Parameter(104))).)/
(4.* (appFs.^2 .* Ka.* Kc.* Parameter(108) + Kc.* Parameter(108).* Parameter(104)));
betas=(- appFs.* Parameter(106) - Parameter(110).* Parameter(106) + sqrt((- appFs.* Parameter(106)
- Parameter(110).* Parameter(106)).^2 - 4.* Parameter(102).* Parameter(110).* Parameter(106).*
(- 2.* appFs.^2.* Ka.* Kb.* Parameter(110) - 2.* Kb.* Parameter(110).* Parameter(106))).)/
(4.* (appFs.^2 .* Ka.* Kb.* Parameter(110) + Kb.* Parameter(110).* Parameter(106)));
appTOTs=appFs.* (1+ s./ (Ks+ appFs) + alphas./ Parameter(108) + betas./ Parameter(110)) + (2.* Ka.*
appFs.^2).*(1 + Kc.* (alphas.^2)./ Parameter(104) + Kb.* (betas.^2)./ Parameter(106));

```

```

%%%%%%%%%%%%%%%%%%%%%%%%%%%%%%%%%%%%%%%%%%%%%%%%%%%%%%%%%%%%%%%%%%%%%%%%
%% check if the difference between the given appTOT and estimated appTOT
% increment count if
% (1) the Difference is larger than the threshold value
% (2) free APPs is negative

```

```

Diff=abs(appTOT- datum);
Diffs=abs(appTOTs- datums);

```

```

u=length(appF);
us=length(appFs);
threshold = 0.00000001;
count=0;
count2=0;
for t=1:u
    if ( Diff(t) > threshold)
        count = count + 1;
    end
    if (appF(t) < 0)
        count2 = count2 + 1;
    end
end
for ts=1:us
    if ( Diffs(ts) > threshold)
        count = count + 1;
    end
    if (appFs(ts) < 0)
        count2 = count2 + 1;
    end
end
% checkpoint: restart if count or count2 < 0
if ((count > 0) || (count2 > 0))
    continue;
else

```

```

%%%%%%%%%%%%%%%%%%%%%%%%%%%%%%%%%%%%%%%%%%%%%%%%%%%%%%%%%%%%%%%%%%%%%%%%
%% Plotting: plot the original data together with simulation results of the model
% See Equations 3.22 and 3.23

```

```

appTOT=appTOT./ 50; %convert back from fmol to nM for plotting
appTOTs=appTOTs./ 50; %convert back from fmol to nM for plotting
appTOT=vertcat(0, appTOT);
appTOTs=vertcat(0, appTOTs);
appFree=vertcat(0, appF);
appFrees=vertcat(0, appFs);
alpha=vertcat(0, alpha);
beta=vertcat(0, beta);
alphas=vertcat(0, alphas);
betas=vertcat(0, betas);
appM=appFree;
appD=Ka.* (appFree.^2);
appMs=appFrees;
appDs=Ka.* (appFrees.^2);

```

```

% without SORLA
figure(3000+ loop)
plot(xdata8P, ydataA8, 'k.', 'MarkerSize', 10)
hold on
fittedal = 2.* (appD).*(Kc.* (alpha.^2)).* Parameter(3)./ Parameter(4); %dimer
fitteda2 = (appM).* alpha.* Parameter(7)./ Parameter(8); %monomer
fitteda1P = fittedal;
fitteda2P = fitteda2;
fitted = fitteda1P+ fitteda2P;
plot(appTOT, fitteda1P, 'g-', 'LineWidth', 2)%dimer
plot(appTOT, fitteda2P, 'm-', 'LineWidth', 2)%monomer
plot(appTOT, fitted, 'k-', 'LineWidth', 2)
xlabel('APP_{Tot} (nM)');

```



```

Kb=p(12);
Kc=p(13);
s=p(14);
Ks=p(15);

%under the influence of SORLA
if (choice==12)%affect Kma monomer and dimer
Kma=p(17);
Kmad=p(16);
Kmb=p(10);
Kmbd=p(6);
elseif (choice==13)%affect Kmb monomer and dimer
Kma=p(8);
Kmad=p(4);
Kmb=p(17);
Kmbd=p(16);
elseif (choice==14)%affect nothing
Kma=p(8);
Kmad=p(4);
Kmb=p(10);
Kmbd=p(6);
end

% Initialization of vectors for the computed amount of free APP in the presence and absence of SORLA
% without SORLA
P = xdata8(:, 1);
w=length(P);
appFSOLVE=zeros(1, w);
% with SORLA
Ps = xdata8s(:, 1);
ws=length(Ps);
appFSOLVEs=zeros(1, ws);

%% SOLVE for free APP given the total amount of APP (without SORLA): see Equations 3.20 and 3.21
for j=1:w
func=@(appF)(appF.* (1+ ((- appF.* p(4) - p(8).* p(4) + sqrt((- appF.* p(4) - p(8).* p(4)).^2 -
4.* p(1).* p(8).* p(4).* (- 2.* appF.^2.* Ka.* Kc.* p(8) - 2.* Kc.* p(8).* p(4)))))./( 4.*
(appF.^2 .* Ka.* Kc.* p(8) + Kc.* p(8).* p(4)))/ p(8)+ ((- appF.* p(6) - p(10).* p(6) +
sqrt((- appF.* p(6) - p(10).* p(6)).^2 - 4.* p(2).* p(10).* p(6).* (- 2.* appF.^2.* Ka.*
Kb.* p(10) - 2.* Kb.* p(10).* p(6)))))./( 4.* (appF.^2 .* Ka.* Kb.* p(10) + Kb.* p(10).*
p(6)))))./( p(10) + (2.* Ka.* appF.^2).* (1 + Kc.* (((- appF.* p(4) - p(8).* p(4) + sqrt((- appF.*
p(4) - p(8).* p(4)).^2 - 4.* p(1).* p(8).* p(4).* (- 2.* appF.^2.* Ka.* Kc.* p(8) - 2.*
Kc.* p(8).* p(4)))))./( 4.* (appF.^2 .* Ka.* Kc.* p(8) + Kc.* p(8).* p(4))))).^2./ p(4) + Kb.*
((( - appF.* p(6) - p(10).* p(6) + sqrt((- appF.* p(6) - p(10).* p(6)).^2 - 4.* p(2).* p(10).*
p(6).* (- 2.* appF.^2.* Ka.* Kb.* p(10) - 2.* Kb.* p(10).* p(6)))))./( 4.* (appF.^2 .* Ka.*
Kb.* p(10) + Kb.* p(10).* p(6))))).^2./ p(6)) - xdata8(j, 1));
appFSOLVE(1, j)=fzero(func, [0 P(j)], optimset('fzero'));
end

%% SOLVE for free APP given the total amount of APP (with SORLA): see Equations 3.20 and 3.21
for js=1:ws
funcs=@(appFs)(appFs.* (1+ ((- appFs.* Kmad - Kma.* Kmad + sqrt((- appFs.* Kmad - Kma.* Kmad).^2 -
4.* p(1).* Kma.* Kmad.* (- 2.* appFs.^2.* Ka.* Kc.* Kma - 2.* Kc.* Kma.* Kmad)))/ (4.*
(appFs.^2 .* Ka.* Kc.* Kma + Kc.* Kma.* Kmad)))/ Kma+ ((- appFs.* Kmbd - Kmb.* Kmbd + sqrt((-
appFs.* Kmbd - Kmb.* Kmbd).^2 - 4.* p(2).* Kmb.* Kmbd.* (- 2.* appFs.^2.* Ka.* Kb.* Kmb -
2.* Kb.* Kmb.* Kmbd)))/ (4.* (appFs.^2 .* Ka.* Kb.* Kmb + Kb.* Kmb.* Kmbd)))/ Kmb + (2.*
Ka.* appFs.^2).* (1 + Kc.* (((- appFs.* Kmad - Kma.* Kmad + sqrt((- appFs.* Kmad - Kma.* Kmad).^2 -
4.* p(1).* Kma.* Kmad.* (- 2.* appFs.^2.* Ka.* Kc.* Kma - 2.* Kc.* Kma.* Kmad)))/ (4.*
(appFs.^2 .* Ka.* Kc.* Kma + Kc.* Kma.* Kmad))).^2)/ Kmad + Kb.* (((- appFs.* Kmbd - Kmb.*
Kmbd + sqrt((- appFs.* Kmbd - Kmb.* Kmbd).^2 - 4.* p(2).* Kmb.* Kmbd.* (- 2.* appFs.^2.*
Ka.* Kb.* Kmb - 2.* Kb.* Kmb.* Kmbd)))/ (4.* (appFs.^2 .* Ka.* Kb.* Kmb + Kb.* Kmb.*
Kmbd))).^2)/ Kmbd) + appFs.* s./ (Ks+ appFs) - xdata8s(js, 1));
appFSOLVEs(1, js)=fzero(funcs, [0 Ps(js)], optimset('fzero'));
end

%%
app=appFSOLVE';
apps=appFSOLVEs';

%% solve for secretases (see Equations 3.21)
% without SORLA
alpha=(- app.* p(4) - p(8).* p(4) + sqrt((- app.* p(4) - p(8).* p(4)).^2 - 4.* p(1).*
p(8).* p(4).* (- 2.* app.^2.* Ka.* Kc.* p(8) - 2.* Kc.* p(8).* p(4)))))./( 4.*
(app.^2 .* Ka.* Kc.* p(8) + Kc.* p(8).* p(4)));
beta=(- app.* p(6) - p(10).* p(6) + sqrt((- app.* p(6) - p(10).* p(6)).^2 - 4.* p(2).*
p(10).* p(6).* (- 2.* app.^2.* Ka.* Kb.* p(10) - 2.* Kb.* p(10).* p(6)))))./( 4.*
(app.^2 .* Ka.* Kb.* p(10) + Kb.* p(10).* p(6)));
%without SORLA

```

```

alphas=(- apps.* Kmad - Kma.* Kmad + sqrt((- apps.* Kmad - Kma.* Kmad).^2 - 4.* Atot.*
Kma.* Kmad.* (- 2.* apps.^2.* Ka.* Kc.* Kma - 2.* Kc.* Kma.* Kmad))./( 4.*
( apps.^2 .* Ka.* Kc.* Kma + Kc.* Kma.* Kmad));
betas =(- apps.* Kmbd - Kmb.* Kmbd + sqrt((- apps.* Kmbd - Kmb.* Kmbd).^2 - 4.* Btot.*
Kmb.* Kmbd.* (- 2.* apps.^2.* Ka.* Kb.* Kmb - 2.* Kb.* Kmb.* Kmbd))./( 4.*
( apps.^2 .* Ka.* Kb.* Kmb + Kb.* Kmb.* Kmbd));

% amount of free APP in monomer and dimer processing
app=appFSOLVE';
apps=appFSOLVEs';
appMon=app;
appDim=Ka.* (app.^2);
appMons=apps;
appDims=Ka.* (apps.^2);

%%%%%%%%%%%%%%%%%%%%%%%%%%%%%%%%%%%%%%%%%%%%%%%%%%%%%%%%%%%%%%%%%%%%%%%%
%% fitting to the experimental data
% without SORLA for dimer processing
fit11 =2.* (appDim) .* Kc.* (alpha.^2).* p(3)./ p(4);% sAPPA
fit21= 2.* (appDim) .* Kb.* (beta.^2).* p(5)./ p(6);% sAPPb
% without SORLA for monomer processing
fit12 = appMon .* alpha.* p(7)./ p(8);% sAPPA
fit22= appMon .* beta.* p(9)./ p(10);% sAPPb
% sum of products w/o SORLA in monomer and dimer
fit1 = (fit11+ fit12); % sAPPA
fit2 = (fit21+ fit22); % sAPPb

% with SORLA for dimer processing
fit11s =2.* (appDims) .* Kc.* (alphas.^2).* p(3)./ Kmad;% sAPPA
fit21s= 2.* (appDims) .* Kb.* (betas.^2).* p(5)./ Kmbd;% sAPPb
% with SORLA for monomer processing
fit12s = appMons .* alphas.* p(7)./ Kma;% sAPPA
fit22s = appMons .* betas.* p(9)./ Kmb;% sAPPb
% sum of products w/ SORLA in monomer and dimer
fit1s = (fit11s+ fit12s); % sAPPA
fit2s = (fit21s+ fit22s); % sAPPb

% RECALL: w and ws denote the number of experimental data without and with SORLA, respectively
err11 = (fit1 - data(:, 2))./ sqrt((sum(data(:, 2))./ w));
err22 = (fit2 - data(:, 3))./ sqrt((sum(data(:, 3))./ w));
err11s = (fit1s - datas(:, 2)) ./ sqrt((sum(datas(:, 2))./ ws));
err22s = (fit2s - datas(:, 3)) ./ sqrt((sum(datas(:, 3))./ ws));
% error vector
err=vertcat(err11, err22, err11s, err22s);
end
end

```

Multi-compartmental model

(For Sections 4.2 – compartmental model with both monomeric and dimeric forms of APP)

```
function MultiCompartmentalModel

%% clear screen
clc

%% declare global variables
global data;
global datas;
global Parameter;

%% load experimental data
PREdata= load('CHO.txt'); %without SORLA
PREdatas= load('CHO_S.txt'); %with SORLA

%% open file to record parameter values that will be estimated
fid = fopen('MultiCompartmentalModel.txt', 'at');

%%%%%%%%%%%%%%%%%%%%%%%%%%%%%%%%%%%%%%%%%%%%%%%%%%%%%%%%%%%%%%%%%%%%%%%%
%% sort experimental data according to the total amount of APP measured in the experiments
data = sortrows(PREdata,1); %without SORLA
datas = sortrows(PREdatas,1); %with SORLA

%% data sets
%without SORLA
xdata = data(:,1).* 50;%convert total APP from nM into fmol
ydataA = data(:,2);%sAPPA
ydataB = data(:,3); %sAPPb
% with SORLA
xdatas = datas(:,1) .* 50;%convert total APP from nM into fmol
ydataAs = datas(:,2);%sAPPA
ydataBs = datas(:,3); %sAPPb
% back up vectors of the experimental data
xdata8=xdata;
ydataA8=ydataA;
ydataB8=ydataB;
xdata8s=xdatas;
ydataA8s=ydataAs;
ydataB8s=ydataBs;
% a copy of vector APP in nM for plotting purpose
xdata8P= data(:,1);
xdata8sP= datas(:,1);

%%%%%%%%%%%%%%%%%%%%%%%%%%%%%%%%%%%%%%%%%%%%%%%%%%%%%%%%%%%%%%%%%%%%%%%%
%% initial loop
loop=1;
%% row denotes the number of repetitions
for row=1:500
    tempflag=row

%% In the process of parameter estimation, the following are assumed
% % Kc3 denotes  $Kc3 \cdot (Kc2.^2)$  from mathematical model in Section~\ref{sec:MultiCompartmentmodel}
% % Kb3 denotes  $Kb3 \cdot (Kb2.^2)$  from mathematical model in Section~\ref{sec:MultiCompartmentmodel}
% % Kg3 denotes  $Kg3 \cdot (Kg2.^2)$  from mathematical model in Section~\ref{sec:MultiCompartmentmodel}
% % Kcs1 denotes  $Kcs1 \cdot Kg1$  from mathematical model in Section~\ref{sec:MultiCompartmentmodel}
% % Kcs2 denotes  $Kcs2 \cdot (Kg3 \cdot (Kg2.^2))$  from mathematical model in
Section~\ref{sec:MultiCompartmentmodel}
% % Kee1 denotes  $Kee1 \cdot (Kcs1 \cdot Kg1)$  from mathematical model in Section~\ref{sec:MultiCompartmentmodel}
% % Kee2 denotes  $Kee2 \cdot (Kcs2 \cdot Kg3 \cdot (Kg2.^2))$  from mathematical model in
Section~\ref{sec:MultiCompartmentmodel}
% % Ks1 denotes  $Ks1 \cdot Kg1$  from mathematical model in Section~\ref{sec:MultiCompartmentmodel}
% % Ks2 denotes  $Ks2 \cdot Kg2$  from mathematical model in Section~\ref{sec:MultiCompartmentmodel}

%%%%%%%%%%%%%%%%%%%%%%%%%%%%%%%%%%%%%%%%%%%%%%%%%%%%%%%%%%%%%%%%%%%%%%%%
%% initial parameter values
Atot=100* rand(1); Btot=100* rand(1);
k6d=100* rand(1); Kmad=100* rand(1); k4d=100* rand(1); Kmbd=100* rand(1);
k6=100* rand(1); Kma=100* rand(1); k4=100* rand(1); Kmb=100* rand(1);
Kg1=100* rand(1); Kg2=100* rand(1);
Kcs1=100* rand(1); Kcs2=100* rand(1); Kee1=100* rand(1); Kee2=100* rand(1);
Kc1=100* rand(1); Kc2=100* rand(1);
```

```

Kb1=100* rand(1); Kb2=100* rand(1);
Kg3=100* rand(1); Kc3=100* rand(1); Kb3=100* rand(1);
Ks1=100* rand(1); Ks2=100* rand(1); SORtotm=100* rand(1); SORtotd=100* rand(1);

%%%%%%%%%%%%%%%%%%%%%%%%%%%%%%%%%%%%%%%%%%%%%%%%%%%%%%%%%%%%%%%%%%%%%%%%
%% call the nonlinear least square function lsqnonlin()
options = optimset('PrecondBandWidth',0);
%27 parameters all in all
[Parameter, resi] = lsqnonlin(@mycurve,[Atot, Btot, k6d, Kmad, k4d, Kmbd, k6, Kma, k4, Kmb, Kg1, Kg2,
Kcs1, Kcs2, Keel, Kee2, Kc1, Kc2, Kbl, Kb2, Kg3, Kc3, Kb3, Ks1, Ks2, SORtotm, SORtotd],[0 0 0 0 0 0 0
0 0 0 0 0 0 0 0 0 0 0 0 0 0 0 0],[],options)

Atot=Parameter(1); Btot=Parameter(2);
k6d=Parameter(3); Kmad=Parameter(4); k4d=Parameter(5); Kmbd=Parameter(6);
k6=Parameter(7); Kma=Parameter(8); k4=Parameter(9); Kmb=Parameter(10);
Kg1=Parameter(11); Kg2=Parameter(12);
Kcs1=Parameter(13); Kcs2=Parameter(14); Keel=Parameter(15); Kee2=Parameter(16);
Kc1=Parameter(17); Kc2=Parameter(18); Kbl=Parameter(19); Kb2=Parameter(20);
Kg3=Parameter(21); Kc3=Parameter(22); Kb3=Parameter(23);
Ks1=Parameter(24); Ks2=Parameter(25); SORtotm=Parameter(26); SORtotd=Parameter(27);

%%%%%%%%%%%%%%%%%%%%%%%%%%%%%%%%%%%%%%%%%%%%%%%%%%%%%%%%%%%%%%%%%%%%%%%%
%% to check if there is negative parameter estimated
if (Parameter(1)>0 && Parameter(2)>0 && Parameter(3)>0 && Parameter(4)>0 && Parameter(5)>0 &&
Parameter(6)>0 && Parameter(7)>0 && Parameter(8)>0 && Parameter(9)>0 && Parameter(10)>0 &&
Parameter(11)>1 && Parameter(12)>1 && Parameter(13)>0 && Parameter(14)>0 && Parameter(15)>0 &&
Parameter(16)>0 && Parameter(17)>1 && Parameter(18)>1 && Parameter(19)>1 && Parameter(20)>1 &&
Parameter(21)>0 && Parameter(22)>0 && Parameter(23)>0 && Parameter(24)>0 && Parameter(25)>0 &&
Parameter(26)>0 && Parameter(27)>0 )

%%%%%%%%%%%%%%%%%%%%%%%%%%%%%%%%%%%%%%%%%%%%%%%%%%%%%%%%%%%%%%%%%%%%%%%%
%% Mathematical representation
APP= appFSOLVE'; %APP_init solved given APP_tot w/ o SORLA
APPms= appFSOLVEms'; %APPms * Kg1 denotes APP_G1 in the presence of SORLA
APPds= appFSOLVEds'; %APPds * Kg2 denotes APP_G2 in the presence of SORLA
datum= xdata8(:,1);
datums= xdata8s(:,1);
% Recall that
% Kc3 = Kc3.* (Kc2.^2)
% Kb3 = Kb3.* (Kb2.^2)
% Kg3 = Kg3.* (Kg2.^2)
% Kcs1 = Kcs1.* Kg1
% Kcs2 = Kcs2.* (Kg3.* (Kg2.^2))
% Keel = Keel.* (Kcs1.* Kg1)
% Kee2 = Kee2.* (Kcs2.* Kg3.* (Kg2.^2))
% Ks1 = Ks1.* Kg1
% Ks2 = Ks2.* Kg2

%% without SORLA
% alpha denotes alpha_init
% beta denotes beta_init
% appTOT denotes APP_init

% see Equations 4.17
alpha = (- (1+ Kc2+ Kc1.* (1+ Kcs1.* APP./ Kma)) + sqrt((1+ Kc2+ Kc1.* (1+ Kcs1.* APP./ Kma)).^2-
4.* (2.* Kc3.* (1+ Kcs2.* APP.^2./ Kmad)).* (- Atot)))/ (2.* (2.* Kc3.* (1+ Kcs2.* APP.^2./ Kmad)));
% see Equations 4.18
beta = (- (1+ Kb2+ Kbl.* (1+ Keel.* APP./ Kmb)) + sqrt((1+ Kb2+ Kbl.* (1+ Keel.* APP./ Kmb)).^2-
4.* (2.* Kb3.* (1+ Kee2.* APP.^2./ Kmbd)).* (- Btot)))/ (2.* (2.* Kb3.* (1+ Kee2.* APP.^2./ Kmbd)));
% see Equations 4.15
appTOT = APP.* (1+ Kg1+ Kg2+ Kcs1.* (1+ Kc1.* ((- (1+ Kc2+ Kc1.* (1+ Kcs1.* APP./ Kma)) + sqrt((1+
Kc2+ Kc1.* (1+ Kcs1.* APP./ Kma)).^2- 4.* (2.* Kc3.* (1+ Kcs2.* APP.^2./ Kmad)).* (- Atot)))/ (2.*
(2.* Kc3.* (1+ Kcs2.* APP.^2./ Kmad)))))/ Kma)+ Keel.* (1+ Kbl.* ((- (1+ Kb2+ Kbl.* (1+ Keel.* APP./
Kmb)) + sqrt((1+ Kb2+ Kbl.* (1+ Keel.* APP./ Kmb)).^2- 4.* (2.* Kb3.* (1+ Kee2.* APP.^2./ Kmbd)).* (-
Btot)))/ (2.* (2.* Kb3.* (1+ Kee2.* APP.^2./ Kmbd)))))/ Kmb)+ ... %monomer processing
2.* (APP.^2).*(Kg3+ Kcs2.* (1+ Kc3.* ((- (1+ Kc2+ Kc1.* (1+ Kcs1.* APP./ Kma)) + sqrt((1+ Kc2+
Kc1.* (1+ Kcs1.* APP./ Kma)).^2- 4.* (2.* Kc3.* (1+ Kcs2.* APP.^2./ Kmad)).* (- Atot)))/ (2.* (2.*
Kc3.* (1+ Kcs2.* APP.^2./ Kmad))))).^2./ Kmad)+ Kee2.* (1+ Kb3.* ((- (1+ Kb2+ Kbl.* (1+ Keel.* APP./
Kmb)) + sqrt((1+ Kb2+ Kbl.* (1+ Keel.* APP./ Kmb)).^2- 4.* (2.* Kb3.* (1+ Kee2.* APP.^2./ Kmbd)).* (-
Btot)))/ (2.* (2.* Kb3.* (1+ Kee2.* APP.^2./ Kmbd))))).^2./ Kmbd)); %dimer processing 1

%% with SORLA
% alphams.* Kc1 = alpha_1
% alphads.* Kc2 = alpha_2
% betams.* Kbl = beta_1
% betads.* Kb2 = beta_2
% Atotms and Atotds denote the conserved amount of alpha in monomer and in dimer, respectively
% Btotms and Btotds denote the conserved amount of beta in monomer and in dimer, respectively

```

```

% see Equations 4.19 and 4.21
alphams = Atotms./ (Kc1.* (1+ Kcs1.* APPms./ Kma));
alphads = (- Kc2 + sqrt(Kc2.^2- 4.* (2.* Kc3.* (1+ Kcs2.* (APPds.^2)./ Kmad)).* (- Atotds)))./ (4.*
Kc3.* (1+ Kcs2.* (APPds.^2)./ Kmad));

betams = Btotms./ (Kb1.* (1+ Kee1.* APPms./ Kmb));
betads = (- Kb2 + sqrt(Kb2.^2- 4.* (2.* Kb3.* (1+ Kee2.* (APPds.^2)./ Kmbd)).* (- Btotds)))./ (4.*
Kb3.* (1+ Kee2.* (APPds.^2)./ Kmbd));

appTOTms = APPms.* (Kg1+ Kcs1.* (1+ Kc1.* alphams./ Kma)+ Kee1.* (1+ Kb1.* betams./ Kmb))+ Ks1.*
(SORTotm./ (1+ Ks1.* APPms)).* APPms;
appTOTds = Kg2.* APPds + 2.* (APPds.^2).* (Kg3+ Kcs2.* (1+ Kc3.* (alphads.^2)./ Kmad)+ Kee2.* (1+
Kb3.* (betads.^2)./ Kmbd))+ Ks2.* (SORTotd./ (1+ Ks2.* APPds)).* APPds;
appTOTs = APP+ appTOTms+ appTOTds;

%%%%%%%%%%%%%%%%%%%%%%%%%%%%%%%%%%%%%%%%%%%%%%%%%%%%%%%%%%%%%%%%%%%%%%%%
%% check if the difference between the given appTOT and estimated appTOT
% increment count if
% (1) the Difference is larger than the threshold value
% (2) free APPs is negative
Diff=abs(appTOT- datum);
Diffs=abs(appTOTs- datums);
u=length(APP);
us=length(APPms);
threshold = 0.00000001;
count=0;
count2=0;
for t=1:u
    if ( Diff(t) > threshold)
        count = count + 1;
    end

    if (APP(t) < 0)
        count2 = count2 + 1;
    end
end
for ts=1:us
    if ( Diffs(ts) > threshold)
        count = count + 1;
    end

    if (APPms(ts) < 0)
        count2 = count2 + 1;
    end

    if (APPds(ts) < 0)
        count2 = count2 + 1;
    end
end

% checkpoint: restart if count or count2 < 0
if ((count > 0) || (count2 > 0))
    continue;
else

%%%%%%%%%%%%%%%%%%%%%%%%%%%%%%%%%%%%%%%%%%%%%%%%%%%%%%%%%%%%%%%%%%%%%%%%
%% Plotting: plot the original data together with simulation results of the model
% See Equations 4.6 - 4.8

appTOT=appTOT./ 50; %convert back from fmol to nM
appTOTs=appTOTs./ 50; %convert back from fmol to nM
appTOT=vertcat(0,appTOT);
appTOTs=vertcat(0,appTOTs);
appFree=vertcat(0,APP);
appFreems=vertcat(0,APPms);
appFreeds=vertcat(0,APPds);
alpha=vertcat(0,alpha);
beta=vertcat(0,beta);
alphams=vertcat(0,alphams);
alphads=vertcat(0,alphads);
betams=vertcat(0,betams);
betads=vertcat(0,betads);
appM=appFree;
appD=(appFree.^2);
appMs=appFreems;
appDs=(appFreeds.^2);

% without SORLA

```



```

%% close the file that is opened earlier
fclose(fid);

%% =====
%% Subroutine to calculate the sum of squared of error by Least Square Method
%% =====
function err = mycurve(p)

%% initial assumptions:
Atot=p(1); Btot=p(2); k6d=p(3); Kmad=p(4); k4d=p(5); Kmbd=p(6); k6=p(7); Kma=p(8); k4=p(9);
Kmb=p(10); Kg1=p(11); Kg2=p(12); Kcs1=p(13); Kcs2=p(14); Keel=p(15); Kee2=p(16); Kc1=p(17);
Kc2=p(18); Kbl=p(19); Kb2=p(20); Kg3=p(21); Kc3=p(22); Kb3=p(23); Ks1=p(24); Ks2=p(25);
SORTotm=p(26); SORTotd=p(27);

%% =====
%% create a vector to be used for APPinit, APPmonomer, and APPdimer
P = xdata8(:,1);
w=length(P);
appFSOLVE=zeros(1,w);
Ps = xdata8s(:,1);
ws=length(Ps);
appFSOLVEs=zeros(1,ws);
appFSOLVEms=zeros(1,ws);
appFSOLVEds=zeros(1,ws);

%% SOLVE for free APP (i.e.\ APP init) given the total amount of APP (without SORLA): see Equations 4.15
for j=1:w
func=@(APP) ( APP.* (1+ Kg1+ Kg2+ Kcs1.* (1+ Kc1.* ((- (1+ Kc2+ Kc1.* (1+ Kcs1.* APP./ Kma)) +
sqrt((1+ Kc2+ Kc1.* (1+ Kcs1.* APP./ Kma)).^2- 4.* (2.* Kc3.* (1+ Kcs2.* APP.^2./ Kmad)).* (-
Atot)))/ (2.* (2.* Kc3.* (1+ Kcs2.* APP.^2./ Kmad))))./ Kma)+ Keel.* (1+ Kbl.* ((- (1+ Kb2+ Kbl.* (1+
Keel.* APP./ Kmb)) + sqrt((1+ Kb2+ Kbl.* (1+ Keel.* APP./ Kmb)).^2- 4.* (2.* Kb3.* (1+ Kee2.*
APP.^2./ Kmbd)).* (- Btot)))/ (2.* (2.* Kb3.* (1+ Kee2.* APP.^2./ Kmbd))))./ Kmb)+ 2.* (APP.^2).*
(Kg3+ Kcs2.* (1+ Kc3.* ((- (1+ Kc2+ Kc1.* (1+ Kcs1.* APP./ Kma)) + sqrt((1+ Kc2+ Kc1.* (1+ Kcs1.*
APP./ Kma)).^2- 4.* (2.* Kc3.* (1+ Kcs2.* APP.^2./ Kmad)).* (- Atot)))/ (2.* (2.* Kc3.* (1+ Kcs2.*
APP.^2./ Kmad))))).^2./ Kmad)+ Kee2.* (1+ Kb3.* ((- (1+ Kb2+ Kbl.* (1+ Keel.* APP./ Kmb)) + sqrt((1+
Kb2+ Kbl.* (1+ Keel.* APP./ Kmb)).^2- 4.* (2.* Kb3.* (1+ Kee2.* APP.^2./ Kmbd)).* (- Btot)))/ (2.*
(2.* Kb3.* (1+ Kee2.* APP.^2./ Kmbd))))).^2./ Kmbd))- xdata8(j,1));
appFSOLVE(1,j)=fzero(func,[0 P(j)],optimset('fzero'));
end

%% SOLVE for free APP (init) given the total amount of APP (with SORLA)
% Since the experimental data for APP_tot with and without SORLA are not measured in 1- 1
% correspondence, thus in order to continue with the analysis of experimental data with SORLA, the
% computation of APP_init done above is repeated for the experimental data with SORLA. Instead of
% xdata8, xdata8s is used

for j=1:ws
func=@(APP) ( APP.* (1+ Kg1+ Kg2+ Kcs1.* (1+ Kc1.* ((- (1+ Kc2+ Kc1.* (1+ Kcs1.* APP./ Kma)) +
sqrt((1+ Kc2+ Kc1.* (1+ Kcs1.* APP./ Kma)).^2- 4.* (2.* Kc3.* (1+ Kcs2.* APP.^2./ Kmad)).* (-
Atot)))/ (2.* (2.* Kc3.* (1+ Kcs2.* APP.^2./ Kmad))))./ Kma)+ Keel.* (1+ Kbl.* ((- (1+ Kb2+ Kbl.* (1+
Keel.* APP./ Kmb)) + sqrt((1+ Kb2+ Kbl.* (1+ Keel.* APP./ Kmb)).^2- 4.* (2.* Kb3.* (1+ Kee2.*
APP.^2./ Kmbd)).* (- Btot)))/ (2.* (2.* Kb3.* (1+ Kee2.* APP.^2./ Kmbd))))./ Kmb))+ 2.* (APP.^2).*
(Kg3+ Kcs2.* (1+ Kc3.* ((- (1+ Kc2+ Kc1.* (1+ Kcs1.* APP./ Kma)) + sqrt((1+ Kc2+ Kc1.* (1+ Kcs1.*
APP./ Kma)).^2- 4.* (2.* Kc3.* (1+ Kcs2.* APP.^2./ Kmad)).* (- Atot)))/ (2.* (2.* Kc3.* (1+ Kcs2.*
APP.^2./ Kmad))))).^2./ Kmad)+ Kee2.* (1+ Kb3.* ((- (1+ Kb2+ Kbl.* (1+ Keel.* APP./ Kmb)) + sqrt((1+
Kb2+ Kbl.* (1+ Keel.* APP./ Kmb)).^2- 4.* (2.* Kb3.* (1+ Kee2.* APP.^2./ Kmbd)).* (- Btot)))/ (2.*
(2.* Kb3.* (1+ Kee2.* APP.^2./ Kmbd))))).^2./ Kmbd))- xdata8s(j,1));
appFSOLVEs(1,j)=fzero(func,[0 Ps(j)],optimset('fzero'));
end

% SOLVE for free APPg1 and APPg2 given the total amount of APP in monomer and in dimer, respectively
% Step-1: solve the conserved total amount of alpha, beta, and APP in monomer and in dimer processing

apps=appFSOLVEs';
alphas = (- (1+ Kc2+ Kc1.* (1+ Kcs1.* apps./ Kma)) + sqrt((1+ Kc2+ Kc1.* (1+ Kcs1.* apps./ Kma)).^2-
4.* (2.* Kc3.* (1+ Kcs2.* apps.^2./ Kmad)).* (- Atot)))/ (2.* (2.* Kc3.* (1+ Kcs2.* apps.^2./ Kmad)));
betas = (- (1+ Kb2+ Kbl.* (1+ Keel.* apps./ Kmb)) + sqrt((1+ Kb2+ Kbl.* (1+ Keel.* apps./ Kmb)).^2-
4.* (2.* Kb3.* (1+ Kee2.* apps.^2./ Kmbd)).* (- Btot)))/ (2.* (2.* Kb3.* (1+ Kee2.* apps.^2./ Kmbd)));

Atotms = (alphas.* Kc1).*(1+ Kcs1.* apps./ Kma);
Atotds = Kc2.* alphas + 2.* Kc3.* (alphas.^2).*(1+ Kcs2.* (apps.^2)/ Kmad);
Btotms = (betas.* Kbl).*(1+ Keel.* apps./ Kmb);
Btotds = Kb2.* betas + 2.* Kb3.* (betas.^2).*(1+ Kee2.* (apps.^2)/ Kmbd);
APPtotms = apps.* (Kg1+ Kcs1.* (1+ Kc1.* alphas./ Kma)+ Keel.* (1+ Kbl.* betas./ Kmb));
APPtotds = Kg2.* apps+ 2.* (apps.^2).*(Kg3+ Kcs2.* (1+ Kc3.* (alphas.^2)/ Kmad)+ Kee2.* (1+ Kb3.*
(betas.^2)/ Kmbd));

```

```

% Step 2: solve for the corresponding free values (APPg1 and APPg2) such that APPms* Kg1 and APPds*
Kg1 correspond to APPG1 and APPG2 in the model representation, respectively. (See Equations 4.19)

for js=1:ws
funcs=@(APPms*(Kg1+ Kcs1.* (1+ Kc1.* (Atotms(js,1)./ (Kc1.* (1+ Kcs1.* APPms./ Kma)))/ Kma)+
Keel.* (1+ Kb1.* (Btotms(js,1)./ (Kb1.* (1+ Keel.* APPms./ Kmb)))/ Kmb)+ Ks1.* (SORtotm./ (1+
Ks1.* APPms)).* APPms - APptotms(js,1));
appFSOLVEms(1,js)=fzero(funcs,[0 APptotms(js)],optimset('fzero'));
end

for js=1:ws
funcs=@(APPds*(Kg2.* APPds + 2.* (APPds.^2).*(Kg3+ Kcs2.* (1+ Kc3.* ((- Kc2 + sqrt(Kc2.^2- 4.*
(2.* Kc3.* (1+ Kcs2.* (APPds.^2)./ Kmad)).* (- Atotds(js,1)))))./(4.* Kc3.* (1+ Kcs2.* (APPds.^2)./
Kmad)).^2)./ Kmad)+ Kee2.* (1+ Kb3.* ((- Kb2 + sqrt(Kb2.^2- 4.* (2.* Kb3.* (1+ Kee2.* (APPds.^2)./
Kmbd)).* (- Btotds(js,1)))))./(4.* Kb3.* (1+ Kee2.* (APPds.^2)./ Kmbd)).^2)./ Kmbd)+ Ks2.*
(SORtotd./ (1+ Ks2.* APPds)).* APPds - APptotds(js,1));
appFSOLVEds(1,js)=fzero(funcs,[0 APptotds(js)],optimset('fzero'));
end

%% SUMMARY of representations
% without SORLA (see Equations 4.17 and 4.18)
% alpha denotes alpha_init
% beta denotes beta_init
% Atot denotes the conserved amount of alpha-secretase
% Btot denotes the conserved amount of beta-secretase
app=appFSOLVE';
alpha = (- (1+ Kc2+ Kc1.* (1+ Kcs1.* app./ Kma)) + sqrt((1+ Kc2+ Kc1.* (1+ Kcs1.* app./ Kma)).^2-
4.* (2.* Kc3.* (1+ Kcs2.* app.^2./ Kmad)).* (- Atot)))/ (2.* (2.* Kc3.* (1+ Kcs2.* app.^2./ Kmad)));
beta = (- (1+ Kb2+ Kb1.* (1+ Keel.* app./ Kmb)) + sqrt((1+ Kb2+ Kb1.* (1+ Keel.* app./ Kmb)).^2-
4.* (2.* Kb3.* (1+ Kee2.* app.^2./ Kmbd)).* (- Btot)))/ (2.* (2.* Kb3.* (1+ Kee2.* app.^2./ Kmbd)));

% with SORLA (see Equations 4.22 and 4.23)
% alphams.* Kc1 denotes alpha_1
% alphads.* Kc2 denotes alpha_2
% betams.* Kb1 denotes beta_1
% betads.* Kb2 denotes beta_2
% Atotms and Atotds denote the conserved amount of alpha in monomer and in dimer, respectively
% Btotms and Btotds denote the conserved amount of alpha in monomer and in dimer, respectively
% appms* Kg1 is APPG1 in the equations shown in Section-\ref{sec:MultiCompartmentmodel}
% appds* Kg1 is APPG2 in the equations shown in Section-\ref{sec:MultiCompartmentmodel}
appms=appFSOLVEms';
appds=appFSOLVEds';
appTOTS=app+ appms+ appds;
%monomer processing with SORLA
alphams = Atotms./ (Kc1.* (1+ Kcs1.* appms./ Kma));
betams = Btotms./ (Kb1.* (1+ Keel.* appms./ Kmb));
%dimer processing with SORLA
alphads = (- Kc2 + sqrt(Kc2.^2- 4.* (2.* Kc3.* (1+ Kcs2.* (appds.^2)./ Kmad)).* (- Atotds)))/ (4.*
Kc3.* (1+ Kcs2.* (appds.^2)./ Kmad));
betads = (- Kb2 + sqrt(Kb2.^2- 4.* (2.* Kb3.* (1+ Kee2.* (appds.^2)./ Kmbd)).* (- Btotds)))/ (4.*
Kb3.* (1+ Kee2.* (appds.^2)./ Kmbd));

%%%%%%%%%%%%%%%%%%%%%%%%%%%%%%%%%%%%%%%%%%%%%%%%%%%%%%%%%%%%%%%%%%%%%%%%
%% fitting to the experimental data (see Equations 4.6 - 4.8)
% with SORLA for monomer processing
fit11=k6.* Kc1.* alpha.* Kcs1.* app./ Kma;% sAPPA
fit21= k4.* Kb1.* beta.* Keel.* app./ Kmb;% sAPPB
% without SORLA for dimer processing
fit12= 2.* k6d.* Kc3.* (alpha.^2).*(Kcs2.* (app.^2)./ Kmad;% sAPPA
fit22= 2.* k4d.* Kb3.* (beta.^2).*(Kee2.* (app.^2)./ Kmbd;% sAPPB
% sum of products w/o SORLA in monomer and dimer
fit1 = (fit11+ fit12); % sAPPA
fit2 = (fit21+ fit22); % sAPPB

% fitting with SORLA monomer(refer to Equations16 in supplementary information)
% with SORLA for monomer processing
fit12s = k6.* Kc1.* alphams.* Kcs1.* appms./ Kma;% sAPPA
fit22s = k4.* Kb1.* betams.* Keel.* appms./ Kmb;% sAPPB
% without SORLA for dimer processing
fit11s=2.* k6d.* Kc3.* (alphads.^2).*(Kcs2.* (appds.^2)./ Kmad;% sAPPA
fit21s= 2.* k4d.* Kb3.* (betads.^2).*(Kee2.* (appds.^2)./ Kmbd;% sAPPB
% sum of products w/ SORLA in monomer and dimer
fit1s = (fit11s+ fit12s); % sAPPA
fit2s = (fit21s+ fit22s); % sAPPB

%RECALL: w and ws denote the number of experimental data without and with SORLA, respectively
% without SORLA
err11 = (fit1 - data(:,2))./ sqrt((sum(data(:,2))./ w));
err22 = (fit2 - data(:,3))./ sqrt((sum(data(:,3))./ w));

```

```
% with SORLA
errAPPs = (appTOTS - datas(:,1))./ sqrt((sum(datas(:,1))./ ws));
err11s = (fit1s - datas(:,2)) ./ sqrt((sum(datas(:,2))./ ws));
err22s = (fit2s - datas(:,3)) ./ sqrt((sum(datas(:,3))./ ws));
% error vector
err=vertcat(errAPPs, err11, err22, err11s, err22s);
end
end
```

DECLARATION/SELBSTÄNDIGKEITSERKLÄRUNG

I, the undersigned, hereby declare that the work contained in this dissertation is my own original work and that I have not previously in its entirety or in part submitted it at any university for a degree.

Hiermit bestätige ich, dass ich die vorliegende Arbeit selbstständig, und nur mit den angegebenen Quellen angefertigt habe. Diese Arbeit wurde weder in Teilen, noch im Ganzen, zur Erlangung von akademischen Graden an anderen Universitäten eingreicht.

Rostock, March 13, 2013

Angelyn Lao

CURRICULUM VITAE

Angelyn Lao

Manila, Philippines

Filipino

30 August 1979

angelynlao@gmail.com

Academic background

- 06.2008- PhD in Computer Science
Rostock University, Rostock, Germany
Department of Systems Biology and Bioinformatics
Thesis title: “A Systems Biology Approach to Understand
the Influence of SORLA on Amyloidogenic Processing in Alzheimer’s Disease”
Supervisor: Prof. Olaf Wolkenhauer
- 06.2005-present PhD in Mathematics
University of the Philippines, Diliman, Philippines
- 09.2001-09.2004 Masters of Science in Mathematics
De La Salle University, Taft Avenue, Manila, Philippines
Thesis title: “Factorization of Pretopological Spaces and Strong Product Graphs”
Supervisors: Dr. Severino Diesto and Dr. Eduardo Mendoza
- 09.2000-07.2001 Certificate of Foreign Studies in Chinese language and literature
Beijing Second Foreign Language University, Beijing, China
- 06.1996-09.2000 Bachelor of Secondary Education in Computer Application
De La Salle University, Taft Avenue, Manila, Philippines

06.1996-09.2000 Bachelor of Science in Mathematics
De La Salle University, Taft Avenue, Manila, Philippines
Thesis title: "Scheduling Conflict-Free Group Activities"
Supervisor: Dr. Severino Gervacio

Professional experience

- 06.2006-03.2008 Lecturer
St. Scholastica's College, Manila, Philippines
- 05.2008 Research assistant
Wep project (http://www.thewep.org/en/philshift_study.php)
headed by Dr. Eduardo Mendoza of the
Ludwig Maximilians University and the University of the Philippines
- 06.2007-04.2008 Research assistant
EUCLIS project (<http://www.bioinfo.mpg.de/euclis/>)
headed by Dr. Eduardo Mendoza of the
Ludwig Maximilians University and the University of the Philippines
- 06.2006-05.2007 Research assistant
Sartorius image analysis project
headed by Dr. Eduardo Mendoza of the
Ludwig Maximilians University and the University of the Philippines
- 09.2005 Passed the "Philippine Licensure Examination for Teachers"
- 09.2002-08.2005 Instructor
De La Salle University, Taft Avenue, Manila, Philippines
- 09.2001-08.2002 Assistant instructor
De La Salle University, Taft Avenue, Manila, Philippines

SCIENTIFIC CONTRIBUTIONS

Peer-Reviewed International Publication

- V. Schmidt, **A. Lao**, K. Baum, K. Rateitschak, Y. Schmitz, C. Munck Petersen, A. Nykjaer, J. Wolf, O. Wolkenhauer, and T.E. Willnow. Quantitative modeling of amyloidogenic processing and its influence by SORLA in Alzheimer's disease. *EMBO J.*, 31(1):187 - 200, January 2012. doi: 10.1038/emboj.2011.352.

V. Schmidt and T.E. Willnow conducted all cell and molecular biology experiments. **A. Lao** carried out the mathematical modelling. **A. Lao** designed and established the model, generated the model equations, performed the simulations, and analyzed the corresponding results. Due to the type of dose-response data used in the study, the creation of the model equations and the implementation of MATLAB codes for parameter estimation were non-trivial. The employed strategies were state-of-the art in systems biology and likely to be of interest to modelers. These strategies were realized and developed by **A. Lao**. Y. Schmitz supported the analysis of the simulations. K. Rateitschak supervised the work of A. Lao. V. Schmidt and K. Baum performed the analyses of enzyme kinetics. The original idea to use enzyme kinetics were from K. Baum and J. Wolf. O. Wolkenhauer and T.E. Willnow conceived the research and supervised the work. T.E. Willnow wrote the initial draft of the manuscript. **A. Lao**, and K. Rateitschak also took part in writing the modeling related parts of the manuscript. The remaining other authors commented on and helped correcting the manuscript. In this study, the biological analysis relied on the mathematical model. However, the choice of journal required extensive experimental evidence for the validation of model. Given that the biological questions and experiments were at the center of this investigation, **A. Lao** was put into second authorship.

- **A. Lao**, V. Schmidt, Y. Schmitz, T.E. Willnow, and O. Wolkenhauer. Multi-compartmental modeling of SORLA's influence on amyloidogenic processing in Alzheimer's disease. *BMC Syst. Biol.*, 6(1):74, June 2012. doi: 10.1186/1752-0509-6-74.

A. Lao conceived and designed the research. **A. Lao** formulated the model, carried out all the calculations, and performed all the simulations. **A. Lao** analyzed the results and wrote the initial draft of the manuscript. V. Schmidt and

Y. Schmitz supported the study conducted by A. Lao by checking assumptions, MATLAB codes, and results. T.E. Willnow, and O. Wolkenhauer supervised the work and contributed to the writing of the final manuscript.

Proceeding(s)

- O. Wolkenhauer, **A. Lao**, S. Omholt, and H. Martens. Systems approaches in molecular and cell biology: making sense out of data and providing meaning to models. *Proceedings of SPIE*, 7343(1): 734318-734318-11, April 2009. doi: 10.1117/12.822742.

Talks

- **A. Lao**. Mathematical modeling of APP processing influenced by SORLA in Alzheimer's disease. *Spring school 2009 on Systems Biology*, Kloster Seeon (Germany), April 2009.
- **A. Lao**. Mathematical modeling of APP processing influenced by SORLA in Alzheimer's disease. *Lecture series on Discrete Mathematics, Informatics, and Systems Biology (DIMISysBio)*, Department of Computer Science, University of the Philippines - Diliman (Philippines), September 2010.
- **A. Lao**. Compartmental modeling of APP processing influenced by SORLA in Alzheimer's disease. *Philippine Computational and Systems Biology (PhilCSBi) lectures*, Department of Computer Science, University of the Philippines - Diliman (Philippines), September 2011.
- **A. Lao**. Mathematical modeling of APP processing influenced by SORLA in Alzheimer's disease. *Gong show 2011*, Faculty of Computer Science and Electrical Engineering, University of Rostock (Germany), September 2011.

Posters

- **A. Lao**, V. Schmidt, K. Rateitschak, O. Wolkenhauer, and T.E. Willnow. Mathematical modeling of APP processing influenced by SORLA in Alzheimer's disease (Part 1). *Mid-term review of the Helmholtz Alliance on Systems Biology*, DKFZ (Heidelberg), January 2010.
- V. Schmidt, **A. Lao**, K. Rateitschak, O. Wolkenhauer, and T.E. Willnow. Quantitative modeling of APP processing influenced by SORLA in Alzheimer's disease. *International conference on Alzheimer's disease*, Honolulu Hawaii, July 2010.
- **A. Lao**, Y. Schmitz, V. Schmidt, K. Rateitschak, J. Wolf, T.E. Willnow, and O. Wolkenhauer. Mathematical modeling of APP processing influenced by SORLA in Alzheimer's disease (Part 2). *International Conference on Systems Biology*, Heidelberg/ Mannheim, August 2011.

- **A. Lao**, V. Schmidt, Y. Schmitz, T.E. Willnow, and O. Wolkenhauer. Multi-compartmental modeling of APP processing influenced by SORLA in Alzheimer's disease. *International Conference on Systems Biology*, Toronto, August 2012.
- **A. Lao**, V. Schmidt, Y. Schmitz, T.E. Willnow, and O. Wolkenhauer. Regulated trafficking of APP by SORLA in Alzheimer's disease. *International Conference on Systems Medicine*, Dublin, September 2012.

Mathematical Modelling of APP Processing influenced by SORLA in Alzheimer's Disease

Angelyn Lao¹, Vanessa Schmidt², Katja Rateitschak¹, Thomas Willnow² and Olaf Wolkenhauer¹

Abstract

Alzheimer's disease (AD) is a neurodegenerative disorder characterized by amyloid plaques in the brain of affected individuals. This project aims at modeling of neurodegenerative processes in AD. Our study focuses on the interconnectome of neuronal factors central to the proteolytic processing of amyloid precursor protein (APP) into A β , the main constituent of senile plaques. Factors considered in this model include proteases, trafficking adaptors, as well as a novel sorting receptor SORLA. Here, we have generated a panel of cell lines in which the amount of APP and of accessory factors can be varied. These novel cell lines are important research tools that have since been applied to produce quantitative data. The quantitative dose-response series have been used to estimate reaction constants of mathematical models describing APP processing. We have established nonlinear ordinary differential equation models describing the cleavage of APP by alpha and beta secretases, and the influence of SORLA herein. We have queried different mathematical models concerning the interactions with SORLA and we have simplified the models based on justifiable steady state approximations. For the resulting algebraic models, we have estimated the model parameters from the dose-response curves by nonlinear optimization methods. These results provide the bases for further modeling of neurodegenerative processes and for determination of individual risk of AD.

APP processing influenced by SORLA – network diagrams

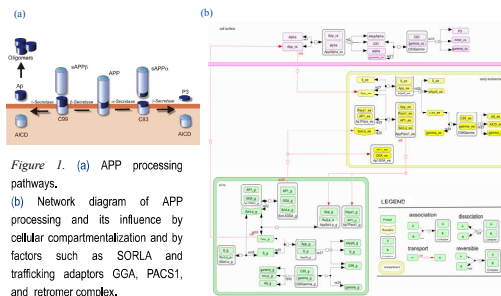


Figure 1. (a) APP processing pathways. (b) Network diagram of APP processing and its influence by cellular compartmentalization and by factors such as SORLA and trafficking adaptors GGA, PACS1, and retromer complex.

Regulated expression of APP in cells

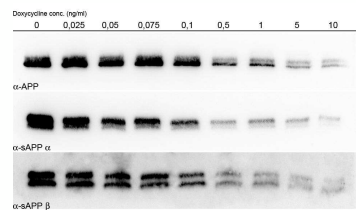


Figure 4. Cells were incubated with doxycycline of the indicated concentrations. Western blot analysis of cell media and lysates showed decreased amounts of APP and its processing products with increasing doxycycline concentration.

Comparison of experimental data and model simulations

Parameter value of the models have been determined on the basis of experimental dose-response series for APP-sAPP α and APP-sAPP β by nonlinear optimization.

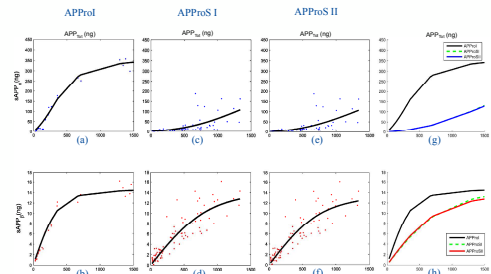


Figure 5. Comparison of experimental dose-response series for APP-sAPP α [blue dots] and APP-sAPP β [red dots] to the simulation of mathematical models with optimized parameters. (a-b) CHO- μ APP [ELISA] with APPProI. (c-d) CHO SORLA- μ APP [ELISA] with APPProSI. (e-f) CHO SORLA- μ APP [ELISA] with APPProSII. (g-h) Putting the respective plots of sAPP α and sAPP β for APPProI, APPProSI and APPProSII together.

Subsystems - mathematical models

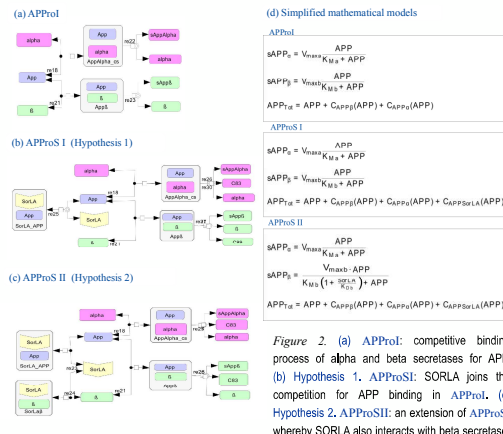


Figure 2. (a) APPProI: competitive binding process of alpha and beta secretases for APP. (b) Hypothesis 1, APPProSI: SORLA joins the competition for APP binding in APPProI. (c) Hypothesis 2, APPProSII: an extension of APPProSI whereby SORLA also interacts with beta secretase. (d) Table of simplified mathematical equations, derived from the rate equations of each subsystem. Nonlinear differential equations are simplified through justifiable assumption of a quasi-steady state and a conservation law. Note that 'APP' (stands for the free APP) in each equations is replaced by their respective function of APP_{tot} (total APP measured in experiments).

Tet-Off inducible APP gene expression - methodology

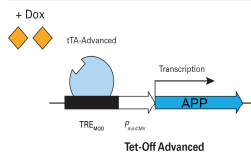


Figure 3. Binding of the Tet-controlled transactivator (ITA) to the tetracycline response element (TRE) induces APP expression. In the presence of doxycycline binding of ITA to TRE is reduced and APP expression is impaired in a dose-dependent manner. (Clontech Laboratories, modified)

Results

- We have established a panel of cell lines in which the amount of APP and regulatory factors can be varied and quantitative data for APP processing can be derived.
- We have produced dose-response series of data (APP-sAPP α and APP-sAPP β) from CHO- μ APP and CHO SORLA- μ APP [Western Blot Analysis and ELISA].
- Our collaboration have shown good agreement between the simulation results of models with optimized parameters and the experimental data.
- We made a comparison of the two alternative hypotheses [APPProSI (Figure 5 (c-d)) and APPProSII (Figure 5 (e-f))]. It suggests that a proposed interaction of beta secretase with SORLA does not impact on APP processing.

Outlook

- Extension of mathematical models by inclusion of additional factors and cellular compartments.
- Validation of models through experimental data in cells and mouse models *in vivo*.

Mathematical Modeling of APP Processing influenced by SORLA in Alzheimer's Disease

Angelyn Lao^{1*}, Yvonne Schmitz¹, Vanessa Schmidt², Katja Rateitschak¹, Jana Wolf², Thomas Willnow², Olaf Wolkenhauer¹

¹Department of Systems Biology & Bioinformatics, University of Rostock, Germany and ²Max-Delbrueck-Center for Molecular Medicine, Berlin, Germany

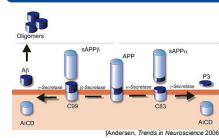
Abstract

Background: Alzheimer's disease (AD) is a neurodegenerative disorder characterized by amyloid plaques in the brain of affected individuals. Our study aims at (i) modeling the interactions of neuronal factors central to the proteolytic processing of amyloid precursor protein (APP) and (ii) evaluating the influence of SORLA/SORL1, an inhibitor of APP processing and important genetic risk factor.

Results: Based on a panel of cell lines in which the amount of APP and of accessory factors can be varied, we have established a model, based on nonlinear Ordinary Differential Equations (ODE), describing the kinetics of APP processing and the influence of SORLA on the processing. The parameter values of the simplified ODE model are estimated by optimization from dose-response series for sAPP α and sAPP β as a function of total amount of APP for cells with or without SORLA. We have systematically compared the goodness of fit of (a) model with only monomer processing, (b) model with only dimer processing, and (c) combined model with both monomer and dimer processing, on a series of dose-response data. In the combined model, the dimeric forms of the secretases only act on the dimeric form of APP and the monomeric forms of the secretases only act on the monomeric form of APP. The complexity of data and model made it necessary to also consider partial parameter estimations in order to capture the dynamical behavior of the experimental data. We performed purely global parameter estimations for all three models and global-local parameter estimation for the combined model. For global-local parameter estimation, all parameters except the parameters describing β -secretase activity in the presence or absence of SORLA are estimated locally.

Conclusions: The simulations, together with our experimental data, support a model whereby SORLA prevents APP oligomerization, thereby causing secretases to switch from allosteric to non-allosteric mode of action. We also performed simulations for intermediate concentrations of SORLA on the combined model with global-local estimate. We predicted a switch from cooperative to less efficient non-cooperative processing on a low amount of SORLA concentration.

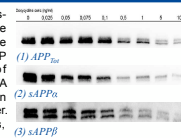
1. APP processing



APP is cleaved by either α - or β -secretase. The sequential cleavage of APP producing A β is called amyloidogenic pathway.

2. Experimental materials and methods

The binding of the Tet-controlled transactivator (tTA) to the tetracycline response element (TRE) in front of the modified CMV promoter induces APP expression. In the presence of doxycycline, the binding capability of tTA to TRE is reduced and APP expression is impaired in a dose-dependent manner. (Figure from Clontech Laboratories, modified)



Multi-compartmental Modeling of APP Processing influenced by SORLA in Alzheimer's Disease

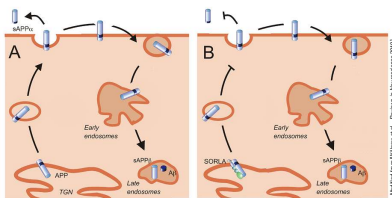
Angelyn Lao^{1*}, Vanessa Schmidt², Yvonne Schmitz¹, Thomas E. Willnow², Olaf Wolkenhauer¹

¹Department of Systems Biology & Bioinformatics, University of Rostock, Germany and ²Max-Delbrueck-Center for Molecular Medicine, Berlin, Germany

Abstract

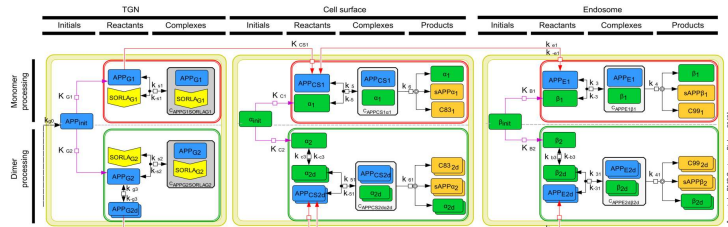
Background: The formation of Aβ plaques from the processing of amyloid precursor protein (APP) is central to the pathology of Alzheimer's disease. Studies concerning APP processing are conventionally conducted in a single-compartment, where the reactants involved are either in a monomeric or a dimeric form of APP. In the single-compartment model we presented earlier, it showed that the sorting receptor-related protein, SORLA, affects APP processing in both its monomeric and dimeric forms. This study raised the interesting question of what the relative contribution of SORLA in each APP processing step is and how this affects the β-secretase? **Results:** To answer this question, we developed a multi-compartment model to simulate the complexity of APP processing in neurons, and to accurately describe the effects of SORLA on these processes. Based on dose-response data, our study concludes that SORLA specifically impairs processing of APP dimer, which is the preferred secretase substrate. Furthermore, our model shows how SORLA alters the dynamical behavior of β-secretase, the enzyme responsible for the initial step in the amyloidogenic processing cascade. **Conclusions:** Our multi-compartment model represents a major conceptual advance over single-compartment models previously used to simulate APP processing; and it identified APP dimers and β-secretase as the two distinct targets of the inhibitory action of SORLA in Alzheimer's disease. **Reference:** A. Lao, V. Schmidt, Y. Schmitz, T.E. Willnow, and O. Wolkenhauer. Multi-compartmental modeling of SORLA's influence on amyloidogenic processing in Alzheimer's disease. *BMC Syst. Biol.*, 6(1):74, June 2012.

1. Influence of SORLA on APP processing



(A) APP traverse from trans-golgi network (TGN) to the cell surface where most APP are cleaved by α-secretase producing sAPPα. Non-processed APP traffic from early to late endosomes and are processed into sAPPβ and Aβ, respectively. (B) SORLA acts as sorting-receptor that traps APP in TGN, guiding the trafficking and processing of APP.

2. Multi-compartmental model



Biochemical network of a multi-compartment model describing the influence of SORLA on APP processing. The three main compartments in the network are the TGN, the cell surface and the endosomes. Each compartment is subdivided into two subcompartments: monomer and dimer processing.

3. Mathematical equations of the model

ODEs

$$sAPP_{TGN} = \frac{k_{s1}}{K_{Mat1}} \alpha_1 \cdot APP_{TGN} + 2 \cdot \frac{k_{s2}}{K_{Mat2}} \alpha_{2d} \cdot APP_{TGN,d}$$

$$sAPP_{Cell} = \frac{k_{c1}}{K_{MPr1}} \beta_1 \cdot APP_{Cell} + 2 \cdot \frac{k_{c2}}{K_{MPr2,d}} \beta_{2d} \cdot APP_{Cell,d}$$

Assumed conservation law

$$\alpha_{Tot} = \alpha_{free} + \alpha_{monomer} + \alpha_{dimer}$$

$$\beta_{Tot} = \beta_{free} + \beta_{monomer} + \beta_{dimer}$$

$$APP_{Tot} = APP_{free} + APP_{monomer} + APP_{dimer}$$

In the absence of SORLA,

$$\alpha_{monomer} = \alpha_1 (\alpha_{Tot} - \alpha_1) + C_{APPC31d} (APP_{TGN,d} \alpha_{Tot})$$

$$\alpha_{dimer} = \alpha_2 (\alpha_{Tot} - \alpha_2) + 2 \cdot C_{APPC32d} (APP_{TGN,d} \alpha_{Tot})$$

$$\beta_{monomer} = \beta_1 (\beta_{Tot} - \beta_1) + C_{APPE11d} (APP_{Cell,d} \beta_{Tot})$$

$$\beta_{dimer} = \beta_2 (\beta_{Tot} - \beta_2) + 2 \cdot C_{APPE21d} (APP_{Cell,d} \beta_{Tot})$$

$$APP_{monomer} = APP_{TGN} (\alpha_{Tot} - \alpha_1) + APP_{Cell} (\beta_{Tot} - \beta_1) + C_{APPC31d} (APP_{TGN,d} \alpha_{Tot}) + C_{APPE11d} (APP_{Cell,d} \beta_{Tot})$$

$$APP_{dimer} = APP_{TGN,d} (\alpha_{Tot} - \alpha_2) + 2 \cdot [APP_{Cell,d} (\beta_{Tot} - \beta_2) + C_{APPC32d} (APP_{TGN,d} \alpha_{Tot}) + C_{APPE21d} (APP_{Cell,d} \beta_{Tot})]$$

In the presence of SORLA,

$$\alpha_{monomer} = \alpha_1 + C_{APPC31d} (APP_{TGN,d} \alpha_1)$$

$$\alpha_{dimer} = \alpha_2 + 2 \cdot [C_{APPC32d} (APP_{TGN,d} \alpha_2)]$$

$$\beta_{monomer} = \beta_1 + C_{APPE11d} (APP_{Cell,d} \beta_1)$$

$$\beta_{dimer} = \beta_2 + 2 \cdot [C_{APPE21d} (APP_{Cell,d} \beta_2)]$$

$$APP_{monomer} = APP_{TGN} (\alpha_1) + C_{APPC31d} (APP_{TGN,d} \alpha_1) + C_{APPE11d} (APP_{Cell,d} \beta_1)$$

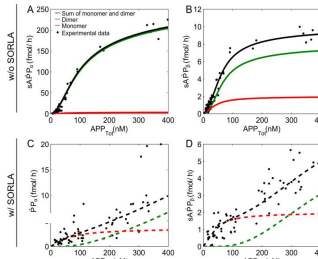
$$APP_{dimer} = APP_{TGN,d} (\alpha_2) + 2 \cdot [C_{APPC32d} (APP_{TGN,d} \alpha_2) + C_{APPE21d} (APP_{Cell,d} \beta_2)]$$

Through justifiable assumptions of quasi-steady state and conservation law, simplified ODEs describe the formation of end products in the APP under the influence of SORLA. Note that subscript '1' was assigned to the reactants and products in monomer processing while subscript '2' for those in dimer processing. In addition, we used subscripts 'C', 'CS', and 'E' for APP in TGN, at the cell surface and in the endosomes, respectively. And for every $f_{(x,y)}$ is a complex function of X and Y . Note that $f_{(x,y)}$ denotes function f dependent on x and y .

7. Conclusions

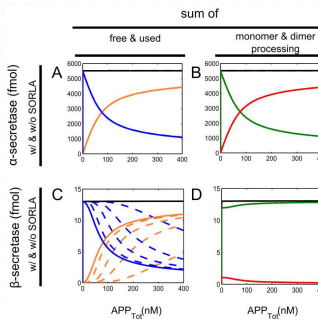
- (1) We successfully confirmed our hypothesis that blockade of APP dimerization is an important aspect of SORLA action on AD.
- (2) Using this model, we are able to uncover that SORLA not only affects amyloidogenic processing through interaction with APP but also specifically targets β-secretase - the enzyme responsible for initial amyloidogenic cleavage.

4. Model simulations fit experimental data



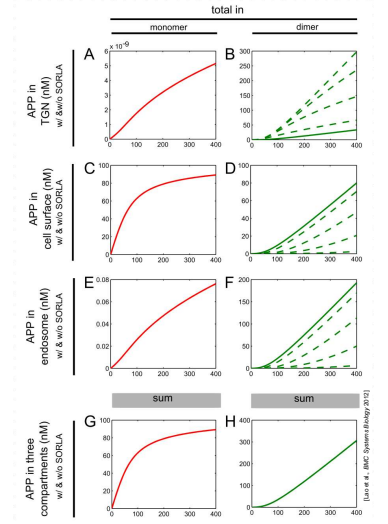
Simulation results of our multi-compartmental model (lines) for the various APP products are shown together with the data points taken from [Schmidt et al., EMBO J, 2012]. In the absence of SORLA, the products produced in the dimer processing pathways more closely resemble the total amount of sAPPα (A) and sAPPβ (B). With SORLA, the amounts of sAPPα and sAPPβ that are produced in dimer processing are significantly reduced as compared to those in monomer processing (C, D).

6. SORLA indirectly affects the dynamical behavior of the β-secretase



The intermediate levels of SORLA include 0% (solid line), 3%, 12%, 30%, and 100% (dashed line) of SORLA_{tot} (where SORLA_{tot} = 2.43 × 10⁶ fmol). Only solid line is visible in a plot when solid and dashed lines are superimposed. (Fig. above) Simulations of the influence of intermediate levels of SORLA on APP processing into the amounts of APP concentrations in the TGN (A-B), at the cell surface (C-D), in the endosomes (E-F), and in all the three compartments (G-H). The simulations for total amount of APP concentrations in monomer processing for the three different compartments (left column) are not influenced by SORLA, while those in dimer processing are affected by the presence of SORLA (right column). (Fig. left) Simulations of the influence of intermediate levels of SORLA on APP processing into the amount of α-secretase (A-B) and β-secretase (C-D) concentration. The term 'free' refers to the secretases that are not bound in a complex. It can be observed that the total amount of β-secretase concentration for both free and used deviated (C), which was not the case for α-secretase (A). This observation suggested that SORLA is indirectly affecting the dynamics of β-secretase but not that of α-secretase.

5. SORLA is more influential in dimer processing than in monomer processing



The intermediate levels of SORLA include 0% (solid line), 3%, 12%, 30%, and 100% (dashed line) of SORLA_{tot} (where SORLA_{tot} = 2.43 × 10⁶ fmol). Only solid line is visible in a plot when solid and dashed lines are superimposed. (Fig. above) Simulations of the influence of intermediate levels of SORLA on APP processing into the amounts of APP concentrations in the TGN (A-B), at the cell surface (C-D), in the endosomes (E-F), and in all the three compartments (G-H). The simulations for total amount of APP concentrations in monomer processing for the three different compartments (left column) are not influenced by SORLA, while those in dimer processing are affected by the presence of SORLA (right column). (Fig. left) Simulations of the influence of intermediate levels of SORLA on APP processing into the amount of α-secretase (A-B) and β-secretase (C-D) concentration. The term 'used' refers to the secretases that are not bound in a complex. It can be observed that the total amount of β-secretase concentration for both free and used deviated (C), which was not the case for α-secretase (A). This observation suggested that SORLA is indirectly affecting the dynamics of β-secretase but not that of α-secretase.



Regulated Trafficking of APP by SORLA in Alzheimer's Disease

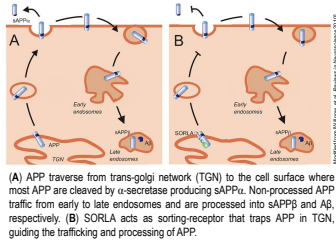
Angelyn Lao¹, Vanessa Schmidt², Yvonne Schmitz¹, Thomas E. Willnow², Olaf Wolkenhauer¹

¹Department of Systems Biology & Bioinformatics, University of Rostock, Germany and ²Max-Delbrueck-Center for Molecular Medicine, Berlin, Germany

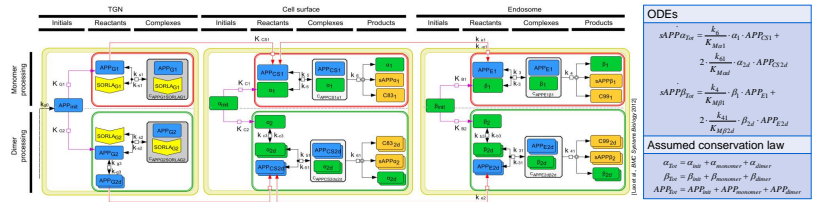
Abstract

Background: Proteolytic breakdown of the amyloid precursor protein (APP) by secretases is a complex cellular process that results in formation of neurotoxic A β peptides, causative of neurodegeneration in Alzheimer's disease (AD). Processing involves monomeric and dimeric forms of APP that traffic through distinct cellular compartments where the various secretases reside. Amyloidogenic processing is also influenced by modifiers such as sorting receptor-related protein (SORLA), an inhibitor of APP breakdown and major AD risk factor. This study aims to (i) model the neuronal factors central to the proteolytic processing of amyloid precursor protein (APP), (ii) trace the trafficking of APP in various compartments, and (iii) evaluate the influence of the SORLA on those factors. **Results:** Using experimental data and literature-based, information we developed a multi-compartment model to simulate the complexity of APP processing in neurons, and to accurately describe the effects of SORLA on these processes. Our model enables regulation of trafficking of APP by SORLA through intracellular compartments. We have successfully confirmed our hypothesis that blockade of APP dimerization is an important aspect of SORLA action on AD. Using this model, we are able to uncover that SORLA not only affects amyloidogenic processing through interaction with APP but also specifically targets β -secretase - the enzyme responsible for initial amyloidogenic cleavage. **Conclusions:** Our model represents a major conceptual advancement by identifying APP dimers and β -secretase as the two distinct targets of the inhibitory action of SORLA in AD. **Reference:** A. Lao, V. Schmidt, Y. Schmitz, T.E. Willnow, and O. Wolkenhauer. Multi-compartmental modeling of SORLA's influence on amyloidogenic processing in Alzheimer's disease. BMC Syst. Biol., 6(1):74, June 2012.

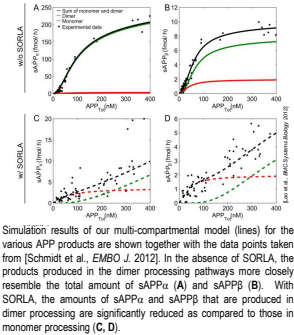
1. Influence of SORLA on APP processing



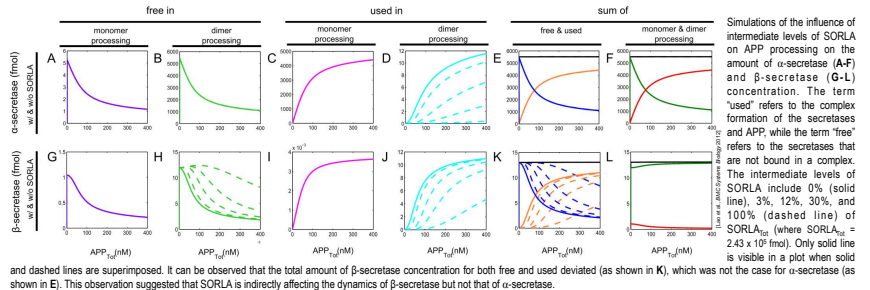
2. Multi-compartmental model



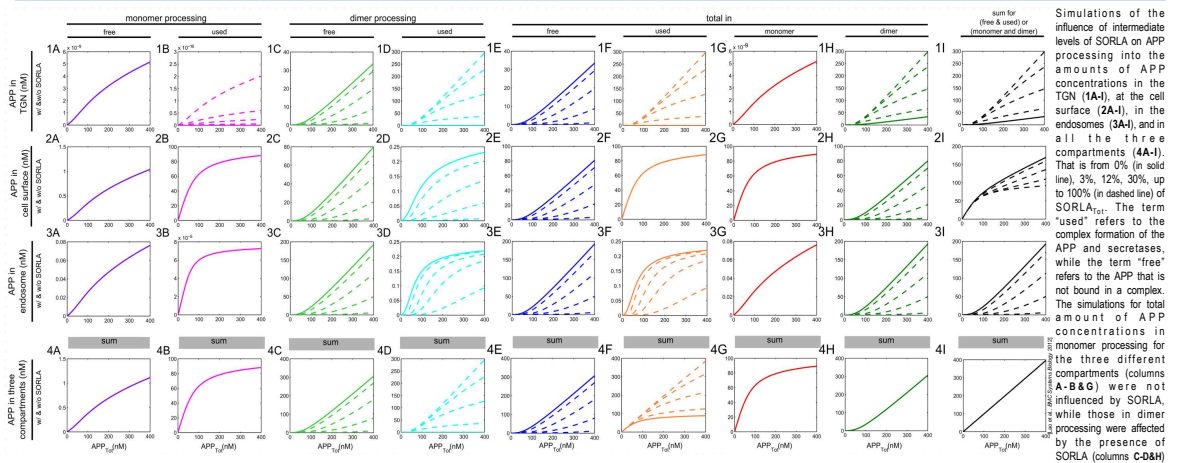
3. Model simulations fit experimental data



4. Regulated trafficking of secretases by intermediate levels of SORLA



5. Regulated trafficking of APP by intermediate levels of SORLA in various compartments



Funding
 Studies in this project were funded in part by a MSBN grant from the Helmholtz Alliance on Systems Biology.

HELMHOLTZ ASSOCIATION
 Alliance on Systems Biology

MDC
 MAX-DELBÜCK-CENTRUM FÜR MOLEKULARE MEDIZIN BERLIN-BUCH
 WIRTSCHAFTS-UNIVERSITÄT BERLIN

Corresponding author:



angelyn.lao@uni-rostock.de
 Department of Systems Biology and Bioinformatics
 University of Rostock, Germany
 www.sbi.uni-rostock.de

THESES

1. The effects of SORLA on APP processing in Alzheimer's disease can be described by a single-compartment model.
2. SORLA concentrations and efficiency of APP processing follow a strict linear relationship.
3. It can be proven that SORLA prevents dimerization of APP, thereby preventing the formation of high affinity substrates for secretases.
4. How SORLA affects APP transport between various cell compartments in neurons can be demonstrated by the multi-compartmental model.
5. With the multi-compartmental model, it can be shown that
 - 4.1. a decrease in the total amount of soluble APP products is due to the high SORLA concentration in dimer processing, and not due to the low SORLA concentration in monomer processing;
 - 4.2. SORLA indirectly affects the dynamic behavior of β -secretase, but not that of α -secretase. This supports the initial biochemical data showing that SORLA can bind to β -secretase; and
 - 4.3. SORLA is more influential in dimer processing than in monomer processing. This confirms our initial hypothesis that blockade of APP dimerization is an important aspect of SORLA action in Alzheimer's disease.
6. For the series of dose response data, nonlinear optimization provides a strategy for parameter estimation.